Altered appetite in Crohn's Disease: Deconstructing the enteroendocrine axis using fMRI

by

Gita Thapaliya BSc, MRes

School of Medicine, University of Nottingham

Thesis submitted to the University of Nottingham for the degree of Doctor of Philosophy

September 2019

Table of Contents

Abstract 8

Acknowledgements 10

List of Abbreviations 12

1 **Literature Review** 17

1.1 Crohn's disease (CD) 17

1.2 Public health Relevance 17

1.3 Environmental risk factors for CD development 18

1.4 Aetiology and Pathophysiology 18

1.5 Disease Classification 20

1.6 Diagnosis 21

1.7 Complications of CD 22

1.8 Symptoms 23

1.9 Management and medication 23

1.10 The role of enteroendocrine cells (EEC) in the control of appetite 24

1.10.1 EEC 25

1.10.2 The role of EEC peptides in the control of appetite 26

1.11 Physiology of appetite regulation 31

1.12 Gut-brain axis 31

1.13 Hedonic control of food intake 32

1.14 Appetite dysregulation 33

2 Investigation of altered appetite in CD using functional MRI 36

2.1 Principles of functional MRI (fMRI) 36

2.1.1 The physiological basis of the BOLD effect 38

2.1.2 Strengths and limitations of the BOLD contrast 40

2.1.3 Functional MRI paradigm designs to study nutrition 41

2.1.4 Functional MRI data analysis 43

2.2 Effect of hunger, thirst and satiety on brain response 52

2.2.1 Nutrient specific effects on brain responses 55

2.2.2 The effects of gut peptides on brain activation 61

2.3 Malnutrition and appetite loss in CD 63

2.4 Intestinal inflammation and modulation of EEC peptides 65

2.4.1 Animal model 66

2.4.2 Human infection cases 66

2.5 EEC peptides and CD 67

2.6 The selection of C12 dodecanoate fatty acid as a test meal in the fMRI paradigm 71
2.7 Hypotheses and Aims 73
2.8 Methods 74
2.8.1 Participant recruitment 74
2.8.2 Experimental Protocol 75
2.8.3 Stimuli, delivery system and bloodletting 76
2.8.4 Scanning protocol 77
2.8.5 fMRI paradigm 78
2.8.6 Plasma gut hormone analysis 79
2.8.7 Statistical analysis for EEC peptides 81
2.8.8 Cytokine analysis 82
2.8.9 fMRI data analysis 83
2.9 Results 85
2.9.1 Recruitment 85
2.9.2 Subject demographics 86
2.9.3 Sensation ratings before and after the fat and saline test meal ... 87
2.9.4 Comparison of baseline and postprandial concentrations of GLP-1, CCK and PYY in ileal CD, colonic CD and HC 89
2.9.5 Comparison of BOLD responses to the fat and saline meals 92
2.9.6 Effect of meal on cortical responses across the whole study group 92
2.9.7 Effect of meal on cortical responses across the combined CD group 97
2.9.8 Comparing the effect of the test meal on cortical responses between the ileal and colonic CD group 100
2.9.9 Effect of meal on cortical responses across the HC group 108
2.10 Discussion 111
2.10.1 Comparison of sensation ratings following the fat and saline test meal 112
2.10.2 Comparison of fasting and postprandial GLP-1, CCK and PYY concentrations 113
2.10.3 Comparison of postprandial BOLD responses to fat and saline 115
2.10.4 Feeding induced DMN activity in CD patients 116
2.10.5 Postprandial increase in BOLD signals in response to fat and saline compared between groups 117
2.11 Conclusion 118

3 Eating behaviour in active CD 120
3.1 Disordered eating and CD 120
3.2 Psychological disturbances and CD 120
3.3 EEC peptides and CD 121
3.4 Aims & Objectives 122
3.5 Methods 123
3.5.1 Eating behaviour constructs 123
3.5.2 Three-Factor Eating Questionnaire (TFEQ) 123
3.5.3 The Binge Eating Scale (BES) 124
3.5.4 The Power of food scale (PFS) 124
3.5.5 CoEQ 124
3.5.6 Go Stop impulsivity paradigm[231] 124
3.5.7 LFPQ 125
3.5.8 Dietary intake 128
3.5.9 Quantitative appetite assessment 129
3.5.10 SQ 131
3.5.11 Statistical analysis 131
3.6 Results 133
3.6.1 Demographics 133
3.6.2 Eating behaviour constructs 135
3.6.3 Correlation of HBI, abdominal pain, mood, QoL and fatigue .. 136
3.6.4 Go stop impulsivity paradigm 137
3.6.5 LFPQ 138
3.6.6 Dietary intake 141
3.6.7 Quantitative appetite assessments 143
3.6.8 Discussion 147
4 A study of brain morphology and it's alterations in patients with CD 159
4.1 Brain morphology 160
4.1.1 Whole-brain development 161
4.2 The association of GMV, WMV, and CT with age 162
4.2.1 GMV 162
4.2.2 CT 163
4.2.3 WMV 164
4.3 Gender-specific differences in GMV, WMV, and CT 165

4.3.1 GMV 165
4.3.2 WMV 166
4.3.3 CT 167
4.4 VBM 167
4.4.1 Limitations of VBM 170
4.4.2 Strengths of VBM 171
4.4.3 Interpretation of VBM results 172
4.5 CT assessment: surface and volume-based methods 173
4.5.1 Surface-based analysis (SBA) of CT 173
4.5.2 Volume-based analysis (VBA) of CT 174
4.5.3 Strengths and weakness of SBA and VBA 175
4.5.4 Interpretation of results 176
4.6 Structural alterations in CD patients 177
4.7 Hypothesis and aims of the study 186
4.8 Methods 187
4.8.1 Symptoms and psychological assessment 187
4.8.2 Plasma gut hormone analysis 187
4.8.3 Cytokine analysis 187
4.8.4 MR Image acquisition 188
4.8.5 VBM 188
4.8.6 CT assessment 190
4.8.7 FreeSurfer: CT analysis 190
4.8.8 CAT12: CT analysis 191
4.9 Results 193
4.9.1 Recruitment 193
4.9.2 Subject demographics 193
4.9.3 VBM of brain volume measures 197
4.9.4 Assessing WMV changes in CD 208
4.9.5 CT: CAT12 213
4.10 Discussion 219
4.10.1 Comparison of GMV and CT, and WMV between CD and HC 220
4.10.2 The association of GMV with age in CD patients and HCs 224
4.10.3 Comparison of GMV and CT, and WMV in CD patients with and without pain 225

4.10.4 Comparison of GMV and CT, and WMV in CD patients with and without EIM 226
4.10.5 Correlation of GMV and CT, and WMV with IBD fatigue scores 227
4.10.6 Comparison of GMV and CT, and WMV ileal and colonic CD and their relationship with fasting gut peptides 228
4.11 Conclusion 229
5 Resting-state fMRI functional connectivity and its alteration in CD 231
5.1 Background 232
5.2 Different RSNs and their behavioural interpretation 234
5.3 RSFC analysis techniques 237
5.3.1 Seed based method 237
5.3.2 Graph theory method 238
5.3.3 ICA 238
5.4 RSFC in healthy subjects 242
5.4.1 The association of age and RSFC 242
5.4.2 Gender-specific differences in RSFC 242
5.4.3 RSFC in fasting and fed states 243
5.5 RFFC alterations in CD 247
5.6 Methods 254
5.6.1 Imaging protocol 254
5.6.2 Pre-processing 255
5.6.3 ICA analysis 256
5.6.4 Group ICA with dual regression 258
5.7 Results 260
5.7.1 Recruitment 260
5.7.2 Participant demographics 261
5.7.3 Comparison of RSFC between CD patients and HCs using a CD and HC network template in dual regression 262
5.7.4 Correlation of pain scores, fatigue scores, disease duration and fasting GLP-1 and PYY in CD patients 264
5.7.5 Comparison of RSFC between CD patients and HCs using HC RSNs as a network template in dual regression 267
5.7.6 Comparison of results between the two dual regression approaches 270
5.8 Discussion 271
5.8.1 Comparison of RSFC between active CD patients and HC 272

5.8.2 Correlation of pain scores, fatigue scores, disease duration and fasting GLP-1 and PYY in CD patients 276
5.9 Conclusion 279
6 Conclusion 280
6.1 Postprandial EEC peptides and BOLD responses in response to the C12 fatty acid test meal 282
6.2 Eating behaviour in active CD 284
6.3 Altered brain structure in CD 285
6.4 Altered RSFC in active CD 286
6.5 Limitations of the study 287
6.6 Future Directions 288
7 References 291
8 Appendix 315

Abstract

Reduced appetite has been observed in patients with ileal Crohn's disease, which has been attributed to the upregulation of enteroendocrine cells and the consequent increase of satiety hormones secretion, therefore possibly negatively affecting appetite signalling to the central nervous system. The specific hypotheses to be tested in this thesis were that Crohn's disease patients with ileal inflammation, when compared with Crohn's disease patients with colonic inflammation and healthy controls, will show A) an alteration in brain-gut stimulation, B) an increase in the postprandial plasma enteroendocrine peptides response (CCK, GLP-1 and PYY) with associated alteration in appetite scores, C) a change in eating behaviour, and D) an alteration in brain structure and resting-state functional connectivity.

Ileal Crohn's disease patients showed greater fasting GLP-1 concentrations compared with healthy controls. No difference was found between ileal and colonic Crohn's disease patients in the fasting and postprandial concentrations of GLP-1, CCK and PYY. The ileal Crohn's disease patients showed a greater postprandial decrease in neuronal activity in the right superior frontal gyrus in the default mode network in response to saline compared with the fat meal. The mechanism underlying this phenomenon is unclear and requires further investigation. Greater neuronal activity was found in areas including the cerebellum, hippocampus, posterior cingulate gyrus, middle temporal gyrus, thalamus and medulla in response to fat, which is in line with the previous literature. The fat induced greater activity of the posterior cingulate gyrus, was driven by Crohn's disease patients, with colonic Crohn's disease patients showing stronger activation in this region compared with the ileal Crohn's disease patients. This finding may be linked with abdominal pain or GLP-1 elevations, which remains to be investigated. Stronger hedonic control of food intake was observed in the ileal CD patients compared with healthy controls, based on their explicit wanting/liking appeal bias for high-fat foods, however, this was not translated into actual increased calorie

intake, perhaps because of fear of triggering or worsening symptoms. Ileal CD patients also exhibited greater impulsivity compared with colonic CD patients. These findings indicate that eating behaviour in ileal Crohn's disease patients is likely to be impulse and reward-driven to alleviate symptoms such as low mood, abdominal pain and chronic fatigue. Therefore, a complex interplay of gut peptides, psychological factors, disease-related symptoms, inflammatory burden may ultimately guide eating behaviour in ileal CD patients.

Grey matter and white matter volume atrophy and cortical thinning were found in active Crohn's disease patients in regions such as the precentral gyrus (motor cortex) and the postcentral gyrus. The relative atrophy of the motor cortex could be a possible central cause of fatigue in Crohn's disease patients. Alterations were found in the resting-state functional connectivity between Crohn's disease patients and healthy controls in the networks implicated in cognition, attention, emotion and pain. These findings may reflect neuroplasticity effects in response to chronic inflammation and disease symptoms such as abdominal pain and fatigue.

This work was carried out between June 2015 and September 2019 at the National Institute of Health Research, Nottingham Biomedical Research Centre at the Queens Medical Centre Campus and the Sir Peter Mansfield Imaging Centre Nottingham. All work described in this thesis was performed by the author, except where indicated.

Acknowledgements

I would like to take this opportunity to thank everyone who has helped in producing the collaborative work forming this thesis.

Firstly, I would like to thank BROAD foundation for generously funding this work. The BROAD foundation's mission is to better understand the aetiology of inflammatory bowel disease and to enable the development of treatments and clinical management strategies for inflammatory bowel disease patients. It goes without saying that this study would not be possible without the participation of patients, who gave up their time to advance our knowledge of Crohn's disease.

I gratefully acknowledge the funding received towards my PhD from the Medical Research Council (MRC). I have carried out this research under the supervision of Dr Gordan Moran and Professor Sue Francis, who have given me endless support, guidance and encouragement, for which I am truly grateful. I would like to give a special thanks to Dr Sally Eldeghaidy for her guidance, mentorship and support. It was a privilege to be part of a multidisciplinary team, all of whom contributed to this work, including Shellie Radford and Adam Novak who had the challenging task of recruiting Crohn's disease patients. I am grateful to Jan, Mehri and Chris at the Sir Peter Mansfield imaging centre (SPMIC) for scanning the study participants. This work was supported by staff at the Biomedical Research Centre (BRC), Nottingham Digestive Disease Centre (NDDC) office and SPMIC who were always so helpful and kind. Many thanks to Melanie, Yirga, Davor, Gulzar and Lissa for analysing the blood data. Thanks to Prof Jens Rehfeld from the University of Copenhagen for his collaboration in

analysing CCK. Thanks to all my fellow PhD students at the NDDC and SPMIC for all the wonderful memories.

This project included collaborations with Dr Michelle Dalton and Dr Graham Finlayson at the University of Leeds. Thanks to Michelle who analysed the computer-based eating behaviour tasks. Also, thanks to David Planes from the University of Murcia for helping me with the questionnaire analysis.

Finally, I would like to thank my wonderful parents and brother for their love, support and motivation throughout my education and life.

List of Abbreviations

AC - Anterior commissure

ACC - Anterior cingulate cortex

ALFF - Amplitude of low-frequency fluctuations

Anti-TNF - Anti-tumour necrosis factor

AP - Area postrema

ARC - Arcuate nucleus

ASL - Arterial spin labelling

AUC - Area under the curve

BBB - Blood brain barrier

BOLD - Blood oxygenation level dependent

CAT12 - Computational anatomy toolbox

CBF - Cerebral blood flow

CBV - Cerebral blood volume

CCK - Cholecystokinin

CD - Crohn's disease

CgA – Chromagranin A

CHO – Carbohydrate

CoEQ - Control of eating questionnaire

CRP – C-reactive protein

CS – Central surface

CSF – Cerebrospinal fluid

CSS – Composite satiety score

CT – Cortical thickness

DAN – Dorsal attention network

DC – Dendritic cells

DMN – Default mode network

DTI – Diffusion tensor imaging

ECN – Executive control network

EEC – Enteroendocrine cells

EIM – Extraintestinal manifestation

ELISA – Enzyme linked immunosorbent assay

FC – Functional connectivity

FCP – Faecal calprotectin

FDR – False discovery rate

FFQ – Food frequency questionnaire

FFX – Fixed effects analysis

fMRI – Functional magnetic resonance imaging

FPN – Frontal parietal network

FWE- Family wise error

FWHM – Full width half maximum

GE-EPI – Gradient echo-echo planar imaging

GI – Glycaemic index

GIP – Glucose dependent insulinotropic peptide

GLM – General linear model

GLP-1 – Glucagon like peptide -1

GM – Grey matter

GMV – Grey matter volume

HADS- Hospital anxiety depression scores

HBI – Harvey Bradshaw index

HC – Healthy control

HFSA – High fat savoury

HFSW – High fat sweet

HRF – Haemodynamic response function

HRP – Horse radish peroxidase

IBD – Inflammatory bowel disease

IC – Independent component

ICA – Independent component analysis

IG – Intragastric

IL-1β – Interleukin-1 beta

IL-6 – Interleukin-6

ImpSS – Impulsive sensation seeking

LB – Large bowel

LFPQ – Leeds food frequency questionnaire

LFSA – Low fat savoury

LFSW – Low fat sweet

MCC – Midcingulate cortex

MD – Mean diffusivity

ME – Median eminence

MHC – Major histocompatibility complex

MNI – Montreal Neurological Institute

MPRAGE – Magnetization prepared rapid gradient echo

MRE – Magnetic resonance enterography

MRI – Magnetic resonance imaging

NF-kB – Nuclear factor kappa light chain enhancer of activated B cells

NgN-3 – Neurogenin-3

NIHR – National institute of health research

NOD2- Nucleotide-binding oligomerization domain-containing 2

NPY/AgRP – Neuropeptide/Agouti related peptide

NPY – Neuropeptide Y

NRES – National research ethics service

NTS – Nucleus tractus solitarius

OFC – Orbitofrontal cortex

PBS – Phosphate buffer solution

PBT – Projection based thickness

PC – Posterior commissure

PCC – Posterior cingulate cortex

PCG – Posterior cingulate gyrus

PE – Parametric estimates

PFC – Prefrontal cortex

PFS – Power of food scale

PHG – Parahippocampal gyrus

Phox2b – Paired like homeobox 2b

POMC/CART – Pro-opiomelanocortin/Cocaine and amphetamine regulated transcript

PYY – Peptide YY

QDEC – Query Design Estimate Contrast

QoL – Quality of life

ReHo – Regional homogeneity

RFX – Random effects analysis

RIA – Radioimmunoassay

ROI – Region of interest

RPS – Resting pre-stimulus state

RSFC – Resting state functional connectivity

RSFG – Right superior frontal gyrus

RS-fMRI – Resting state functional Magnetic Resonance Imaging

RSN – Resting state network

RYGB – Rous-en-Y gastric bypass

SB – Small bowel

SBA – Surface based analysis

SBCE – Small bowel capsule endoscopy

SCFA – Short chain fatty acid

SMA – Supplementary motor area

SN – Substantia nigra

SNP – Single nucleotide polymorphism

SNR -signal to noise ratio

SPM – Statistical Parametric Mapping

SPMIC – Sir Peter Mansfield Magnetic Resonance Imaging Centre

SQ – Satiety quotient

SS- Structural scan

T2DM – Type 2 diabetes

TA – acquisition time

TE – echo time

TFCE – Threshold free cluster enhancement

TFEQ – Three factor eating questionnaire

TIV – Total intracranial volume

TMB – Tetramethylbenzidine

TR – repetition time

Ube4A – Ubiquitination

UC- Ulcerative colitis

VAS – Visual Analogue Scale

VBA – Volume based analysis

VBM -Voxel based morphometry

VF – Verbal fluency

VTA – Ventral tegmental area

WM – White matter

WMD – White matter distance

WMV – White matter volume

1 **Literature Review**

1.1 Crohn's disease (CD)

Crohn's Disease (CD) is a chronic, relapsing systemic inflammatory disease, primarily affecting the gastrointestinal tract. CD may have a pan-enteric distribution and predominantly affects the distal ileum and colon[1]. About 60% of small bowel (SB) CD cases are localised in the terminal ileum. CD is characterised by skip lesions and transmural inflammation whereby the full thickness of the intestinal wall is inflamed[2,3].

1.2 Public health Relevance

CD is most commonly presented in adolescence and young adulthood, with 30 years of age being the median age of diagnosis[4]. However, with the rise in the ageing population, the elderly onset of CD is also becoming more common[5].

In Europe, the prevalence of CD is 322 per 100,000 persons and in North America is 319 per 100,000 persons[6]. Similarly, the annual incidence of CD was found to be 12.7 per 100,000 person-years in Europe, 5.0 person-years in Asia and the Middle East and 20.2 per 100,000 person-years in North America[6]. The rising incidence of CD and the lack of cure has led to significant cost implications particularly in relation to treating and managing complications. For instance, in 2010 the estimated cost attributed to inflammatory bowel disease (IBD) treatment was £1 billion, where the annual cost for any CD patient was approximately £6156.44[7].

1.3 Environmental risk factors for CD development

A number of environmental risk factors are thought to be involved in the development of CD such as westernised lifestyle, Helicobacter pylori[89]. People emigrating from countries of low CD prevalence to countries with higher prevalence are at an increased risk of developing CD. The migrant populations from South Asia, Africa, and South America have presented with IBD in their adopted western countries, indicating a potential genetic and environmental interaction leading to high CD and UC susceptibility[10]. Epidemiological data have shown that Helicobacter pylori infection may exert a protective effect on IBD development[11]. Smoking has been associated with increased risk of CD[12]. It has been postulated that prolonged use of oestrogen containing oral contraceptive pills increase the risk of CD development and this risk reverts back to normal when discontinued[13]. Also, childhood antibiotic exposure has been positively linked with increased risk of CD development[14].

1.4 Aetiology and Pathophysiology

The aetiology of CD is still not fully understood. Epigenetic factors and altered immune response to intestinal microbiota in genetically susceptible individuals are thought to be involved in the pathogenesis of CD[15]. Twin studies have demonstrated 30.3 % concordance in monozygotic twins compared with 3.6% in dizygotic twins, which suggests that there is a genetic component to CD heritability[16]. Furthermore, genome-wide association studies have identified 143 susceptibility loci associated with CD[17]. Amongst all of these genes, polymorphisms in the ligand recognition domain of the Nucleotide-binding

oligomerization domain–containing-2 (NOD2) receptor and single nucleotide polymorphism (SNP) in the autophagy gene ATG16L has been strongly linked to increased susceptibility to CD[18,19]. Dendritic cells (DC) with the CD variant of NOD2 gene show impaired autophagic induction, evidenced by reduced localization of bacteria in autophagolysosomes[20]. Presence of T300A variant makes ATG16l1 protein more susceptible to caspase-3 proteolytic degradation resulting in increased cellular stress and increased apoptotic stimuli and impairment in the autophagy pathway[21]. Impairment in the autophagic process leads to incomplete destruction of bacterial fragments and inadequate generation of major histocompatibility complex (MHC) class II antigen-specific CD4+ T cell responses in DCs resulting in a persistence of bacterial fragments that could act as a constant stimulus on other pattern recognition receptors contributing to the overproduction of pro-inflammatory cytokines[20,22]. The bacterial persistence gives mechanistic insight into the secondary inflammatory responses of CD. Additionally, CD mutant NOD2 located in mucosal cells shows impaired activation of the nuclear factor kappa-light-chain-enhancer of activated B cells (NF-κB) signalling pathway, resulting in altered cell function through reduced expression of α defensins[23]. Defensins are secreted to protect the integrity of the mucosal layer; with the reduced defensins level compromising the permeability of the mucosal layer allowing unwanted and pathogenic bacteria to invade the epithelial mucosal layer leading to severe symptoms[24]. Impairment in autophagic induction, bacterial factors and impaired antigen presentation and intestinal membrane permeability play a role in the pathogenesis of CD.

1.5 Disease Classification

The Montreal classification of CD based on age onset (A) and disease location (L) and disease behaviour (B) is described in **Table 1**[25]. Figure 1 shows the different phenotypes of CD

Montreal classification of CD		
Age at diagnosis (A)	**Disease location (L)***	**Disease Behaviour (B)**
A1 16 years or younger	L1 Terminal ileum	B1nonstricturing nonpenetrating
A2 17-40 years	L2 Colon	B2 stricturing
A3 over40 years	L3 Ileocolon	B3 penetrating
	L4 Upper gastrointestinal tract	

Table 1 Summary of Montreal CD classification

*** A perianal disease modifier may be added in the presence of perianal fistulas.**

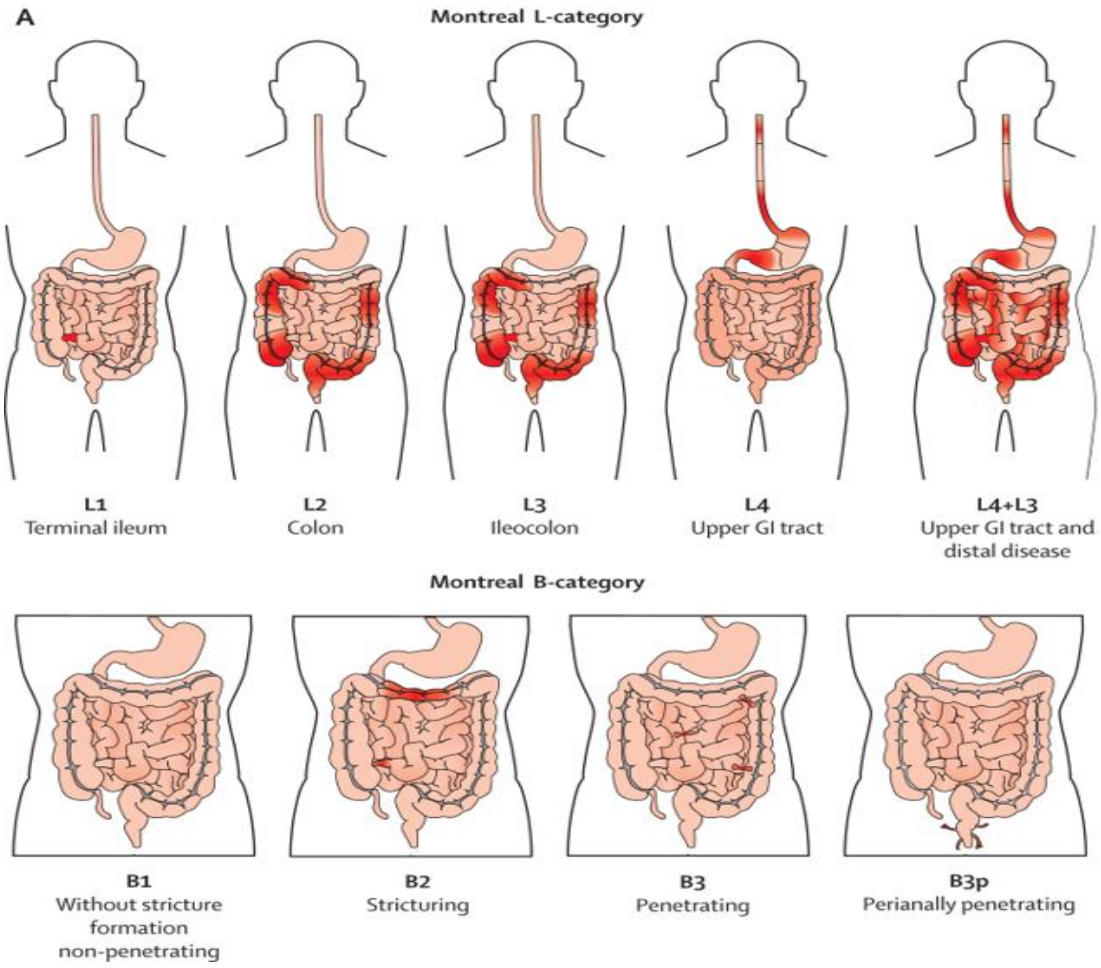


Figure 1 shows the various phenotype of CD[26]

1.6 Diagnosis

Extensive investigations are required to confirm CD diagnosis because the symptoms presented in CD can be non-specific and shared with other gastrointestinal disorders. A combination of clinical presentation, endoscopic appearance, radiological, histological, biochemical and serological tests are performed to establish a diagnosis [3]. CD patients are most commonly diagnosed with anaemia, high white cell count, thrombocytosis and increased pro-inflammatory markers [3]. Full blood count test is carried out to test for anaemia and thrombocytosis, also C-reactive protein (CRP), an acute-phase protein synthesized by the liver is assessed as a surrogate measure for acute phase

inflammation. Stool samples are used to test for faecal calprotectin (FCP) level, as a biomarker of gut inflammation and *Clostridium difficile* to rule out infectious diarrhoea[3]. FCP has been commonly used as a marker of disease activity and predictor of relapse in CD. However, FCP is found to be less sensitive as a predictor of relapse risk in patients with ileal CD relative to colonic CD in remission[27].

Different imaging techniques are used in the diagnosis and evaluation of disease severity and to assess potential complications of CD. A colonoscopy is considered to be the gold standard investigation, as an endoscopic examination allows for closer inspection of the intestinal mucosa and obtain histological samples for the microscopic analysis of the disease[3]. However, colonoscopy is less useful in the diagnosis of ileal disease compared to colonic disease due to difficulties in accessing the proximal region of the bowel[3]. Small bowel capsule endoscopy (SBCE) is a highly sensitive technique useful for detecting small bowel disease, but SBCE is not easily available and results may be biased due to inter-observer variability, moreover, SBCE cannot be used to investigate extraluminal disease extent[28]. Additionally, magnetic resonance imaging (MRI) and computed tomography have been extensively used because of their accuracy in detecting SB inflammatory lesions[3].

1.7 Complications of CD

CD has a negative impact on patient's quality of life (QoL) and psychological wellbeing. The embarrassing symptoms, active flare-ups and frequent hospitalisations can negatively impact on social life, education, employment and insurance[2]. In young people, CD may impair growth and sexual development. Iatrogenic factors such as steroids, immunosuppressants and surgery could even

lead to impotence or intestinal failure in some cases[2]. Other complications include the formation of abscesses and fistulas in perianal skin, bladder and genital area[2]. Due to the systemic nature of inflammation, CD also causes several extraintestinal manifestations (EIM) such as iritis, arthritis, pyoderma gangrenosum and erythema nodosum[2]. CD patients are at higher risk of developing colorectal and SB cancers[29].

1.8 Symptoms

Symptoms observed in CD depend on factors such as the severity of the disease, location, behaviour and EIM of the disease[26]. Extraintestinal symptoms are also observed in some CD patients, involving the skin, eyes, joints, liver, biliary tract, kidneys and bones indicating the systemic nature of inflammation[26]. For example, colonic distribution of the disease presents with chronic diarrhoea and rectal bleeding, whereas patients with SB CD tend to present with a change in bowel habits, abdominal pain and other obstructive symptoms[26]. Such a presentation is not exclusive, and patients may present with a variety of symptoms. Other common symptoms of CD include fatigue, loss of appetite, malnutrition, mouth ulcers and fever [3].

1.9 Management and medication

The principles of CD management is based on the severity, the site and behaviour of the disease[3]. Nutritional supplementation, smoking cessation, drug therapy and surgery in severe cases of stricturing and penetrating disease are the options applied in the clinical management of CD[30]. Calcium and vitamin D supplements are recommended to prevent the risk of fractures and osteoporosis[26]. Smoking cessation is strongly recommended as it is known to

reduce the risk of relapse by 65% relative to patients that continue to smoke, therefore patients are encouraged to quit smoking through the provision of counselling services and nicotine replacement therapy[26]. A number of drugs are commonly prescribed for the induction and maintenance of remission such as corticosteroids, immunosuppressants (azathioprine, mercaptopurine and methotrexate) or anti- tumour necrosis factor α (anti-TNFα) therapy such as infliximab and adalimumab[3]. Other drugs include antibiotics, and antibodies $\alpha_4\beta_7$ integrins on migrating T lymphocytes[31]. Despite the medical and nutritional interventions some patients will eventually require surgery, to mitigate symptoms and complications. Only 10% of CD patients achieve long term clinical remission whereas majority of patients undergo surgery[32]. Risk of surgery 5 years after CD diagnosis was found to be 33.3% and after 10 years was 46.7%, demonstrating that maybe the risk of surgery has decreased over the last decades[33].

1.10 The role of enteroendocrine cells (EEC) in the control of appetite

Appetite can be described as the "the internal driving force for the search, choice and ingestion of food"[34]. The intake of food results in satiation that decreases the drive to eat thereby terminating the eating episode which leads to a feeling of satiety that inhibits hunger and determines the quantity of food consumed at the next eating episode[35]. Food intake is governed by complex neurohormonal appetite networks involving homeostatic and hedonic factors. Reduced food intake due to appetite loss is one of the major causes of undernutrition in CD patients[36].

1.10.1 EEC

The enteroendocrine gut-brain axis plays a critical role in the homeostatic regulation of appetite. The enteroendocrine system is the largest endocrine organ in the human body and it is made up of EEC[37]. EEC is found distributed as single cells throughout the intestinal tract and are located within intestinal crypts and villi and represents 1% of the epithelial cells[37]. Gastrin, ghrelin, somatostatin, cholecystokinin (CCK), glucose-dependent insulinotropic peptide (GIP), glucagon-like peptide (GLP-1) and peptide YY (PYY) are some of the regulatory peptides secreted by the EEC[38]. Some of the EEC peptides more relevant to this thesis has been described in detail in section **1.10.2**

EEC act as sensors of the nutrient contents of the lumen and secrete peptides and amines that regulate postprandial gut secretion and motility[39]. The EEC peptides act on vagal afferents in the gastrointestinal tract directly relaying to sites in the central nervous system that regulate ingestive behaviour[40].

1.10.2 The role of EEC peptides in the control of appetite

Several appetite regulatory hormones are secreted from the gut which enhances or suppress appetite as shown in **Table 2**. For example, ghrelin is secreted by the stomach and enhances appetite[41] whereas CCK, PYY and GLP-1 suppress appetite [42].

	Hormone	**Site of secretion**	**Major receptors**	**Major actions**
Anorectic	PYY	Gastrointestinal L cells (distal ileum)	Y2	Delays gastric emptying Vagal and CNS effects
	GLP-1	Gastrointestinal L cells	GLP-1	Glucose-dependent insulin release Delays gastric emptying CNS effects
	CCK	Intestinal I cells (duodenum and jejunum) some numbers in the ileum	CCK 2	Gall bladder contraction Delays gastric emptying Pancreatic enzyme secretion
Orexigenic	Ghrelin	Gastric fundal A cells	GHS-R	Increases gastric motility Growth hormone release

Table 2 Summary of some gut hormones and their major actions

1.10.2.1 CCK

CCK is one of the first endogenous gut hormones documented to affect appetite and a neuropeptide that is abundantly found in the CNS[43]. CCK is synthesized and released from the I cells of the proximal duodenum and jejunum in response to luminal content particularly protein and fat[44]. It has a short half-life of 1-2

minutes (i.e. rapidly deactivated after release). It has been found that only long-chain fatty acids of chain length C12 can stimulate I cells to release CCK[45] via G- protein-coupled receptor 40[46]. CCK exerts its effects via receptors CCK-1 and CCK-2. CCK-1 is found in the gastrointestinal tract and CCK-2 is expressed in the CNS[35]. CCK binds to its CCK-1 receptor on the sensory terminals of the vagus nerve relaying satiety signals to the arcuate nucleus (ARC) in the hypothalamus and vagotomy has shown to remove this effect[47] Peripheral administration of CCK is shown to reduce appetite and decrease meal size in rodents and humans[48]. Furthermore, the CCK-1 receptor knockout rat model has shown to increase food intake and develop an obese phenotype, which was attributed to the overexpression of neuropeptide Y (NPY)[49]. These findings indicate the role of CCK in the regulation of food intake. Moreover, a high dose of intravenous administration of CCK has shown to cause nausea and abdominal discomfort which would also contribute to the reduction in food intake[50].

CCK levels rise over 10-30 minutes after food ingestion and act to stimulate gall bladder contraction, pancreatic secretions and delay gastric emptying which collectively contributes to the feeling of fullness, and satiety[51]. Central administration of CCK via intracerebroventricular injection CCK agonists have shown a reduction in food intake[52]. However, the central administration of CCK with leptin has shown to induce weight loss indicating CCK role in the central regulation of appetite [53].

1.10.2.2 GLP-1

GLP-1 is released from the L cells in the distal small intestine and proximal colon proportionately to ingested calories[43]. GLP-1 is released rapidly into the

circulation with a biphasic response to food intake mainly carbohydrates (CHO). It is released 10-15 minutes postprandially and again peaks after 30-60 minutes[35]. The initial release of GLP-1 is vagally mediated[54], or due to stimulation of GLP-1/GIP co-expressing K cells. The later release of GLP-1 is due to direct stimulation of ileal L cells[55].

Studies have shown that peripheral and central administration of GLP-1 and GLP-1 receptor agonists exendin-4 reduced food intake in rodents[56]. It has been found that the GLP-1 receptors in the CNS rather than vagus nerve contributed to the complete anorectic response to the GLP-1 agonist liraglutide, suggesting that GLP-1 receptors in the CNS are involved in weight loss[57]. It has been postulated that GLP-1 signals converge on the Nucleus Tractus Solitarius (NTS) and in the area postrema (AP) and directly activates Pro-opiomelanocortin/Cocaine- and amphetamine-regulated transcript (POMC/CART) and indirectly inhibits the NPY/ Agouti-related peptide (NPY/AgRP) via GABAergic transmission to reduce food intake[58]. Moreover, it has been shown in animal models, that fluorescently labelled liraglutide penetrates the brain activating GLP-1 receptor-expressing neurons in the ARC to induce weight loss[59].

The GLP-1 analogue liraglutide has been found to alter brain activity in response to highly palatable food cues in Type 2 diabetic patients (T2DM)[60]. This finding is in agreement with another study that showed liraglutide improved hypo responsiveness to palatable food in obese T2DM patients relative to lean healthy individuals indicating the role of GLP-1 in the hedonic control of food intake[61]. GLP-1 is also an incretin hormone that stimulates insulin biosynthesis by acting on pancreatic β cell receptors in response to glucose load and regulates glucose

homeostasis[48]. GLP-1 also exerts its satiating effects via ileal brake a feedback mechanism where distal intestinal signals inhibit proximal gastrointestinal motility and gastric emptying[51]. Furthermore, the presence of GLP-1 receptors in the (AP) has been linked to nausea and vomiting side effects of GLP-1 analogues, as the AP is thought to be involved in the regulation of symptoms like nausea which has a negative impact on food intake[62].

1.10.2.3 PYY

PYY synthesized and released from the L cells in the ileum and colon in response to food intake especially fat and fermentable CHO[43]. PYY concentrations are low in a fasting state and rise postprandially, in proportion to the energy intake signalling the appetite-regulating circuits to subsequently reduce food intake[63]. As with GLP-1, PYY also shows a biphasic response with levels rising within 30 mins after meal intake[64]. The early increase in PYY is CCK mediated[65] while the later increase is due to direct nutrient stimulation of the L cells in the ileum[66].

PYY binds to G protein receptors Y1 and Y2[35] and exerts its anorectic effects by acting on the Y2 receptor, as evidenced by the inhibition of food intake in response to Y2 agonist[67] and this effect being dampened by Y2 antagonist[68]. Y2R is expressed on both NPY and (AGRP) neurons in the hypothalamus and induces its anorectic effects by inhibiting NPY/ARGP neurons via Y2R thereby activating the appetite-suppressing POMC neurons which are inhibited by NPY/AGRP neurons[69]. Furthermore, Y2R is also expressed by the vagal afferent terminals, it has been shown in murine models that the peripheral administration of PYY induced anorectic effects via the arcuate neuronal activation and this effect was abolished by vagotomy or transection of hindbrain-hypothalamic

pathways[70]. In addition to PYY's direct central effect on appetite, PYY also modulates gut motility via ileal brake, through delay in gastric emptying and gastrointestinal transit time[71] resulting in a sensation of fullness and satiety[63]. It has also been reported that supraphysiological intravenous infusions of PYY induced nausea in humans, thereby having a negative impact on food intake[72].

1.10.2.4 Interactions between multiple EEC peptides

The aforementioned gut peptides bind to their respective receptors at the vagus nerve fibre terminals, where the vagal afferent discharge is suppressed in the presence of appetite stimulator ghrelin and is increased for appetite-suppressing peptides CCK, PYY and GLP-1[41].

It is important to note that, multiple receptors are co-expressed on one cell body in the vagus nerve, and their stimulation can have an additive, synergistic or antagonistic effect on food intake[73]. *In vivo* and *in vitro* experiments have shown that CCK and leptin have a combined additive effect on appetite suppression relative to CCK treatment on its own[74]. CCK promotes the translocation of early growth response -1 transcription factor into the nucleus that upregulates the expression of appetite-suppressing CART[74]. Additionally, leptin upregulates EGR1 expression, thereby synergistically suppressing appetite with CCK. In contrast, ghrelin inhibits the actions of both CCK and leptin with respect to EGR-1 nuclear localisation and upregulation, consequently enhancing appetite[74]. GLP-1 and PYY are expressed in the intestinal L cells, where the postprandial increase in PYY and GLP-1 was found to be correlated indicating that the hormones are possibly complementary, therefore co-localized within the same cell[66].

1.11 Physiology of appetite regulation

Appetite regulation starts with the cephalic phase whereby the anticipation and exposure to food stimulate pre-absorptive physiological responses to external cues such as sight, smell, thought of food, location and time of the day[75]. Cephalic phase responses prepare the gastrointestinal tract for the arrival of food and digestion/absorption of nutrients[76]. Food induced stretching of the stomach muscle wall signals through the gastric mechanoreceptors and activate the vagus nerve. The vagus nerve is the 10th cranial nerve that sends signals from the digestive tract to the central nervous system. The vagus nerve is made up of both afferent fibres (visceral sensory nerve) and efferent fibres (motor nerves)[77]. Peripheral vagal afferent fibres are scattered along the mucosal and submucosal layers of the digestive tract and send signals from appetite regulatory gut peptides to the central nervous system through the NTS [78].

1.12 Gut-brain axis

Appetite regulation involves complex interactions of homeostatic and hedonic factors. Hypothalamus is central in the homeostatic control of food intake and other neural circuits integrate environmental and emotional cues to constitute the hedonic drive of appetite regulation. The ARC of the hypothalamus plays a pivotal role in the integration of signals regulating appetite. Due to the presence of a relatively leaky blood-brain barrier (BBB) and the ARC proximity to the median eminence (ME), circulating peripheral hormonal signals have relatively greater access to receptors in the ARC than other brain areas[79]. ARC comprises of neurons that integrate signals of nutritional status and energy expenditure. Neurons that express (POMC) and (CART) are anorexigenic that decrease appetite and increase energy expenditure. Neurons that express (AgRP) and

(NPY) increase appetite and decrease energy expenditure[80]. Peripheral hormonal signals act in the hypothalamus to inhibit or activate ARC neurons to alter appetite. Furthermore, ARC neurons also communicate with other orexigenic and anorexigenic neurons in other nuclei of the hypothalamus to regulate food intake[81]

1.13 Hedonic control of food intake

Overeating is thought to be driven by the hedonic desire for food, perpetuated by easy access and availability of cheap, highly palatable, energy-dense foods [82]. Food intake is a rewarding and pleasurable experience that activates the reward pathways of the brain. These reward pathways comprise of the dopaminergic neurons that originate in the ventral tegmental area (VTA) and *substantia nigra* (SN) in the midbrain with neuronal projections throughout the brain. Dopaminergic signals are received and integrated into the *nucleus accumbens*, striatum and orbitofrontal cortex (OFC), these regions are activated in response to food cues and ingestion during fMRI scans in humans[83]. It is thought that the homeostatic and hedonic systems are integrated via the lateral hypothalamic area[84] and through its projections regulate the VTA and brainstem nuclei such as the NTS, which is pivotal in the modulation of gut hormones and satiety signals[85].

In addition to acting as homeostatic appetite regulatory signals, CCK, GLP-1 and PYY also stimulate the reward circuitry either directly or through projections from the hypothalamus and brainstem nuclei such as the NTS[82]. It has been shown that GLP-1 concentration correlates with increased cerebral blood flow (CBF) in the dorsolateral prefrontal cortex (PFC) which has been implicated in satiation and inhibition control[86]. Inhibition control has been closely linked to

impulsivity traits which may negatively influence self-regulation of food intake. For example, laboratory tests of impulsivity have shown that obese adults[87] and children [88] display higher impulsivity which relates to higher energy intake, weight gain and poorer compliance to treatments and interventions[88]. This suggests that non-homeostatic control of food intake also involves factors such as memory, learning, executive behaviours and their interaction with the neurohormonal network. Also, PYY has found to activate the left caudolateral OFC which predicts subsequent feeding behaviour[89].

1.14 Appetite dysregulation

Appetite dysregulation is a phenomenon observed in different pathologies. For example, following Roux-en-Y gastric bypass (RYGB) surgery fasting obese patients have lower activation in the brain reward regions such as the OFC, amygdala, caudate nucleus, nucleus accumbens and hippocampus in response to viewing pictures of high calorie and palatable foods resulting in a lower appeal for these foods[90]. Moreover, an increase in plasma PYY and GLP-1 levels were reported following a high energy palatable test meal in patients that underwent (RYGB) relative to patients with gastric banding surgery and BMI matched controls[90]. It has also been shown that octreotide (somatostatin analogue) suppresses postprandial PYY and GLP-1 after RYGB. The reduction in plasma PYY and GLP-1 with octreotide positively correlated with an increase in BOLD signal in the brain reward system. These findings suggest that alteration in the anatomy and physiology of the gut and the enhanced satiety gut hormones alters the regulation of the reward-based eating behaviour in obese individuals[91].

Lower activation of the reward-based centres of the brain are commonly observed in the fed state[92] and in a fasted state the reward-based centres are in

favour of high-calorie food[93]. Obese T2DM patients show lower activation in the insula (one of the reward centres) compared to healthy lean individuals after the consumption of highly palatable chocolate milk. However, after treatment with GLP-1 receptor agonists liraglutide, there was increased activation in the insula and caudate nucleus in response to chocolate milk suggesting that palatable food intake may be increased to compensate for the under stimulation of reward areas [61].

Reduced appetite has been observed in ileal CD patients, which has been attributed to the upregulation of EEC and the consequent increase of satiety hormones secretion, therefore possibly negatively affecting appetite signalling to the CNS[94–96] as described in detail in section **2.5** of this thesis

Specific hypotheses to be tested in this thesis were that ileal CD patients, when compared with colonic CD patients and healthy controls (HC) s, will show A) an alteration in brain-gut stimulation, B) an increase in the postprandial plasma EEC peptides response (CCK, GLP-1 and PYY) with associated appetite scores, C) a change in eating behaviour, and D) an altered brain structure and resting-state functional connectivity (RSFC).

The overall purpose of the study is to investigate the role of the gut-brain axis and the EEC pathways in the control of food intake using MRI. The primary objective of this thesis was to compare the relevant changes in measures of brain activity following the C12 fatty acid test meal between ileal and colonic CD and age-, BMI- and gender-matched HCs. The secondary objectives were to compare the following measures amongst the ileal and colonic CD groups and the HC cohorts:(i) the postprandial EEC hormones (CCK, GLP-1 and PYY) response

(ii) changes in appetite and eating behaviour (iii) fasting plasma levels of interleukin-1 β (IL-1β), interleukin -6 (IL-6) and TNFα (iii) structural and RSFC measures.

2 Investigation of altered appetite in CD using functional MRI

Malnutrition and appetite loss represent a major problem in the clinical management of CD. Reduced appetite observed in ileal CD has been attributed to the upregulation of EEC and the consequent increase of satiety hormones secretion, therefore possibly negatively affecting the appetite signalling to the CNS. The hypothesis of this chapter is that in ileal CD patients an elevated fasting and postprandial EEC peptide concentrations will be observed with differential postprandial CNS responses and appetite-related sensations based on the CD location.

2.1 Principles of functional MRI (fMRI)

Functional MRI (fMRI) is the most widely used method for mapping brain activity. This method typically uses the Blood Oxygenation Level Dependent (BOLD) contrast, which measures brain activity indirectly through the haemodynamic changes related to neural activation. The mechanism of BOLD contrast relies on the magnetic properties of the haemoglobin molecule. It was demonstrated by Pauling and Coryell[97] in 1936, that oxyhaemoglobin (oxygen bonded to haemoglobin) is diamagnetic, whereas deoxyhaemoglobin is paramagnetic. These haemodynamic MRI properties were investigated by Thulborn et al[98], who demonstrated that the transverse relaxation time (T_2*) of the blood relies strongly on its oxygenation state, with a decrease in blood oxygen levels resulting in a decrease in the T_2* relaxation time. This phenomenon was shown to be even more pronounced at high magnetic field strength[99]. The first animal experiment by Ogawa et al[100] using BOLD contrast

imaging on rat brains used a very high-resolution gradient echo sequence at high field strength (7 Tesla). They reported that the manipulation of the amount of oxygen in the rat's blood (a reduction in oxygen) led to signal loss in the blood and around the tissues surrounding the blood vessels throughout the cerebral cortex, this was described as the T_2* effect. This signal loss is now termed BOLD contrast. Following Ogawa's observations, BOLD contrast was successfully used to generate functional images of the human brain[101,102].

The magnetic susceptibility difference between blood and surrounding tissues has given rise to the widespread use of the BOLD endogenous contrast. Since oxygenated blood is diamagnetic, it exhibits similar magnetic properties to that of brain tissues, whereas paramagnetic deoxyhaemoglobin in blood vessels induces a susceptibility difference within and around the vessels[103,104].

When the brain is at rest, the deoxyhaemoglobin concentration in blood vessels is higher relative to the active state, resulting in local magnetic field distortions within and around these vessels. This local field distortion causes the spins to dephase, reducing the T_2 and T_2* signal in these regions[104]. Upon activation, blood flow increases the oxygen delivery to active brain regions, increasing the T_2 and T_2* signal, thereby reducing the susceptibility difference between the vessels and surrounding tissue. Hence, the MRI signals in active brain regions exhibit an increase in MR intensity with respect to inactive brain areas. This effect is observed using T_2*- and T_2-weighted sequences, gradient echo and spin echo schemes respectively[103,104]. Figure 2 shows the schematic representation of the haemodynamic changes which lead to a BOLD signal.

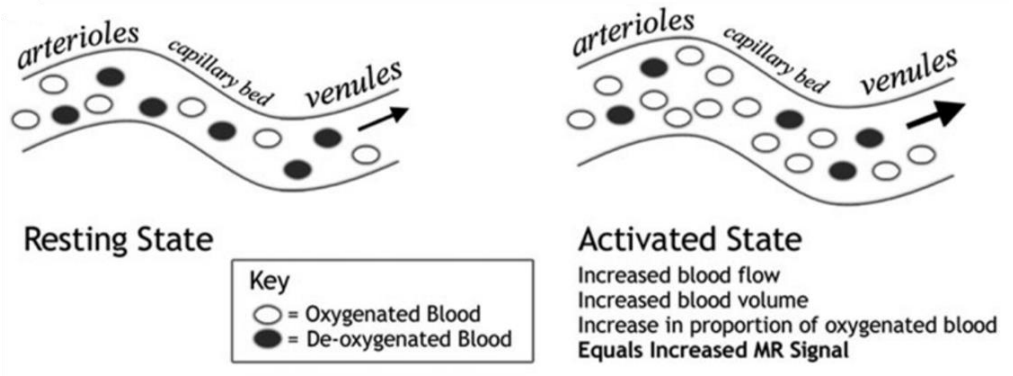


Figure 2 Schematic representation of the haemodynamic changes leading to a BOLD signal[104]

The changes observed in the BOLD signal originate within and around capillaries and veins, which are partially or significantly deoxygenated[105]. The BOLD signal depends on vessel size, shape, and orientation of the vessels with respect to the external magnetic field (B_0)[106]. For example, vessels oriented perpendicular to the static field show a large susceptibility difference, compared to those which are parallel that have little or no susceptibility difference[106].

2.1.1 The physiological basis of the BOLD effect

A complex interplay between CBF, cerebral blood volume (CBV) and cerebral metabolic rate of oxygen determines the BOLD signal. However, the mechanisms linking neural activity and the BOLD signal are complex and still not fully understood[107]. In response to a stimulus, neurons in a particular brain region begin to fire causing rapid neural activation, in turn causing vessel dilatation, increase in blood volume and blood flow to this region. Consequently, the oxygen supply in the capillary and veins increases along with oxygen consumption. However, an over-compensatory action occurs, where there is an increase in CBF, and thus, the supply of oxygenated blood, which increases to a level greater than that required by demand[104]. This results in a local increase in

blood oxygenation in active brain regions, leading to a local increase in the T_2/ T_2* relaxation time and thus a small, but detectable, increase in the MR image intensity termed the BOLD response[98]. The time course of the BOLD signal associated with the neural activity is known as the Haemodynamic Response Function (HRF). The HRF is characterised by 3 distinct phases: the initial dip, the positive peak, and the post-stimulus undershoot. It is thought that the initial dip takes place immediately after neural stimulation, this is found to be small in amplitude and to last for 1-2 seconds[108,109]. Its existence is still debatable, and it is thought to be reflective of an immediate increase in oxygen consumption in the capillary bed with close proximity to the site of neuronal activity[107]. This initial dip is followed by a large positive rise that peaks after approximately 6 seconds. This is the main feature of the HRF, which results from the increased CBV and CBF, leading to an oversupply of oxygenated blood, hence an increase in BOLD signal[107]. This positive BOLD signal change is the component typically assessed using BOLD fMRI and for strong stimuli can reach of the order of 3-5% at 3T[110]. The width of the peak and the shape of the HRF is proportional to the stimulus duration. After the end of the stimulus, the amplitude of the BOLD signal declines and displays a negative post-stimulus undershoot before returning to baseline, which may take approximately 30 seconds[107]. This post-stimulus undershoot is thought to arise from deoxygenated blood

concentration remaining elevated, due to a mismatch either between CBV and CBF or between CBV and oxygen consumption[111,112]

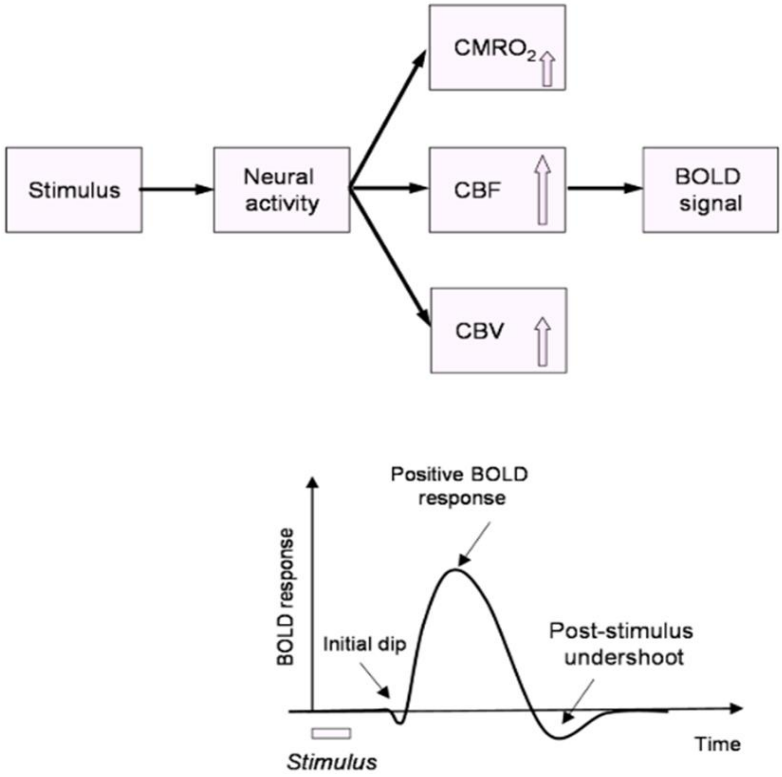


Figure 3 Physiological events that follow neuronal activation leading to a BOLD signal and the HRF [104].

2.1.2 Strengths and limitations of the BOLD contrast

BOLD-fMRI is a non-invasive technique, which can be repeatedly used. However, it only measures secondary blood flow and not direct neural activity. It is still in its early stages for clinical use and surgical planning in patients[104].

One of the major advantages of BOLD imaging is its high spatial resolution[104]. However, the BOLD signal originates from brain tissues, with varying sizes of blood vessels and dephasing effect around these vessels[107]. The micro and macrovascular haemodynamic activity of the tissues influences the neurovascular coupling relationship, which may mislead the exact site of the

neuronal activity which generates the BOLD signal. The spatial resolution typically used in BOLD-fMRI at 3T is 3 mm isotropic, whilst submillimetre resolution can be achieved using an ultra-high field (7T) scanner[99]. The main limitation of the BOLD technique arises from its vascular origin limiting its temporal resolution and quantitation[113,114]. Due to its vascular origin, the BOLD signal may be contaminated by the distribution of large veins, which may cover a significant fraction of the volume in a voxel, rather than the signal generated from the actual site of neural activity i.e. capillary bed and grey matter (GM)[107,115]. Further, the temporal resolution is the major limitation of this technique due to the inherent physiological changes associated with neural activity[115].

2.1.3 Functional MRI paradigm designs to study nutrition

During fMRI data acquisition, a set of BOLD images covering the whole brain (a brain volume) is taken every 2-3 seconds during the presentation of a stimulus[104]. To increase the sensitivity of brain areas activated by the stimuli, hundreds of brain volumes are collected during many repeats of a stimulus, making fMRI paradigms typically last 10-20 mins. Due to the difficulty in detecting the low BOLD signal changes in the presence of background physiological noise signals and fluctuations, statistical processing and signal averaging are required[116]. BOLD sensitivity can be improved using ultra-high-field MR scanners due to its supra-linear relationship with magnetic strength[99].

Two types of experimental designs can be used for fMRI paradigms, block or event-related designs[117]. A block or boxcar design consists of two or more conditions. In each condition (block) the stimulus is continuously presented for

a discrete epoch of time (ON period). The stimuli blocks are usually separated by a rest block (OFF period), which allows the haemodynamic response to return to baseline and hence maximise the detectable BOLD amplitude[115]. Alternatively, in an event-related design, stimuli events are presented as isolated brief events (e.g. 1 sec) separated in time from one another, and individual haemodynamic responses can be identified to each event, as shown in Figure 4.

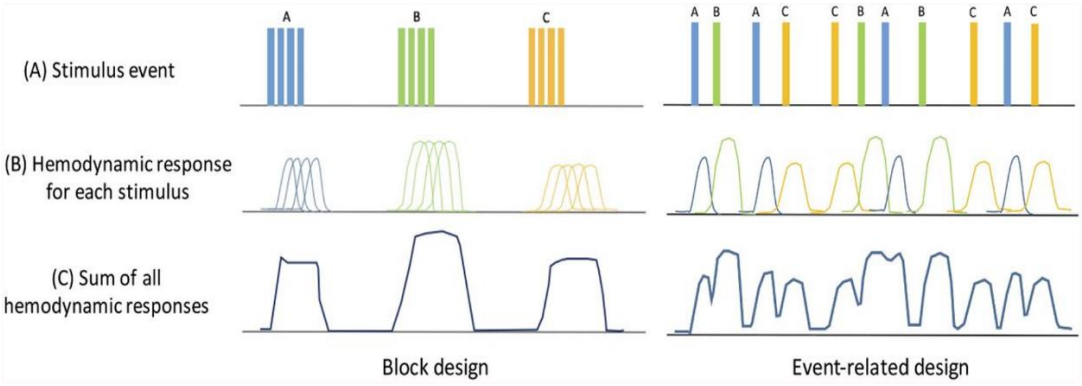


Figure 4 Illustration of a block and event-related designs, each bar represents a stimulus[117]

The methods commonly used in nutrition research include the presentation of taste, aroma, or flavour stimuli or food images in a block design, where stimuli are presented for a period of time after a period of rest[104]. The BOLD response to a meal or food cues can be measured under different physiological condition i.e. fasted state compared with fed state or in the presence of exogenously administered of endogenously produced gut hormones[118]. For example, a nutrient can be infused into the gut after a short baseline period, where the BOLD signal over a time period is compared with the baseline[119]. This technique is similar to that of pharmacological interventions which use psychoactive drug infusions instead of nutrients[120].

2.1.4 Functional MRI data analysis

As the BOLD signal is typically of the order of 1-5% at 3T, underlying noise in the data can make the analysis of fMRI data challenging[107]. Sources of noise include system noise, thermal noise and physiological noise (respiration, cardiac pulsation) and head motion[115]. fMRI analysis can be divided into two stages: the first stage consists of a number of pre-processing steps, used to eliminate non-task related variability in the data due to noise and to increase the signal to noise ratio (SNR)[115]. The second includes statistical analysis to identify and infer which voxels in the images show a response to the stimulus[115]. In this thesis, Statistical Parametric Mapping (SPM) software https://www.fil.ion.ucl.ac.uk/spm/software/ was used to perform the fMRI analysis. Figure 5 shows the steps involved in fMRI data analysis

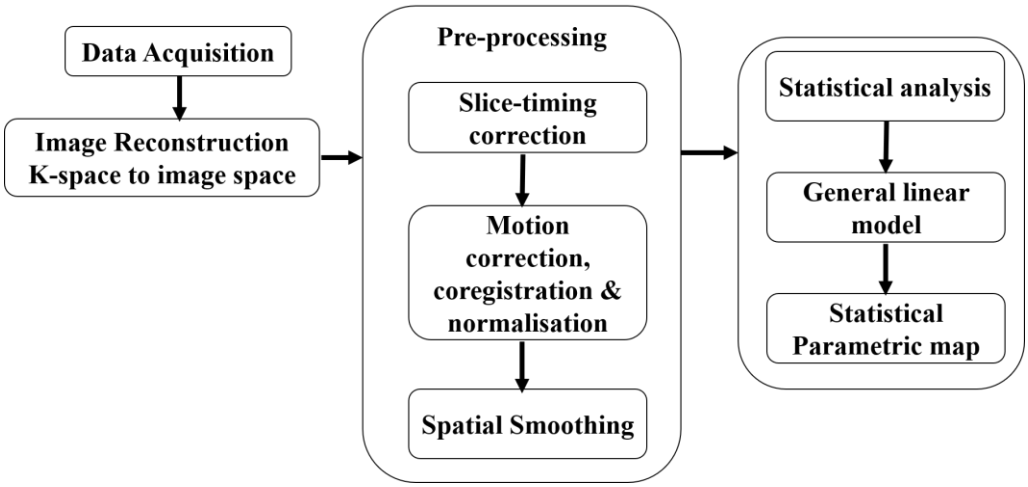


Figure 5 The fMRI data processing pipeline illustrates the steps involved in an fMRI experiment

2.1.4.1 Pre-processing

After the data were acquired it was first transformed from "k-space" to "image" space on the scanner. The following post-processing steps are then performed.

Slice timing correction during fMRI data acquisition, slices within a given volume are acquired sequentially i.e. ascending, descending or interleaved (for example, 34 slices are acquired per volume in a repetition time (TR) of 2.5 s this thesis chapter). Each slice is thus acquired at a slightly different time with respect to the other slices. For instance, in ascending acquisition, the lower slice is acquired at acquisition time, TA=0, whilst the acquisition of the top slice is delayed by a full TR period, i.e. TA = TR. These time differences cause a phase shift in the BOLD haemodynamic response. Haemodynamic modelling assumes that all slices within a volume are captured at the same time. Thus, slice timing correction is used to shift each voxel's time series (within each slice) to a reference slice (usually the first slice acquired). In this way, all voxels within the same volume 'appear' as if they had been acquired at the same time[115].

2.1.4.1.1 Head motion correction

fMRI analysis relies on measuring the haemodynamic response within the same location (voxel) throughout the experiment[115]. However, participants will make small movements during scanning, usually between 1-2 mm, resulting in a change in the voxel location across the fMRI time series[115]. This is an issue particularly at tissue boundaries or the edge of the brain, where the intensity difference between two adjacent regions is the highest. Head motion becomes a substantial problem when it is task correlated, i.e. the stimulus itself causes head

movement (e.g. swallowing during food-related experiments)[115]. If motions are not sharp and visibly obvious, these movements can be mistaken for the haemodynamic response creating false-positive activations[115]. Motion correction or spatial realignment is routinely used to remove gross head motions. SPM implements an automated image registration algorithm, to estimate the extent of head motion compared to a reference image, which is usually the first image in the time series[115]. All images are then realigned to the reference image, which minimises the sum of squared differences between images[115]. This realignment is performed using a six-parameter rigid body transformation: three translations about the x-, y- and z-axes and three rotations around each of the axes. Realignment transformations for translation and rotations are shown in Figure 6 for an fMRI series comprising 350 volumes.

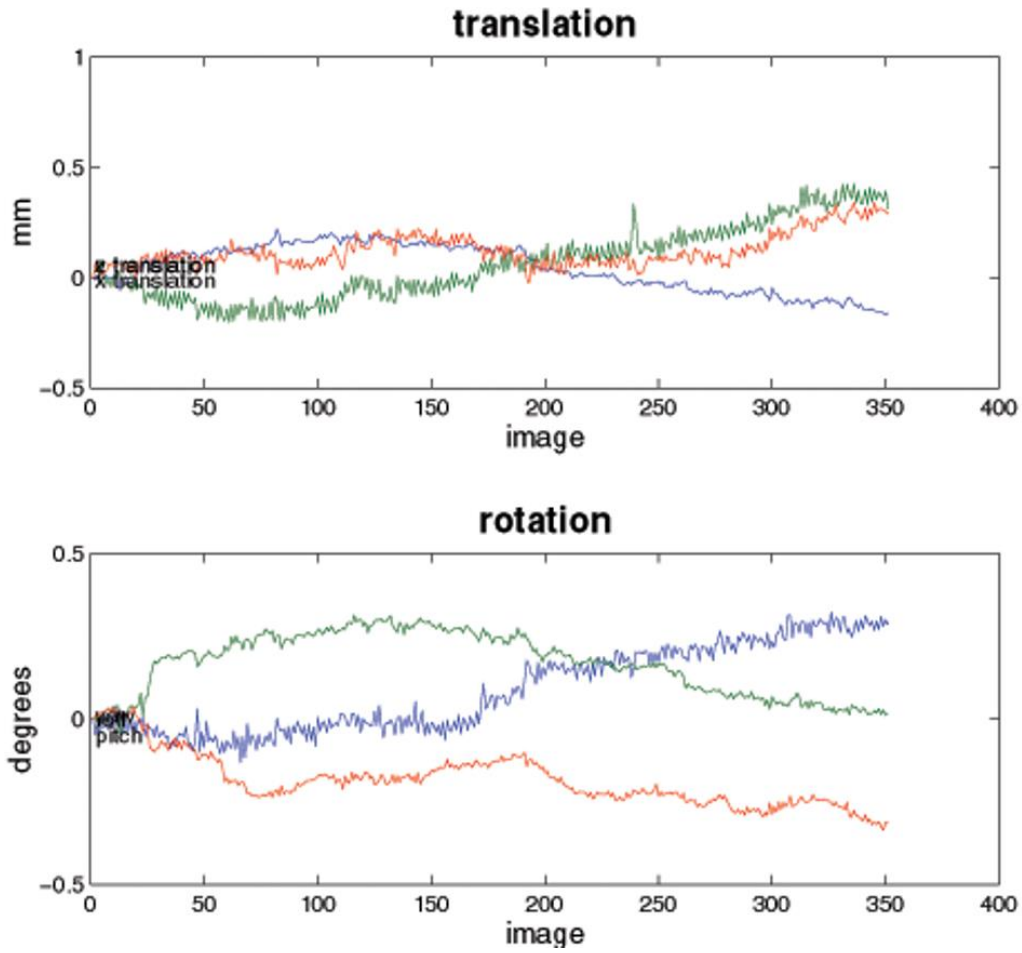


Figure 6 Plots showing translation and rotation correction used in an fMRI data set of 350 volumes.

These transformations should be inspected for excessive motion. In this thesis, any participant moving more than two voxels (>6mm) is discarded from the study. It is important to note that the rigid body technique does not consider sharp and signal distortion that arises from cardiac pulsation or respiration, which mask the task-induced BOLD response, and introduce temporal and spatial correlations in the data[115].

2.1.4.1.2 Spatial Normalisation

Individual brains vary in shapes, sizes and orientations and the number of sulci and gyri, therefore, it is essential to transform the data from each subject into standard template space when forming a group activation map[115]. This process

is known as spatial normalisation. Spatial normalisation is performed by matching the shape, size and orientation of an individual brain to a template by applying 12 linear parameters; translation (x, y and z); rotation (roll, pitch and yaw); resizing in three dimensions; and three shearing deformations[115]. The most commonly used template spaces are the Montreal Neurological Institute (MNI) space and Talairach space[121]. The MNI space template has been formed from the average of 152 T_1-weighted brain images of right-handed normal controls[121]. MNI space is used for all fMRI data sets that have been analysed in this thesis. Figure 7 shows the normalised MNI template and an individual subjects anatomical scan which has been normalised.

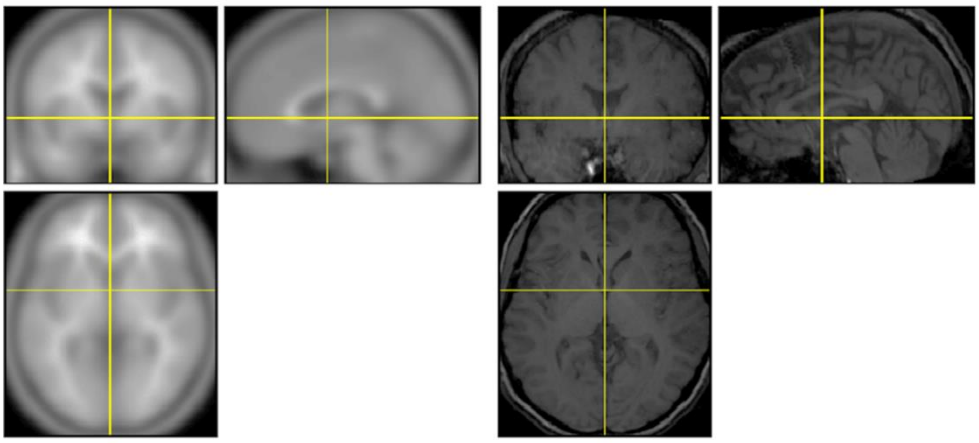


Figure 7 MNI template image and associated normalised anatomical image.

2.1.4.1.3 Spatial smoothing

After the normalisation step, spatial smoothing or filtering is applied to the fMRI data. Spatial smoothing is performed to increase the SNR, to enable averaging across subjects, and to make the data follow a normal distribution to allow the application of the Gaussian Random Field theory[122] in the statistical analysis. Spatial smoothing is achieved by convolving each volume of the fMRI data with

a 3D-Gaussian kernel of a specific full-width-half-maximum (FWHM). Smoothing is usually performed to a level of two to three voxel sizes (between 3 and 12 mm FWHM). However, the smoothing level may reduce the underlying signal. The smoothing level should typically match the size of the expected activated region. Spatial smoothing removes high spatial frequency noise and blurs sharp edges of the image, thus enhancing SNR[115]. Although individual brains are spatially normalised (to MNI space), different brains have a different cortical organisation, hence in group analysis data are smoothed at a higher level to increase the chances of overlapping activity across subjects[115]. fMRI data in this thesis were smoothed with a Gaussian filter of 6 mm FWHM.

2.1.4.1.4 Temporal Filtering

Temporal filtering is used to remove unwanted components in the fMRI time series. In SPM software, a high-pass filter is implemented in the statistical analysis stage to remove unwanted slow varying signals, such as scanner drifts and physiological noise i.e. cardiac and respiration[115]. A high-pass filter of 3000s was used in this thesis, which is not typical due to the nature of the fMRI paradigm and fMRI data TA.

2.1.4.2 Statistical analysis

The statistical analysis determines which brain regions show a significant signal change in response to the fMRI task or stimulus. Most fMRI analyses are performed independently on each voxel i.e. the univariant approach and tested under the null hypothesis, that the voxels of interest are not activated[115]. The general linear model (GLM)[123] is one of the most commonly used methods to analyse fMRI data and is the approach implemented in the SPM software used

in this thesis. In the GLM, the expected BOLD responses are linearly modelled by convolving the stimulus waveform function with a canonical HRF[115]. In a block design, the stimulus waveform is represented by a box-car function, while in event-related design the stimulus waveform is represented by a series of stick functions[115]. A GLM is often formulated in matrix notation as:

$\mathbf{Y} = \beta\mathbf{X} + \boldsymbol{\epsilon}$, where **Y** is the vector of observed data, **X** is the design matrix, β is the vector parameters to estimate and **€** is the vector of residual error, which is assumed to be independent and normally distributed. The design matrix **X** represents the experimental design (the model). Figure 8 shows an example of a design matrix modelled with HRF.

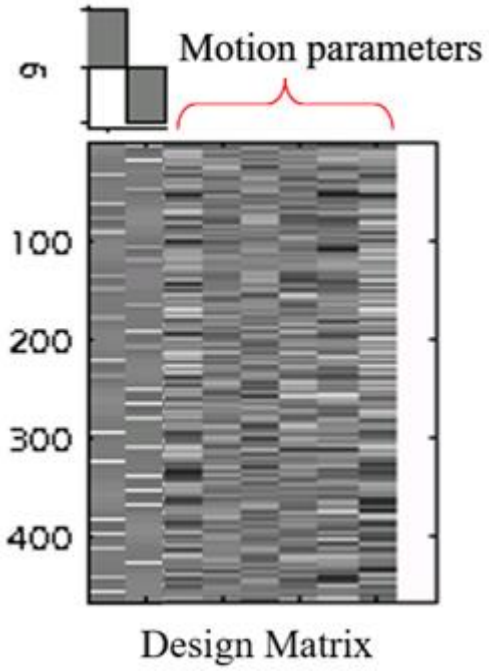


Figure 8 An example of a design matrix. Each row represents a point in time (volume), and columns correspond to experimental conditions and confounds. The first two columns represent the experimental conditions (with white lines depicting stimulus periods) and the last six columns show the motion parameters as regressors of no interest

Each row in the design matrix corresponds to the one-time point (volume) in BOLD time series and each column corresponds to an experimental condition (onset time for stimulus) and/or confounds, such as the estimated motion

parameters. Here motion parameters are included as regressors-of-no-interest to eliminate signal fluctuations correlated to confounds[115]. The parameter β is then estimated for each column by fitting the model to each voxel's time series[115].

To test the statistical significance of activated voxels, a parametric test (T- or F-statistics) is performed on a voxel-by-voxel basis, under the null hypothesis. T-tests are used to examine the statistical difference in the mean and standard deviation of the BOLD response for data modelled using the canonical HRF only[115]. A contrast vector is set up, where the condition of interest is assigned to a value of 1, and 0. For instance, to test if condition A has statistically more activated areas than condition B (in a design matrix of two conditions (A and B) and six motion parameters of no interest), the contrast vector is defined as (1 -1 0 0 0 0 0 0) as shown in Figure 8. F-tests are used when more than one basis function is used to model the BOLD response[115].

The resulting T (or F) values of the activated voxels are distributed in accordance with the T/F distribution, these values are then converted to z-score and probability (P) maps. These statistical parametric maps (SPMs) are then colour coded and superimposed on a normalised anatomical T_1-weighted image or the MNI template. Data may be displayed at uncorrected probability (typically $P < 0.001$). However, since fMRI analysis is performed on a voxel-by-voxel basis, thousands of statistical tests are performed for each data set, hence increasing the chance of false positives, known as the multiple comparisons problem[124]. For example, in each dynamic of an fMRI data set, there may be 100,000 voxels inside the brain, at a threshold of $P = 0.05$ i.e. 0.5 % by chance, giving 5000 false activations, or at $P = 0.01$ there are 1000 false activations. To minimise the number of false positives, while maximising the number of the truly active

voxels, the probability threshold may be corrected for multiple comparisons[124]. Two methods are commonly used: Family Wise Error (FWE) correction[122] and False Discovery Rate (FDR)[125], which are both implemented in SPM and used throughout this thesis. FWE rate controls the chance of any false positives, using random field theory[123].

2.1.4.3 Group analysis

Two statistical approaches are typically used in fMRI group analysis, fixed-effects and random-effects analyses[115]. Fixed effects analyses (FFX), or first-level analysis, is based on the assumption that the experimental effect is constant, i.e. fixed and that all participant's brains are affected similarly to the stimulus. Hence, the FFX approach only considers the within-subject variability of the group being studied and can only be used to make inferences about these specific participants studied[115]. Random effects analysis (RFX), or second-level analysis, consider the variability across subjects, and also within-subject variability, allowing inferences to be made about the study population as a whole[125].

In FFX analysis, a single large design matrix is created which includes all participants datasets in the group. The statistical maps generated represent the averaged brain areas activated in the group across subjects. In contrast in RFX analysis, a design matrix is formed and statistical analysis is carried out for each individual participant[115]. This is followed by the statistical parametric maps from each subject being pooled at the second-level analysis where the variance is computed across subjects[115]. Figure 9 illustrates a group analysis using FFX and RFX.

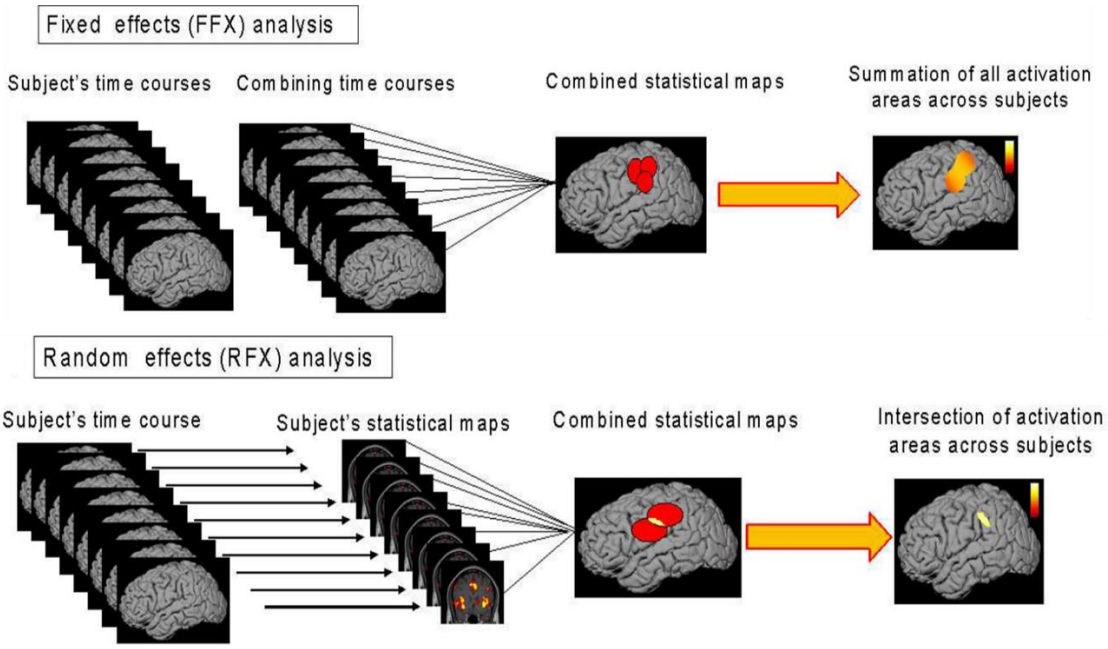


Figure 9 Group fMRI analysis using FFX and RFX[115]

2.2 Effect of hunger, thirst and satiety on brain response

The functional MRI response has been shown to vary between the fasted and fed state. In general, an increase in the BOLD response has been found in the fasted/ hunger state in the OFC, anterior cingulate cortex (ACC), amygdala, insula, thalamus, hypothalamus, and caudate[104,118]. Further, the BOLD response in these brain regions has also been shown to be reduced in the satiated/fed state[104,118], accompanied by an increase in the BOLD response in the PFC and inferior parietal lobe. However, there remain inconsistent findings in the literature in relation to brain activation and deactivation in fasted and fed states[118]. These discrepancies could be due to the difference in nutrients ingested, administration methods such intragastric (IG), oral or intravenous methods and differences in the paradigms used in the fMRI environment[118], or variations in the time between nutrient administration and MR imaging examination. For example, in some studies, fMRI data are collected immediately after nutrient delivery[89,126–128],

whilst in other cases, the data are acquired 5-120 min following nutrient administration[90,129–131]. The hypothalamus is a well-established brain region involved in the homeostatic regulation of food intake[132,133]. However, the modulation of the hypothalamus by feeding has been inconsistent across BOLD studies, possibly due to its small structure and its proximity to the sinus cavity making imaging of this region difficult[104].

In addition to studying BOLD response to meal administration, the food-cue or food picture paradigm is popular, in this a block design involving high/low energy-dense food pictures are shown together with non-food pictures in a randomised manner during the fMRI acquisition. Viewing food images in a fasted or hunger state has been shown to regulate the response in appetite-related brain regions such as the amygdala, Para hippocampal gyrus (PHG) and lateral OFC compared with the fed state[134–137]. Also, manipulating food motivation through displaying high or low-calorie food images has been associated with fMRI activation in the hypothalamus, ventral striatum, cerebellum, frontal middle gyrus in response to high-energy food images relative to low energy images[93,134,137,138]. Figure 10 shows those brain regions reported to be involved in the homeostatic and hedonic control of food intake.

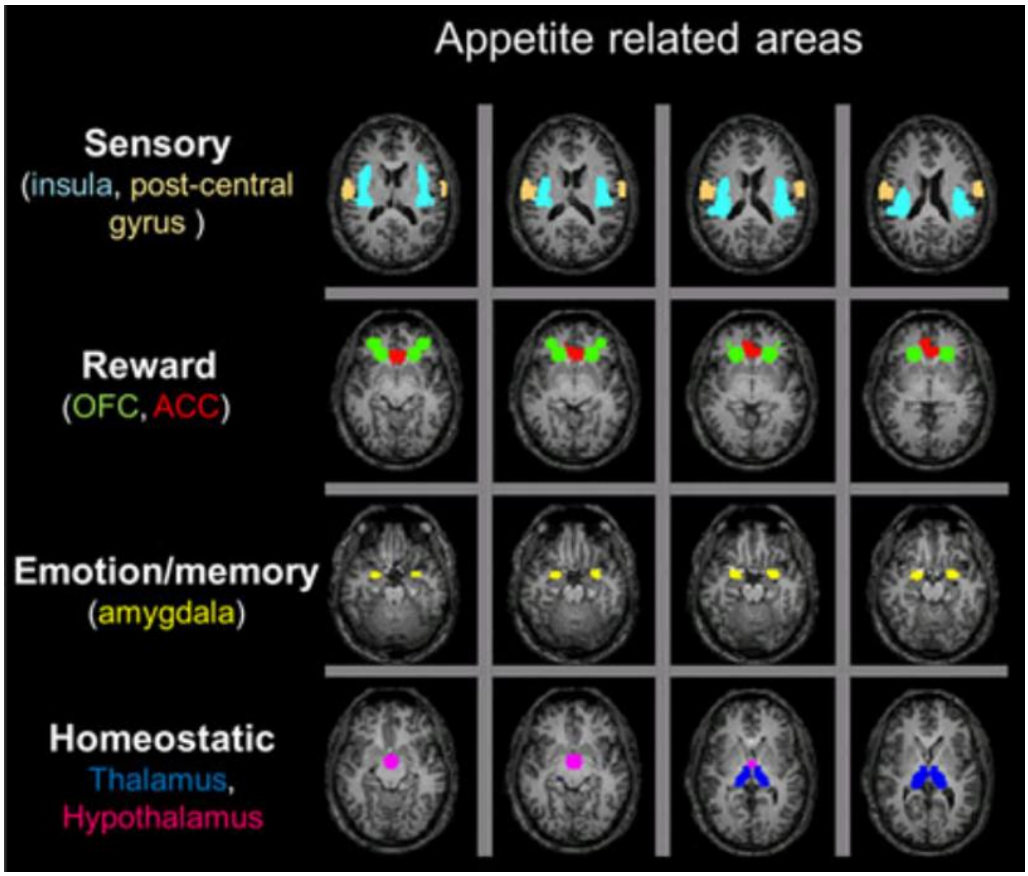


Figure 10 Images of those brain regions reported to be involved in homeostatic and hedonic control of food intake[104].

RSFC methods (described in detail in Chapter 5), as well as task-based fMRI, have also been employed to study the human brain in fasted and fed states. Some studies have shown a feeding induced reduction in default mode network (DMN) activity, possibly linked with the activity of the cholinergic and glutamatergic neurotransmitter systems[139]. For example, postprandial glucose-induced reduction in DMN connectivity in the posterior cingulate cortex (PCC) and precuneus has been reported in HCs[139]. Similarly, a decreased BOLD signal in the PCC (part of the DMN) has been reported following glucose drink ingestion[140]. Reduction in DMN connectivity has also been found after acute loading of the amino acid tryptophan[141]. Changes in RSFC and BOLD responses have also been reported in response to a non-nutrient stimulus (e.g. plain water), where regions such as the PCC and precuneus have been implicated in a thirsty

state. For example, a linear decrease in BOLD response in the precuneus[142] (part of the DMN) with increasing fluid consumption has been reported. Similarly, other studies have also found a decrease in neuronal activity in the PCC[143,144] and precuneus[144] immediately following drinking water to satiation.

2.2.1 Nutrient specific effects on brain responses

Brain responses to a test meal are not just a function of calorie intake, but such responses have been shown to be nutrient specific, with differential brain responses to sugars, lipids and proteins being reported[119].

Most studies have demonstrated a glucose-induced decrease in hypothalamic BOLD response[145–152], with a few exceptions[153,154]. It was found that glucose ingestion showed a stronger reduction in BOLD response than intravenous administration, indicating that the incretin effect is important in the hypothalamic response[148]. Additionally, glucose drinks at lower temperatures have been shown to result in a stronger homeostatic and hedonic response, as evidenced by stronger BOLD signals in the hypothalamus and VTA[151]. Glucose mediated BOLD responses are found to be CCK-independent, unlike lipid-mediated BOLD effects[149]. Fructose-induced BOLD responses have been shown in reward areas of the brain relative to glucose[150,152,153,155,156]. Finally, non-nutritive sugars (aspartame, allulose, sucralose) have been shown to not have the same satiating effects as nutritive sugars (glucose/sucrose), as demonstrated by their diminished BOLD responses in key homeostatic and hedonic brain regions[140,147,152]. Table 3 summarises the key fMRI studies investigating brain responses to different types of sugars.

Unlike glucose, lipid-driven BOLD responses are abolished by the CCK1 receptor antagonist dexloxiglumide, indicating a CCK dependent pathway[157]. Lipid-activated BOLD responses have also been shown to be also suppressed by ghrelin[126], indicating ghrelin's role in attenuating the gut-derived satiety signals. In general, fats attenuate the BOLD response in reward areas of the brain[130,158], exerting stronger satiating effects, and may also play a role in alleviating low mood[130]. Table 4 summarises the key fMRI studies investigating brain responses to fat/fatty acid.

High protein meals have been shown to exhibit stronger satiating effects compared with low protein meals and glucose and fat, as evidenced by attenuated BOLD responses in the hippocampal regions[159] and the amygdala[160]. Table 5 summarises the key fMRI studies investigating the brain responses to protein and amino acids.

Author	**Nutrients received (sugars)**	Paradigm	Main findings
Liu et al, 2000[145]	Ingestion of D-dextrose (75 g) or water	On-off treatment-related block design	A decrease in hypothalamic BOLD signal
Smeets et al 2005[146]	Glucose solution (25 or 75 g) or water	On-off treatment-related block design	- Prolonged decrease of the fMRI signal in the hypothalamus, - The observed response was dose-dependent i.e. a larger glucose load resulted in a larger signal decrease.
Smeets et al 2005[147]	Ingestion of one of the following 4 stimuli (300 mL of each): water (control), a glucose solution, aspartame (sweet taste) solution, or maltodextrin (nonsweet CHO) solution	On-off treatment-related block design	-Glucose ingestion resulted in a prolonged and significant signal decrease hypothalamus -No hypothalamic BOLD decrease following artificial sweetener (aspartame) or non-sweet maltodextrin -Indicating both sweet taste and energy content needed to achieve a hypothalamic response
Smeets et al 2007[148]	- ingestion of glucose solution 75 g or water (300 ml), and -iv infusion of 40% glucose solution 35g or, - infusion of saline	On-off treatment-related block design	-Glucose ingestion resulted in a stronger BOLD signal decrease in the hypothalamus compared with the glucose infusion, -indicating the incretin effect is an important factor in the hypothalamic response to nutrient ingestion
Purnell et al 2011[153]	Intravenous: 0.3mg/kg Glucose Fructose Saline	On-off treatment-related block design	-Neither glucose nor fructose infusions significantly altered the BOLD signal in the hypothalamus. -The BOLD signal in the cortical control areas increased during glucose infusion. -BOLD signal decreased in the cortical control areas during fructose infusion
Kroemer et al 2012[161]	Glucose 75g	fMRI- food cue	-Glucose administration led to decreased activation for food versus control pictures in the right basal ganglia, the right medial frontal gyrus, the left middle temporal gyrus, and the left ACC. -Increased activation was found in the anterior precuneus and in occipital regions
Lennerz et al 2013[162]	High glycaemic index (GI) Low GI	fMRI-CBF	-High-GI meal elicited greater brain activity in the right nucleus accumbens, right striatum and the olfactory region.

Little et al 2014[149]	IG infusion (250 ml) of: -1 M glucose + predosing with dexloxiglumide (CCK1 receptor antagonist), - 1 M glucose + placebo, - 0.9% saline (control) + placebo	On-off treatment-related block design	- Glucose decreased BOLD signal, relative to saline, in the brainstem, hypothalamus, the cerebellum, right occipital cortex, putamen and thalamus. - The glucose +dex arm showed a CCK1receptor-dependent increase in BOLD signal only in the motor cortex (significance unclear) - Most glucose-mediated BOLD responses were CCK independent.
Heni et al 2014[163]	Glucose 75g Water ingestion	fMRI- food cue	-Bodyweight substantially impacted on the brain's response to visual food cues after glucose versus water ingestion. -Overweight subjects showed increased activity to food cues in response to glucose and water ingestion in the putamen and occipital cortex compared with lean subjects
Dorton et al 2017[164]	-a drink containing 75 g of glucose and 0.45 g of non-sweetened cherry flavouring dissolved in 300 ml of water.	On-off treatment-related block design	-a positive correlation between added sugar intake and BOLD response to food cues in the dorsal striatum and a similar trend in the nucleus accumbens after glucose were found, but not after water consumption
Van Opstal et al 2018[151]	- plain tap water at room temperature (22°C), plain tap water at 0°C - a glucose-containing beverage (75 g glucose dissolved in 300 mL water) at 22°C, and a similar glucose drink at 0°C	On-off treatment-related block design	-All glucose drinks resulted in a direct, significant decrease in BOLD response in the hypothalamus compared with baseline. -In the VTA, a significantly decreased BOLD response compared with baseline was found after the ingestion of stimuli containing glucose at 0°C and 22°C. -indicating that the low temperature leads to a response from the hypothalamus and might strengthen the response of the VTA (hedonic response).
Stopyra et al 2019[154]	glucose or water infusion directly into the stomach using a nasogastric tube,	fMRI-food cue	No significant differences in brain activation depending on glucose load (i.e. glucose vs. water) when processing food stimuli.
Van Opstal et al 2019[152]	50 g of glucose, fructose, or sucrose, or 0.33 g of sucralose dissolved in 300 mL tap water. The control condition consisted of 300 mL of plain tap water.	On-off treatment-related block design	-A decrease in BOLD signal in the hypothalamus was found after ingestion of glucose, -A lesser but delayed BOLD response was found after ingestion of sucrose and fructose. -Sucralose led to a smaller and transient response from the hypothalamus. - In the VTA, sucralose led to a very similar response to water, indicating its lack of satiating effects

Table 3 Summary of the key fMRI studies investigating brain responses to different types of sugars.

Author	**Nutrients received (lipids/fatty acids)**	Paradigm	Main findings
Lassman et al 2010[127]	IG administration: -Lipid (dodecanoic acid, 250ml) - saline -CCK-1 receptor antagonist dexloxiglumide (600mg orally)	On-off treatment-related block design	-Lipid activated bilaterally the brain stem, pons, hypothalamus, cerebellum and motor cortical areas. -These activations were abolished by dexloxiglumide, indicating a CCK-mediated pathway.
Oudenhove et al 2011[165]	-IG: 250 ml 0.05 mol/l dodecanoic acid (C12) or -saline	fMRI- visual cue	BOLD responses to sad emotion induction were attenuated by fatty acid infusion in the right medulla/pons, left hypothalamus, right hippocampus and the MCC
Jones et al 2012[126]	-intravenous ghrelin in a postprandial state -intravenous infusion of ghrelin alone -intravenous infusion of ghrelin after IG lipid (dodecanoate, C12)	On-off treatment-related block design	-IG C12 led to strong bilateral activation of the brain stem, hypothalamus and limbic areas which was attenuated by exogenous ghrelin. -Suggests the role of ghrelin in the suppression of gut-derived satiety signals, thus increasing food intake.
Byrne et al 2016[166]	-control inulin (10g) -inulin-propionate ester (IPE) 10g – food supplement that increases colonic propionate production	Food cue	-Increasing colonic propionate production reduced BOLD signal during food picture evaluation in the caudate and nucleus accumbens. -Reduction in BOLD signal in the caudate was driven specifically by a lowering of the response to high-energy food. -Indicating the role of short-chain fatty acids (SCFA) in attenuating reward-based eating behaviours
Eldeghaidy et al 2016[130]	- prior consumption of a 250-mL High Fat Meal [rapeseed oil, emulsifier, sucrose, flavour cocktail] or - water load -during fMRI: flavoured no-fat control stimulus (CS) (sucrose+flavour+water)): or flavoured fat stimulus (FS) (rapeseed oil): rapeseedoil+sucrose+flavour+water	On-off treatment-related block design	-Prior high fat meal consumption caused reduced amygdala activation in response to the fat stimulus compared to the control stimulus in the fMRI environment indicating fat-related satiety

Table 4 A summary of the key fMRI studies investigating the brain responses to fat

Author	**Nutrients received (proteins/amino acids)**	Paradigm	Main findings
Li et al 2012[160]	-250 g glucose solution/L; -257 g whey protein solution/L -111 g soybean oil emulsion/L -0 kcal distilled water/L. -all 4 solutions were orange flavoured	On-off treatment-related block design	-Ingested macronutrients similarly reduced the BOLD signal in the middle insula, thalamus, PHG, caudate, and lateral OFC. -Protein ingestion reduced the BOLD signal in the amygdala more effectively than did fat and glucose ingestion
Leidy et al 2013[159]	-350-kcal normal protein NP (13 g protein) cereal-based breakfasts, -350-kcal high protein HP egg and beef-rich (35g protein) breakfasts, -or continued breakfast skipping (BS)	fMRI- food cue	-Both meals reduced predinner amygdala, hippocampal, and midfrontal corticolimbic activation compared with breakfast skipping. -High protein meal led to additional reductions in hippocampal and PHG activation compared with a normal protein meal.

Table 5 A summary of key fMRI studies investigating the effect of protein/amino acids on the brain.

2.2.2 The effects of gut peptides on brain activation

A systematic review by Zanchi et al[118] (including 40 original studies) investigated the effect of appetite-regulating hormones such as ghrelin, insulin, leptin, PYY, GLP-1 and CCK on brain activation. Figure 11 shows the regions that were identified as the main targets for gut peptides.

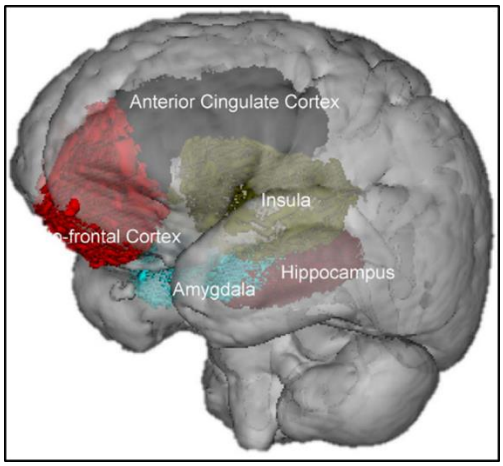


Figure 11 The main target regions for gut peptides[118]

The key findings of this systematic review were as follows:

i) Plasma levels of appetite enhancing hormone ghrelin correlated positively with activity in the OFC, ACC, PFC, amygdala and insula and negatively correlated with activity in subcortical areas such as the hypothalamus, thalamus, hippocampus and striatum.

↑ Plasma ghrelin → ↑ BOLD signal in OFC, ACC, PFC, amygdala and insula

↑ Plasma ghrelin → ↓ BOLD signal in hypothalamus, thalamus, hippocampus and striatum

ii) Plasma levels of satiety-stimulating hormones (insulin, leptin, PYY, GLP-1 and CCK) correlated negatively with the same cortical areas and positively with subcortical areas.

↑ Plasma satiety hormones → ↓ BOLD signal in OFC, ACC, PFC, amygdala and insula

↑ Plasma satiety hormones → ↑ BOLD signal in hypothalamus, thalamus, hippocampus and striatum

The mechanistic pathway based on the findings from this systematic review[118] can be illustrated as follows. Following food intake, hormones like ghrelin and insulin act on the receptors on neurons in the hypothalamus via the leaky BBB. The postprandial satiety signals penetrate the subcortical areas, such as the amygdala and striatum. The hypothalamus then sends signals to the cortical areas such as the OFC, ACC and insula as part of the reward- hedonic circuitry, where information (such as sensory properties of food, habitual, sociocultural emotional influences) is integrated with adiposity signals, thus regulating food intake.

2.3 Malnutrition and appetite loss in CD

Malnutrition is a major problem in the clinical management of CD. Disease-related malnutrition may be represented by poor nutritional intake, impaired utilisation or loss nutrients, or maybe a result of acute or chronic inflammation[167]. Protein-energy malnutrition, altered body composition and micronutrient deficiencies are some of the main characteristic features of malnutrition in CD [168]. It has been reported that up to 75% of hospitalised patients are malnourished and 50% are in a state of negative nitrogen balance [169]. Malnutrition in CD may be attributed to inadequate nutrient intake, loss of absorptive surfaces in the ileum due to disease activity or surgical resections[170]. The negative nitrogen balance is related to the increased protein catabolism rates in CD[171] in response to the increased protein requirements as a result of the intestinal and systemic inflammation (e.g. acute-phase protein, inflammatory cytokine and FCP production). Several other factors such as disease burden, appetite loss, and other associated symptoms such as nausea, diarrhoea contribute to malnutrition with a negative impact on patients' QoL.

Issues regarding food and nutrition are a major concern for CD patients. For example, a survey in a UK cohort of IBD patients showed that both UC and CD patients found nutritional issues to be either important or extremely important in 62.5% of the respondents, with virtually all (94%) of the CD participants having had problems with unintentional weight loss[172]. Another survey investigating dietary beliefs and behaviours in a UK IBD cohort found that 48% believed diet was the initiating factor in IBD and 57% believed it could trigger a flare[173]. Certain foods such as (sugary food, coffee/tea, carbonated beverages, milk/milk products, raw vegetables/fruits, alcohol, fatty food and spicy food) were

implicated in worsening symptoms[173]. These findings are in line with studies in Spanish[174] and Dutch[175] IBD cohorts where the same food groups were avoided to reduce symptoms.

The aetiology of weight loss in CD is multifactorial. Although malabsorption and catabolism are considered to be the major contributors to weight loss, other factors such as suppressed appetite, early satiety and reduced food intake are also clinically relevant in elucidating nutritional abnormalities[176].

The IBD research priority setting partnership[177] placed diet and nutrition in the top 5 priorities in IBD research to promote self-management for patients with mildly active or inactive CD to achieve a better QoL. Table 6 describes the possible factors that could lead to malnutrition in CD

Reasons	Contributing factors
Increased nutritional requirements	Active inflammation
Increased nutrient losses	Diarrhoea, intestinal and fistulae and protein losses
Impaired dietary intake	Nausea, vomiting, appetite loss
Nutrient malabsorption	Bacterial overgrowth, secondary lactose malabsorption
Iatrogenic factors (drug-related, surgery-related)	Drug-nutrient interactions, reduced intestinal absorptive area.

Table 6 Contributing factors to malnutrition in CD[176]

Food intake is a physiological need to maintain energy homeostasis. However, food intake is also a social phenomenon influenced by factors illustrated in **Table 7**. Physiological mechanisms regulating energy homeostasis may be

overridden by environmental and psychological factors that may influence eating habits.

Factors	Examples
Psychological/cognitive factors	Learned habits (habitual mealtimes, familiar foods) health/religious beliefs/ dietary restraint, anxiety, depression.
Sensory factors	Thought, smell, the sight of food, food composition
Environmental factors	Food availability, social circumstances, cultural influences, stress and boredom

Table 7 Factors that influence food intake

Disordered eating in CD patients during active disease has been previously reported by our research group[178]. It was found that CD patients had greater anxiety/depression, lower positive mood, greater binge eating tendencies, lower craving control, greater craving for sweet, savoury foods and reduced protein consumption. These findings indicate that CD patients have stronger hedonic desires for food and emotional eating patterns possibly attributed to low mood, anxiety and depression[178]

2.4 Intestinal inflammation and modulation of EEC peptides

The inflammatory response per se may be a cause of weight loss in CD. Hypophagic eating behaviour during intestinal inflammation may be partly attributed to the increase in proinflammatory cytokines such as IL-1[179], IL-6[180] and TNFα[181]. These regulators of inflammatory response may influence metabolism, induce fever and result in loss of appetite[182]. Intracerebroventricular

infusion of pro-inflammatory cytokines such as TNFα and IL-1β have shown to reduce food intake in rats, indicating that inflammation may play a role in the central regulation of appetite[183]. However, several animal and human models have shown that EEC peptides play a critical role in appetite regulation and linked with the adverse symptoms during intestinal inflammation as described below:

2.4.1 Animal model

The role of the EEC axis in the induction of altered eating behaviour has been described in a *Trichinella spiralis* induced intestinal inflammation murine model[184]. It has been found that T spiralis induces CCK upregulation in mice which correlates with the peak severity of enteritis and reduction in food intake. The food intake was increased by the administration of the CCKR1 antagonist dexloxiglumide. In contrast, the induction of extra intestinal inflammation via T spiralis larvae encyst in skeletal muscle of the mice, resulted in an attenuated hypophagic response in the absence of CCK upregulation. These findings indicate the importance of the enteroendocrine axis in the abnormal eating behaviour in intestinal inflammation[184].

2.4.2 Human infection cases

Early studies of intestinal inflammation demonstrated that patients suffering from tropical malabsorption had elevated levels of gut hormones [185]. A significant increase in postprandial CCK was observed in patients with giardiasis or acute upper gastrointestinal infection[50]. After treatment with tinidazole, plasma CCK levels were normalised and symptoms such as nausea, bloating and anorexia in these patients were ameliorated[50]. It has been suggested that the

endogenous increase in CCK may contribute to symptoms such as nausea and discomfort observed during intestinal inflammation[50]. Reduction in food intake during a gut infection is thought to be an immunological response that acts as a protective mechanism against environmental contamination. Moreover, CCK was also found to reduce bacterial translocation [186] and increase luminal IgA secretion[187].

2.5 EEC peptides and CD

Reduced appetite observed in ileal CD has been attributed to the upregulation of EEC and the consequent increase of satiety hormones secretion, therefore possibly negatively affecting appetite signalling to the CNS[94–96]. For instance, a study[94] investigating key appetite secreting EEC subtypes and EEC markers using terminal ileal tissue from patients with (i) active ileal disease (n=38), (ii) inactive ileal disease (n=5) and colonic tissue from patients with (iii) active colonic disease (n=12) (iv) inactive colonic disease (n=4) and HCs (n =60) reported a significant increase in terminal ileal Chromagranin A (CgA) (EEC marker) expressing cells, in active ileal CD group compared with HCs terminal ileal samples. No change in CgA expressing cells was found in the active colonic CD tissues. A 2.5-fold increase in GLP-1 positive cells was seen in the active ileal CD tissues compared with HCs tissues. However, no change in terminal ileal PYY expressing cells or mRNA expression was seen between active ileal CD tissue and HCs. Furthermore, a 3.3 fold increase in CgA mRNA expression, 3.1 fold increase in GLP-1 expression, a 2.2 fold increase in ubiquitination protein 4a Ube4A expression (EEC gene implicated in CD), a 1.8 fold increase in neurogenin-3 (Ngn-3) gene expression (a transcription factor involved in the epithelial cell differentiation to the EEC lineage) was found in ileal CD

compared with HCs. Finally, paired like homeobox 2b (Phox2b) (another gene implicated in CD) was found to be colocalised to EEC and showed a 1.5-fold increase in ileal CD. A further study[95], investigating EEC peptides and appetite-related symptoms in response to a mixed nutrient test meal in active ileal CD patients (n=12), inactive ileal CD patients (n=6), active colonic CD patients (n=5) and HCs (n=13) found a 2 fold increase in pre and postprandial PYY plasma levels in active ileal CD group compared with HCs and active colonic CD. Plasma PYY positively correlated with symptoms of nausea and bloating in the ileal CD group. No difference in pre or postprandial GLP-1 levels was seen between the groups. The authors postulated that GLP-1 was less likely to play a part in altered appetite in CD. Postprandial elevation in ghrelin was found in the active ileal CD group compared with controls. The reassessment of active ileal CD patients in remission showed that the postprandial PYY and ghrelin levels reverted to normal HCs levels. This finding is limited by the small number of patients restudied in remission (n=6). A further study[188] investigating postprandial gut hormone levels and gastric emptying in response to a standardised breakfast meal in moderately active CD patients (n=13) (4 ileal, 4 colonic, 5 ileal-colonic), in active UC patients (n=10) and diverticulitis patients (n=7) found a 3 fold increase in postprandial plasma CCK levels compared with HCs and was associated with delayed gastric emptying. It was also found that postprandial CCK plasma concentrations were significantly higher in CD patients with exclusively ileal disease compared with the patients with colonic and ileal-colonic disease, but this finding is limited by the small sample size of exclusively ileal patients (n=4). No difference in postprandial PYY and GLP-1 was found between CD and HCs. Finally, another study[189] also investigating

postprandial gastric emptying and gut hormones response to a test meal in 24 HCs, active CD patients (n=14) and active UC patients (n=14) found that fasting CCK levels and maximal postprandial concentrations were similar between IBD patients and HCs, however, patients with UC had significantly lower postprandial CCK levels than HC and CD patients. In this study, there was no association between plasma levels and gastric emptying which contrasts with the previous finding by this group. The authors attributed this inconsistency to the test meal composition which contained less lipids and protein, that primarily stimulate CCK, also this study only had one CD patient with ileal disease which may explain the absence of difference between groups, as in the previous study the postprandial difference between CD patients and controls was driven by the exclusive ileal CD patients. In this study, Fasting PYY and postprandial PYY was similar between IBD and HC. Fasting GLP-1 was also similar between IBD patients and HCs. However, postprandial GLP-1 responses were increased in IBD (including CD-HC and UC-HC) compared with HCs and was associated with delayed gastric emptying, the reassessment of IBD patients in remission showed accelerated gastric emptying and normal postprandial increase in GLP-1, indicating the increased release of GLP-1 from the inflamed gut mucosa in IBD may result in delayed gastric emptying.

Taken together, these findings suggest elevated EEC activity in ileal CD, however, these studies are limited by patient standardisation with variations in distribution and severity of inflammation, concomitant medication use, genotypes and triggers and the nutrient composition of test meals used to assess postprandial physiological effects. It has been postulated that the increase in EC expression at the tissue and plasma level in ileal CD might affect appetite

regulation through changes in CNS signalling pathways. It is important to reiterate, the increase in tissue and plasma EEC peptide expression was only observed in patients with ileal CD whereas patients with exclusive colonic disease were found to have a normal ileal expression of EEC peptides and normal postprandial responses to GLP-1 and PYY[94,95], thereby suggesting disease location may differentially affect postprandial meal responses. Therefore, the colonic CD group was used in this study to dissect the effect of inflammation on the postprandial meal response in the absence of EEC peptide upregulation.

Despite the difference in pathophysiology to ileal CD, similar gut hormone elevations have been found in obese patients that have undergone RYGB surgery (involves bypassing most of the stomach and first section of the small intestine), where an increase in plasma PYY, GLP-1, CCK and decrease ghrelin was found[190,191]. In these obese patients postoperatively, lower activation in brain-hedonic responses to food has been reported in relation to elevated postprandial gut hormones[192–194]. For example, an increase in plasma PYY and GLP-1 levels was found following an ad libitum test meal in obese patients that underwent (RYGB) relative to patients with gastric banding surgery and BMI matched controls. It was found that octreotide (somatostatin analogue) induced suppression of postprandial PYY and GLP-1 after RYGB correlated positively with an increase in BOLD signal in the brain reward system, indicating the role of GLP-1 and PYY in the hedonic response to food[91]. Similarly, inhibition of GLP-1 using receptor antagonist exendin 9-39, resulted in increased BOLD response in the caudate nucleus in response to food pictures and in the insula in response to chocolate milk. These same regions had shown a decrease in BOLD response to the chocolate milk, in the absence of the GLP-1 receptor antagonist,

indicating the role of GLP-1 in reward-driven food intake[91]. Similar findings have been reported following the parenteral administration of GLP-1 and PYY in healthy subjects[129].

Therefore, in the present study, it was hypothesised in ileal CD patients a similarly elevated fasting and postprandial EEC peptide response will be observed with differential postprandial effects based on disease location. Although an exaggerated EEC hormone response to food intake has been described in ileal CD, the gut-brain axis has not yet been investigated. To date, no published studies have performed food-related tasks in the fMRI environment using visual stimuli or meal administration in CD. Task-based fMRI studies published in IBD have mainly involved cognitive/psychological tasks, mental stress, visceral/thermal pain induction tasks *(Readers note: please find a table of summary of these fMRI studies in the appendix of this thesis*).

2.6 The selection of C12 dodecanoate fatty acid as a test meal in the fMRI paradigm

CCK is one of the well understood gastrointestinal satiety signals, which is released by the enteroendocrine I cells of the upper small intestinal epithelium in response protein or fat, especially fatty acids with an acyl chain length greater than C12[195]. The use of CCK-1 receptor antagonist, dexloxiglumide in humans has demonstrated a fatty acid-induced slowing of gastric emptying, hence reducing meal size and increasing satiety through a CCK dependent pathway[196]. It has been found that CCK binds to its CCK-1 receptors expressed on the terminals of the vagus afferent neurons[197,198], indicating vagally mediated gut-brain signalling processes regulating food intake. In animal models, vagotomy has been shown to reduce gastric emptying in response to lipid perfusion of the

duodenum[199], further supporting vagal mediation of CCK signal transduction pathways.

An fMRI study investigating the role of CCK in C12 fatty acid-induced brain activations assessed postprandial BOLD signals in response to (i) a nasogastric infusion of C12 fatty acid or saline (ii) and a nasogastric infusion of C12 fatty acid or saline with or without prior administration of the CCK-1 receptor antagonist dexloxiglumide. It was found that lipid infusion increased BOLD signals in the medulla, pons, hypothalamus, motor cortex and cerebellum compared with saline, and this effect was diminished by dexloxiglumide pre-treatment, suggesting a CCK mediated CNS response to C12 fatty acid in the absence of any nutrient awareness cues. **Figure 12** shows the brain regions activated in responses to C12 fatty acid. Other fMRI studies that have studied fat specific brain responses are summarised in **Table 4**.

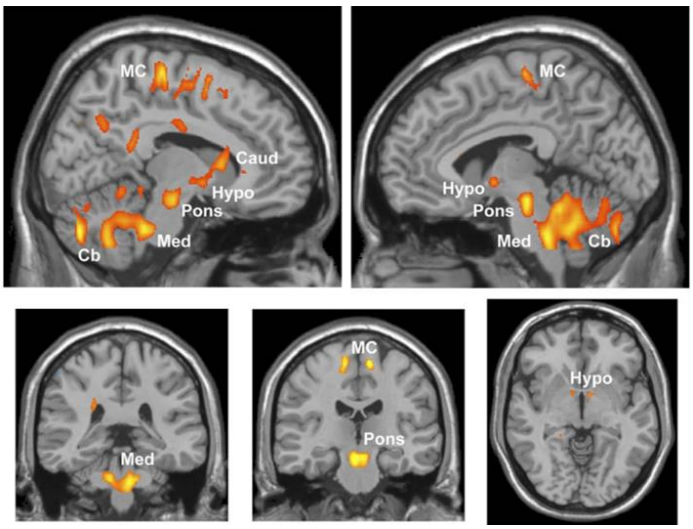


Figure 12 The CCK dependent increase in BOLD signal in the brainstem, pons, hypothalamus, cerebellum and motor cortical areas in response to IG infusion of C12 (dodecanoate)[157] compared with saline.

2.7 Hypotheses and Aims

The hypothesis to be tested is that in patients with CD and ileal inflammation A) an increase in the postprandial plasma EEC peptides response and associated appetite scores will be observed, and B) an alteration in brain-gut stimulation will be observed,

Specific aims of the chapter are to:

- Quantify fasting and postprandial plasma EEC peptide response and associated appetite scores.
- Quantify relevant changes in measures of brain activity following the C12 fatty acid test meal.

2.8 Methods

The following outlines the methods performed in this PhD thesis to assess fasting and postprandial fMRI BOLD responses in CD patients and HCs.

2.8.1 Participant recruitment

The study was conducted between June 2015 and March 2019 at the National Institute of Health Research [NIHR] Nottingham Biomedical Research Centre [NDD BRC] at the Queens Medical Centre Campus and the Sir Peter Mansfield Imaging Centre [SPMIC], Nottingham, UK https://clinicaltrials.gov/ct2/show/NCT02772458. CD patients were recruited from IBD Clinic by the study Principal Investigator and research nurse. Patients were identified through a clinical database search, expression of interest list. Patients who fit the study inclusion criteria were sent an invitation letter and patient information sheet. HCs were recruited from an existing participant database in the Nottingham BRC and from the local healthy populations of Nottingham University Hospitals and the University of Nottingham. This study was advertised through study fliers and social media. For CD patient's disease activity was defined through objective markers of inflammation: FCP of >250 µg/g, CRP of > 5 g/dL, through recent ileocolonoscopy, CT, magnetic resonance enterography [MRE] showing active inflammatory and uncomplicated disease [not of a stricturing or penetrating behaviour]. CD clinical symptoms were measured with a Harvey-Bradshaw Index [HBI] score recorded at inclusion. Potential participants presenting with recent corticosteroid use [in the past 3 months], pregnancy, breastfeeding, or significant comorbidities were excluded from the study. Stable doses of immunosuppressive agents or anti-TNFα agents were permitted. All CD patients and healthy volunteers gave their informed consent before recruitment. Exclusion criteria included malignant disease, BMI <18 or 35 kg/m^2, significant cardiovascular or respiratory disease, diabetes mellitus, current infection, neurological or cognitive impairment;

significant physical disability. Other exclusions were significant hepatic disease or renal failure, abnormal blood results other than those explained by CD including bleeding diatheses (apart from in the case of HC where all unexplained blood results are exclusion criteria), pregnancy or breastfeeding or if MRI is contraindicated (e.g. pacemaker). Severe CD where a delay in a change in medical treatment for 1-2 weeks would not be clinically advisable was also an exclusion criterion.

Participants attended two MRI scan sessions (approximately 1 week apart) involving nasogastric infusion of saline or fatty acid. Figure 13 shows the participants journey through this study.

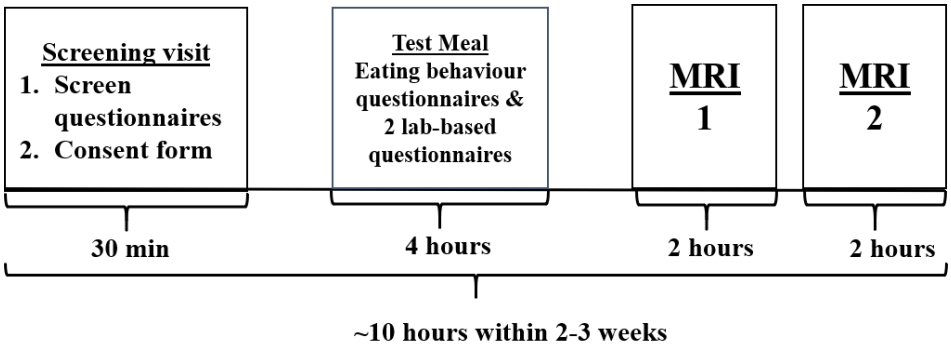


Figure 13 Participant journey: Two MRI scan sessions were required for the fatty acid and saline test meals, the order of which was randomised across participants.

2.8.2 Experimental Protocol

On the MRI study days, participants arrived at 8:00 am, following an overnight fast. In each fMRI scan session, a training scan (dummy scan) was performed to familiarize the subjects with the scanner prior to cannulation and the noise made by the MR sequence. In this scan, a 10-minute resting pre-stimulus state (RPS) fMRI data set was collected to assess RSFC. This was done to ensure that RPS CNS data acquisitions were free of the confounding effects of stress-induced by the invasive procedure. In addition, a whole head 1mm isotropic resolution T_1-

weighted structural scan (SS) was acquired. **Figure 14** shows the general fMRI experimental paradigm.

2.8.3 Stimuli, delivery system and bloodletting

After the baseline data acquisition, an IG tube was inserted in the nose and into the volunteer's stomach by a trained senior research nurse (Shellie Jean Radford). This was used to deliver the test meals, thus avoiding the confounding effects of taste on the CNS data acquired. BOLD measurements were carried out prior to and following IG delivery of test solutions. On each occasion, the participant received either an IG 250ml control solution of phosphate buffer solution (PBS) 7.4 (1X) liquid or 250 mL of 0.05 mol/L dodecanoate (C12 fatty acid; lauric acid; Sigma–Aldrich, Gillingham, Dorset, England)[18]. To prepare the fatty acid solution, 2.6 g of dodecanoic acid was mixed with 3.90ml of Polysorbate 80 and 256.1ml of PBS, the solution was heated and stirred until the fatty acid was fully dissolved at ~60° C, the solution was then cooled down to 35°-37° C and kept in a hot water bath until the time of meal delivery. **Table 8** details the participants, intervention, comparator and outcome of this study

Participants	17 patients with ileal CD 17 patients with colonic CD 17 HCs
Intervention	An IG bolus of 250ml of 0.05 mol/L dodecanoate (fatty acid)
Comparator	An IG bolus of 250 ml-of PBS
Outcome	BOLD response after the fatty acid test meal

Table 8 The participants, intervention, comparator and outcome

Participants were also cannulated by the senior research nurse (SJR) for the blood measurements of gut hormones (GLP-1, PYY, CCK) and cytokines. The first 2 mL of each blood draw was discarded to avoid contamination with the

saline used to maintain patency. Ice-chilled lithium heparin-treated tubes (BD Diagnostics, UK) containing aprotonin (Sigma-Aldrich, UK) were used to collect plasma.

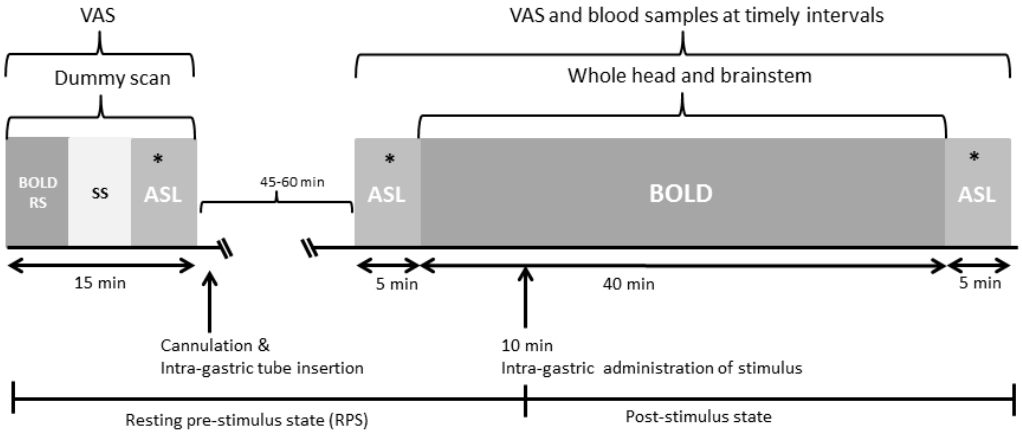


Figure 14 General fMRI paradigm used in this study. A 15 min-dummy scan was performed prior to the cannulation and IG tube insertion. * Arterial Spin Labelling (ASL) measures of CBF, BOLD RPS, BOLD acquisition, SS=Structural Scan

2.8.4 Scanning protocol

BOLD data were collected on a 3T Achieva scanner (Philips Medical Systems, Best, Netherlands) with a 32 channel receiver head coil using a double-echo gradient-echo EPI (GE-EPI) acquisition scheme with echo time (TE) 20/49ms, 64 x 64 matrix, 3x3x3 mm^3, 34 axial slices, TR=2.5 s. An optimized double-echo gradient echo-echo planar imaging acquisition was used to increase BOLD sensitivity in areas with short T2*, such as the amygdala and hypothalamus which have particular importance to reward and feeding. Each acquisition lasted for ~35 mins, yielding 840 volumes per subject. A high resolution T_1-weighted image was also acquired using a magnetization-prepared rapid gradient echo [MPRAGE] sequence (1mm isotropic resolution; TE/TR = 8.3/3.8 ms, flip angle = 8 º, SENSE factor =2, 160 slices, 256 x256 matrix). **Figure 15** shows an example of the slice acquired during BOLD data acquisition

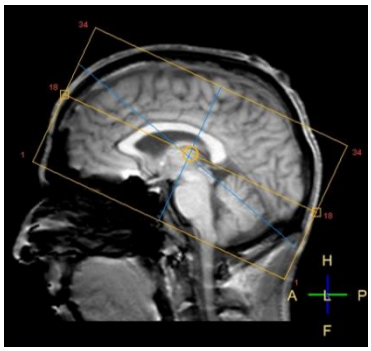


Figure 15. An example of the 34-slice alignment during BOLD data acquisition

2.8.5 fMRI paradigm

Following the IG tube insertion and cannulation. Participants were placed inside the scanner and asked to remain as still as possible. Extra padding was placed on the head to minimise motion. Firstly, a survey scan was performed, then ASL (CBF) baseline data were collected, after which a 5-minute baseline BOLD fMRI data were acquired. This was followed by the IG infusion of the test meal (fatty acid or saline).

Patients were cannulated for serial (every 15 mins) blood measurements of gut hormones (GLP-1, PYY, CCK) during the fMRI scan. Participants also rated subjective feelings of hunger, fullness and nausea using a handheld controller moving a cursor along a scale from 1 (minimum) to 100 (maximum) on a visual analogue scale (VAS), every 5 minutes. Subjects had their eyes open and scales were projected onto a screen visible from inside the scanner once every 5 min for the duration of the scan.

Following data acquisition participants were asked to remain inside the scanner for 15 minutes until the final blood sample was taken. Figure 16 illustrates the complete details of the fMRI paradigm.

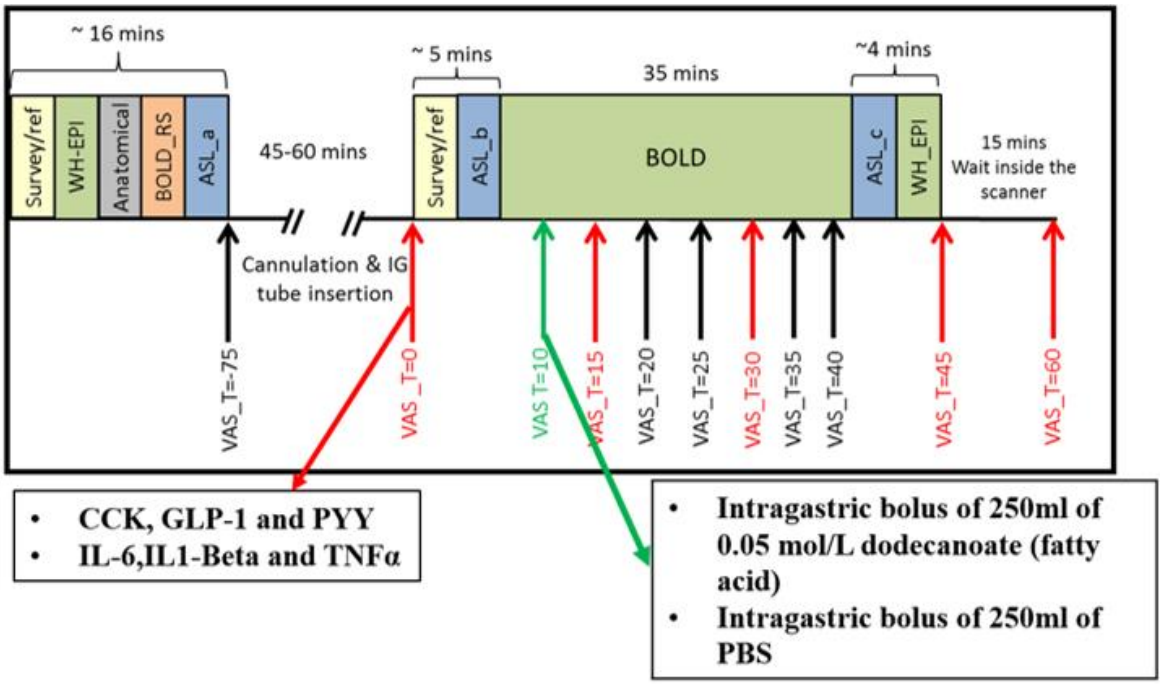


Figure 16. The MRI protocol which comprises the acquisition on a 3T Philips Achieva scanner of the resting-state BOLD fMRI data, structural data and task-induced fMRI data to assess the BOLD response to a nasogastric infusion of fatty acid or saline.

2.8.6 Plasma gut hormone analysis

Centrifugation was performed at the end of the fMRI data acquisition, for 10 mins at 3000g at 4 ºC for plasma and 1000 g at room temperature for 10 mins for serum. The samples were aliquoted and stored at –80ºC.

From the blood plasma samples, total PYY and GLP-1 were assayed in duplicates with commercially available Enzyme-Linked Immunosorbent Assay (ELISA) (total PYY (catalogue no. EZHPYYT66K), (total GLP-1 catalogue no EZGLP1T-36K) kits, Millipore, Billerica, MA, USA as previously described[97], with results read on electronic plate reader Spectra Max 340PC. The assays were performed by lab technicians Melanie Lingaya and Yirga Falcone at the Biomedical Research Centre (BRC) lab. The PYY and GLP-1 ELISAs were performed as follows:

PYY	**GLP-1**
1) Human PYY molecules (both 1~36 and 3~36) were bound in the sample by rabbit anti-human PYY IgG and immobilizing the resulting complex to the wells of a microtiter plate coated by a pre-titered amount of anti-rabbit IgG antibodies and the simultaneous binding of a second biotinylated antibody to the PYY **3)** Unbound materials were washed away, followed by conjugation of horseradish peroxidase (HRP) to the immobilized biotinylated antibodies, **4)** Free enzyme conjugates were washed away	**1)** GLP-1 total molecules were captured from samples to the wells of a microtiter plate coated by a pre-titered amount of anti- GLP-1 polyclonal antibody **2)** Unbound materials from samples were washed away. **3)** A biotinylated anti- GLP-1 monoclonal antibody was bound to the captured molecules **4)** Unbound materials from samples were washed away followed by conjugation of HRP to the immobilized biotinylated antibodies **5)** Free enzyme conjugates were washed away

These steps were followed by the quantification of immobilized antibody-enzyme conjugates by monitoring HRP activities in the presence of the substrate 3, 3', 5, 5'- tetra-methylbenzidine (TMB). The enzyme activity was measured spectrophotometrically by the increased absorbency at 450 nm, corrected from the absorbency at 590 nm, after acidification of formed products. Since the increase in absorbency is directly proportional to the amount of captured GLP-1 Total and captured human PYY (both 1~36 and 3~36) in the unknown sample, the latter can be derived by interpolation from a reference curve generated in the

same assay with reference standards of known concentrations of human GLP-1 and PYY.

CCK plasma was analysed by our collaborators at Copenhagen University Hospital (Prof. Jens. F. Rehfeld). The technique involved the use of activated charcoal in the radioimmunoassay (RIA), using the rabbit antibody 92128 that binds to sulphated CCK-8[200]. *(Readers note: please find the CCK RIA analysis protocol in the appendix of this thesis).*

Please note: The CCK radioimmunoassay was discontinued by its manufacturer Euro Diagnostica in October 2017. Several alternative ELISA kits were used; however, the results were unsatisfactory (later found high cross-reactivity with gastrin). CCK RIA optimisation was being carried out by Dr Gulzar Singh in our lab, however, this process was time-consuming, therefore samples were sent to Copenhagen University for analysis.

2.8.7 Statistical analysis for EEC peptides

The three groups were compared using a two-way ANOVA and Bonferroni post hoc multiple comparisons for observed means. Repeated measures ANOVA were used to identify differences in EEC peptides between postprandial time points. Values for incremental AUC (iAUC) were calculated using differences from baseline. Values were considered positive when they were higher than baseline values, and negative when they were lower than baseline values. The area above or below the baseline was calculated using the trapezoid rule[201]

2.8.8 Cytokine analysis

Serum levels of IL-6, IL-1 β, TNFα were measured using immunoassay kit (Duoset ELISA Development, R&D Systems, Inc, USA). The ELISA was performed by PhD student Lissa Sutherland at the School of Life Sciences (University of Nottingham). The assay was performed as follows:

1. IL-6, IL-1 β and TNFα specific capture antibodies were bound to 384 well microplates. The unbound capture antibodies were washed away. The plates were then blocked and washed.

2. The serum samples or standards were added, and any analyte present was bound by the immobilised antibody. The unbound materials were washed away.

3. Streptavidin-HRP was used to bind to the detection antibody. The unbound streptavidin-HRP was washed away.

4. TMB substrate solution was added to the wells developing a blue colour in proportion to the amount of analyte present in the sample. The colour development was stopped using a stop solution to prevent turning the colour in the wells to yellow.

5. The amount of IL-6, TNFα and IL-1β were determined by measuring absorbance at 450nm. All samples and standards were measured in duplicates. IL-6, IL-1 β, and TNFα were expressed in pg/ml.

2.8.9 fMRI data analysis

fMRI data were pre-processed using SPM 12 https://www.fil.ion.ucl.ac.uk/spm/software/spm12/ [SPM12; Wellcome Department of Cognitive Neurology, University of London] running on MATLAB [The MathWorks, Natick, MA]. Slice timing correction was applied to the first and second echo EPI images. The first echo images were then motion corrected to the first volume data space and the motion parameters were subsequently applied to the second echo images. The individual registration motion parameters for the fMRI data were inspected visually and any subject who moved more than two voxels (>6mm) during the fMRI paradigm was excluded from the study. T_2* maps were calculated from the four echo data sets using a pixel-by-pixel, linear weighted least-squares fit and used for weighted summation[1] of the two datasets acquired during the fMRI session. T_2* maps were calculated and the combination of the two fMRI datasets was performed for each subject for each session using in-house programs written by Prof. Susan Francis. The fMRI datasets were then co-registered to the anatomical 160 slices dataset, followed by the normalisation of the anatomical 160 slices data set to the standard SPM EPI template. The fMRI dataset was then spatially normalised to the standard SPM EPI template using these co-registration and normalisation parameters. Spatial smoothing was 6 x 6 x6 mm FWHM, global scaling and temporal filtering with a 3000s high pass filter was applied to remove any drift in the fMRI data during the long acquisition. A GLM was formed, where individual motion parameters, and white matter (WM) and cerebrospinal fluid (CSF) signals were included in the design matrix as covariances-of-no-interest.

The fat and saline were modelled as a 5-minute box function convolved with a canonical HRF.

Contrast vectors were formed to identify the CNS response to the fatty acid and saline in each group. **Table 9** shows the contrast vectors used to create statistical maps of brain regions associated with a decrease/increase in BOLD signal. Since the time course of the BOLD response was unknown, and different regions may have different temporal responses. Two analyses were performed: (i) Baseline compared to all post feed bins, and (ii) Baseline compared to post feed bin5 maps. These results were pooled in a second level, random-effects group analysis (RFX) and active brain areas displayed at a $P < 0.005$, uncorrected k > 10.



Post feed all bins	Bin5 only
• (baseline > post feed all bins) saline • (baseline > post feed all bins) fat • (post feed all bins > baseline) saline • (post feed all bins > baseline) fat	• (baseline > bin5) saline • (baseline > bin5) fat • (Bin 5 > baseline) saline • (Bin 5 > baseline) fat

Table 9 Contrasts used to create statistical maps of brain regions with an increase/decrease in BOLD signal

Please note that at the time of this analysis, CCK concentrations could not be used as a parametric modulator in the 1st level analysis in the fMRI model (results of the analysis of CCK data arrived from Copenhagen only one week before this thesis deadline), but these will be used in future work, see Discussion.

2.9 Results

2.9.1 Recruitment

Figure 17 shows the number of participants included in the brain fMRI data analysis. Please refer to Figure 70 in Chapter 6 which shows the summary consort diagram of the number of participants that appeared in each chapter.

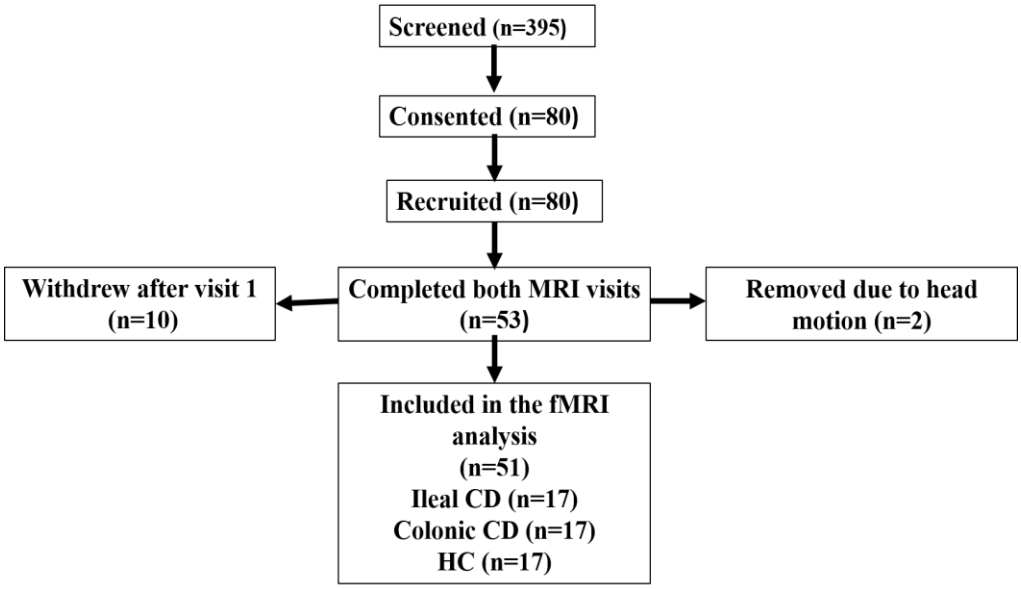


Figure 17 Consort diagram illustrating the number of participants included in this chapter.

2.9.2 Subject demographics

17 active ileal CD patients, 17 colonic CD patients and 17 age, BMI, and gender-matched HCs were included in the postprandial fMRI assessment. Demographics for the CD and HC groups are provided in Table 10

	Ileal [n=17]	**Colonic [n=17]**	**HC [n=17]**	**Significance [2-tailed]**
Age [years]	33.5 ± 3.5	36.2 ± 4.1	33 ± 3.2	NS
BMI [kg/m^2]	25.7 ± 1.2	25.2 ± 1.2	24 ± 0.8	NS
Gender [M/F]	11 M, 6F	11 M, 6F	11M, 6F	
Disease duration [years]	8 ± 2	6 ± 1		NS
HBI	4.0 ± 0.6	4.4 ± 0.8		NS
IBD-QoL	4.3 ± 0.2	4.7 ± 0.3		NS
IBD-Fatigue	11.4 ± 0.8	10.4 ± 1.3		NS
CRP [mg/dl]	9.5 ± 2.0	37 ± 18		NS
FCP [µg/g]	624 ±210	734 ± 182		NS
TNF alpha [pg/ml]	92.0 ± 72	120 ± 61	65 ± 50	NS
IL-6 [pg/ml]	47 ± 16	92 ± 36	50 ± 17	NS
IL-1β [pg/ml]	141 ± 115	254 ± 109	58 ± 21.5	NS

Table 10 Demographic and clinical characteristics of ileal CD, colonic CD and HC. Values presented as mean ± SEM. HBI scores (<5 remission, 5-7= mild disease, 8-16 = moderate disease, >16 = severe disease IBD QoL scores (ranges from 1 to 7, where 1= poor , 7= optimum), IBD fatigue score= (ranges from 0 to 20, where 0 = no fatigue, 1 to 10 = moderate fatigue, 11 to 20 = severe fatigue. 49% of CD patients were on Anti-TNF therapy and 36% were on immunosuppressants and 14.3% on nil treatment

2.9.3 Sensation ratings before and after the fat and saline test meal

Figure 18 shows the sensation ratings for fullness, bloating, distension, abdominal pain and nausea/sickness. Bloating is indicated by the sensation of abdominal swelling, whereas abdominal distension is defined by an actual increase in measured abdominal size[202].

In response to the fat meal, HCs showed a significant postprandial increase in fullness and bloating ($P<0.05$). Significant postprandial increase in fullness was found in HCs in response to the saline meal ($P<0.05$). No significant increase was found in the distension, abdominal pain, nausea/sickness in response to both saline and fat meal in HCs.

Ileal CD patients showed a significant postprandial increase in fullness, bloating, distension, pain, nausea in response to the fat meal ($P<0.05$). In response to the saline meal, ileal CD patients showed a significant increase in fullness and bloating ($P<0.05$), however, no increase was found in sensations of distension, pain and nausea. Colonic CD patients showed a significant increase in fullness, bloating, abdominal pain ($P<0.05$), but not in distension and nausea in response to both the fat and saline meal.

Group comparison showed that in response to the fat meal, the ileal CD patients showed greater fullness compared with HCs, whilst the colonic CD patients showed greater distension than HCs. In response to saline intake, ileal CD patients had greater bloating than HCs, and ileal CD patients had greater abdominal pain than HCs. However, the multivariate analysis showed no group meal interactions

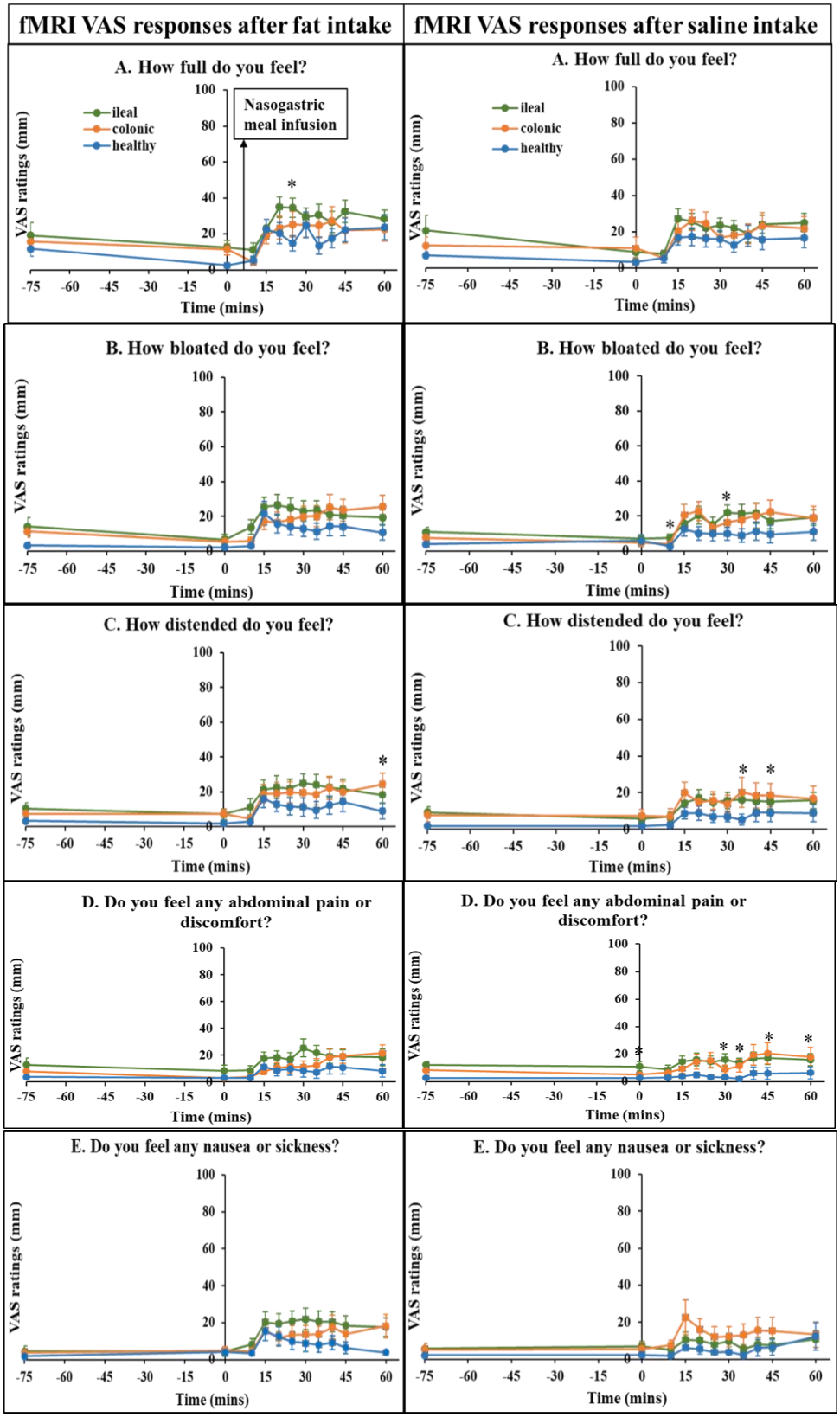


Figure 18 fMRI VAS responses after fat intake (column 1) and after saline intake (column 2) and associated significant difference for A) Fullness – Ileal > HC, for fat at time point 25 (P<0.05). B) Bloating at time points T10 and T30 for saline Ileal> HC (P<0.05).C) Distension – Colonic >HC at time point 60 (P<0.05) for fat and timepoints T35 and T45 for saline ileal > HC P<0.05 D) Abdominal pain and discomfort – timepoints T0, T30, T35, T45, T60 for saline for Ileal >HC P<0.05. E) Nausea or sickness. Two-way multivariate analysis showed no disease location- meal interactions.

2.9.4 Comparison of baseline and postprandial concentrations of GLP-1, CCK and PYY in ileal CD, colonic CD and HC

Figure 19 shows the fasting and postprandial GLP-1, PYY and CCK concentrations in response to fat and saline in the ileal CD, colonic CD and HC groups.

A significant difference was found in the fasting concentrations of GLP-1 ($P<0.05$) between ileal CD patients and HC. No difference was found in the fasting PYY and CCK concentrations between the groups.

GLP-1 : Group comparisons showed significant differences between ileal-HC at T0 and ileal-HC at T45 in response to fat. In response to saline, group comparisons showed a significant difference between ileal-HC at T0, ileal-HC at T15. The aforementioned postprandial differences were a result of the higher fasting baseline GLP-1 concentrations seen in the ileal CD patients.

PYY: Group comparisons showed no significant differences between the groups in response to fat. Group comparisons showed significant differences between ileal-HC at T15 and colonic-HC at T60 in response to saline. Similar to GLP-1, the postprandial differences observed were a result of variations in the fasting baseline PYY concentrations between the groups.

CCK:. As anticipated, a significant postprandial increase in CCK concentrations was found in the ileal CD, colonic CD and HC group in response to fat. However, group comparisons showed no significant differences between the groups in response to fat and saline.

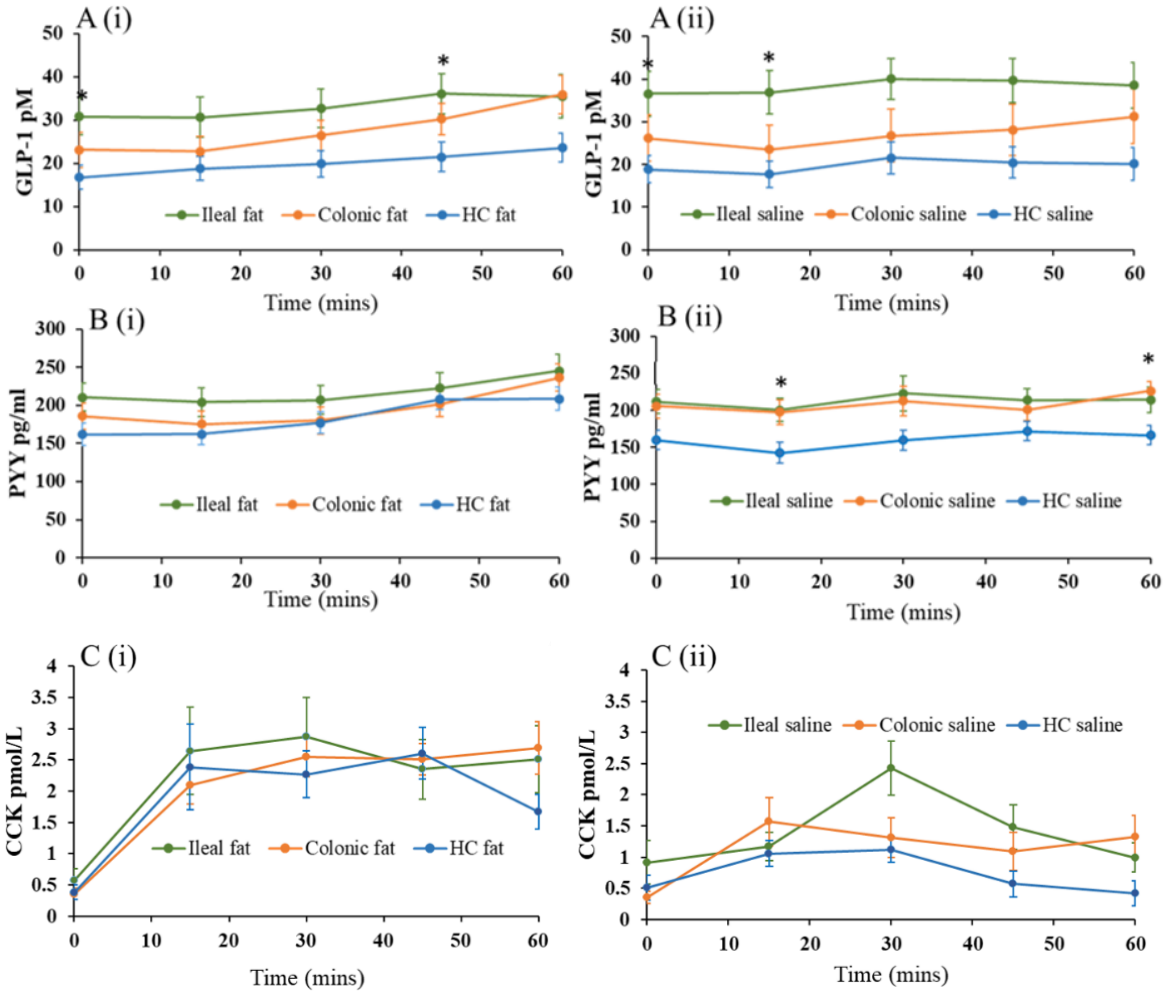


Figure 19 A. Postprandial GLP-1 concentrations in response to (i) fat and (ii) saline in the ileal CD, colonic CD and HC group. B. Postprandial PYY concentrations in response to (i) fat and (ii) saline in the ileal CD, colonic CD and HC group. C. Postprandial CCK concentrations in response to (i) fat and (ii) saline in the ileal CD, colonic CD and HC group. *P<0.05, significant differences between groups, using 2 way ANOVA and post-doc Bonferroni multiple comparisons between groups for each meal. Multivariate analysis showed no interactions between the groups and meals.

GLP-1: No significant difference in GLP-1 concentrations was found in the postprandial iAUC between the fat and saline meal in the ileal group and colonic CD group respectively, but a significant difference was found in the HC group between meals. For the fat meal condition, a significant difference was found at the fasting baseline between ileal-HC (P<0.05), no difference was found in the iAUC between the three groups. For the saline meal condition, a significant difference was found at fasting baseline, no difference was found in the iAUC between the three groups.

PYY: No significant difference in PYY concentrations was found in the postprandial iAUC between the fat and saline meal in the ileal CD group, colonic CD group and HC. For both the fat and saline meal condition, no difference was found in the iAUC between the 3 groups.

CCK: Significant differences in CCK concentrations were found in the postprandial iAUC between the fat and saline meal in the ileal CD group, the colonic group and HC group. For both the fat and saline meal conditions, no significant difference was found in fasting baseline and iAUC between the 3 groups.

Table 11 shows the baseline and area iAUC above or below baseline using trapezoid rule for GLP-1, PYY and CCK.

			Ileal	Colonic	HC
PYY (pg/ml)	Baseline fasting values	Fat	211 ± 18	186 ± 17	162 ± 15
		Saline	212 ± 16	206 ± 16	160 ± 13
	Incremental (AUC)	Fat	280 ± 537	928 ± 384	1288 ± 358
		Saline	-87 ± 370	899 ± 803	413 ± 315
GLP-1 (pM)	Baseline fasting values	Fat	31 ± 4 **	23 ± 4	17 ± 3**
		Saline	37 ± 5	26 ± 5	19 ± 3
	Incremental (AUC)	Fat	105 ± 64	169 ± 84	201 ± 47*
		Saline	108 ± 106	96 ± 71	56 ± 51*
CCK (pmol/L)	Baseline fasting values	Fat	0.6 ± 0.2	0.4 ± 0.1	0.4 ± 0.1
		Saline	0.9 ± 0.3	0.4 ± 0.1	0.5 ± 0.2
	Incremental (AUC)	Fat	102 ± 28***	104 ± 14***	106 ± 18***
		Saline	29 ± 18***	44 ± 13***	13 ± 16***

Table 11 Fasting and iAUC values (above or below baseline values using trapezoid rule) for PYY, GLP-1 and CCK for the ileal, colonic and HC in the fat and saline condition. *P<0.05 iAUC GLP-1 (fat vs saline meal), **P<0.05 GLP-1 baseline fasting values (Ileal CD-HC), ***P<0.05 iAUC CCK (fat vs saline meal)

2.9.5 Comparison of BOLD responses to the fat and saline meals

In this section, the increase/decrease in BOLD response to fat and saline is assessed. This is first studied for the whole study population (combined CD+HC participants) to determine key brain regions that respond to saline and fat separately. The analysis is then separately assessed for the (i) combined CD group, (ii) ileal CD group, (iii) colonic CD group, and (iv) HCs.

2.9.6 Effect of meal on cortical responses across the whole study group

This section provides results of the whole group (CD+HC) effect of the BOLD response to each of the fat and saline meals. **Figure 20** shows the BOLD response to the (baseline > postprandial) contrast for fat and saline separately, highlighting a decrease in BOLD activation in the DMN and superior frontal gyrus following each of the meals. Note a greater decrease in BOLD response following the saline meal compared to the fat meal in the superior frontal gyrus. Note: The baseline BOLD signal is contrasted to the post-feed BOLD signal in all bins (bins 1 – 5) in maps shown in A (i) and B(i), whilst baseline is contrasted to bin 5 in maps shown in A (ii) and B(ii). This was performed in order to determine if different regions may have different temporal responses, which will be investigated in future by incorporating CCK concentrations in the fMRI model. It can be seen that the strongest responses are observed for baseline contrasted to post feed all bins (bins 1 – 5), and so this model is used for subsequent results figures.

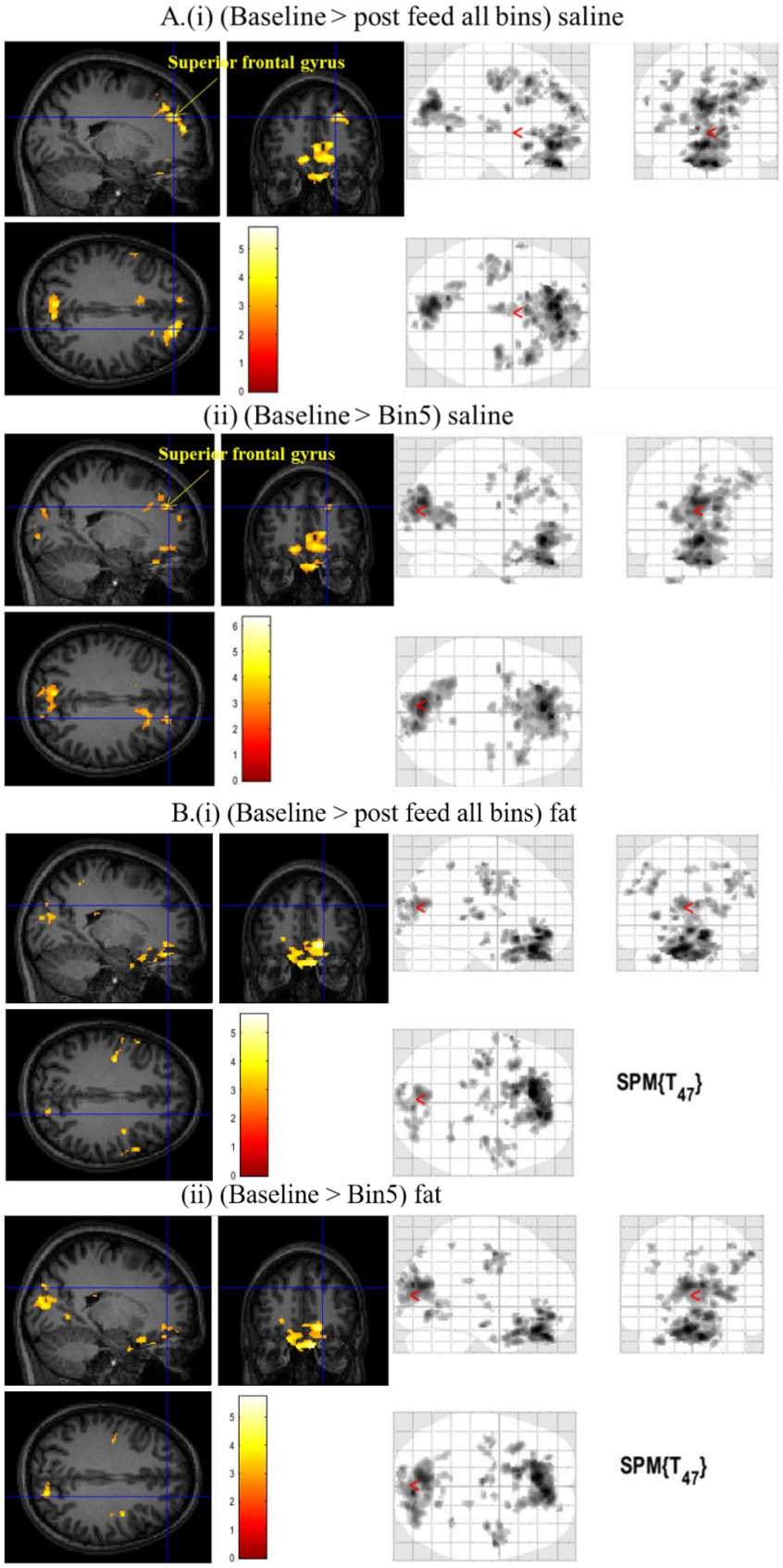


Figure 20 (Baseline > postprandial) responses highlighting activity in the DMN and superior frontal gyrus. Greater activation was found in the superior frontal gyrus for saline compared to fat. Data are shown in for saline in A(i) (Baseline > post feed all bins) saline and (ii) (Baseline > Bin5) saline, and for fat in B(i) (Baseline > post feed all bins) fat (ii) (Baseline > Bin5) fat. Images displayed at P<0.005, uncorrected, k=10, T=2.68.

Table 12 details those areas showing significant responses to the (baseline >post feed all bins) contrast for the saline meal across the whole study group.

Area	uncorrected p (peak level)	Z score (voxel level)	MNI coordinates x	y	z	Cluster size (k)
Frontal medial cortex (DMN)	0.000	4.97	-4	38	-30	2142
Left cuneus (DMN)	0.000	4.70	-6	-76	22	1291
Superior frontal gyrus	0.000	4.34	20	44	30	717
Subcallosal cortex	0.000	4.10	0	10	-16	60
Right accumbens	0.000	4.02	8	18	-4	70
Right precentral gyrus	0.000	3.99	38	-16	38	198
Left lateral ventricle	0.000	3.95	-14	12	26	74
Central opercular cortex	0.000	3.72	-38	-8	20	56
Anterior cingulate gyrus	0.000	3.69	-2	-14	46	159
Precentral gyrus	0.000	3.68	-32	-22	44	143

Table 12 Areas showing significant responses to baseline >postprandial for the saline condition across the whole study group, P<0.005, uncorrected.

Table 13 details the areas showing significant responses to (baseline >post feed all bins) contrast for the fat meal across the whole study group.

Area	uncorrected p (peak level)	Z score (voxel level)	MNI coordinates x	y	z	Cluster size (k)
Frontal medial cortex	0.000	4.90	-14	32	-26	2496
Temporal pole	0.000	3.93	-32	14	-34	90
Left putamen	0.000	3.91	-32	-18	6	56
Left postcentral gyrus	0.000	3.89	-34	-12	36	160
Left cuneus	0.000	3.87	-4	-72	18	710
Right precentral gyrus	0.000	3.67	36	-14	38	269
Left thalamus	0.000	3.57	-14	-36	4	15
Left precentral gyrus	0.000	3.55	-58	12	28	11
Right superior parietal lobule	0.000	3.52	36	-46	52	40
Left occipital pole	0.000	3.51	-8	-96	20	34
Right lateral ventricle	0.000	3.45	16	-30	20	30
Middle frontal gyrus	0.000	3.43	-50	16	38	21

Table 13 Areas showing significant responses to baseline >postprandial for the fat condition, across the whole study group, P<0.005, uncorrected.

Figure 21 shows the (postprandial > baseline) BOLD responses for all bins. Greater BOLD responses were found postprandially in areas including the cerebellum, hippocampus, thalamus, and brain stem. **Table 14** details those areas showing significant responses to (postprandial > baseline) for the saline meal across the whole study group and **Table 12** shows the brain regions for the fat meal. *Please note*, since there was a stronger response for (post feed all bins > baseline) than (bin5> baseline), therefore the latter is not shown for this

condition. Further comparing the meals, there was a greater BOLD response in the PCG to the fat meal as compared with the saline meal, **Figure 21**.

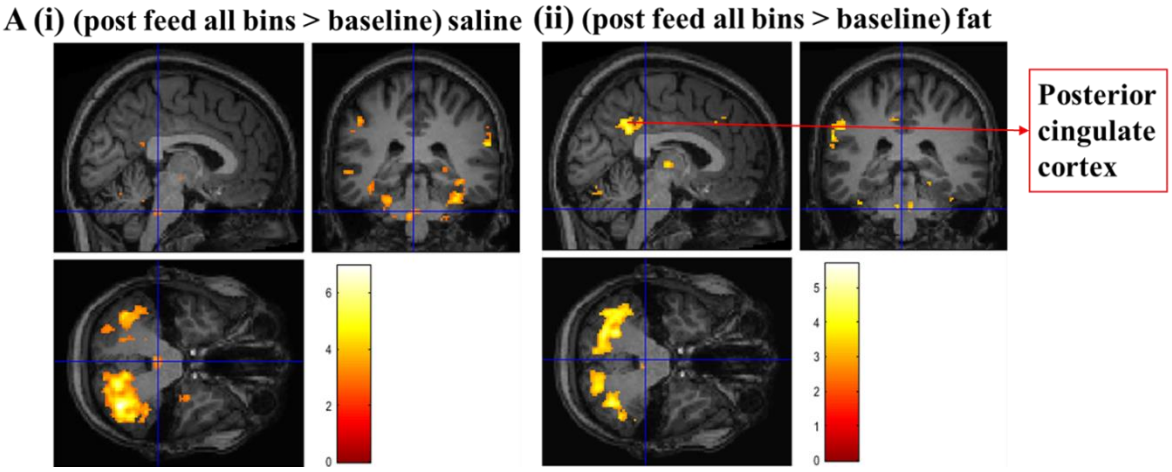


Figure 21: Postprandial > baseline responses for A(i) (post feed all bins > baseline) saline (ii) (post feed all bins > baseline) fat. Greater PCG activation was found in response to fat compared with saline. Images displayed at P<0.005, uncorrected, k=10, T=2.68.

Area	uncorrected p (peak level)	Z score (voxel level)	MNI coordinates x	y	z	Cluster size (k)
Cerebellum	0.000	5.73	38	-68	-36	7337
Right inferior parietal lobule	0.000	4.24	62	-36	22	92
Right thalamus	0.000	4.18	8	-16	-2	85
Left insular cortex	0.000	4.14	-36	-10	-10	107
Right inferior parietal lobule	0.000	4.08	58	-44	32	25
Right middle temporal gyrus	0.000	3.85	60	-8	-12	28
Brain stem	0.000	3.75	-6	-36	-40	62
Supra-marginal gyrus	0.000	3.68	-54	-32	30	64
Left amygdala	0.000	3.39	-24	-2	-24	22
Left lateral orbital gyrus	0.000	3.38	-40	42	-14	36
Left middle temporal gyrus	0.000	3.36	-58	-34	-2	26
Left fusiform gyrus	0.000	3.34	-40	-36	-16	62
Left PCG	0.001	3.23	-4	-46	22	12
Right angular gyrus	0.001	3.22	56	-58	16	19
Left angular gyrus	0.001	3.20	-42	-58	28	24
Right middle cingulate gyrus	0.001	3.05	2	-12	32	14
Left middle temporal gyrus	0.001	3.00	-54	-16	-16	10
Right supramarginal gyrus	0.001	2.99	60	-22	22	17

Table 14 Areas showing significant responses to postprandial > baseline for the saline condition across the whole study group, P<0.005, uncorrected.

Area	uncorrected p (peak level)	Z score (voxel level)	MNI coordinates x	y	z	Cluster size (k)
Cerebellum	0.000	4.93	36	-64	-36	4269
Right hippocampus	0.000	4.73	40	-10	-18	367
Right supramarginal gyrus	0.000	4.34	64	-24	22	46
Left PCG	0.000	4.17	-2	-50	32	269
Left supramarginal gyrus	0.000	4.07	-56	-34	32	175
Left middle temporal gyrus	0.000	4.05	-56	-60	10	385
Left temporal pole	0.000	3.76	-52	10	-4	84
Right mid temporal gyrus	0.000	3.68	58	-6	-14	12
Left thalamus	0.000	3.53	-2	-16	2	60
Right fusiform gyrus	0.000	3.36	34	-28	-24	54
Right central operculum	0.001	3.28	52	6	-2	21
Medulla	0.001	3.27	2	-32	-30	61
Right middle temporal gyrus	0.001	3.22	50	-52	10	101
Left fusiform gyrus	0.001	3.16	-40	-38	-32	17
Left supramarginal gyrus	0.001	3.11	-56	-48	26	12
Right frontal pole	0.001	3.11	42	38	-6	18
Right frontal pole	0.001	3.08	32	48	-2	16
Left cerebellum	0.001	3.00	-32	-74	-58	16
Left supramarginal gyrus	0.002	2.99	-58	-24	22	15
Right planum polare	0.002	2.97	42	14	-16	13
Left temporale pole	0.002	2.94	-46	14	-12	15
Superior middle frontal gyrus	0.002	2.87	-4	30	38	13
Right lingual gyrus	0.003	2.77	22	-74	-4	11

Table 15 Areas showing significant responses to postprandial > baseline for the fat condition, across the whole study group, P<0.005, uncorrected.

2.9.7 Effect of meal on cortical responses across the combined CD group

In this section, the BOLD response to the fat and saline meal in the combined CD group (i.e. ileal CD + colonic CD) only is assessed **Figure 22A** shows the

(baseline > postprandial) responses, in the CD group only a greater decrease in BOLD response following the saline meal compared to fat meal was found in the superior frontal gyrus. **Figure 22B** shows the (postprandial > baseline) responses, greater PCG activation was found in response to fat compared with saline in the combined CD group. **Table 16** and **Table 17** detail the areas in the combined CD group showing significant responses to (postprandial > baseline) for the saline and fat condition respectively.

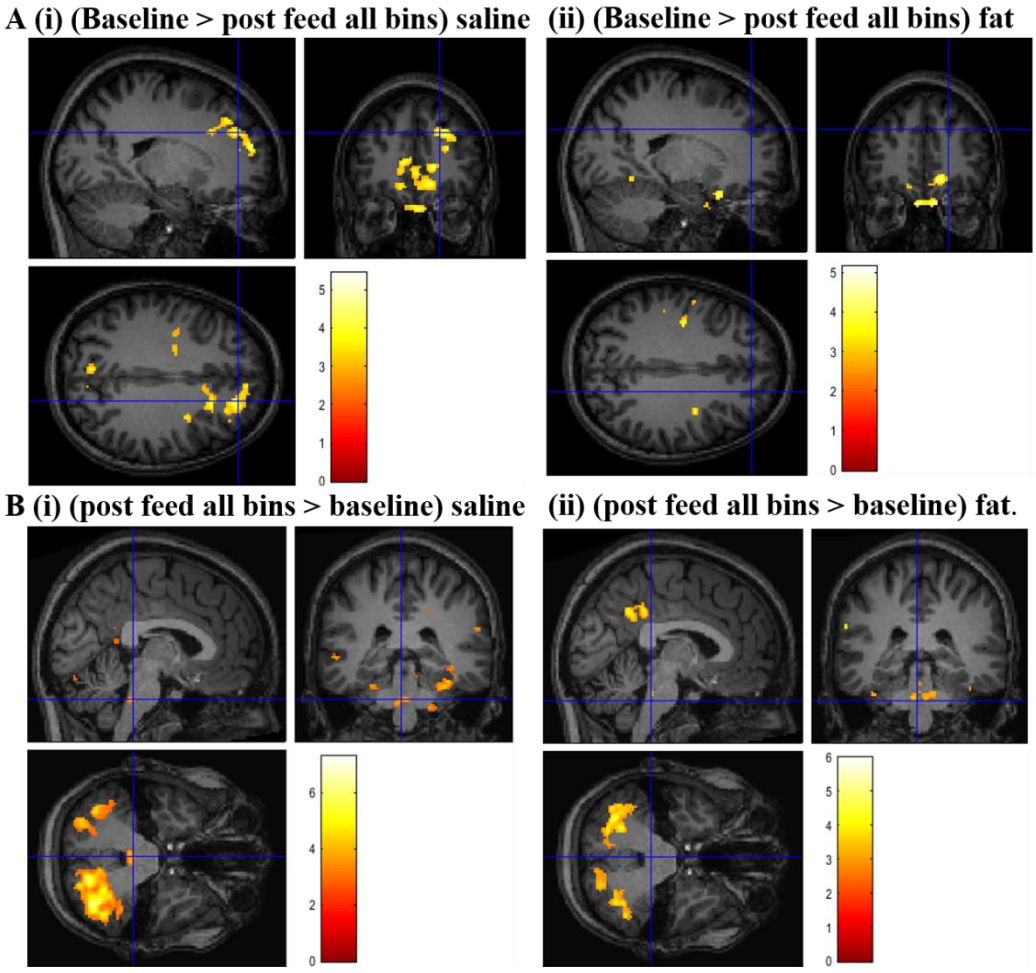


Figure 22 A) (Baseline > postprandial) responses, greater activation was found in the superior frontal gyrus for saline compared to fat in the combined CD group. (i) (Baseline > post feed all bins) saline (ii) (Baseline > post feed all bins) fat. B) shows postprandial > baseline responses, where greater PCG activation was found in response to fat compared with saline in the combined CD group (i) (post feed all bins >baseline) saline (ii) (post feed all bins >baseline) fat. Images displayed at P<0.005, uncorrected, k=10, T=2.7.

Area	uncorrected p (peak level)	Z score (voxel level)	MNI coordinates x	y	z	Cluster size (k)
Right cerebellum	0.000	5.52	42	-64	-28	5411
Left cerebellum	0.000	5.01	-42	-64	-34	1322
Right posterior insula	0.000	4.18	40	-2	10	97
Right thalamus proper	0.000	4.02	10	-18	-2	67
Left fusiform gyrus	0.000	4.02	-26	-32	-26	70
Left inferior occipital gyrus	0.000	3.99	-46	-74	-16	189
Brain stem	0.000	3.79	-4	-38	-38	48
Left temporal gyrus	0.000	3.56	-56	-36	-2	22
Right inferior occipital gyrus	0.000	3.42	42	-66	2	65
Left PCG	0.001	3.40	-4	-50	10	21
Left inferior temporal gyrus	0.001	3.30	-42	-18	20	36
Left amygdala	0.001	3.29	-26	-2	-26	13
Right temporal pole	0.001	3.21	54	10	-16	29
Left middle temporal gyrus	0.001	3.18	-50	-52	14	25
Left middle temporal gyrus	0.001	3.17	-54	-64	12	115
Right supramarginal gyrus	0.001	3.15	60	-36	22	11
Right middle temporal gyrus	0.001	3.13	50	-56	8	21
Left cerebellum	0.001	3.08	-20	-40	-42	21
Left middle occipital gyrus	0.001	3.08	-44	-72	12	10
Left PCG	0.001	3.06	-4	-48	22	13
Left planum polare	0.001	3.03	-48	4	-12	15
Left cerebellum	0.001	3.03	-12	-46	-34	16
Right thalamus proper	0.001	2.99	22	-32	4	13
Left cerebellum	0.002	2.97	-22	-86	-30	12
Right supramarginal gyrus	0.002	2.88	56	-44	30	10
Left angular gyrus	0.002	2.79	-42	-64	16	10

Table 16 Areas showing significant responses to postprandial > baseline for the saline condition, in the combined CD group, P<0.005, uncorrected.

Area	uncorrected p (peak level)	Z score (voxel level)	MNI coordinates x	y	z	Cluster size (k)
Right cerebellum	0.000	4.84	52	-68	-28	1567
Right insular cortex	0.000	4.36	38	-8	-12	230
Left cerebellum	0.000	4.33	-34	-64	-40	1006
Right middle temporal gyrus	0.000	3.84	60	-6	-14	11
Right frontal pole	0.000	3.84	40	36	-6	68
Left frontal pole	0.000	3.80	-40	38	0	20
Left PCG	0.000	3.79	0	-52	34	198
Left inferior temporal gyrus	0.000	3.77	-46	-64	-12	92
Right planum temporale	0.000	3.59	58	-56	14	24
Left supramarginal gyrus	0.001	3.56	-62	-34	24	10
Left temporale pole	0.001	3.52	-50	10	-4	43
Left frontal operculum	0.001	3.47	-40	26	2	62
Brain stem	0.001	3.46	4	-34	-32	144
Left fusiform gyrus	0.001	3.39	-40	-42	-22	26
Right fusiform gyrus	0.001	3.20	26	-40	-20	13
Left angular gyrus	0.001	3.20	-30	-58	28	14
Right middle occipital gyrus	0.001	3.16	36	-78	40	38
Left cerebellum	0.001	3.16	-38	-66	-58	15
Right inferior lateral ventricle	0.001	3.15	24	-18	-12	32
Left superior temporale gyrus	0.001	3.13	-56	-52	14	20
Left planum polare	0.001	3.07	-52	-4	2	12
Right lateral occipital cortex	0.001	2.97	28	-56	36	11

Table 17 Areas showing significant responses to postprandial > baseline for the fat condition in the combined CD group.

2.9.8 Comparing the effect of the test meal on cortical responses between the ileal and colonic CD group

Here, the BOLD responses in the ileal and colonic CD groups alone to the fat and saline meals are assessed and contrasted. **Figure 23A** shows the (baseline >

postprandial) response. In the ileal CD group, a greater decrease in BOLD response following the saline meal compared to the fat meal was found in the superior frontal gyrus. **Figure 23B** shows the (postprandial > baseline) responses, there was greater PCG activation in response to fat than saline in the ileal CD group, there was greater cerebellum activity in response to saline than fat. **Table 18** and **Table 19** detail the areas showing significant responses to (postprandial > baseline) for the saline condition and fat condition in the Ileal CD group. For comparison, colonic CD group BOLD responses to the fat and saline meal are shown in **Figure 24**. **Figure 24A** shows (baseline > postprandial) responses, a greater decrease in BOLD response in the DMN was found for saline compared to fat, however no decrease in BOLD response was found in the superior frontal gyrus in the colonic group, indicating this activation in the combined CD group was driven by the ileal CD group. **Figure 24B** shows the (postprandial > baseline) responses in the colonic group. Greater PCG activation was found in response to fat compared with saline in the colonic CD group and highlights that the PCG activation in the CD group response is driven by the colonic group. **Table 20** and **Table 21** detail the areas showing significant responses in the colonic CD group to (postprandial > baseline) for the saline and fat condition.

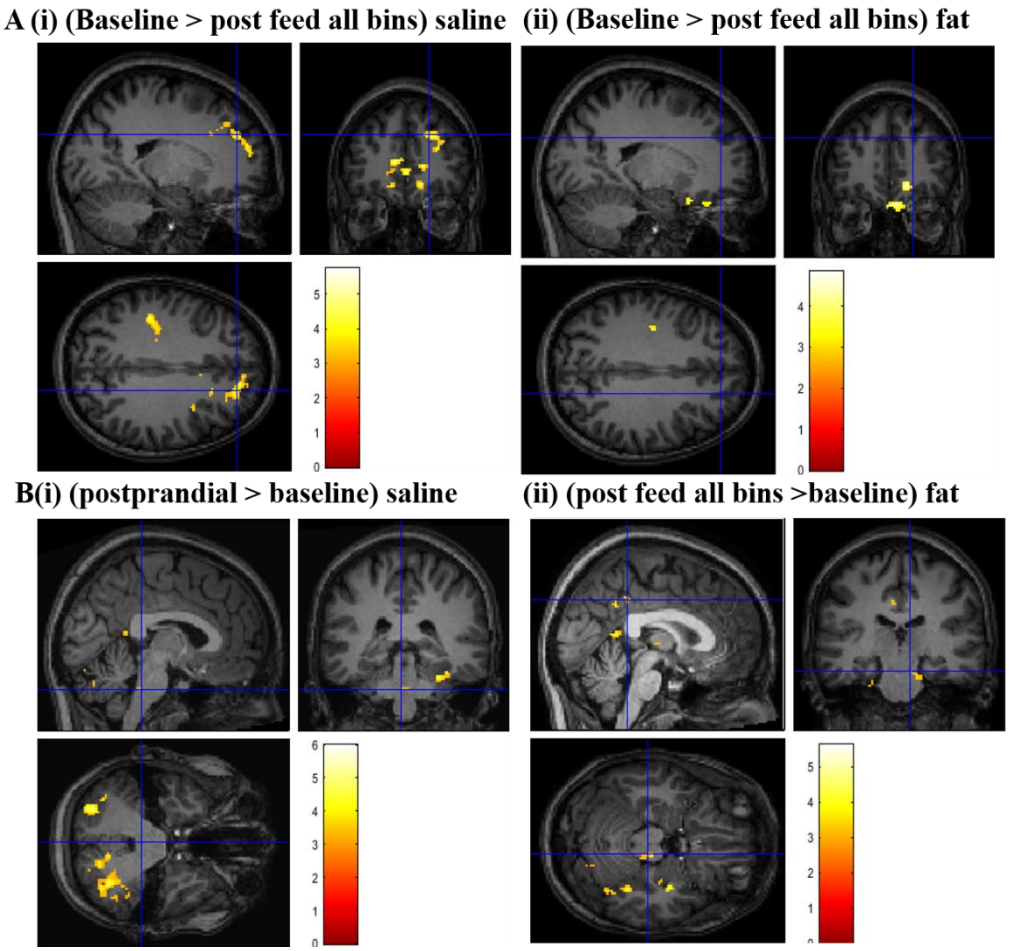


Figure 23 Baseline > postprandial responses, where greater DMN activation was found in the superior frontal gyrus for saline compared to fat in the ileal CD group. **A(i)** (Baseline > post feed all bins) saline **(ii)** (Baseline > post feed all bins) fat **B(i)** shows postprandial > baseline responses, where greater PCG activation was found in response to fat compared with saline in the ileal CD group (post feed all bins >baseline) saline **(ii)** (post feed all bins >baseline) fat.

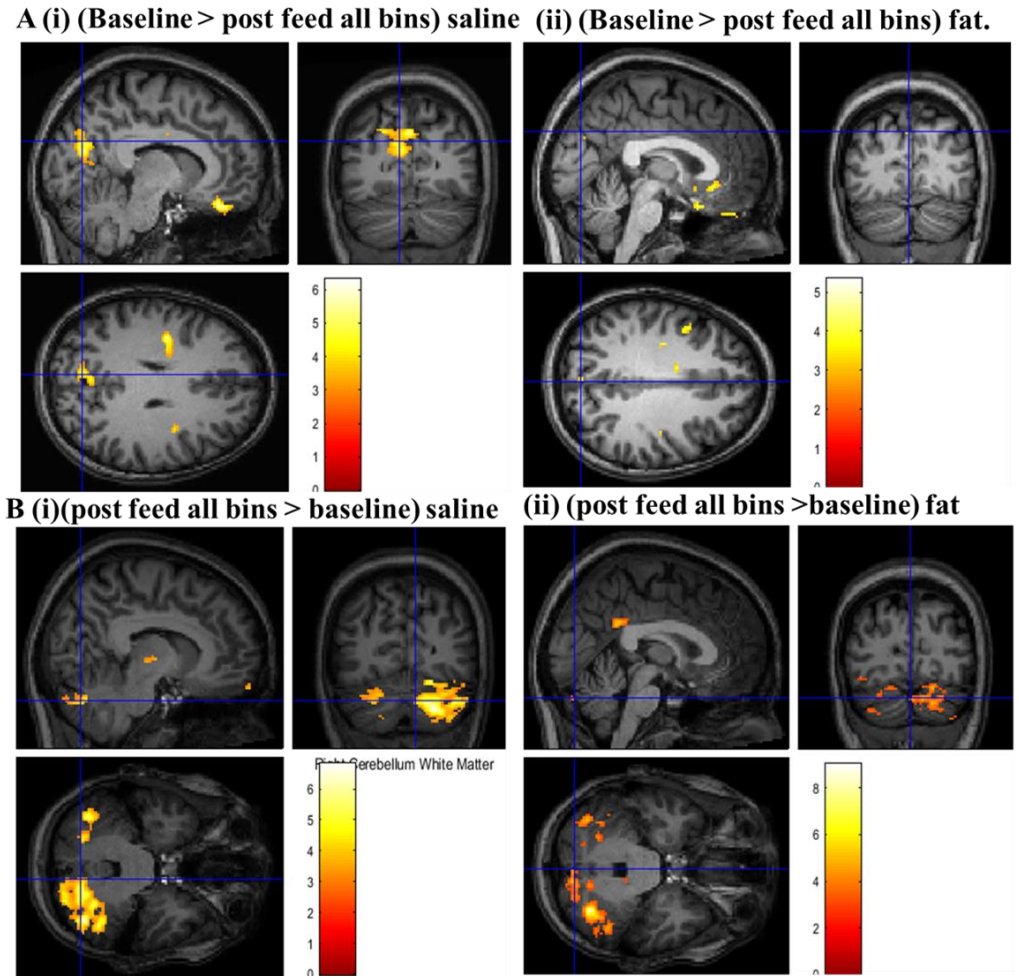


Figure 24 A) shows baseline > postprandial responses, where greater DMN activation was found for saline compared to fat in the colonic CD group. (i) (Baseline > post feed all bins) saline – *note superior frontal gyrus did not survive* (ii) (Baseline > post feed all bins) fat. B) shows postprandial > baseline responses, where greater PCG activation was found in response to fat compared with saline in the colonic CD group (i) (post feed all bins > baseline) saline (ii) (post feed all bins >baseline) fat -note this activation is stronger in the colonic group compared with the ileal CD group.

Area	uncorrected p (peak level)	Z score (voxel level)	MNI coordinates x	y	z	Cluster size (k)
Right PHG	0.000	4.28	20	-14	-32	136
Right cerebellum	0.000	4.06	34	-64	-40	1387
Left cerebellum	0.000	3.93	-30	-80	-42	263
Left lateral occipital cortex	0.000	3.55	-32	-68	18	187
Left occipital fusiform gyrus	0.000	3.49	-34	-64	-6	74
Right precuneus	0.000	3.46	10	-62	20	24
Left inferior occipital gyrus	0.000	3.44	-46	-74	-16	32
Left lingual gyrus	0.000	3.43	-12	-84	-12	10
Right fusiform gyrus	0.000	3.35	38	-12	-28	55
Right cerebellum	0.000	3.35	16	-72	-38	64
Right middle temporal gyrus	0.000	3.32	46	-50	4	64
Left fusiform gyrus	0.000	3.30	-26	-32	-26	21
Left inferior temporal gyrus	0.000	3.28	-44	-20	-20	26
Left lingual gyrus	0.001	3.20	-20	-60	-6	10
Left middle temporal gyrus	0.001	3.17	-50	-50	6	13
Left middle occipital gyrus	0.001	3.14	-44	-80	16	14
Left PCG	0.001	3.11	-2	-48	12	10
Left cerebellum	0.001	3.02	-42	-48	-32	22
Right cerebellum	0.001	2.97	42	-52	-46	16
Brain stem	0.001	2.86	4	-38	-36	13
Left cerebellum	0.001	3.10	-26	-70	-24	15

Table 18 Areas showing significant responses to postprandial > baseline for the saline condition in the Ileal CD group.

Area	uncorrected p (peak level)	Z score (voxel level)	MNI coordinates x	y	z	Cluster size (k)
Right amygdala	0.000	4.12	38	-6	-20	77
Right supramarginal gyrus	0.000	3.94	66	-22	22	38
Right thalamus proper	0.000	3.71	8	-18	0	30
Left PCG	0.000	3.49	2	-52	10	42
Right insular cortex	0.000	3.46	36	-6	2	13
Left PHG	0.000	3.40	-26	-22	-32	11
Right cerebellum	0.000	3.39	48	-50	-34	50
Right occipital fusiform gyrus	0.000	3.32	36	-64	-18	28
Right fusiform gyrus	0.000	3.27	32	-8	-34	15
Left precuneus	0.001	3.26	0	-52	34	15
Left cerebellum	0.001	3.23	-38	-64	-42	57
Brain stem	0.001	3.07	10	-22	-22	38
Right cerebellum	0.001	3.55	26	-70	-44	22
Left cerebellum	0.001	3.55	-20	-66	-48	13
Left frontal operculum	0.001	3.53	-38	28	6	14
Right occipital fusiform gyrus	0.002	3.49	16	-82	-4	27
Right central operculum	0.002	3.48	54	-16	20	11
Right putamen	0.002	3.44	30	-18	-8	21
Left middle temporal gyrus	0.002	3.42	-52	-58	-2	15
Left midcingulate gyrus	0.002	3.41	-2	-24	36	10
Right cerebellum	0.002	3.38	16	-78	-24	12
Left precuneus	0.002	3.38	0	-44	42	17
Right temporal occipital fusiform cortex	0.002	3.33	24	-8	-44	12

Table 19 Areas showing significant responses to postprandial > baseline for the fat condition in the ileal CD group.

Area	uncorrected p (peak level)	Z score (voxel level)	MNI coordinates x	y	z	Cluster size (k)
Right cerebellum	0.000	4.45	30	-58	-30	2420
Left cerebellum	0.000	4.37	-42	-66	-36	361
Right hippocampus	0.000	4.29	36	-28	-12	699
Right opercular cortex	0.000	3.74	48	-4	2	20
Left putamen	0.000	3.62	-16	0	-8	34
Left temporale pole	0.000	3.54	-44	14	-14	38
Brain stem	0.000	3.41	-2	-50	-38	25
Left temporal fusiform cortex	0.001	3.39	-38	-34	-20	27
Brain stem	0.001	3.33	-4	-36	-44	21
Left lateral ventricle	0.001	3.22	-18	-40	24	60
Right thalamus proper	0.001	3.15	8	-18	-2	32
Paracingulate gyrus	0.001	3.09	2	-48	-30	11
Right frontal pole	0.001	2.98	-14	40	12	21
Left occipital fusiform cortex	0.002	2.89	-36	-66	-8	13
Left putamen	0.002	2.88	-30	-12	-6	13
Left cerebellum	0.002	2.82	-20	-32	-28	16

Table 20 Areas showing significant responses to postprandial > baseline for the saline condition in the colonic CD group, P<0.005, uncorrected.

Area	uncorrected p (peak level)	Z score (voxel level)	MNI coordinates x	y	z	Cluster size (k)
Right cerebellum	0.000	5.10	34	-68	-34	1008
Left PCG	0.000	3.81	0	-48	28	114
Left cerebellum	0.000	3.81	-28	-70	-38	392
Right fusiform gyrus	0.000	3.73	44	-54	-14	154
Right anterior insula	0.000	3.62	32	28	-2	191
Left posterior orbital gyrus	0.000	3.59	-36	24	-10	19
Left temporale pole	0.000	3.51	-50	14	-16	25
Right PCG	0.000	3.51	14	-16	34	10
Right amygdala	0.000	3.44	28	-6	-24	63
Right fusiform gyrus	0.000	3.41	38	-16	-42	12
Right angular gyrus	0.000	4.30	58	-56	24	11
Right central operculum	0.000	4.29	50	8	0	24
Right insular cortex	0.000	4.19	38	-8	-12	25
Left cerebellum	0.001	3.98	-12	-78	-42	46
Left cerebellum	0.001	3.94	-28	-86	-42	25
Left occipital fusiform gyrus	0.001	3.92	-40	-76	-18	18
Right inferior temporal gyrus	0.001	3.82	52	-60	-14	25
Right amygdala	0.001	3.81	22	-8	-14	14
Left cerebellum	0.001	3.74	-46	-56	-34	11
Left cerebellum	0.001	3.70	-32	-70	-52	14
Left cerebellum	0.001	3.70	-26	-62	-46	38
Right middle temporal gyrus	0.001	3.65	56	-6	-36	11
Right superior temporal gyrus	0.001	3.65	58	-44	12	13

Table 21 Areas showing significant responses to postprandial > baseline for the fat condition in the colonic CD group, P<0.005, uncorrected.

2.9.9 Effect of meal on cortical responses across the HC group

As a comparator, this section shows results in the HC group alone. **Figure 25A** shows (baseline > postprandial) responses. A greater decrease in BOLD response in the DMN was found following the saline meal compared to the fat meal in the HC group. **Figure 25B** shows the (postprandial > baseline) responses, little PCG activation was found indicating this activation is driven by CD patients, particularly the colonic CD group.

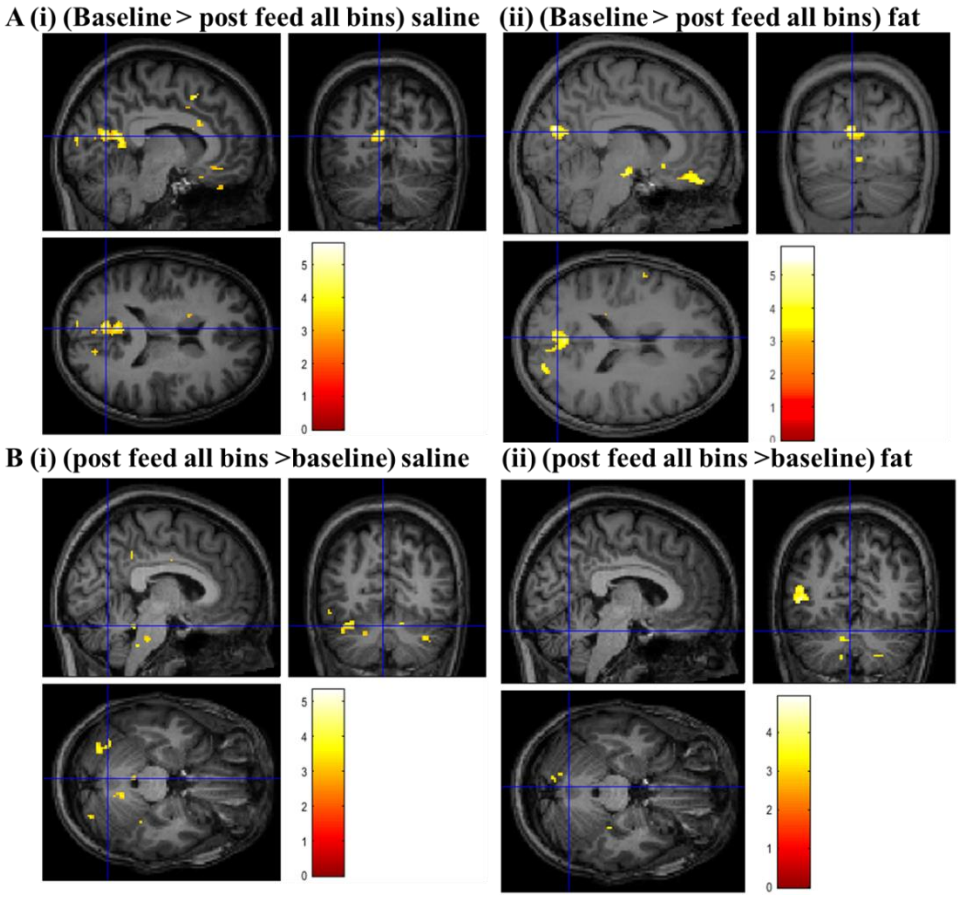


Figure 25 A) shows baseline > postprandial responses, where greater DMN activation was found in the saline condition compared to fat in the HC group. (i) (Baseline > post feed all bins) saline (ii) (Baseline > post feed all bins) fat. B) shows postprandial > baseline responses, where *no PCG activation* was found in response to fat compared with saline in the HC group (i) (post feed all bins >baseline) saline (ii) (post feed all bins >baseline) fat.

Table 22 and **Table 23** detail the areas showing significant responses in the HC group to (postprandial > baseline) for the saline and fat condition respectively.

Area	uncorrected p (peak level)	Z score (voxel level)	MNI coordinates x	y	z	Cluster size (k)
Right posterior insula	0.000	3.94	40	-2	-4	42
Left postcentral gyrus	0.000	3.78	-44	-26	36	36
Right parietal operculum	0.000	3.67	62	-24	22	23
Right parietal operculum	0.000	3.48	-24	-2	-20	13
Left entorhinal area	0.000	3.48	38	-4	-14	52
Brain stem	0.000	3.47	-6	-40	28	11
Right supramarginal gyrus	0.000	3.47	62	-34	22	19
Inferior frontal gyrus	0.000	3.41	54	16	-2	33
Right fusiform gyrus	0.000	3.35	40	-24	-16	43
Left parietal operculum	0.000	3.34	-48	-40	30	11
Right cerebellum	0.000	3.32	34	-76	-32	41
Left middle frontal gyrus	0.000	3.29	-34	44	10	28
Right inferior occipital gyrus	0.001	3.28	42	-78	-18	33
Brain stem	0.001	3.22	2	-30	-42	66
Right cerebellum	0.001	3.22	14	-64	-24	65
Right cerebellum	0.001	3.22	34	-68	-38	62
Left cerebellum	0.001	3.21	-44	-64	-34	117
Left lateral orbital gyrus	0.001	3.21	-40	48	-16	28
Left fusiform gyrus	0.001	3.20	-38	-42	-10	29
Left middle temporal gyrus	0.001	3.19	-52	-58	-8	13
Right midcingulate gyrus	0.001	3.18	6	-8	32	15
Right inferior temporal gyrus	0.001	3.17	56	60	-16	45

Table 22 Areas showing significant responses to postprandial > baseline for the saline condition in the HC group, P<0.005, uncorrected.

Area	uncorrected p (peak level)	Z score (voxel level)	MNI coordinates x	y	z	Cluster size (k)
Left middle temporal gyrus	0.000	3.74	-54	-50	4	296
Left supramarginal gyrus	0.000	3.50	-54	-34	34	98
Left middle frontal gyrus	0.000	3.48	-38	46	12	17
Right planum polare	0.000	3.47	42	-10	-18	24
Left cerebellum	0.000	3.41	-20	-70	-34	136
Left middle occipital gyrus	0.000	3.35	-34	-78	36	28
Right cerebellum	0.000	3.35	10	-36	-42	10
Left cerebellum	0.000	3.31	-40	-74	-34	22
Right supramarginal gyrus	0.000	3.30	62	-24	26	18
Right occipital fusiform gyrus	0.001	3.21	36	-84	-16	12
Left putamen	0.001	3.09	-32	0	-2	69
Left middle frontal gyrus	0.001	3.65	-38	40	22	17
Right cerebellum	0.001	3.62	24	-48	-20	18
Right ventral	0.001	3.59	20	-20	-6	10
Right cerebellum	0.002	3.46	20	-68	-48	12
Right fusiform gyrus	0.002	3.36	38	-30	-22	11
Left cerebellum	0.002	3.34	-12	-64	-44	12

Table 23 Areas showing significant responses to postprandial > baseline for the fat condition in the HC group.

2.10 Discussion

This chapter studies the postprandial gut hormone and BOLD responses in patients with active ileal and colonic CD and HCs. The key findings are:

- CD patients had significantly higher ratings compared with HC for fullness, distension, bloating, abdominal pain and discomfort.
- Fasting baseline concentrations of GLP-1 in the ileal CD patients were significantly higher compared with HC, no difference was found between ileal and colonic CD patients. No difference was found in the postprandial GLP-1 concentrations iAUC between the three groups
- No significant difference was found in the fasting baseline concentrations of PYY between the 3 groups. No difference was found in the postprandial PYY concentrations iAUC between the three groups
- A significant postprandial increase in CCK concentrations was found in ileal CD, colonic CD and HC group in response to fat. No significant difference was found in the fasting baseline and postprandial CCK concentrations iAUC between the 3 groups for both fat and saline conditions. The probable explanation for this is that the absence of co-localisation of intestinal inflammation and the location of the CCK secreting I cells in the proximal gut rather than in the distal ileum and colon.
- In all subjects, both saline and fat-induced a decrease in BOLD response following the meal in the DMN, in addition, there was a greater decrease in the superior frontal gyrus for the saline meal compared with the fat

meal. It was found that this response in the superior frontal gyrus was driven by the ileal CD patients.

- In all subjects, in the postprandial time points, there were greater BOLD responses in areas including cerebellum, hippocampus, PCG, middle temporal gyrus, thalamus and medulla in response to fat, which is in agreement with previous findings by Lassman et al[157]. In the PCG, the BOLD response was greater following the fat meal compared with the saline meal. The activity of this region was driven by CD patients, with colonic CD patients showing stronger activation in this region compared with the ileal CD patients.

2.10.1 Comparison of sensation ratings following the fat and saline test meal

In response to the fat meal, HCs showed a significant postprandial increase in fullness and bloating. Significant postprandial increase in fullness was found in response to the saline meal. No significant increase was found in the distension, abdominal pain, nausea/sickness in response to both saline and fat meal in HCs. Ileal CD patients showed a significant postprandial increase in fullness, bloating, distension, pain, nausea in response to the fat meal. In response to the saline meal, ileal CD patients showed a significant increase in fullness and bloating, however, no increase was found in sensations of distension, pain and nausea. Colonic CD patients showed a significant postprandial increase in fullness, bloating, abdominal pain, but not in distension and nausea in response to both the fat and saline meal.

Group comparison showed that in response to the fat meal, the ileal CD patients showed greater fullness compared with HCs, whilst the colonic CD patients

showed greater distension than HCs. In response to saline intake, ileal CD patients had greater bloating than HCs, and ileal CD patients had greater abdominal pain than HCs. However, the multivariate analysis showed no group meal interactions. These findings indicate that ileal CD patients are more sensitive to meal-induced symptoms such as nausea and abdominal pain, which is in agreement with a previous study[95], These symptoms could have been driven through the central anorectic effects of GLP-1 or through a state of intestinal hypomotility in the CD patients as our research has very recently shown[203]

2.10.2 Comparison of fasting and postprandial GLP-1, CCK and PYY concentrations

This section discusses the fasting and postprandial changes in GLP-1, CCK and PYY in response to the fat and saline test meal.

The fasting baseline concentration of GLP-1 in the ileal CD patients was significantly higher compared with HCs, no difference was found between the ileal and colonic CD patients. This is the first study to show an increase in fasting plasma GLP-1 concentrations in ileal CD patients, which is in line with previous findings that showed an increase in GLP-1 positive cells in the ileal tissue of active CD patients[94]. Significant differences were found between ileal-HC at T0, and ileal-HC at T45, in response to fat. This finding is reflective of higher baseline concentrations seen in the ileal CD group. No difference was found in the iAUC in response to fat between these three groups. These findings contrast with a previous study[95] where no significant difference was found in the postprandial GLP-1 levels between the ileal CD, colonic CD and HCs. This inconsistency could be due to differences in the test meal nutrient composition, which had a low protein and fat content. However, an increase in postprandial

GLP-1 has been reported in active CD patients relative to HCs [188,189] in response to higher fat and protein content test meals, where an elevated GLP-1 level was associated with delayed gastric emptying[189]. Group comparisons showed a significant difference between ileal-HC at T0, ileal-HC at T15 in response to saline, which could be attributed to the differences seen in the fasting GLP-1 concentrations between the two groups. It could be that the lack of nutrient stimulation leading to more power in detecting differences between the groups, whereas the fat meal would have stimulated a response, abolishing any differences between groups. Although, no difference was found in the postprandial GLP-1 iAUC in response to saline

No difference was found in the fasting baseline and postprandial PYY concentrations between the 3 groups in response to fat. This finding contrasts with a previous study[95], where ileal CD patients showed greater postprandial PYY concentrations compared with colonic CD patients and HCs. This inconsistency may be attributed to differences in the test meal nutrient composition, where a lower fat/protein meal was used. In contrast, other studies that used higher fat/protein test meals reported no postprandial differences in the PYY concentrations between CD patients and HCs[188,189]. In response to saline, significant differences were found between ileal-HC at T15 and colonic -HC at T60. These findings may be reflective of baseline differences between groups and the lack of nutrient stimulation leading to more power in detecting differences between the group. No difference was found in the postprandial PYY iAUC in response to saline.

As anticipated, a significant postprandial increase in CCK concentrations was found in the ileal CD, colonic CD and HC group in response to fat, although no

significant difference was found between the three groups. The probable explanation for this is that the absence of co-localisation of intestinal inflammation and the location of the CCK-secreting I cells in the proximal gut rather than in the distal ileum and colon. The aforementioned finding of this present study, contrasts a previous study[188], where a significant difference in CCK postprandial concentrations was found between CD patients and HCs, however, the difference in that study was found to be driven by only 4 patients with exclusive ileal CD. A significant postprandial increase in CCK concentrations was found in the ileal CD patients at T30, but not in the colonic CD and HC groups in response to saline, no significant difference was found between the three groups. The saline induced postprandial increase in CCK may be attributed to gastric distension.

2.10.3 Comparison of postprandial BOLD responses to fat and saline

To determine key brain regions that response to saline and fat, the whole study population was first grouped together resulting in greater statistical power to study meal specific BOLD responses. The ileal CD, colonic CD and HCs were then assessed separately to determine group specific BOLD responses to the fat and saline meals.

In the whole group maps, a greater decrease in BOLD response following the meal was found in the superior frontal gyrus in the DMN for the saline condition compared with the fat condition. Previous studies have reported feeding induced decrease in DMN activity in response to glucose[139,140] and amino acids[141]. Non-nutrient stimulus (e.g. plain water) induced decrease in DMN activity has also

been reported, where a linear decrease in BOLD response was shown in the precuneus[142,144](part of the DMN) with increasing water consumption.

The increase in postprandial BOLD activity in the brainstem (medulla), thalamus, cingulate gyrus and middle temporal gyrus and cerebellum **Table 15** in response to the C12 fat meal is in agreement with the previous findings[157]. In this study, greater BOLD activity was found in the PCG compared to baseline for the fat condition compared with saline.

2.10.4 Feeding induced DMN activity in CD patients

Both ileal and colonic CD patients were combined (i.e. ileal CD + colonic CD) to assess the meal specific BOLD responses in patients. Similar to the whole study group findings, a greater decrease in BOLD response following the meal was found in the right superior frontal gyrus (RSFG) in the DMN for the saline condition compared with the fat condition in the combined CD group. Analysis of the ileal CD, colonic CD and HC groups separately, showed that the greater decrease in BOLD response following the meal in the RSFG in the saline condition was preferentially driven by the ileal CD patients (as the RSFG was only activated in the ileal CD group and not in colonic CD and HC groups). The frontal lobe of the brain has been implicated in impulsive behaviours[204], and in particular, the RSFG[205] has been implicated in the control of impulse response. Studies have shown a feeding induced reduction in DMN activity. The mechanisms underlying this phenomenon is not understood and is thought to be linked with the activity of the cholinergic and glutamatergic neurotransmitter systems[139] as described in section 2.2 of this thesis.

2.10.5 Postprandial increase in BOLD signals in response to fat and saline compared between groups

The greater activity in the PCG in the fat condition was found to be driven by the CD patients, where colonic CD group showed a greater response than ileal CD patients and HCs showed no activation of this region. The activity of the cingulate cortex has been implicated in CD, where the PCC is thought to have a role in self-monitoring of sensory stimuli such as visceral pain[206]. Studies in CD patients in remission have shown increased anterior and PCG activity in response to visceral pain[207], and greater midcingulate activity has been reported in response to mental stress[208]. Reduction in PCG activity has been reported following anti-TNF α treatments in CD patients in response to a test of implicit attribution biases regarding sickness/health[209]. In the present study, the PCG activation is specific to CD patients in response to fat. Both colonic and ileal CD patients showed a significant postprandial increase in abdominal pain in response to the fat meal. It could be postulated that abdominal pain may be one of the factors inducing the greater PCG activity in CD patients. Although, lower BOLD activations in the anterior[90] and PCG[210] have been reported in obese patients after RYGB surgery in response to viewing high-calorie foods[90], with reduced desire to eat, and reduced liking of high-calorie foods possibly linked with elevated postoperative GLP-1 and PYY concentrations[90]. As shown in the eating behaviour chapter of this thesis, ileal CD patients exhibited explicit liking and wanting bias for high-fat foods, which may be related to emotional and comfort eating behaviours to alleviate symptoms such as low mood, abdominal pain and chronic fatigue. In HCs, the sad emotion-induced activity of the PCG is found to be attenuated by C12 fatty acid infusions[165]. It could be postulated

that the lower activity in PCG in the ileal CD patients, could be linked with the upregulation GLP-1 hormone and not driven by inflammation as, no difference was found in the proinflammatory cytokines (TNFα, IL-6, IL-1β) between the ileal and colonic CD groups and HCs. Therefore, it is not possible to postulate whether the reduced PCG activity is a fat-induced attenuation in homeostatic-hedonic response compared to colonic CD, or a response linked with abdominal pain

2.11 Conclusion

This chapter assessed the postprandial gut hormone and BOLD responses in patients with active ileal and colonic CD. A greater postprandial decrease in BOLD response was found in the RSFG in the DMN in response to the saline meal compared with the fat meal, which was driven by ileal CD patients. The greater postprandial activity in the PCG was found to be driven by the CD patients, where colonic CD group showed a greater response than ileal CD patients and HCs showed no activation of this region. To confirm, if the PCG activity is linked with CCK, GLP-1 or PYY, further analysis is required including these measures in the fMRI model. At the time of completing this work, the CCK plasma data were not available. For future analysis, statistical maps will be formed of those regions which correlate with CCK levels and fullness ratings by using these measures as parametric modulators and results pooled in a second level, random-effects group analysis.

This experiment has its limitations. The experiments were not blinded to the student. Patient standardisation was another limitation, due to variations in disease duration, the severity of inflammation and medication use. The test meal

used in this study specifically stimulated CCK, a different test meal with mixed nutrients (protein, CHO and fat) may have shown stronger postprandial responses in GLP-1 and PYY. The habitual diets of the participants were not assessed using FFQ or weighed food records, to see if the fat stimulus was comparable between groups. However, based on the 24-hour recall there was no difference in fat intake between the 3 groups.

3 Eating behaviour in active CD

This chapter studies eating behaviour traits, impulsivity traits, subjective hedonic measures of explicit liking and implicit wanting for food, dietary intake and satiety in patients with active ileal CD, colonic CD and in HCs.

3.1 Disordered eating and CD

Disordered eating might be linked with a disruption in homeostatic and hedonic balance. Presently, the cross-link between eating behaviour and active CD is still in its infancy. Patients with gastrointestinal disorders are at higher risk of disordered eating patterns such as meal skipping, food restriction and binge eating[211,212]. A disordered eating behaviour may be described with a two-path theoretical model[211,212]. The first pathway describes feelings of heightened anxiety about unfamiliar foods and overestimation of the negative consequences linked with their disease. The second pathway describes the type of behaviour which employs techniques to lose weight to counteract weight gain induced by medical or dietary interventions. 62.5% of IBD patients consider dietary issues to be extremely important, with patients specifically with CD having suffered from unintentional weight loss[213]. Three-fourths of patients with IBD with the active disease suffer from appetite loss[173], with 37% of CD patients showing abnormal eating patterns[214].

3.2 Psychological disturbances and CD

Psychological disturbances have been reported in CD with strong associations with surgical history, disease complications (such as EIM), smoking and female gender[215,216]. In theory, malnutrition could influence mood due to abnormal

metabolism of monoamines such as serotonin, dopamine and noradrenaline by the CNS as a result of deprivation of nutrients involved in the synthesis of these neurotransmitters [217]. Mood disorders have been found to be more prominent in the active phase of the disease than remission with higher rates in CD than UC [218]. CD patients are more likely to require hospitalisation, medical and surgical procedures increasing financial burden and stress that could worsen psychological symptoms [215]. Higher incidences of mood swings have also been reported in female patients with CD [219].

In the UK, there is inadequate access to psychological support services for IBD patients[220]. Studies have shown that psychological therapy/antidepressant interventions, resulted in significant improvements in fatigue and energy levels, emotional, social functioning and QoL in IBD patients[221–225]. At present, a long-term follow-up study is still required to demonstrate whether the beneficial effects of psychological support are sustainable, and a cost-effectiveness analysis needs to be carried out to provide additional evidence of the value of psychological services for IBD patients. Based on the available evidence, psychological interventions and dietetic advice may have a positive impact on rectifying disordered eating behaviours in active CD.

3.3 EEC peptides and CD

Appetite and satiety involve complex interactions between homeostatic and hedonic factors. The enteroendocrine-gut brain axis is critical to homeostatic control of food intake, and other neural circuits integrate emotional and environmental cues to constitute the hedonic drive of appetite regulation[226]. EEC play a central role in orchestrating physiological functions in the gastrointestinal

tract. Sensing the nutrient content of the lumen, they secrete multiple peptides and amines that control gut secretory and motor function. Gut hormones act on vagal afferents in the gastrointestinal tract, directly relaying to key CNS nuclei that interface within the hypothalamus and other cortical areas to regulate food intake. Reduced appetite observed in ileal CD has been attributed to the upregulation of EEC and the consequent increase of satiety hormones secretion, therefore possibly negatively affecting appetite signalling to the CNS[94–96] (as described in detail in section 2.5 of this thesis)

3.4 Aims & Objectives

The aim of this study was to compare between ileal CD, colonic CD and HC groups i) eating behaviour traits ii) impulsivity traits (iii) subjective hedonic measures of explicit liking and implicit wanting for food (iv) dietary intake (v) appetite sensations following a preload and satiety capacity of an ad libitum test meal between ileal CD, colonic CD and HC groups

3.5 Methods

The following outlines the methods performed in this PhD thesis to assess eating behaviour traits in CD.

3.5.1 Eating behaviour constructs

Eating behaviour traits were measured through four validated self-reported questionnaires: Three-Factor Eating Questionnaire (TFEQ) Restraint, Disinhibition and Hunger subscales[227], the binge eating scale [228], the Power of Food Scale (PFS)[229]. Control of eating questionnaire (CoEQ) was used to assess perceptions of food cravings and control over meal intake during the previous 7 days[230]. Eating behaviour states were measured through laboratory behavioural tasks; the Go Stop impulsivity paradigm[231] and the Leeds Food Preference Questionnaire (LFPQ)[232].

3.5.2 Three-Factor Eating Questionnaire (TFEQ)

The TFEQ contains 51 items and measures three dimensions of human eating behaviour: Cognitive Restraint of Eating [I], Disinhibition [II], and Hunger [III][233]. Restraint refers to concern overweight control and strategies which are adopted to achieve this. Disinhibition reflects a tendency towards overeating and eating opportunistically in an obesogenic environment. Hunger is concerned with the extent to which hunger feelings are perceived and the extent to which such feelings evoke food intake[234]. Each item scores either 0 or 1 point. The minimum score for factors I, II, and III is therefore 0, with the possible maximum scores being 21, 16, and 14, respectively.

3.5.3 The Binge Eating Scale (BES)

The BES is a 16-item questionnaire that assesses the severity of binge eating tendencies. Eight questions describe the behavioural manifestations of binge eating behaviour and eight describe the feelings and cognitions associated with binge eating. Scores are summed to produce a total score ranging from 0 to 46. Cut-off points have previously been reported denoting mild [≤17], moderate [18–26], and severe [≥27] binge eating behaviours[228,235].

3.5.4 The Power of food scale (PFS)

The PFS is a 15-item questionnaire reflecting the psychological influence of the food environment. It measures the appetite for, rather than consumption of, palatable foods and may be a useful measure of the hedonic impact of food environments replete with highly palatable foods[229]. Items are grouped into three domains according to food proximity; food available but not physically present; food present but not tasted; and food tasted but not consumed.

3.5.5 CoEQ

The CoEQ is a 21-item questionnaire designed to assess the severity and type of food cravings experienced over the previous 7 days. The CoEQ has four subscales: Craving Control, Craving for Savoury, Craving for Sweet, and Positive Mood. Items on the CoEQ are assessed by 100-mm VAS, with items relating to each subscale being averaged to create a final score[236].

3.5.6 Go Stop impulsivity paradigm[231]

Behavioural inhibitory control was measured using a computerised Go-No-Go task, which assesses participants' ability to inhibit a 'go' response when a 'stop'

signal is present. Participants were required to attend to a series of five-digit numbers presented in quick succession and respond via mouse-click when a number matched the previous number displayed (the 'go' signal). If the colour of the number changed from black to red (the 'stop' signal), participants were required to withhold the response. The parameters were set as two blocks with seven-stop trials, 28 no-stop trials and 56 novel trials. Stimuli were presented for 500ms with a 600ms washout between presentations. Four intervals between the 'go' and 'stop' signals were used: 50ms, 150ms, 250ms and 350ms, presented in a randomised order throughout the trials. Percentage correct inhibition on the 'stop' trials was averaged over the four intervals and two blocks to produce a mean response inhibition value (i.e. "Inhibitory Control"). A lower inhibitory control score represents a greater level of impulsivity.

3.5.7 LFPQ

The LFPQ provides a measure of implicit wanting, explicit liking, and explicit wanting. In addition, an 'Appeal Bias' score can be calculated for fat and taste[232]. The computerised procedure included photographs of food items categorised based on fat content (high or low) and taste (sweet or savoury) i.e. (i) high fat and sweet (HFSW), (ii) low fat and sweet (LFSW), (iii) high fat and savoury

(HFSA) (iv) low fat and savoury (LFSA). Table 24 shows a list of food images used in the LFPQ.

Savoury		**Sweet**	
High fat	Low fat	High fat	Low fat
Garlic bread	Salad (baby spinach, cucumber, tomatoes)	Chocolate fingers	Mixed fruit (strawberries and blueberries)
Chips	Broccoli	Doughnut	Smarties
Crisps	Pilau rice	Blueberry muffin	Haribo
Sausage roll	Bread roll	Chocolate bar	Banana

Table 24 Food images used in LFPQ to assess liking and implicit wanting

Participants were given the opportunity to screen the images of food. If there were any food items on the list that participants would never/rarely eat or did not recognise, those foods were replaced by alternative food items. To measure explicit liking, single presentation of a food item was shown, and participants had to rate "how pleasant would you find the taste of this food right now?" on a VAS (100 unit). To measure explicit wanting, an image of a single food item was presented, and participants had to rate "how much do you want some of this food now?" on a VAS (100 unit). To measure implicit wanting, a paired presentation of images of food items was shown where participants had to select their most wanted food ("select the food which you most want to eat right now?") as quickly and accurately as possible. Over 150 trials of each food item were paired against each alternative food item in the list. Participants were not aware of the measurement of their reaction time for each choice, therefore, this measure provided an indication of non-verbal, implicit motivational forces[232,237]. As shown by previous research[238] reaction times were transformed to a standardized 'd-score' (D-RT) using a validated algorithm[239] to improve statistical reliability

and reduce individual variability in total average response speed. A higher implicit wanting score indicated a faster relative reaction time for that food type.

Further analysis was done to compute fat and sweet appeal bias as follows:

1) Fat appeal bias, explicit liking (mean score for high fat, explicit liking – mean score for low fat, explicit liking)
2) Fat appeal bias, explicit wanting (mean score for high fat, explicit wanting – mean score for low fat, explicit wanting)
3) Sweet appeal bias, explicit liking (mean score for sweet, explicit liking – mean score for non- sweet, explicit liking)
4) Sweet appeal bias, explicit wanting (mean score for sweet, explicit wanting – mean score for non- sweet, explicit wanting)
5) Fat appeal bias, implicit wanting (mean score for high fat, implicit wanting – mean score for low fat, implicit wanting)
6) Sweet appeal bias, implicit wanting (mean score for sweet, implicit wanting – mean score for non-sweet, implicit wanting

Further details about the LFPQ outcome measures can be found in Table 25

Outcome measure	Range	Interpretation
Implicit wanting	-100 - 100	A positive score indicates a more rapid preference for the given food category relative to alternative categories, whereas a negative score reflects the opposite.
Explicit liking	0 - 100	A higher score indicates a greater liking for that category.
Explicit wanting	0 - 100	A higher score indicates a greater wanting for that category.
Fat appeal bias	-100 - 100	A positive score indicates a bias for high-fat versus low-fat foods. There are fat appeal bias scores for implicit wanting, explicit liking, and explicit wanting.
Sweet appeal bias	-100 – 100	A positive score indicates a bias for sweet versus savoury foods. There are taste appeal bias scores for implicit wanting, explicit liking, and explicit wanting.

Table 25 Details of the LFPQ outcome measures

3.5.8 Dietary intake

24-hour dietary recall: The Automated Multiple-Pass Method was used to perform the single spontaneously administered 24-h dietary recall. This five-step questionnaire can accurately assess dietary consumption and may be administered face-to-face[240]. AN and GT conducted all interviews. A copy of the dietary assessment textbook Carbs and Cals was provided to each participant to facilitate the dietary recall and estimate portion sizes. This book contains over 1700 food and drink photographs and was primarily used to assist in identifying the appropriate food type and portion size consumed. Diet logs were analysed using Nutritics dietary analysis software [Nutritics v4.312 Academic Edition, Ireland].

3.5.9 Quantitative appetite assessment

Figure 26 shows the timeline for the quantitative appetite experiment. Participants arrived at 7:30 am and completed a fasting baseline questionnaire using VAS at 8 am. Participants were given a fixed calorie breakfast meal at 8:15 am and asked to finish it within 15 mins. Appetite sensations were measured using VAS at 30 mins intervals throughout the experiment. Participants received an ad libitum test meal at 1130am, they were asked to eat as much as they could in 15 minutes until they felt comfortably full. The VAS ratings pre and post the Ad libitum eating episode were used to calculate the satiety quotient (SQ) of the Ad libitum meal. In the waiting time period between the preload and ad libitum meal, participants performed the computer-based tasks (LFPQ and Go Stop) and 24-hour recall was also administered.

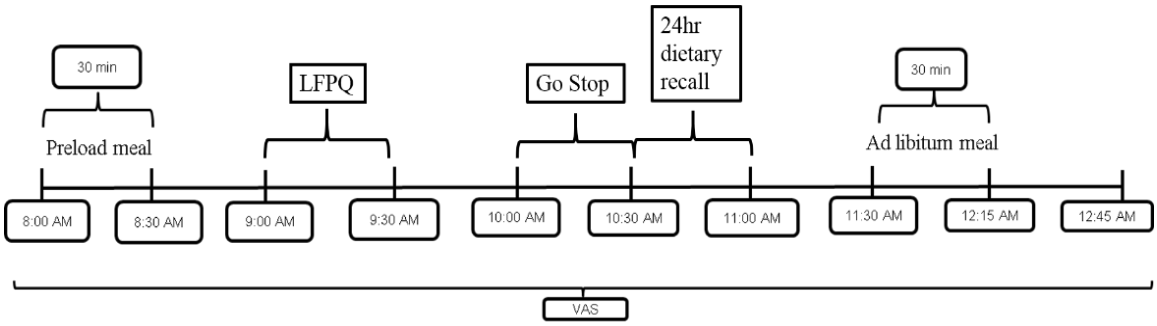


Figure 26. Timeline for quantitative appetite experiment.

3.5.9.1 Fasting and post preload VAS measurements

A fixed quantity preload meal was used in conjunction with appetite ratings as an index of satiety[241]. Participants consumed the preload meal (653 kcal fixed breakfast: 48% protein, 27% fat and 36% CHO defined by % adult reference intake), within 15 minutes. The preload breakfast consisted of 220 ml of orange

juice, 40g bran flakes, 170 ml semi-skimmed milk and, 2 slices of wholemeal bread, each slice with 10g of margarine and one slice with 10g strawberry jam, and the other slice with an 8g slice of cheese Table 26.

Food item	Energy (kcal)	Protein (g)	Fat (g)	CHO (g)
220ml of Sainsbury's basics orange juice from concentrate	88	1.1	1.1	18.5
40g of Sainsbury's wholegrain bran flakes	145	4.0	1.2	27
170 ml semi-skimmed milk	85	6.1	3.1	8.2
2 slices of wholemeal bread	206	11	2.6	32.3
20 g of Sainsbury's sunflower spread	84	0.1	9	0.84
10g of Sainsbury's strawberry jam, basics	24.7	0.05	0.05	5.98
8g Sainsbury's cheesy slices	20.4	1.3	1.4	0.7
total	**653**	**24**	**19**	**93.52**

Table 26 Macronutrient composition of the preload breakfast meal.

Subjective appetite sensations were measured using a 100 mm VAS at 30-minute intervals. The following questions were asked to assess appetite:

"How strong is your desire to eat now?" (Very weak- very strong)

"How hungry do you feel now?" (Not hungry at all- extremely hungry)

"How full do you feel now?" (Not at all – Very full)

"How much food do you think you could eat now?" (Nothing at all – A very large amount)

Composite Satiety Score (CSS) was using the measures for fullness, desire to eat, hunger and prospective food consumption =

[Fullness + (100 – Desire to eat) + (100 – Hunger) + (100 – Prospective food consumption)]/4

3.5.10 SQ

Three hours after finishing the preload meal, satiation was measured with a subsequent ad libitum meal in conjunction with appetite ratings to calculate an SQ. An 800g portion of Tomato and mozzarella pasta bake from Sainsbury's (35% protein, 22% CHO, 19% fat as defined by % adult reference intake and an energy content of 4.73kJ/g) per 400g pack was initially provided followed by 250g portions at constant intervals to refill the plate until the participant reported being comfortable full. Participants were asked to finish their meal within 15 minutes. VAS was measured to 60 minutes after completed the ad libitum test meal to measure SQ. SQ is a measure of the satiating capacity of foods relative to energy content (as shown in the equation below)[241,242]. SQ was used to assess the effect of preload on satiety at the ad libitum meal

SQ (mm/kcal) = [rating pre-eating episode - rating post eating episode] mm/ [energy intake of eating episode kcal] x 100

3.5.11 Statistical analysis

Data were analysed using SPSS version 20 for Windows. Parametric or non-parametric nature of the data were determined by a normality test. Data are presented as mean ± [SEM]. For the questionnaire and dietary data analysis, a one-way ANOVA (for parametric data) or Kruskal Wallis test (for non-parametric data) was used to assess differences between the ileal CD, colonic

CD and HCs. In the cases, where the ileal CD and colonic CD patients were combined (i.e. CD patients vs HC) an independent t-test was used for parametric data and Mann-Whitney test was used for non-parametric data. All correlations were performed with the appropriate Spearman or Pearson test. P values less than 0.05 were deemed significant.

Group differences in response to the test meal and group-meal interactions were determined using a two-way ANOVA analysis, followed by post-doc Bonferroni multiple comparisons between groups. Values of iAUC for appetite ratings were calculated using differences from baseline. Values were considered positive when they were higher than baseline values, and negative when they were less than baseline values. The area above or below baseline was calculated using the trapezoid rule[201].

The Go Stop Impulsivity test data and the LFPQ data were analysed by our collaborator at the University of Leeds Dr Michelle Dalton. For the LFPQ data analysis, food intake selection according to fat content (high or low) and taste (sweet or non-sweet) were examined by 2*2 repeated measures ANOVA. For the four categories of food image (taste – sweet or non-sweet; and fat – high or low) were examined by separate 2*2 ANOVA. For the Go Stop Impulsivity test, a one-way ANOVA was used to examine the differences in mean response inhibition values between the groups.

3.6 Results

Figure 27 shows the number of participants that were screened, consented, recruited and included in the data analysis. Please refer to Figure 70 in Chapter 6 which shows the summary consort diagram of the number of participants that appeared in each chapter. **All subjects in this chapter appeared in Chapter 1**

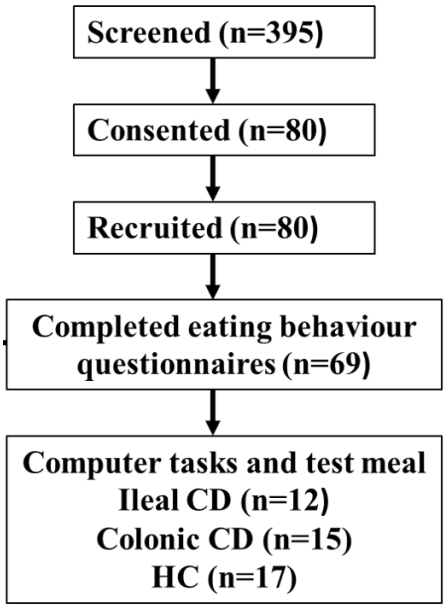


Figure 27 Consort diagram illustrating the number of participants included in this chapter

3.6.1 Demographics

18 ileal CD patients, 17 colonic CD patients and 34 HCs a completed the eating behaviour questionnaires. Twelve out of 18 ileal CD patients, 15 out of 17 colonic patients, and 17 out of 34 HCs completed the computer tasks and test meal experiment.

	Ileal [n=18]	Colonic CD [n=17]	HC [n=34]
Age [years]	32.9 ± 3.39	36.2 ± 4.12	34.5 ± 2.63
BMI [kg/m^2]	25.6 ± 1.14	25.2 ± 1.21	25.4 ± 0.83
Gender [M/F]	11M, 7F	9M, 8 F	20 M, 14 F
Abdominal pain score	27 ± 8.2	34.4 ± 8.23	
IBD QoL	4.13 ± 0.43	4.23 ± 0.55	
HBI	3.0 ± 1.0	5.3 ± 1.44	
IBD- Fatigue	12.4 ± 1.46	11 ±1.95	
CRP [mg/dl]	8.9 ± 2.8	42 ± 31	
FCP [µg/g]	855 ± 254	751 ± 256	
TNF α [pg/ml]	86.9 ± 68.3	120 ± 61.3	87.6 ± 37
IL-6 [pg/ml]	44.9 ± 14.8	91.6 ± 36.5	63.4 ± 20
IL-1β [pg/ml]	132.7 ± 108.6	254.4 ± 109.4	50.4 ± 16.0

Table 27 Demographics of ileal CD, colonic CD and HC (mean ± SEM). 49% of CD patients were on Anti-TNF therapy and 36% were on immunosuppressants and 14.3% on nil treatment

* IBD – fatigue; 0= no fatigue, 1 to 10 = moderate fatigue, 11 to 20 = severe fatigue * IBD QoL = score ranges from 1 to 7, 1= poor, 7=optimum

3.6.2 Eating behaviour constructs

Table 28 provides the eating behaviour questionnaire scores in ileal CD, colonic CD and HCs. No significant difference was found in the BES, PFS, CoEQ and TFEQ scores between the 3 groups. Although, when the ileal and colonic CD patients were combined and compared with HCs, CD patients showed significantly lower positive mood than HC

	Ileal CD [n=18]	**Colonic CD [n=17]**	**HC [n=33]**	**P values**
BES	6.7 ± 1.38	6.4 ± 1.6	6.4 ± 0.9	NS
PFS	32.4 ± 2.6	31.7 ± 2.9	33.3 ± 2.2	NS
PFS: Available	10.7 ± 1.0	10.9 ± 1.38	11.1 ± 0.93	NS
PFS: Present	10.6 ± 0.95	9.9 ± 0.9	9.8 ± 0.7	NS
PFS: Tasted	11.2 ± 0.9	10.9 ± 1.0	12.4 ± 0.8	NS
CoEQ: Control	66.2 ± 4.1	67.3 ± 6.1	66.6 ± 2.7	NS
CoEQ: Sweet	42.9 ± 6.0	46.9 ± 7.3	36.2 ± 3.1	NS
CoEQ: Savoury	40.2 ± 5.2	36.3 ± 6.2	44.8 ± 3.2	NS
CoEQ: Positive Mood	*52.6 ± 3.6	55.9 ± 3.1	*65.4 ± 2.5	P=0.009
TFEQ: R	5.6 ± 0.9	6.8 ± 1.0	7.8 ± 0.79	NS
TFEQ: D	4.8 ± 0.78	5.2 ± 0.93	5.2 ± 0.58	NS
TFEQ: H	3.9 ± 0.58	3.9 ± 0.97	4.7 ± 0.57	NS

Table 28 Eating behaviour questionnaire scores in CD and HC (mean ± SEM). One-way ANOVA was used to assess the difference between the 3 groups. An independent t-test was used to assess the difference between the combined CD patients and HCs * P<0.05

3.6.3 Correlation of HBI, abdominal pain, mood, QoL and fatigue

Figure 28 shows a correlation plot of HBI, abdominal pain, mood, QoL and fatigue scores. The yellow end of the scale represents a strong correlation and the blue end of the scale represents a weak correlation between the scores.

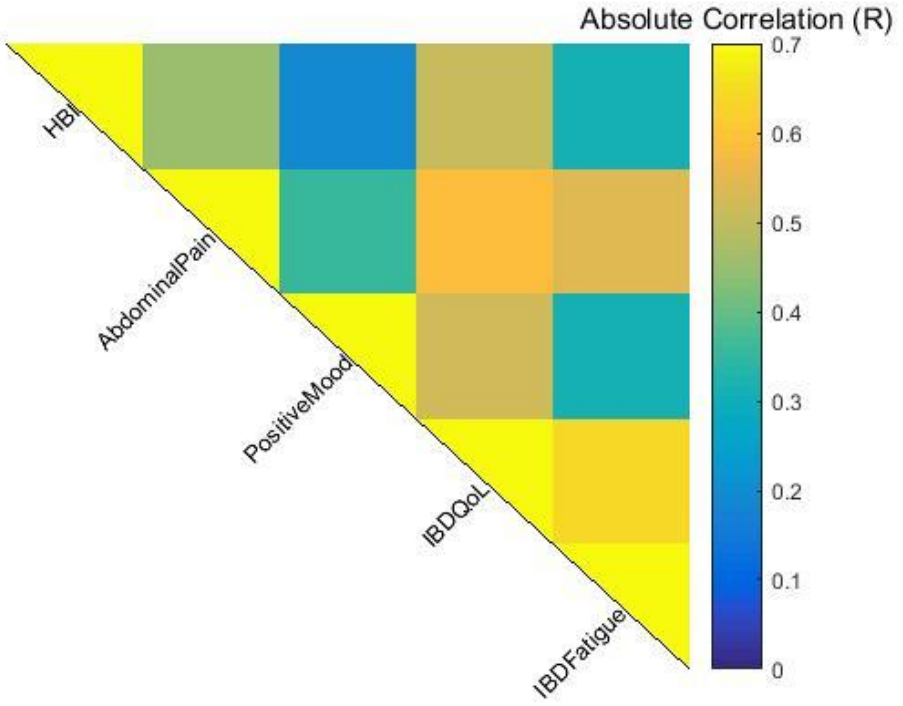


Figure 28 Correlation plot of different behavioural measures

Table 29 provides the correlation coefficient and the (*) represents a significant correlation between scores ($P<0.05$)

Spearman rho correlation	HBI	Abdominal pain	Positive Mood	IBD QoL	IBD Fatigue
HBI	1	0.449*	-0.186	-0.506*	0.316
Abdominal pain	0.449*	1	-0.357*	-0.583*	0.538
Positive Mood	-0.186	-0.357*	1	0.517*	-0.307
IBD QoL	-0.506*	-0.583*	0.517*	1	-0.635*
IBD Fatigue	0.316	0.538*	-0.307	-0.635*	1

Table 29 Spearman correlation coefficient between different measures

3.6.4 Go stop impulsivity paradigm

This section assesses inhibition control (impulsivity traits) between ileal CD, colonic CD patients and HC

3.6.4.1 All participants

As expected, there was a main effect of test block with participants being more impulsive on the first block [M: 58.6, SE: 3.3] compared to the second [M: 66.5, SE: 3.5] [$F(1, 40) = 10.4$, $p<.005$]. There was no interaction between test block and group [$F(2, 40) = .372$, $p=.69$].

3.6.4.2 Inhibitory control

Table 30 shows the mean response inhibition values across the ileal CD, colonic CD patients and HCs. A significant difference was found in inhibitory control in the 350 milliseconds Stop trials [$F(2, 40) = 4.0$, $p<0.05$] with greater inhibitory control in the patients with colonic CD compared to patients with ileal CD ($p<0.05$). There were no other differences in inhibitory control across trials or groups.

Inhibitory control	Ileal CD [n=12]	Colonic CD [n=15]	HC [n=17]	P values
All trials	53.3 ± 3.9	70.3 ± 6.2	62.7 ± 5.2	NS
50ms trials	73.8 ± 5.7	87.3 ± 5.0	82.4 ± 6.0	NS
150ms trials	64.3 ± 5.3	75.5 ± 7.2	72.7 ± 6.2	NS
250ms trials	45.9 ± 5.0	62.3 ± 7.4	56.7 ± 5.9	NS
350ms trials	*29.2 ± 5.5	*56.1 ± 7.3	39.1 ± 6.4	P=0.026

Table 30 Inhibitory control across stop trials in patients with ileal CD, colonic CD and HC Mean ± SEM. A one-way ANOVA was used to examine the difference between the groups* (P<0.05)

3.6.5 LFPQ

This section assesses the implicit wanting, explicit liking, and explicit wanting scores and 'Appeal Bias' scores for fat and taste for the four different food categories

3.6.5.1 Implicit wanting

Table 31 shows the implicit wanting scores for the 4 food categories across the 3 groups. No significant group and category interaction were found across the 3 groups and when the ileal CD and colonic CD patients were combined and compared with HC [F (6, 123) = 6.51, p=.79]

	Ileal CD [n=12]	Colonic CD[n=15]	HC [n=17]	P values
HFSA	3.4 ± 7.6	-17.2 ± 8.1	-15.8 ± 6.7	NS
LFSA	-18.4 ± 8.3	-13.8 ± 7.5	-11.34 ± 8.7	NS
HFSW	1.1 ± 6.5	5.4 ± 6.7	14.8 ± 12.9	NS
LFSW	13.9 ± 5.4	25.8 ± 7.2	12.4 ± 10.3	NS

Table 31 Implicit wanting scores for the four food categories in patients with ileal CD, colonic CD and HC. Mean ± SEM

3.6.5.2 Explicit liking

Table 32 shows the explicit liking scores for the 4 food categories across the 3 groups. No significant group and category interaction were found across the 3 groups. [F (6, 123) = 1.73, p=. 12]. When the ileal CD and colonic CD patients were combined and compared with HC, a lower explicit liking for low-fat savoury foods was found in the combined CD patients compared with HC.

	Ileal CD [n=12]	Colonic CD [n=15]	HC [n=17]	P-values
HFSA	28.04 ± 6.8	14.4 ± 3.5	23.5 ± 5.5	NS
LFSA	15.9 ± 4.1	18.0 ± 4.7	31.0 ± 5.7	*0.026
HFSW	31.4 ± 6.9	25.0 ± 6.6	36.9 ± 6.5	NS
LFSW	36.0 ± 7.7	29.3 ± 6.2	42.2 ± 5.9	NS

Table 32 Explicit liking scores for the four food categories in ileal CD, colonic CD and HC. Mean ± SEM *P<0.05

3.6.5.3 Explicit wanting

Table 33 shows the explicit wanting scores for the 4 four food categories across the 3 groups. There was no group x category interaction across the 3 group [F (6, 123) = 1.49, p=.19]. When the ileal CD and colonic CD patients were combined and compared with HCs, the combined CD patients showed significantly lower explicit wanting for low-fat savoury foods compared with HC.

	Ileal CD [n=12]	Colonic CD [n=15]	HC [n=17]	P values
HFSA	19.4 ± 4.8	12.5 ± 3.7	19.5 ± 4.3	NS
LFSA	12.2 ± 3.4	14.8 ± 3.5	28.7 ± 5.6	P=0.023
HFSW	23.5 ± 6.3	19.7 ± 5.6	31.2 ± 5.5	NS
LFSW	25.2 ± 6.6	27.0 ± 5.8	36.6 ± 5.7	NS

Table 33 Explicit wanting scores for the four food categories in ileal CD, colonic CD and HC. Mean ± SEM. *P<0.05

3.6.5.4 Appeal bias

Table 34 shows appeal bias scores for the LFPQ outcome measures in patients with ileal CD, colonic CD and HC. Ileal CD patients had a greater explicit liking [F (2, 43) = 3.4, p=.04] and explicit wanting appeal bias for high-fat foods [F (2, 43) = 4.1, p=.02] compared with HCs. No significant differences were found in the implicit wanting fat appeal bias or sweet appeal bias between the two groups.

	Ileal CD [n=12]	Colonic CD [n=15]	HC [n=17]	P values
Implicit wanting				
Fat appeal bias	4.5 ± 8.3	-11.9 ± 9.6	-1.04 ± 11.3	NS
Sweet appeal bias	15.0 ± 9.5	31.1 ± 10.0	27.2 ± 10.1	NS
Explicit liking				
Fat appeal bias	3.8 ± 3.1	-4.0 ± 3.3	-6.5 ± 2.1	P=0.044
Sweet appeal bias	11.7 ± 3.3	11.0 ± 3.8	12.3 ± 3.4	NS
Explicit wanting				
Fat appeal bias	2.7 ± 2.7	-4.7 ± 2.5	-7.3 ± 2.3	P=0.023
Sweet appeal bias	8.5 ± 3.2	9.6 ± 3.6	9.8 ± 3.2	NS

Table 34 Appeal bias scores for the LFPQ outcome measures in patients with ileal CD, colonic CD and HC

3.6.6 Dietary intake

Table 35 provides the energy, CHO, protein, fat, saturated fat, fibre, sugars and sodium intake in the ileal CD, colonic CD patients and HCs. No difference was found in the macronutrient intake between the ileal CD, colonic CD and HC group.

	Ileal CD [n=12]	Colonic CD [n=15]	HC [n=17]	P values
Energy (Kcal)	1755 ± 166	1762 ± 203	2160 ± 139	NS
CHO (g)	211 ± 19	227 ± 23	246 ± 24	NS
Protein (g)	71 ± 7	67 ± 8	97 ± 12	NS
Fat (g)	69 ± 11	64 ± 11	84 ± 5	NS
Sat Fat (g)	23 ± 4	23 ± 4	30 ± 3	NS
Fibre (g)	15.4 ± 4	20 ± 3	24 ± 4	NS
Sugars (g)	77 ± 9	90 ± 10	104 ± 8	NS
Sodium (mg)	2131 ± 377	1735 ± 163	2270 ± 245	NS

Table 35 Dietary intake in ileal CD, colonic CD and HC *P<0.05 colonic-HC

Table 36 provides the macronutrient intake of the combined CD patients with HCs. Dietary Reference Values (DRVs) are shown to compare values with daily nutrient requirements. The combined CD patients showed a significant reduction in energy and protein intake compared with HCs.

	(ileal +colonic CD) [n = 27]	HC [n = 17]	P values	DRV
Energy (Kcal)	1759 ± 133	2160 ± 139	P<0.05	2000
CHO (g)	220 ± 15	246.4 ± 24.0	NS	260
Protein (g)	69 ± 5.2	96.7 ± 11.5	P<0.05	50
Fat (g)	66.6 ±7.6	84.1 ± 5.3	NS	70
Sat Fat (g)	22.8 ± 2.96	30.3 ± 2.6	NS	20
Fibre (g)	18.2 ± 2.4	23.7 ± 4.0	NS	14
Sugars (g)	84.0 ± 6.7	104 ± 7.9	NS	90
Sodium (mg)	1911 ± 188	2270 ± 245	NS	1600

Table 36 Dietary intake ileal and colonic CD combined and compared with HC

3.6.7 Quantitative appetite assessments

This section assesses the appetite sensations following a fixed calorie breakfast meal. The appetite sensations measured were as follows: the desire to eat, hunger, fullness, prospective food consumption and a CSS was also calculated. In addition, SQ was used to assess the effect of preload on satiety at the ad libitum meal.

3.6.7.1 Fasting and preload VAS measurements

Figure 29 shows the appetite sensation ratings following a fixed calorie breakfast meal. As anticipated, a significant postprandial reduction in the desire to eat, hunger and prospective food consumption, and a significant increase in fullness and CSS was found in response to the breakfast meal.

Figure 29**A.** A significant difference was found in the desire to eat between ileal CD and HC at T30, T60, T90 and between colonic CD and HC at T30, T60 T90, T120, T150. **B**. A significant difference was found in hunger between ileal CD and HC at T60, and between colonic CD and HC at T60 and T90. **C**. No significant difference was found in fullness between the groups. **D.** A significant difference in prospective food consumption was found between ileal CD and HC at T30, T60, T90 and between colonic CD and HC at T60 and T90. **E.** A significant difference in CSS was found between ileal CD and HC at T30, T60, and T90 and between colonic CD and HC at T60, T90. **F**. The incremental/decremental AUC showed no difference in the postprandial appetite sensations between the three groups

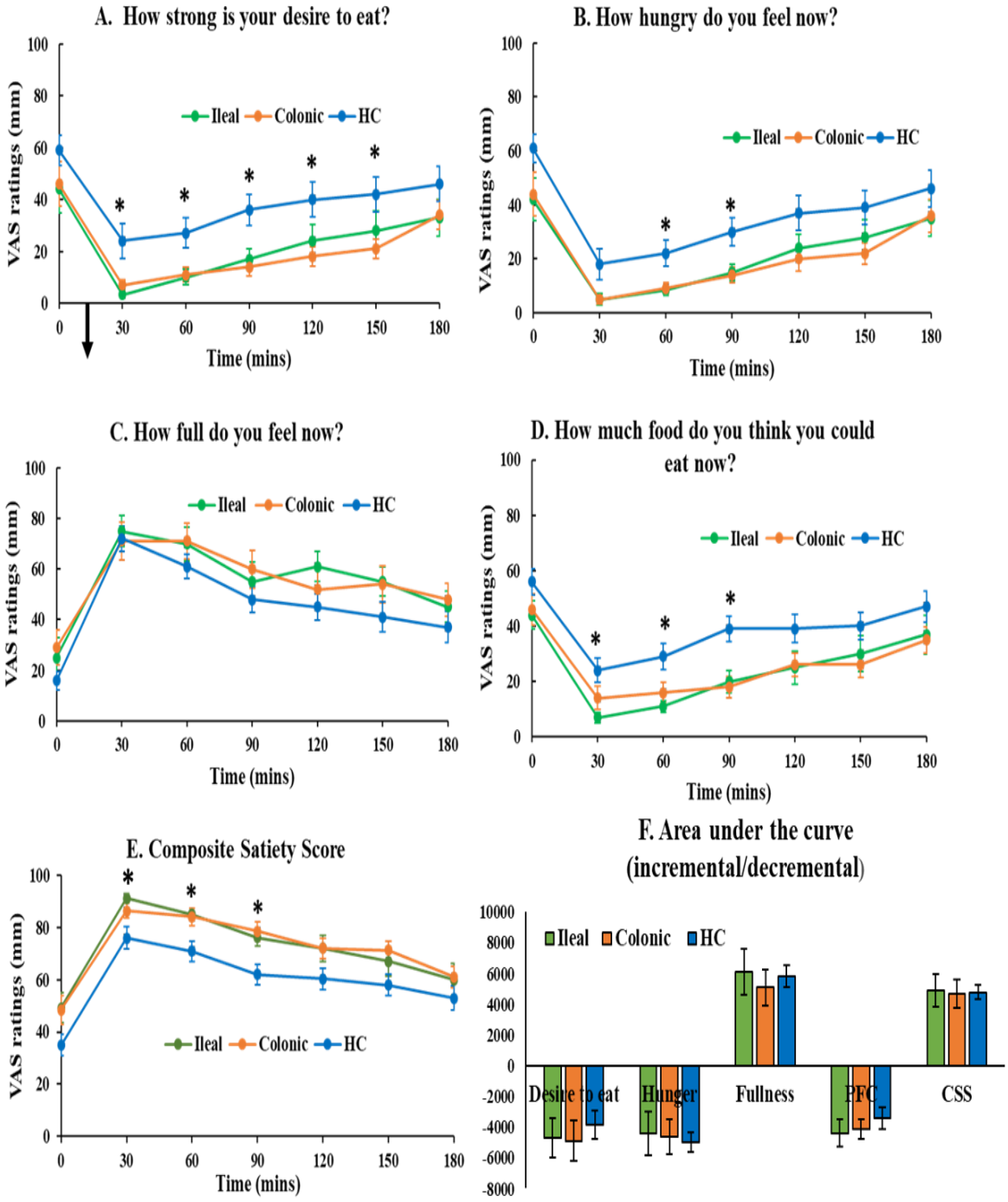


Figure 29 Appetite sensations following fixed calorie breakfast meal.

3.6.7.2 SQ

SQ was used to assess the effect of preload on satiety at the ad libitum meal. Figure 30 shows the SQ (mm/kcal) for the desire to eat, hunger, fullness and prospective food consumption in ileal CD, colonic CD and HCs. No significant difference was found in the SQ between the 3 groups, even the combined CD patients compared with HCs showed no difference in SQ (data not shown). However, the kilocalories of the ad libitum test meal consumed was significantly different between ileal CD and HC

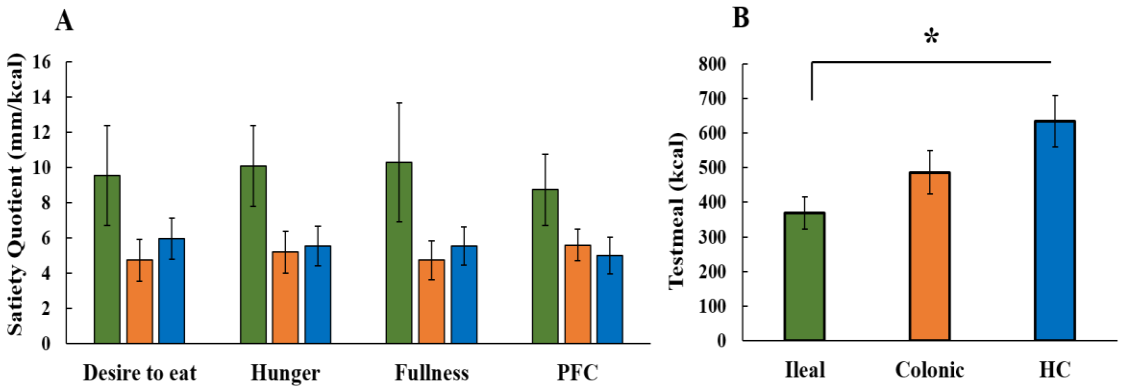


Figure 30 A. SQ (mm/kcal) for the desire to eat, hunger, fullness, prospective food consumption ileal CD, colonic CD and HC. B. Energy (kcal) of ad libitum test meal consumed by ileal CD, colonic CD and HC, *Ileal-HC

3.6.8 Discussion

This chapter studies eating behaviour traits, impulsivity traits, subjective hedonic measures of explicit liking and implicit wanting for food, dietary intake and satiety in patients with active ileal CD, colonic CD and in HCs. The key findings are:

- No significant difference was found in the BES, PFS, CoEQ and TFEQ scores between the 3 groups. Although, when the ileal and colonic CD patients were combined and compared with HCs, CD patients showed significantly lower positive mood than HC.
- Ileal CD patients showed lower inhibitory control (i.e. greater impulsivity) compared with colonic CD patients
- Ileal CD patients had a greater explicit liking and explicit wanting appeal bias for high-fat foods compared with HCs.
- Combined CD patients compared with HC, showed a lower explicit liking and explicit wanting for low-fat savoury foods compared with HC
- No difference was found in the macronutrient intake between the ileal CD, colonic CD and HC group. However, the combined CD patients showed a significant reduction in energy and protein intake compared with HCs.
- In response to the fixed calorie breakfast meal, both ileal CD and colonic CD patients exhibited reduced appetite sensations compared with HC. No significant difference was found between the ileal CD and colonic CD patients

- No significant difference was found in the SQ between the 3 groups, even the combined CD patients compared with HCs showed no difference in SQ in response to the ad libitum test meal. However, the kilocalories of the ad libitum test meal consumed was significantly lower in ileal CD patients than HC.

3.6.8.1 Eating behaviour questionnaire outcomes

No significant differences were found between the ileal CD, colonic CD and HC group in the BES, PFS, TFEQ. (CoEQ) showed no difference in craving control, craving sweet, craving savoury. However, there was a significant difference in CoEQ positive mood between the ileal CD and HC group, where the ileal CD group showed lower positive mood compared with HC (P=0.009). CoEQ positive mood assessment involved rating VAS questions such as "How happy have you felt?", "How anxious have you felt?", "How alert have you felt?" and "How contented have you felt?" This finding is in agreement with a previous study by our research group which also showed a lower positive mood in patients with active CD [178]. In this study, it was found that positive mood was negatively correlated with abdominal pain and IBD fatigue Figure 28. This finding is in agreement with a previous study that also found an association between low mood and abdominal pain [243]. Mood disorders are found to be prevalent in other chronic inflammatory conditions such as rheumatoid arthritis [244], psoriasis [245] and also in gastrointestinal disorders such as irritable bowel syndrome (IBS) and functional dyspepsia [246]. Proinflammatory cytokines (such as TNFα, IL-6 and IL-1β) are soluble regulatory proteins produced by immune cells and have the ability to interact with the CNS via the vagus nerve or directly with the BBB via cytokine receptors and can cross the BBB via transporter or compromised leaks

in BBB[247]. It has been shown that cytokines can affect the metabolism of neurotransmitters such as glutamate, serotonin, dopamine in the nucleus accumbens, amygdala and hippocampus, which are regions are involved in emotional regulation [248]. In the present study, we found no difference in the serum levels of proinflammatory cytokines IL-6, TNF alpha and IL1-β between the active CD patients and HC despite these patients having objective evidence of disease activity. This could be because despite having active disease, patients were partially treated with 49% of CD patients with anti-TNF therapy and 37% with immunosuppressants. Therefore, psychological disturbance in CD is a complex issue that could be a manifestation of several issues, such as lower socioeconomic status[249], poor QoL, malnutrition, chronic abdominal pain, fatigue, chronic inflammation, other disease-related symptoms/ complications and medication use.

3.6.8.2 Personality trait assessment in active CD

The Go Stop task results showed that ileal CD had lower inhibitory control i.e. greater impulsivity compared with colonic CD. Impulsivity has been described as 3 distinct psychological manifestations i.e. impulsive choice, impulsive action and reflection impulsivity[250]. An impulsive choice which has been described as a measure of reward sensitivity whereby a person tends to accept small or immediate rewards instead of larger future outcomes[251]. Impulsive action which is measured by the Go Stop task represents the inability to inhibit an inappropriate reaction to prepotent stimuli[251]. Reflection Impulsivity describes the failure to gather essential information and evaluate this information before making a decision[252]. A study which examined different personality traits in IBD[253], where impulsive choice was assessed using the Eysenck Impulsivity

Inventory[254], found that IBD patients (both with UC and CD) had higher impulsivity compared with controls. Elevated impulsivity was correlated with low levels of physical and mental health and poorer QoL in IBD patients, which was more characteristic of female gender[253]. Another study[255] which investigated "impulsive sensation seeking" (ImpSS) personality characteristic in IBD found that smokers with CD had higher ImpSS scores than smokers with UC. Smokers with CD also scored higher on the nicotine dependence scale than smokers with UC[255]. Impulsivity is a personality trait that has found to be predisposing toward rewarding behaviour, which may explain smoking behaviours in CD due to the rewarding properties of nicotine which is linked with the mesolimbic dopaminergic system[256]. The mesolimbic dopaminergic system also dictates the reward and pleasure-driven liking and wanting of food[257]. In this study, the significantly lower inhibitory control or greater impulsivity seen in ileal CD compared with colonic CD may explain reward-driven explicit liking and wanting fat appeal bias in relation to food preference. Inhibitory control plays an imperative role when there is a conflict between health concerns and impulse to give in to temptation for high-calorie palatable foods. If inhibitory control is impaired, the motivational drive may become more dominant dictating eating behaviours causing failure to resist palatable foods. A study which used stop a signal task that was adapted to train participants to react impulsively (i.e. act fastly) to one palatable food stimuli and inhibit responding to another palatable food stimuli found that participants with lower inhibitory control consumed more of the palatable food used in the manipulation compared with participants with higher control abilities. Moreover, the inhibition manipulation training had the desired effect of reducing palatable food consumption in participants with

low levels of inhibitory control[258]. In the present study, the Go Stop impulsivity paradigm did not include any food stimulus, so future research could use food-based impulsivity task to better understand the lower inhibitory control observed in ileal CD patients relative to colonic CD patients. It is thought that alterations gut microbes could affect the dopaminergic mesolimbic reward circuit, which is involved in addiction, impulsive choice and food reward[259]. In this study, the gut microbiota of the ileal and colonic CD was not compared. It is still not understood how dysregulation of appetite-suppressing hormones in ileal CD is linked with impulsivity, but it could be speculated that impulsive traits dictate the preference for palatable foods for momentary pleasure than future health concerns.

3.6.8.3 Food preference in active CD

The two neuropsychological factors dictating food reward are the "liking" and "wanting" components of food intake. The "liking" component is dependent on the person's physiological state (fasting or fed state), sensory properties of the food and past experiences associated with the pleasure derived from that food[260,261]. Liking has been measured objectively in human and animal models using taste reactivity patterns which involved assessing facial expressions following bitter or sweet stimuli[262]. The "wanting" component involves an incentive motivational demand to seek out and consume food as reward-related stimuli[261]. In humans, liking and wanting has been measured using computer-based paradigm which assessed liking through pleasantness rating and wanting through forced-choice paired food image comparison that varied in fat (high-low) and taste (sweet and savoury). In this method wanting was measured using the frequency of the choices made between the paired foods. It was found that

liking and wanting could be dissociated in humans because of differences in these two measures observed in a hungry or satiated state[263], following on from this method, another computer-based paradigm was developed called LFPQ to measure explicit liking and wanting of food. As previously described explicit liking and wanting was measured using pleasantness ratings whereas implicit wanting was measured based on the reaction time of the choices made in the paired food comparison task. It was found that in a fed state, hunger, explicit liking and wanting for foods decreased whereas implicit wanting remained unchanged suggesting implicit wanting is independent of the homeostatic control of food intake[232]. In the present study, ileal CD patients had a greater explicit liking and explicit wanting appeal bias for high-fat foods compared with HCs but there was no difference in fat intake between ileal CD and HC. Differences in hedonic measures of eating behaviour between active CD patients (not exclusively ileal CD patients) and HCs have been reported before by our research group [178]. In healthy populations, implicit wanting and explicit liking have been associated with disordered eating patterns such as binge eating[264]. Similarly, explicit liking fat appeal bias has been associated with a low satiety phenotype (as defined by a lower SQ to standardised test meal) in healthy individuals[265]. The explicit liking and wanting fat appeal bias seen in ileal CD is likely to be a more complex phenomenon involving reward and impulse-driven food choices to alleviate symptoms such as low mood, abdominal pain and chronic fatigue. In relation to mood and fat appeal bias, an fMRI study in healthy individuals showed attenuation of neural and behavioural response to experimentally induced sad emotion following a fatty acid infusion [165]. BOLD response in key hedonic brain regions, including midbrain, dorsal and ventral

striatum, left ACC right hippocampus and homeostatic regions such a as hypothalamus and brainstem were attenuated by the fatty acid infusion in an experimentally induced sad mental state [165]. A metanalysis of neuroimaging studies of emotion also showed the same aforementioned regions of the brain activated after negative emotion induction[266]. In addition, CCK dependent increase in the BOLD response of the same brain regions has been reported following fatty acid infusion [157]. Taken together, these studies highlight a possible interplay between gut peptides, mood and appetite for high fat foods possibly explaining an underlying neurobiological basis for comforting eating behaviours in CD patients.

In the present study combined ileal and colonic (active CD), exhibited significantly lower explicit liking and wanting for low-fat savoury foods compared with HC. Low-fat savoury foods comprised of salad (baby spinach, cucumber, and tomatoes), broccoli, pilau rice and bread roll. This finding demonstrates that active CD patient's food preferences are more reward-driven than motivated by health concerns. The avoidance of these foods could also be due to fear of worsening flare, it has been reported that 86% of active CD patients avoid certain types of food to prevent symptom exacerbation[174].

3.6.8.4 Dietary intake in active CD

No significant difference was found in the macronutrient intake between ileal CD and colonic CD. The ileal and colonic combined active CD patients had lower energy and protein intake. Lower protein intake in active CD patients has been reported by our research group before[178] and also in paediatric cases of CD in remission[267]. In contrast, some previous studies have shown no difference in

macronutrient intake in both active and inactive disease[268,269]. Reduced protein and energy intake observed in this present study may be explained by the two paths theoretical model whereby anxiety about food intake in CD patients may lead to restriction of food groups to minimise fear of worsening flare[212]. It is thought that CD is linked with increased food monitoring behaviours often seen in people with gastrointestinal disorders[178,211,212]. In a questionnaire-based study of 400 IBD patients in the UK, patients felt that diet was a factor that triggered their IBD and involved in subsequent relapses. Majority of patients reported that their IBD symptoms were triggered by food, with two-thirds of patients depriving themselves of their favourite food to achieve symptom control[173]. A study in 1271 IBD patients found that patients with active disease avoided spicy foods, fat, fibre, legumes, meat, dairy products, raw vegetables, fruit, eggs and fish compare to when in remission. This is in line with the findings from this present study where protein and energy intake were significantly reduced in CD patients and that their preference for low-fat savoury foods was significantly lower than HC.

The single administered 24-hour recall has its limitations in terms of assessing dietary intake and its accuracy might have been improved by performing this test on 3 consecutive days then one day. The 24-recall technique is memory dependent, and the participant's potential bias in reporting good/bad foods may affect the accuracy of the outcome. In this study, 24 h recall data were collected by 2 interviewers (AN, GT) which may have introduced interrater variability in the data collected. If the manufacturer's nutritional label was not available, the portion size was obtained using Carbs and Cals, which may have affected the estimation of the portion size. Future studies should use additional methods such

as weighted food records, food diary, food frequency questionnaire (FFQ) and quantitative assessment in free-living conditions, to measure food intake in active CD patients.

3.6.8.5 Quantitative appetite assessment in active CD

The intake of food results in satiation that decreases the drive to eat thereby terminating the eating episode which leads to a feeling of satiety that inhibits hunger and determines the quantity of food consumed at the next eating episode [35]. Experimental protocols used in appetite studies are either in free-living or laboratory conditions. Free-living conditions have more external validity in relation to normal eating behaviour, however, the participants may not adhere to the protocol. Moreover, food diaries and FFQ have reporting bias (i.e. over or underreporting) and in free-living conditions, external confounders such as (stress, availability of food and eating out) cannot be controlled. In a laboratory setting, one can ensure that participants follow the protocol of a controlled intervention and outcome measures, with good internal validity. However, there is a lack of external validity for normal eating behaviour. It has been suggested that data from free-living conditions could complement data acquired in the laboratory with scope for overlapping protocols[270]. In the present study, a single course meal was used as an ad libitum test meal. However, given the explicit liking/wanting appeal bias for fatty foods in ileal CD group relative to HC, it might be more revealing to use a buffet-style test meal in future studies comprising of (high-fat sweet/savoury, low-fat sweet/savoury), in this way the effect of preload manipulation on food preference could be assessed. The fasting and preload VAS measurements showed no difference in the appetite sensations (desire to eat, hunger, fullness, prospective food consumption) and CSS between

ileal and colonic CD. Significant differences were found between ileal-HC and colonic-HC at multiple time points for the appetite sensations shown in Figure 29. The reduced appetite following the preload test meal could be due to fear of aggravating abdominal symptoms such as diarrhoea and abdominal pain, the increase in satiety hormones in the ileal CD group may also contribute to reduced appetite. However, fasting and postprandial gut peptides were not measured for this part of the study. It is important to note, the pitfalls of analysing satiety data at multiple individual time points are that it does not account for satiety responses as a function of multiple time points and that these individual time points are not physiologically statistically independent, it may also introduce type 1 statistical errors by inflating experiment wide error rated[270]. The data presented in Figure 29 are for display purposes only, and the incremental/decremental AUC measures are more robust and reliable for satiety score data[270].

SQ reflects the change in fullness or suppression of hunger based on the energy content of the food consumed[242]. There was no difference in the SQ between ileal CD, colonic CD and HCs. However, ileal HC group consumed significantly less of the ad libitum meal, perhaps in a bigger sample, a significant difference in the SQ would have been observed.

3.6.8.6 Summary of eating behaviour traits and hedonic measures between combined (ileal CD and colonic CD) and HC

The combined CD groups had lowered positive mood compared with HC. There was no difference in inhibitory control between the combined CD groups and HC. In relation to food preference, combined CD group had a significantly reduced explicit liking and wanting for low-fat savoury foods. Furthermore, the

combined CD group had reduced energy and protein intake compared with HC. Combined CD group showed significantly reduced appetite than HC following the preload test meal. There was no difference in the SQ between combined CD and HC, however, the CD group ate significantly less of the test meal compared with HC. Taken together, reduced appetite, dietary intake and the lack of preference of low-fat savoury foods, could be attributed to food avoidance linked with fear of worsening symptoms.

3.6.8.7 Summary of eating behaviour traits and hedonic measures between ileal CD, colonic CD and HC

Ileal CD exhibited greater impulsivity than the colonic CD. Ileal CD had a lower positive mood than HC and showed stronger explicit liking and wanting fat appeal bias in relation to food preference relative to HC. However, there was no difference in dietary intake across the 3 groups. The preload meal did not show a difference in appetite measures between the ileal and colonic CD groups. However, both ileal CD and colonic CD separately showed reduced appetite compared with HC. Lastly, no difference in the SQ was found across the 3 groups, however, the ileal CD ate significantly less of the ad libitum test meal compared with HC. Taken together, eating behaviour in ileal CD is likely to be impulse and reward-driven to alleviate symptoms such as low mood, abdominal pain and chronic fatigue. Stronger hedonic control of food intake was observed in the ileal CD patients based on explicit wanting/liking appeal bias for high-fat foods, however, this is not translated into actual increased calorie intake, perhaps because of fear of triggering or worsening symptoms. Therefore, a complex interplay of gut peptides, psychological factors, disease-related symptoms, inflammatory burden may ultimately guide eating behaviour in ileal CD patients.

Therefore, firm dietetic advice and psychotherapy may help improve appetite and nutritional status inducing remission and preventing relapse.

4 A study of brain morphology and it's alterations in patients with CD

Structural brain alterations in grey matter volume (GMV), cortical thickness (CT) and white matter volume (WMV) have been previously documented in adult CD patients in remission, however, the data are inconsistent and not available in the active disease state. This chapter aims to investigate the differences in GMV, WMV and CT between patients with active CD and HCs. Brain measures in active CD are correlated with clinical and behavioural scores, and an exploratory analysis is performed to determine if disease location (i.e. ileal CD compared with colonic CD) differentially affects brain structure and if such changes are linked with appetite regulatory peptides.

This work has been presented at the following events:

• *Investigating the brain anatomical changes in active Crohn's disease. British Chapter ISMRM, 25th Post-Graduate Symposium, King's College London, March 2017. Oral presentation.*

• *Investigating the brain anatomical changes in active Crohn's disease. The British Society of Gastroenterology (BSG) Conference- Manchester, - June 2017. Poster presentation.*

• *Investigating the brain anatomical changes in active Crohn's Disease 13th Congress of European Crohn's and Colitis organisation ECCO – Inflammatory Bowel Diseases, Vienna February 2018. Poster presentation.*

• *Alteration in cortical thickness and grey matter volume in patients with active Crohn's disease. The British Society of Gastroenterology (BSG) Conference- Liverpool, - June 2018. Poster presentation.*

• *Volume and surface-based analyses in active Crohn's Disease Patients International Society for Magnetic Resonance in Medicine ISMRM, Paris 2018. Poster presentation.*

4.1 Brain morphology

Brain morphology is the study of the structure of the brain, particularly that of the cerebral cortex in relation to its volume and shape and its internal structures. Eighty-two per cent of brain mass is composed of the cerebral cortex, comprising both GM and WM, with 42 % of the brain mass consisting of cerebral GM[271].

The brain is protected by three layers of tissues known as meninges composing the i) dura mater, the archnoid layer, and the pia mater. The cerebral cortex is a highly folded sheet of GM, lying between the CSF and the WM. The regions of GM folded inwards are called sulci whilst the regions folded outwards are termed gyri. The cortical GM is composed of approximately 7 billion neuronal cells and 9 billion non-neuronal cells such as glial cells[271]. Figure 31 shows the inner surface, outer surface and the central surface (CS), which contains six layers termed lamina I-VI. The CT is described by the distance between the inner surface and outer surface, with the CT ranging from 1 to 4.5 mm, and having an average thickness of 2.5 mm [272].

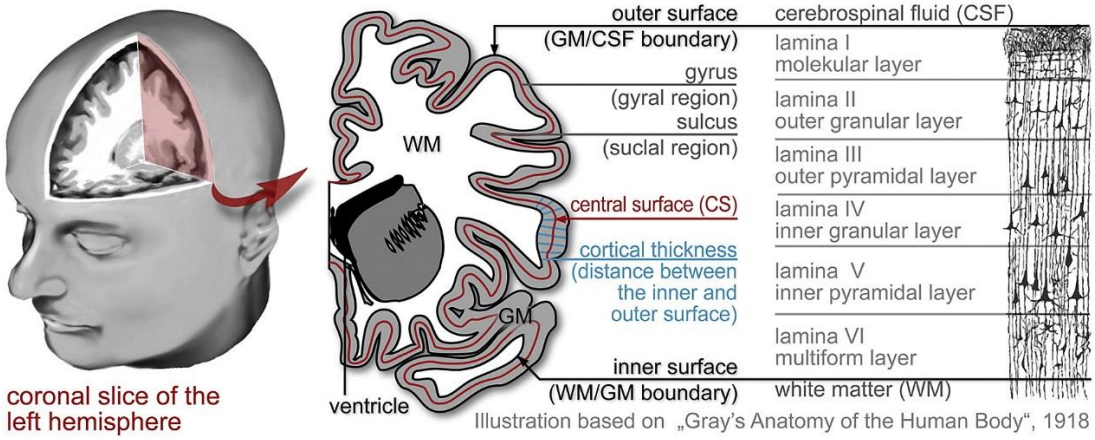


Figure 31 Illustration of the macro- and micro-structure of the cerebral cortex.

The cortex has evolved into distinct cytoarchitectectonic areas with neurons arranged in horizontal layers or laminae and vertical (radial) columns or modules that have expanded in size, number and complexity during human evolution[273]. It is well known that the expansion of the cortex has occurred mainly in the surface area rather than in thickness[273]. The cortical surface is determined by the number of radial ontogenetic columns, and the CT is determined by the number of cells within the column[273].

GMV is defined as the amount of GM lying between the grey-white interface and pia mater. GMV is a function of surface area and CT, where CT and surface area measurements are genetically and phenotypically independent[274]. It has been demonstrated that GMV has a closer linear correlation with the cortical surface area than the CT[274].

The study of brain morphology has been widely used to gain a better understanding of normal brain development and changes in the brain in diseased states. In diseased states, region-specific atrophy over time can give an insight into the aetiology or manifestation of a disease.

4.1.1 Whole-brain development

Brain size increases significantly by the age of two, reaching 80-90% of adult brain volume driven by a GMV increase[275], whilst WMV continues to grow until 20-25 years of age[276]. CSF increases with advancing age in a nonlinear (quadratic fashion). This is thought to be due to GM and WM converting into CSF later in life [277].

4.2 The association of GMV, WMV, and CT with age

The association of GMV, CT, and WMV with age are described in Sections 4.2.1, 4.2.3 and 4.2.2.

4.2.1 GMV

GMV develops rapidly in the first two years of life and reaches 80% of its volume by 1-2 years of age[275,276,278] reaching its peak at approximately 8 years of age[279]. Factors such as prenatal/childhood malnutrition[280,281], childhood trauma[282], and preterm birth[283,284] can negatively affect GMV in the developing brain. It has been well established that whole-brain GMV declines in a linear fashion with age[276,277,279,285]. After 20 years of age, the regional GMV demonstrates either a negative linear correlation with age in the (superior frontal, lateral OFC, putamen, precentral, rostral anterior cingulate, cuneus, rostral middle frontal, accumbens area, inferior parietal, supramarginal, PCC) or a nonlinear correlation with age in the (precuneus, cerebellum cortex, postcentral, hippocampus, PHG, thalamus proper, isthmus cingulate, insula, lateral occipital, paracentral and amygdala)[277]. But discrepancies have been found in the regional effects of ageing on the brain between voxel-based morphometry (VBM) studies, possibly due to differences in the sample size and limitations of the VBM approach (as described in Section 4.4.1). Age-related GMV decline in the frontal and temporal regions and the preservation of GMV in the hippocampus and the amygdala has been a consistent finding across most studies[277,286–288]. Figure 32 demonstrates the brain regions that have been shown to have a negative correlation with age.

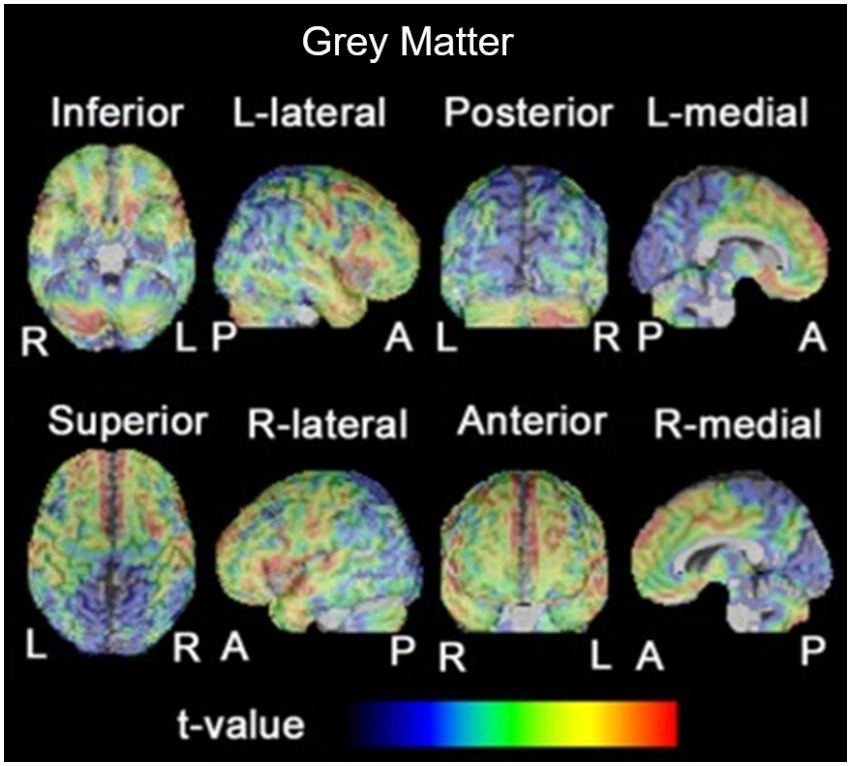


Figure 32 VBM analysis: age-related atrophy in GM in 159 healthy individuals aged 20 to 74 years with more prominent GMV loss in the frontal and temporal regions[289]

4.2.2 CT

Studies have found that CT increases rapidly from birth to 2 years of age reaching 97% of adult brain CT[290,291]. Cortical thickening of the posterior brain regions' occurs between 5 to 6 years of age[292]. In the pre-adolescent years, cortical asymmetry has been reported in the medial occipital lobe and inferior gyrus between hemispheres, followed by a post-adolescent asymmetry in the frontal and parietal lobes[293]. Over the life course, the effect of ageing is widespread, exhibiting an anterior-posterior gradient with frontal and parietal regions showing greater atrophy than temporal and occipital regions[293].

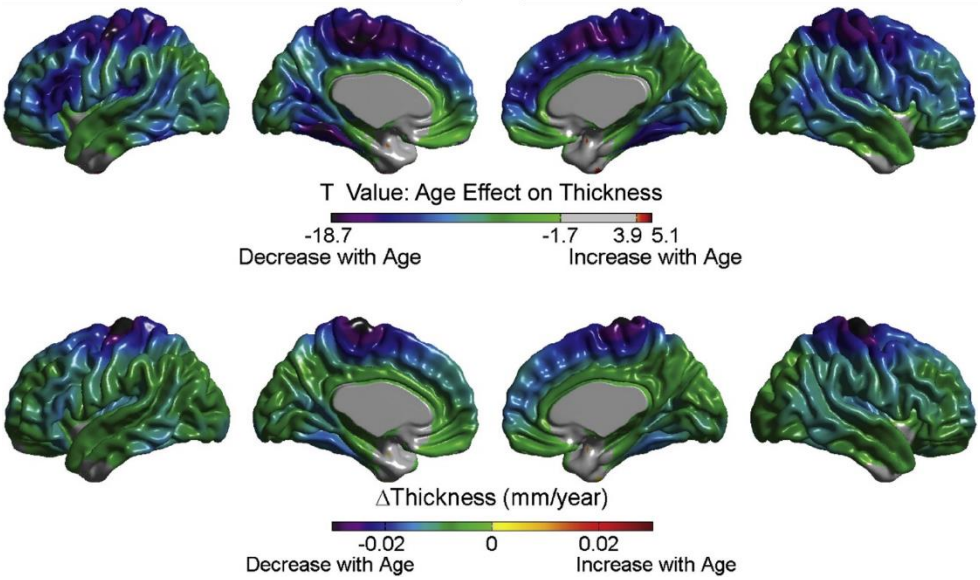


Figure 33 Brain regions that show alterations in CT with age in healthy individuals[293]

4.2.3 WMV

WM is formed of myelinated axons called tracts. Myelin is a fatty insulating sheath from oligodendrocytes that wraps around axons increasing conduction velocity[294]. GM and WM form parts of the same neural circuitry and interact with each other throughout the life span. However, they have quite different developmental trajectories[294]. A study that investigated the association of WMV with age, on brain volumes in 563 healthy adult brains using a volume-based approach (i.e. Computational anatomy toolbox (CAT12) reported that WMV had a non-linear quadratic relationship with age[277]. It was found that WMV increases with age, reaching a peak in the fourth decade following by a significant decline in older age[277]. This finding is in line with other studies[289,294–296] that also found an increase in WMV during adulthood thought to be due to the ongoing maturation of WM occurring during the normal ageing process. In contrast, some other studies have found a widespread decline in WMV with age[285,297,298]

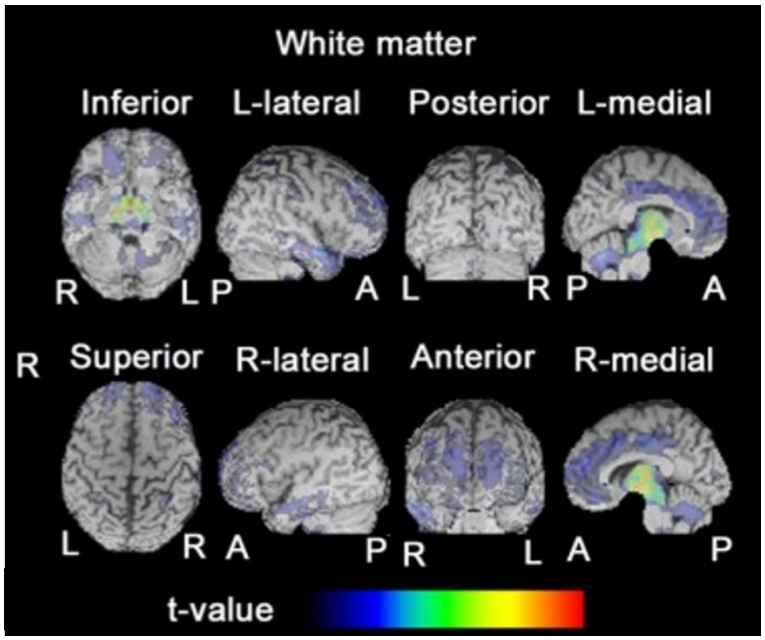


Figure 34 VBM analysis: age-related atrophy in WM in 159 individuals aged 20 to 74 years with more prominent loss in the frontal cortex and brain stem[289]

4.3 Gender-specific differences in GMV, WMV, and CT

Gender-specific differences in GMV. WMV and CT are described in the sections 4.3.1, 4.3.2 and 4.3.3.

4.3.1 GMV

Two large studies by Lotze et al[299] and Ruigrok et al[300] have attempted to clarify the inconsistencies in previous findings of single studies in relation to gender-specific GMV differences.

Lotze et al 2018[299]		Ruigrok et al 2014 [300]	
Larger GMV in men	Larger GMV in women	Larger GMV in men	Larger GMV in women
○ amygdala ○ hippocampus ○ temporal pole ○ fusiform gyrus ○ visual primary cortex and motor areas (premotor cortex, putamen, anterior cerebellum)	○ inferior and middle frontal gyrus ○ ACC ○ right OFC ○ right insula ○ lateral occipital cortex ○ Heschl gyrus ○ Thalamus ○ precuneus	○ amygdala ○ hippocampus, ○ PHG, ○ precuneus, ○ putamen ○ temporal poles, ○ cingulate gyrus cerebellum	○ frontal pole ○ inferior/middle frontal gyrus ○ planum temporale/parietal operculum ○ anterior cingulate gyrus ○ right insular cortex ○ Heschl's gyrus ○ thalamus ○ precuneus ○ PHG ○ lateral occipital cortex

Table 37 GMV differences in men and women as reported in Lotze et al[299] and Ruigrok et al [300]

The structural differences seen between men and women are due to complex biological and environmental factors and understanding gender-specific effects on the brain can shed light on psychopathological disorders that disproportionately affect one gender over the other. For example, the female gender has been shown to be a strong predictor of anxiety and depression in patients with CD[215]. Other factors such as prenatal malnutrition, stress, maternal health, sex-biased gene expression, and steroid hormones could all play a role in gender-specific brain differences[300].

4.3.2 WMV

Several studies have reported no gender-specific differences in WMV[285,295,296,298]. In contrast, other studies have found that WMV increases throughout childhood and adolescence in males and females, but more rapidly in adolescent males[301]. Larger WMV has been found in young adult women

compared with young adult males in the bilateral anterior frontal regions and left Broca's area[302].

4.3.3 CT

One of the largest studies of gender-specific effects on CT found that females have a thicker cortex across most of the brain[303], whilst males have increased CT in the right insula[303]. It was reported that in females, the motor and somatosensory regions in the parietal lobe, the frontal pole and PHG show higher thickness but males show relatively higher volume and surface area[303].

4.4 VBM

VBM is a classical quantitative method based purely on the volumetric representation of the brain[304]. The local amount of tissue is measured from the intensity within each voxel from an anatomical scan. This technique typically uses a T_1-weighted high-resolution 3D sequences such as an MPRAGE scheme that is spatially normalised to a standard template in stereotactic space[305]. Figure 35 shows an example of a T_1-weighted MPRAGE image.

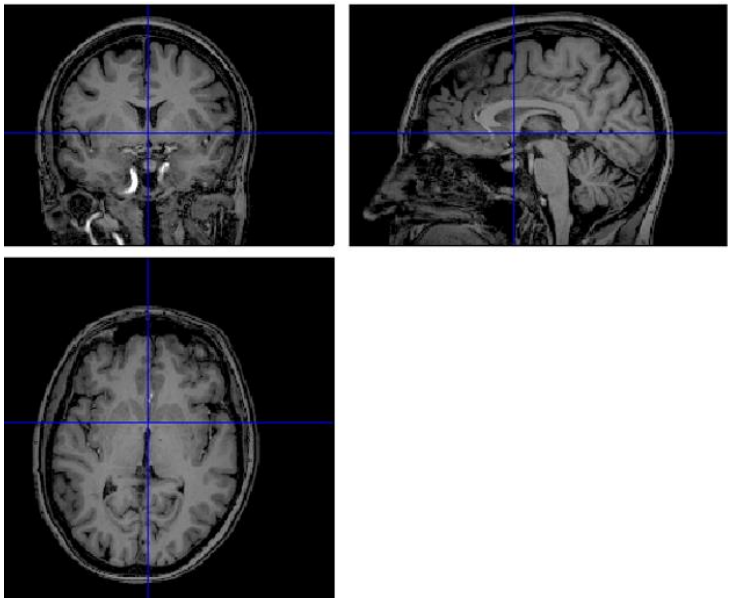


Figure 35 An example of T_1-weighted MPRAGE image

Spatial normalisation deforms different shape and sized brains to fit a standard template image, so that one location in a given subject's brain corresponds to the exact same location in another subject's brain scan, establishing a voxel-for-voxel correspondence across subjects[306]. A standard template that is popularly used is the MNI-152, which was created using 3D MRI brain images of 152 normal subjects[307,308]. Figure 36 shows the MNI-152 template.

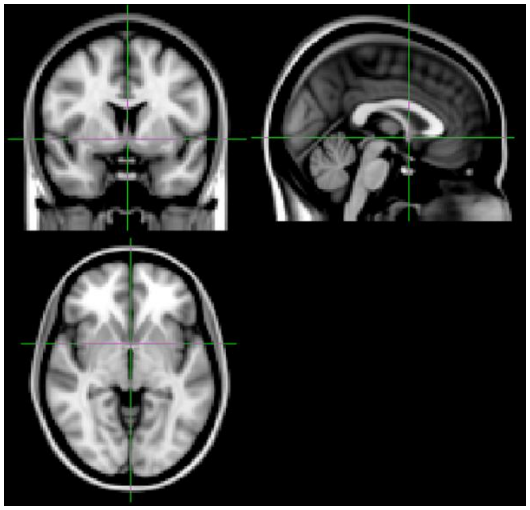


Figure 36 MNI-152 template

Stereotactic space is a coordinate system of Talairach and Tournoux used to identify different brain regions based on two reference landmarks, the anterior commissure (AC) and posterior commissure (PC), where AC is the origin coordinate, i.e. (0, 0, 0)[309]. For VBM, following spatial normalisation MPRAGE images are segmented into GM and WM and smoothed using an isotropic Gaussian kernel[305]. Smoothing with an isotropic Gaussian kernel ensures that each voxel in the image has the average amount of GM with respect to its neighbouring voxels in all directions, where the region surrounding the voxel is defined by the FWHM kernel ranging from (8-12mm)[305]. Smoothing ensures the data follows a Gaussian or normal distribution given by the central limit theorem, allowing for parametric statistical tests[305]. Also, smoothing allows for the compensation of any inaccuracies in the spatial normalisation step[305].

Statistical analysis of the smoothed segmented images is then performed using parametric statistics using a GLM. Figure 37 shows an example of using a GLM, to compare GMV or WMV differences between two experimental groups.

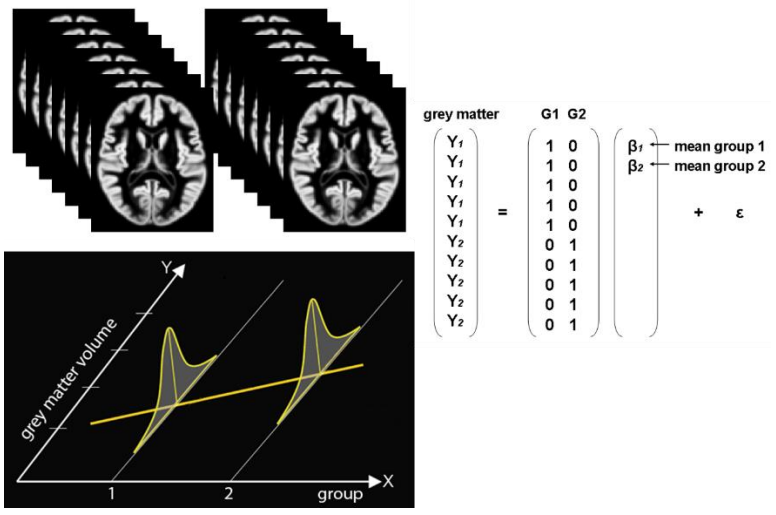


Figure 37 Using the GLM for VBM

Subjects total intracranial volume (TIV) and age are included in the model as covariates of no interest, to account for differences in brain size and the effect of ageing. The GLM is described by

$$V = \beta_1(\text{patients}) + \beta_2(\text{control}) + \beta_3(\text{covariates}) + \beta_4(\text{TIV}) + \mu + \varepsilon,$$

where V is the intensity for each voxel which is modelled by a function that accounts for differences between experimental groups, μ is the population mean, and ε is error. Using the random field theory equation, a voxel-wise comparison of GM in the experimental groups is then performed correcting for multiple comparisons to prevent the occurrence of false positives[305,310]. Two types of correction can be applied, FWE correction and FDR. FWE correction uses a Bonferroni correction method to control the chance of false positives across the whole brain, whereas the FDR correction controls the expected proportion of false positives among suprathreshold voxels. An uncorrected threshold of $P<0.001$ can also be used followed by small volume correction to reduce the number of comparisons being performed and increase the sensitivity of identifying significant results in a particular region of interest (ROI). This method involves, placing an ROI over particular structures and analysing these regions[311].

4.4.1 Limitations of VBM

For optimal results, it is advisable that the T_1-weighted structural images are acquired on the same scanner with identical imaging parameters for all subjects to prevent any significant technical effects from the scanner (e.g. differences in gradients resulting in slight differences in voxel volume) or MR sequence contrast differences[310]. Another limitation is the difficulty of spatially

normalising atypical brains, where group-specific misregistration may occur due to specific patterns of abnormal anatomy[310]. Motion artefacts may also influence the segmentation process, leading to classification differences[310]. Another consideration of the VBM approach is that it combines both CT and surface area measures into one single measured value. It has been shown that CT and surface area are two separate measures that can change independently of each other[274], therefore global or local changes in these measures can be cancelled and diluted by measuring GMV (i.e. increased CT and decreased surface area) and will not be accounted for in the VBM approach. Finally, regional variation in normalisation accuracy or smoothness can result in varying statistical sensitivity of VBM across the brain[312].

4.4.2 Strengths of VBM

VBM is a user-friendly technique, freely available in the SPM software (https://www.fil.ion.ucl.ac.uk/spm/). It allows for reproducible hypotheses-free assessment of the whole brain. Due to its high degree of automation, large samples can be analysed in a reasonable amount of time[310]. VBM results have been compared to regional manual volumetry, the gold standard of *in-vivo* neuroanatomy, measuring multiple regions of interests from unmanipulated MR images[288]. Comparison between these two methods when investigating the effects of ageing showed good correspondence, with only discrepancies in regions of increased inter-voxel variability[288]. VBM analysis resulted in strong age-related differences in the regions bordering CSF and WM regions and a more non-linear age volume relationship[288].

4.4.3 Interpretation of VBM results

Comparison between VBM studies may pose some issues, due to several factors that can affect the results. For example, the processing steps may vary between studies, with the use of different degrees of smoothing, registration, and segmentation algorithms[311]. Also, different options for multiple comparison correction and lack of standardisation as to the p-value applied to each statistical analysis result in variability. Variation in p-values and multiple comparison tests applied will change the number of voxels that exceed the significance threshold affecting the final conclusions of the study[311]. Other confounding factors include sample size, differences in age, BMI, gender ratios and disease severity across groups. To reliably compare results across VBM studies, the patient group should ideally be analysed using the same statistical model, same pre-processing steps and a standardised reporting system must be established. In relation to the biological meaning of VBM results, in the case of Alzheimer's disease[313], dementia, and other neurodegenerative disorders[314], neuronal loss is thought to be the cause of GM atrophy. However, the subtle changes in brain structure attributed to neurological and psychiatric dysfunction can be harder to interpret, where GM density is not the same as cell packing density measured cytoarchitectonically[310]. In relation to improvement in brain function, studies have demonstrated that new skill acquisition leads to brain structural brain plasticity in normal human brains[315]. For example, juggling[316], spatial navigation training[317], learning a foreign language[318], dancing[319], and music playing[320] have all been shown to be associated with an increase in regional GMV. It has been speculated that these structural changes are attributed to use-dependent plasticity, possibly due to the proliferation of neuronal progenitor cells, increase

in synaptic density through dendritic branching axonal sprouting, stabilisation of synapses for neural rewiring and possible changes in the glial cell numbers and morphology[315]. In contrast, other studies have shown training-related decreases in GMV[321,322], which are speculated to be due to the selective elimination of synapses[322]. It is important to note that, presently the underlying physiological mechanisms of both an increase and decrease in GMV remain to a great extent speculative.

4.5 CT assessment: surface and volume-based methods

The methods for estimating CT from MR images can be categorised as surface-based or volume-based methods. Both of which use an initial segmentation step to separate GM, WM, and CSF.

4.5.1 Surface-based analysis (SBA) of CT

FreeSurfer is an established software (http://surfer.nmr.mgh.harvard.edu/ version 5.3) that uses the surface-based approach for assessment of CT and is considered to be the gold standard method for CT measurements. The first step of this SBA is the extraction of the cortical surface, where non-brain tissue is removed, then segmentation of the subcortical WM and deep GM volumetric structures is performed[323,324]. The cortex is then surface modelled as a mesh of triangles, the points where the corners of the triangle meet are called a vertex. The coordinates (X, Y, and Z) are the parameters of the model at each vertex. The 2D spherical coordinates of a vertex are adjusted to match the curvature (aligning the gyri and sulci) across subjects for group analysis[306]. The images are then spatially normalised in a nonlinear fashion, allowing the parts of the surface to be compressed or stretched to match the curvature, and then

transformed into a common group space (i.e. Talairach space). Intensity normalisation is performed to ensure the accurate labelling of each voxel with a tissue type[325]. This is followed by tessellation of the GM and WM boundary and topology correction (to ensure any voxel misclassifications are corrected)[326]. Additionally, surface deformation is performed to enable the detection of tissue boundaries[327]. The CT is then calculated as the distance between the white and pial surface. The CT is then smoothed and fed into the group analysis to compare across groups at homologous points on the cortex. General linear modelling is applied to the data **y=X*beta, where y** is the vector observed data (i.e. CT for each subject at a vertex), **X** is the known design matrix (i.e. age, gender), and **beta** is the vector of unknown parameter estimates (PEs). PEs can be interpreted based on how **X** is constructed. For instance, they could be interpreted as indicating the degree of linear change of CT with age.

4.5.2 Volume-based analysis (VBA) of CT

The CAT12 in the SPM software (https://www.fil.ion.ucl.ac.uk/spm/) uses a volume-based approach based to estimate CT based on projection-based thickness (PBT)[328], where the information of blurred sulci is used to create a CT map. This method is fully automated and performs the reconstruction of the CS and can measure CT in one step[328]. The reconstruction of the surface involves topology correction, which corrects topological defects using spherical harmonics[329]. Spherical mapping is applied to reparametrize the surface mesh into a common coordinate system[330] and spherical registration adapts the volume-based diffeomorphic DARTEL algorithm[331] to the surface. Tissue segmentation is used to estimate the white matter distance (WMD), from which the local maxima (which is equal to the CT) is then projected to other GM voxels

by using a neighbour relationship described by the WMD, as shown in Figure 38.

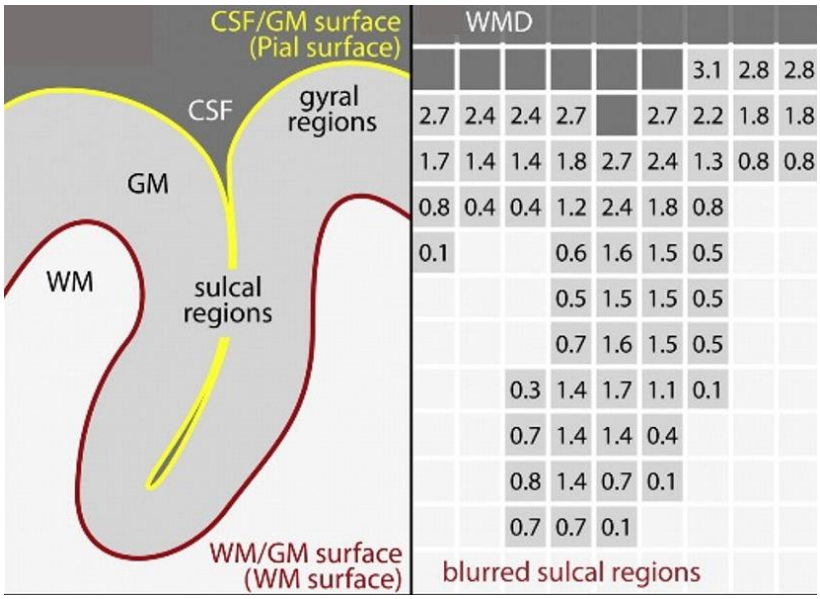


Figure 38. VBA of CT, for which the WMD is used to project CT values from the outer boundary[328]

4.5.3 Strengths and weakness of SBA and VBA

The SBA method using FreeSurfer (gold standard tool) has been validated against both histological analysis[332] and manual measurements[333]. This method has been shown to provide good test-retest reliability across both scanner manufacturers and scanner field strengths[334,335]. The CAT12 has been validated as a suitable alternative tool to FreeSurfer[336,337]. Table 38 outlines the strengths and weaknesses of the SBA and VBA methods in the assessment of CT.

	Surface-based method (FreeSurfer)	**Volume-based method (CAT12)**
Strengths	○ High accuracy/gold standard as the entire surface is modelled	○ Faster processing time (one hour per subject) without extensive reconstruction of the surface. ○ User-friendly ○ Validated to have the same high-quality results as surface-based method
Weakness	○ Longer processing times ~ 24 hours per subject, as the entire cortical surface is reconstructed. ○ It requires high computational resources. ○ Not ideal to process large numbers of subjects. ○ Manual intervention may be needed when any of the reconstruction steps fail	○ Not ideal if the research question requires extensive surface reconstruction steps.

Table 38 Strengths and weaknesses of surface-based and volume-based approaches for CT measurements

4.5.4 Interpretation of results

Studies have shown that surface and VBA methods give comparable results[336,337]. However, just as for VBM techniques, the pre-processing steps, smoothing kernel and multiple comparison tests used for CT measures must be the same to compare the outcomes across studies. Cortical thickening is thought to be influenced by the extent of myelination, synaptogenesis synaptic density and changes in cell size[338], dendritic arborisation, and alterations in inhibitory or excitatory neuronal circuits[339]. These types of changes occur during maturation and ageing[292], during skill acquisition[315], following injury[340] and drug treatments[341]. In patients with chronic bowel disorders[342–344] and chronic pain[341],

prolonged exposure to increased nociceptive input may result in increased volume/CT based on use-dependent plasticity[315,316,345] in brain regions involved in nociceptive processing. Cortical thinning has been attributed to a decrease in cell size, apoptosis of glial cells and astrocytes, fewer dendritic spines and reduced synaptic density[341].

4.6 Structural alterations in CD patients

Multiple factors such as systemic inflammatory response, fatigue, abdominal pain, psychological comorbidities, and medication use, may be linked with brain structural and functional abnormalities in CD. Intestinal inflammation and pain may activate central sensitization pathways that convey visceral nociceptive afferent signals from the gut to the brain[342,346], leading to brain structural changes. Additionally proinflammatory cytokines such as TNFα, IL-1β, IL-6 are soluble regulatory proteins produced by immune cells and have the ability to interact with the CNS via the vagus nerve or directly with the BBB via cytokine receptors and can also cross the BBB via transporters or compromised leaks in BBB, propagating inflammatory signals within the brain via the activation of the endothelial cells, glial cells and macrophages[347]. Figure 39 shows the gut-brain interactions that may lead to structural and functional brain changes.

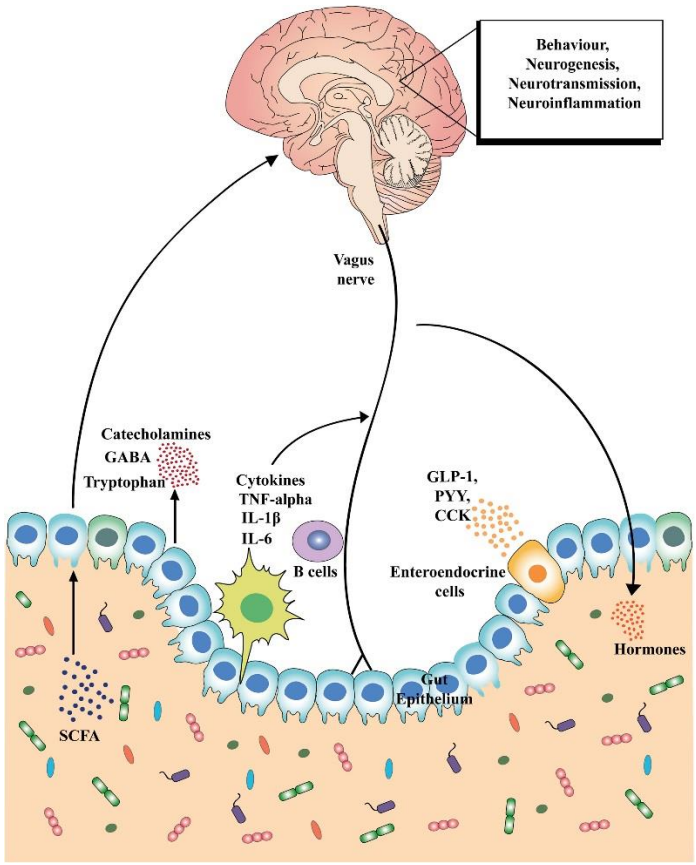


Figure 39 Illustration of gut-brain interactions[348]

In adult CD patients in remission, studies have reported alterations in both GMV and CT[208,339,349–355]. In addition, a small number of studies have assessed additional cortical measures of the gyrification index[351] (a metric quantifying the amount of cortex buried within the sulcal folds relative to the amount of cortex on the outer visible cortex)[356] and cortical surface area[339,351] (the area of the cortical surface, which is more closely related to GMV than CT) as shown in Table 39.

Author, Country	Study population	Methods	Main Findings	Analysis of correlation Findings
Bao et al 2017, CHINA[349]	-21 CD patients with abdominal pain in remission -26 CD patients without abdominal pain in remission -30 HCs	VBM, SPM12 -3T, Siemens scanner,	**GMV: CD with pain < CD without pain and HC** in the insula and ACC [P<0.05, FDR corrected] **GMV: CD without pain > CD with pain and HC** in HIPP/PHG [P<0.05, FDR corrected] **CD with/without pain >HC in putamen** [P<0.05, FDR corrected]	The **GMV** of the insula and ACC were significantly negatively correlated with daily pain scores in patients with abdominal pain P < 0.005 (uncorrected), then FDR corrected using small volume correction
Agostini et al 2017, ITALY[208]	17 CD patients in remission 17 HCs	VBM, SPM8 -3T, GE 750	**GMV:** No difference found between HC and CD groups	N/A
Van Erp et al 2017, the Netherlands[350]	20 CD patients with fatigue in remission -17 HCs	VBM, FSL -3T, Philips Ingenia	**GMV: CD < HC** GMV in left superior frontal gyrus P-value < 0.05, corrected for multiple comparison	N/A
Mrakotsky et al 2017	37 paediatric CD patients 17 HCs	FreeSurfer	**CT: CD <HC** in posterior brain regions (bilateral inferior parietal, superior parietal, supramarginal [all pFDR < 0.05]) **GMV CD < HC** subcortical volume (bilateral hippocampi and thalami	
Thomann et al, Germany 2016[351]	15 CD in remission (of which 9 with EIM) 6 CD patients with no EIM 15 HCs	FreeSurfer -3T MAGNETOM Skyra	**CT:** No differences in CT were identified in the group and subgroup comparisons **Surface area: CD with EIM>HC** left rostral middle frontal gyrus **Gyrification index (GI): CD>HC** CD with EIM subgroup showed elevated local GI in the left lingual gyrus, extending to precuneus, cuneus, PHG and isthmus cingulate **CD with EIM vs. CD without EIM:** elevated GI in right rostral ACC, extending to superior frontal gyrus and lower GI in the right insula**.**	None of the observed alterations was significantly correlated with disease duration

Nair et al 2016, USA[339]	19 CD in remission and 20 HC	FreeSurfer 3 T GE 750	**CT: CD<HC** middle and superior frontal, superior temporal, superior parietal, precuneus, and pericalcarine regions. **(P<0.001, uncorrected).** **CT: CD > HC** in left superior frontal region **(P<0.05, corrected),** lateral occipital, post-central, and the superior and inferior temporal regions **(P<0.001, uncorrected).** **CT: CD>HC** in the right middle temporal, post-central, lateral occipital, and inferior parietal regions (P<0.001, uncorrected). **Subcortical volume**: **CD < HC** Left putamen, left pallidum, right putamen, right pallidum **(P<0.05, uncorrected)** **Cortical surface area: CD <HC** left precuneus, pars opercularis, fusiform, paracentral, superior temporal and caudal middle frontal and insular regions **(P=0.09, uncorrected)** **Cortical surface area: CD> HC** temporal pole, superior frontal regions **(P=0.09, uncorrected)**	The surface area of the left middle temporal region correlated negatively with VF test. The VF test was performed outside the scanner, using Controlled Oral Word Association Test, which measured the spontaneous production of words beginning with 'F,' 'A,' and 'S' in three respective 1-min trials.
Mrakotsky et al 2015, USA[357]	25 paediatric CD patients, 10 HCS	FreeSurfer	**CT: CD<HC** posterior regions (bilateral inferior parietal, superior parietal, supramarginal [<0.001–0.01]) and middle frontal gyrus (<0.05) **Subcortical volume: CD<HC** posterior regions (bilateral inferior parietal, superior parietal, supramarginal [<0.001–0.01]) and middle frontal gyrus (<0.05),	Inflammation during active disease was associated with cortical thinning (<0.001–0.05) Higher disease severity and steroid medication were negatively associated with brain structures (<0.001–0.05), as was lifetime use of steroids.
Bao et al 2015, CHINA[358]	44 CD remission and 33 HC	VBM (SPM8) and FreeSurfer -3T SIEMENS TRIO Covariates:	**GMV: CD <HC** bilateral ACC, SMA, insula, postcentral gyrus, precentral gyrus, superior frontal cortex, dorsomedial [dmPFC], middle frontal cortex, superior temporal cortex, right MCC, left middle OFC, inferior frontal cortex, middle temporal cortex, inferior temporal cortex,	Negative correlations were found between disease duration and GM volume of the right ACC, dmPFC, and left insula. Disease duration was also negatively correlated with the CT of the left insula and OFC

		total GM volumes, gender, age, weight, anxiety, and depression	and inferior parietal cortex. [p < 0.05, FDR corrected]. **GMV: CD>HC** periaqueductal grey [PAG], bilateral putamen, left pallidum, HIPP, thalamus, precuneus, posterior parietal cortex [PPC], right amygdala, and cerebellum. [p < 0.05, FDR corrected] **CT: CD <HC** bilateral OFC, superior frontal cortex, inferior parietal cortex, superior temporal cortex, left insula, rostral [rACC], caudal middle frontal cortex, pars triangularis, postcentral gyrus, middle temporal cortex, PHG, right [PCC], precentral gyrus, and fusiform gyrus **[p < 0.05, corrected]** **CT: CD >HC none**	
Zikou et al 2014, GREECE[359]	18 IBD (11 CD and 7 UC), 20 HC	VBM, FSL -1.5 T Philips	**GMV: CD <HC** right fusiform, left inferior temporal, left fusiform, right inferior temporal, right precentral, right SMA, right middle frontal, left superior parietal. [P<0.05, FWE, corrected] **GMV: CD >HC** none	
Agostini et al 2013, ITALY[360]	20 CD patients in remission 18 HCs	VBM, FSL -3T Philips	**GMV:** No difference was found between groups	
Agostini et al 2013, ITALY[355]	18 CD in remission and 18 HC	VBM, SPM5 3 Tesla Philips TIV and age	**GMV: CD <HC** middle and superior frontal gyrus, and**. (P<0.001, uncorrected)** after ROI approach SVC in the anterior MCC **GMV: CD > HC** none	Negative correlation with disease duration and GMV in the left precentral gyrus, RSFG, left/right middle frontal gyrus, and superior frontal gyrus, left subgenual anterior cingulate, right posterior midcingulate, left PCC, left/right PHG, right superior temporal gyrus, left inferior temporal gyrus, [P<0.001, uncorrected]

Table 39 Literature on structural brain changes in CD

Bao et al[349] examined GMV differences in CD patients in remission with abdominal pain, CD patients without abdominal pain and HCs. CD patients with abdominal pain had reduced GMV in the insula and ACC compared with CD without abdominal pain and HCs, these brain regions also negatively correlated with daily pain scores measured on a 0-10 VAS. The average pain score in this cohort of CD patients ranged from 1 to 5.4, indicating mild abdominal pain. CD patients without abdominal pain showed higher GMV in the hippocampal and PHG[349]. The increased GMV in the hippocampal and PHG was speculated to be a compensatory increase in GMV in the absence of pain. The findings of this study are in agreement with previous studies which also found a decrease in GMV in the insula[361] and ACC[355,361] and an increase in GMV in the hippocampal cortex[361]. In this study by Bao et al[349], anxiety and depression scores were used as covariates in the data modelling. This addition was redundant and may have influenced the final outcome of this study because despite showing a significant difference in HAD scores between groups, the scores were still in the normal range <7[362].

Studies by Agostini et al have reported inconsistent findings, with one study[355] reporting a decrease in GMV in the middle/superior frontal gyrus and the anterior MCC in CD patients compared with controls[355]. In this paper, they reported a negative correlation between GMV in various brain regions (right ACC, dmPFC and left insula) and disease duration, also CT of the left insula and OFC was negatively correlated with disease duration as shown in Table 39. A limitation of disease duration in the correlation analysis is that it does not account for the number and severity of relapses, surgical history and the type and duration of treatments and in general disease duration, it is not a good surrogate for disease burden, which is the disease variable that may have an effect on CT. In contrast,

two other studies by the same group found no difference in GMV between CD patients and HC[208,360]. This inconsistency was attributed to the small sample size, and the authors suggested the use of patients with a range of disease activity in future research.

Van Erp et al[350] reported reduced GMV in the left superior frontal gyrus in CD patients in remission with fatigue[350] compared to HC without fatigue. This study did not have a negative control group of CD patients without fatigue, therefore it is not possible to conclude whether the differences in GMV observed were related to CD per se or reflective of patients with both CD and fatigue. Just like pain assessments, fatigue assessments are also limited by the subjective nature of self-reporting.

A further study by Thomann et al[351], comparing CD patients in remission with a history of EIM (n=9), those without a history of EIM (n=6), and HCs (n=15), found no difference in the CT, cortical area and gyrification index in the combined CD group (n=15) compared to HCs. However, in a subgroup analysis, they showed that CD patients with EIM had a higher surface area in the left rostral middle frontal gyrus and higher gyrification index in the left lingual gyrus, precuneus, cuneus, PHG and isthmus cingulate. Also, a comparison between CD with EIM and without EIM showed higher gyrification index in the CD with EIM in the right rostral ACC and superior frontal gyrus, and lower gyrification in the right insula[351]. One of the biggest limitations of this study was the sample size, with only 9 CD patients with a history of EIM. In this study, cortical surface area and gyrification index were used as markers of brain development. This is the first study to speculate that structural brain changes might precede the clinical diagnosis of CD. The susceptibility to EIM is thought to be genetically determined

and attributed to the systemic nature of CD, so it has been proposed that the effect of systemic inflammation may be more severe in CD patients with EIM[351].

A study by Nair et al[339] showed cortical thickening in the left superior frontal region in CD patients in remission compared with HCs, this finding contradicts the findings of Bao et al [352] which showed cortical thinning of the same region. Other structural alterations reported in this study[339], but not surviving multiple comparison corrections, are provided in Table 39. In this study, the surface area of the left middle temporal region was found to be negatively correlated with verbal fluency (VF) test scores in the CD group and positively correlated in the HC group. This VF test was described by a controlled oral word association test performed outside the scanner, which measured the spontaneous production of words beginning with 'F' 'A' and 'S' in three respective 1-min trials, which can assess attention, verbal memory, and word knowledge. However, it is important to note that the difference in the surface area between CD and HC did not survive multiple comparisons and no difference in the VF test scores was found between the groups. It was postulated that the reason for no difference in the VF task between groups was because CD patients' brains may have undergone a compensatory mechanism. This proposed compensatory mechanism was based on another fMRI experiment by the same research group[363] which used the same VF task inside the scanner, where CD patients recruited more of the right hemisphere regions compared to HC during fMRI task performance.

Bao et al[352] examined a larger sample size of CD patients in remission, including 44 CD patients and 33 HCs. Comparison between the two groups showed higher GMV in the putamen, pallidum, thalamus, amygdala, and other regions and lower GMV in the frontal and temporal regions as shown in Table 39. Also cortical

thinning was found in the CD group compared with HCs in the insula, cingulate cortex, PHG, and other cortical regions and no cortical thickening was reported in the CD group Table 39. In this study, repeated analysis of the group differences and correlation analysis was performed using anxiety and depression scores as covariates, along with gender, age and weight in the data model which gave different results. Significant differences in GMV that appeared in the right SMA, precentral gyrus, superior frontal cortex, middle frontal cortex, left middle OFC, inferior frontal cortex disappeared following the inclusion of HAD scores in the model. Similarly, after HAD scores were included in the statistical model, the differences in CT in the left PHG lost significance, and the intensity of the differences decreased in the RSFG, left insula, right ACC, postcentral gyrus, and right precentral gyrus. It is important to note that, despite showing a significant difference in HAD score between groups numerically, both groups were in the normal range i.e. <7, making the addition of these scores to the model redundant, hence the results before the inclusion of HAD score in the model should be considered when comparing between studies.

Zikou et al[359] examined 18 IBD patients (including 11 CD patients and 7 ulcerative colitis UC) and found reduced GMV in the right fusiform, left inferior temporal, left fusiform, right inferior temporal, right precentral, right supplementary motor area (SMA), right middle frontal, left superior parietal compared with HC. The loss of GMV in the inferior temporal, precentral, SMA, middle frontal and superior parietal is in line with findings by Bao et al[358].

In summary, presently there are no consistent regions or patterns across studies implicating the structural brain changes in CD. The inconsistences in findings between these published studies could be attributed to variability in disease

location, disease activity, disease duration, and medication use. Additionally, the inconsistencies could also be due to differences in analysis methodology, identity/version of the processing software, size of smoothing kernel used, and the choice of covariates used in the statistical model. The cross-sectional nature of the studies mean there is a small window to assess the association between mild abdominal pain or fatigue and structural brain measures. Furthermore, it is hard to describe the chronology of events in the pathogenesis of CD and whether brain involvement precedes CD diagnosis or is a manifestation of the disease.

In this chapter, an exploratory analysis was performed to determine if disease location (i.e. ileal CD compared with colonic CD) differentially affects brain structure and if such changes are linked with appetite regulatory peptides.

4.7 Hypothesis and aims of the study

- The hypothesis is that the GMV, WMV and CT will be affected in patients with active CD

The aims are as follows:

- To investigate the differences in GMV, WMV and CT between patients with active CD and HCs.
- To correlate brain measures in active CD with clinical and behavioural scores.
- To determine if disease location and EEC peptides are associated with brain structure
- To investigate differences in these brain measures in CD patients with and without EIM

4.8 Methods

The following outlines the methods performed in this PhD thesis to assess structural changes in CD.

4.8.1 Symptoms and psychological assessment

Abdominal pain scores were assessed using a 100 mm VAS. Fatigue scores were measured using the first section of IBD-Fatigue self-assessment scale, reporting on identifying fatigue, its severity, frequency, and duration, where 0= no fatigue, 1 to 10= moderate fatigue, 11 to 20 = severe fatigue. CRP and FCP values were collected at inclusion as part of standard patient care. CD symptoms were measured with an HBI[364] score recorded at inclusion. HBI being a simple index based on 5 items assessing symptoms and complications (including general wellbeing, abdominal pain, number of liquid or soft stools per day, abdominal mass and EIM).

4.8.2 Plasma gut hormone analysis

From the blood plasma samples, total PYY and GLP-1 were assayed in duplicates with commercially available ELISA (total PYY (catalogue no. EZHPYYT66K), (total GLP-1 catalogue no EZGLP1T-36K) ELISA Kits, Millipore, Billerica, MA, the USA as previously described[365] (described in detail in section 2.8.6)

4.8.3 Cytokine analysis

Serum levels of IL-6, IL-1 β and TNFα were measured using immunoassay kit (Duoset ELISA Development, R&D Systems, Inc, USA). The ELISA was performed by PhD student Lissa Sutherland at the School of Life Sciences (University of Nottingham) as described in detail in section 2.8.8

4.8.4 MR Image acquisition

The MRI data were acquired at the SPMIC, on a 3T Philips Achieva scanner (Philips Medical Systems, Best, Netherlands) with a 32-channel receive head coil, at the SPMIC, Nottingham UK. Structural MRI scans were acquired with a T_1-weighted [MPRAGE] sequence collected axial-oblique along the AC-PC line (1 mm isotropic resolution; TE/TR = 8.3/3.8 ms, flip angle = 8°, SENSE factor = 2, 160 slices, 256 x 256 matrix).

4.8.5 VBM

4.8.5.1 Preprocessing

Structural images were pre-processed using SPM12 [SPM12; Wellcome Department of Cognitive Neurology, University of London] and the associated toolbox CAT12 running on MATLAB [The MathWorks, Natick, MA] with default parameters given by the CAT12 toolbox. The T_1-weighted image data were segmented into different tissue classes: GMV, WM, CSF and then transferred into a stereotactic coordinate system MNI. The images were normalised using the high- dimensional DARTEL normalization[304]. After that, images were smoothed with a Gaussian smoothing kernel of 12 mm (FWHM) to allow parametric comparisons and compensate for possible inaccuracies from the spatial normalisation step. The final smoothed, modulated, and normalised images had a 1.5 mm isotropic voxel size.

4.8.5.2 VBM: Statistical analysis

Voxel wise GM differences between CD and HC were assessed using a two-sample t-test. Different GLM designs including the following covariates-of-no-interest were assessed: (i) TIV only; (ii) TIV and age; (iii) TIV, age and gender;

(iv) TIV, age, gender, and BMI. In this way, the effect of age, gender, BMI and variation in brain sizes were removed from the data and the effect of adding different covariates to the data could be assessed[366]. Possible edge effects between tissue types were avoided by excluding all voxels with GM values of less than 0.1 (absolute threshold masking). The statistical threshold for assessing voxel-wise differences was set at [P<0.05, FDR corrected], cluster size > 5. A multiple regression model was used to investigate the potential associations between GMV and clinical variables such as fatigue, abdominal pain, CRP, FCP, and pro-inflammatory cytokines [IL-6, IL-1β, TNF α] and fasting gut peptides [GLP-1, PYY and CCK], with results thresholded at [P<0.05, FDR corrected], cluster size > 5

In addition to standard parametric methods, a non-parametric, permutation-based threshold-free cluster enhancement was used (TFCE). This method has been found to be an effective method to deal with smoothness non-stationarity in VBM analyses[367] and its influence on cluster-based inference[368]. The number of permutations was set to 5000. The TFCE method with randomisation testing produces maps of cluster-enhanced t-statistics and p-values that correct for multiple comparisons across space[369]. Voxels were considered to be significantly different between groups at P < 0.05.

4.8.5.3 VBM: ROI analysis

Brain regions that showed a significant correlation in VBM statistical analysis were independently selected for correlation analysis using the ROI extraction tool in MaRSBar in the SPM toolbox https://www.fil.ion.ucl.ac.uk/spm/. Brain

volumes extracted from different regions were correlated with variables of interest in SPSS (IBM SPSS Statistics 24)

4.8.6 CT assessment

CT assessment was performed using both CAT12 and FreeSurfer for comparison of methods.

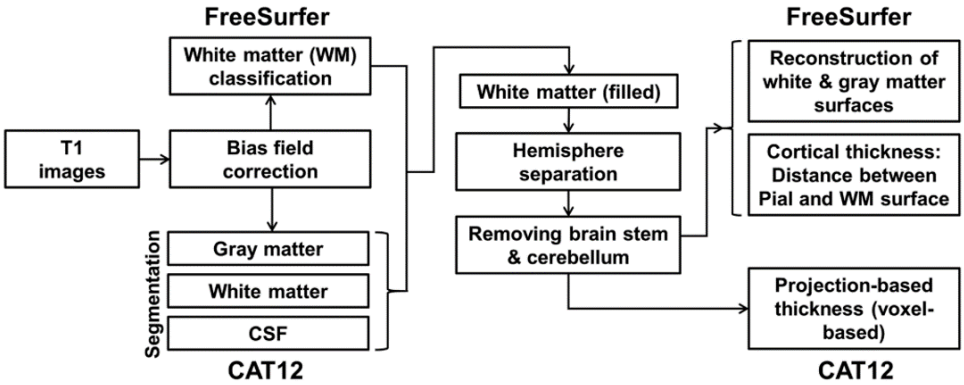


Figure 40 Flow chart shows the pre-processing steps used for both FreeSurfer and CAT 12 approaches [336]

4.8.7 FreeSurfer: CT analysis

All participants' data were processed with the FreeSurfer software [https;//surfer.nmr.mgh.harvard.edu/ version 5.3] using the "recon-all" processing stream with default parameters to create a 3-dimensional cortical surface model[272]. Non- brain tissue was removed using a hybrid watershed algorithm[370]. Subcortical WM and cortical GM were segmented using automated Talairach transformation. After that, intensity normalisation[325] and tessellation of the GM/WM boundary was performed. This was followed by automated correction of topological defects to ensure that the surface had the topological properties of a sphere, and surface deformation to form the GM and WM boundary[327]. CT was determined as the difference between the pial and WM surface. A smoothing kernel of 15 mm was

used prior to the estimation of a vertex specific GLM. The minimal processing time for a subject was 10 hours and the maximal time was 24 hours.

The Query Design Estimate Contrast (QDEC) interface of FreeSurfer, which uses a GLM approach, was used to perform a vertex wise analysis of CT, area and gyrification over the entire cortical mantle to assess significant differences between CD patients and HC. Monte Carlo Simulation was used to correct for multiple comparisons with 10000 iterations and cluster analysis was applied to determine contiguous clusters of significant cortical parameters between groups at a $P<0.05$. The estimated mean CT values were extracted and transferred to SPSS (IBM SPSS Statistics 24) to be used for further analysis.

4.8.8 CAT12: CT analysis

All participants were processed with the CAT12 toolbox ((http://www.neuro.uni-jena.de/cat/ version r1109) within SPM12 (http://www.fil.ion.ucl.ac.uk/spm/software/spm12/ version 6225) using MATLAB (8.3) to gather CT estimates. Firstly, volumes were segmented using surface and thickness estimation for ROI analysis in the writing options. Estimation of the CT and the CS was performed in one step, based on the PBT method[328]. Tissue segmentation was used to estimate the WMD, which projects the local maxima to other GM voxels [equal to the CT] by using a neighbour relationship described the WMD. The PBT method allows the handling of partial volume information, sulcal blurring, and asymmetries. The surface pipeline uses topology correction, spherical mapping, estimation of local surface complexity and local gyrification. A smoothing kernel of 15 mm was used prior to the estimation of vertex specific GLM.

4.8.8.1 CAT12: ROI analysis

Mean CT values were extracted using CAT12 toolbox defined by atlases, [aparc Desikan-Killiany atlas[371] and aparc 2009s[372,373]], which are automatic parcellations of the human brain cortical gyri and sulci using standard anatomical nomenclature. The estimated mean CT values were transferred to SPSS (IBM SPSS Statistics 24) to be used for further analysis.

4.9 Results

4.9.1 Recruitment

The consort diagram below shows the number of participants that were screened, consented, recruited and included in the brain structural data analysis. Please refer to Figure 70 in Chapter 6 which shows the summary consort diagram of the number of participants that appeared in each chapter. **28 CD patients and 17 HCs in this chapter appeared in Chapter 1.**

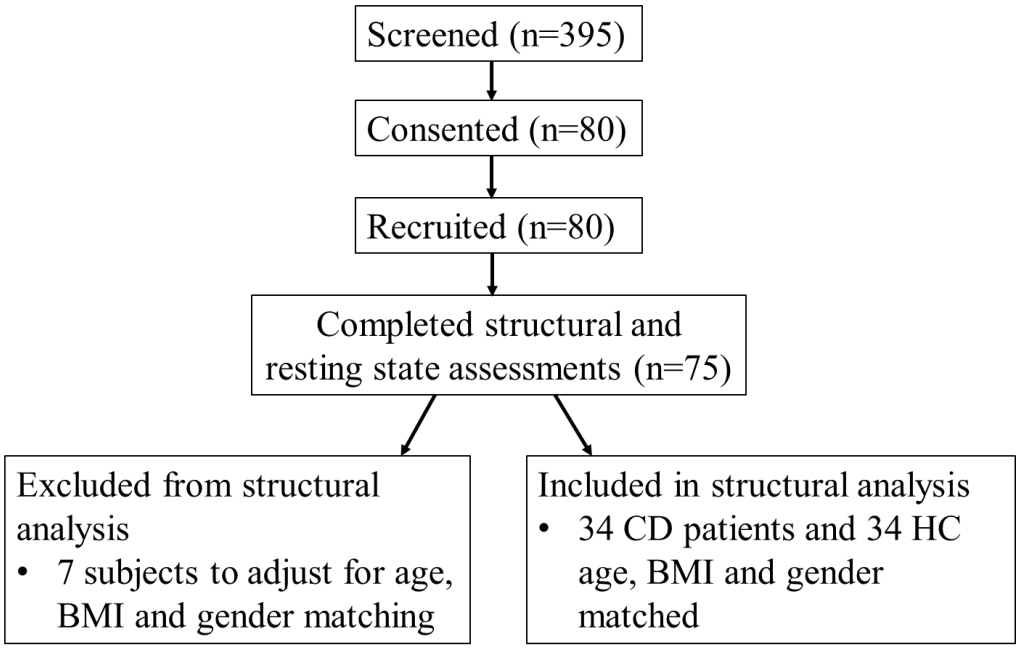


Figure 41 Consort diagram illustrating the number of participants included in this chapter

4.9.2 Subject demographics

34 active ileal/colonic CD patients and 34 age, BMI, and gender-matched HCs HCs were included in the structural assessment. Demographics for the CD and HC groups are provided in Table 40.

	CD **[n=34]**	**HC** **[n=34]**	**Significance** **[2-tailed]**
Age [years]	34.0 ± 3.0	35.0 ± 2.3	NS
BMI [kg/m^2]	25.0 ± 0.8	25.0 ± 0.6	NS
Gender [M/F]	20 M, 14 F	20 M, 14 F	NS
Abdominal pain score	21 ± 3.5	0 ± 0	P<0.05*
Disease duration [years]	6.7 ± 1.0	-	-
HBI	4.1 ± 0.5	-	-
IBD- Fatigue	10.5 ± 0.76	-	-
CRP [mg/dl]	20.3 ± 9.2	-	-
FCP [µg/g]	647.4 ± 140	-	-
Fasting GLP-1 [pM]	32.1 ± 3.44	17.7 ± 2.9**	0.009
Fasting PYY [pg/ml]	199.6 ± 11.3	158 ± 12.8**	0.031
EIM	10 with EIM, 24 without EIM		

Table 40 Demographic and clinical characteristics of CD patients and HC. Values are presented as mean ± SEM. **17 HC instead of 34 HCs are presented as (gut peptide analysis has only been performed on the plasma samples of 17 HCs). 49% of CD patients were on Anti-TNF therapy and 36% were on immunosuppressants and 14.3% on nil treatment

As an exploratory analysis, to assess whether disease location differentially affects brain structure and if any such changes are related to appetite regulatory gut peptides, CD patients were categorised into patients with ileal inflammation (ileal CD) and patients with colonic inflammation (colonic CD).

Table 41 expands details of the CD patients based on disease location, with 17 ileal, 17 colonic CD patients. Note 17 HCs are presented as a comparator group (gut peptide analysis was performed on the plasma samples of these 17 HCs). Fasting GLP-1 levels were significantly higher in the ileal CD patients compared with the HCs, whereas PYY levels showed a non-significant trend for ileal CD > HCs.

	Ileal [n=17]	**Colonic [n=17]**	**HC [n=17]**	**Significance [2-tailed]**
Age [years]	33.0 ± 3.4	35.0 ± 4.0	33.0 ± 3.2	NS
BMI [kg/m^2]	25.6 ± 1.1	25.0 ± 1.2	24.0 ± 0.8	NS
Gender [M/F]	10 M, 7 F	10M, 7F		
Abdominal pain score	23.0 ± 5.3	21.0 ± 6.0	0.0 ± 0.0	NS
Disease duration [years]	8.0 ± 2.0	6.0 ± 1.0	-	NS
HBI	4.0 ± 0.6	4.1 ± 1.0	-	NS
IBD-QoL	4.4 ± 0.2	5.0 ± 0.3	-	NS
IBD-Fatigue	11.4 ± 0.9	10.0 ± 1.3	-	NS
CRP [mg/dl]	9.5 ± 2.0	36.0 ± 16	-	NS
FCP [µg/g]	624 ± 210	669 ± 177	-	NS
TNF alpha [pg/ml]	87.0 ± 68	114 ± 58	65.3 ± 50.0	NS
IL-6 [pg/ml]	45 ± 15.0	87.0 ± 35	50.0 ± 17.0	NS
IL-1β [pg/ml]	133 ± 109	241 ± 104	59.0 ± 22.0	NS
GLP-1 [pM]	*35 ± 5.0	24 ± 4.0	*18 ± 3.0	P=0.013
PYY [pg/ml]	209 ± 16	195 ± 16	158 ± 13.0	P=0.070

Table 41. Demographic and clinical characteristics of ileal CD, colonic CD, and HC. Values presented as mean ± SEM. *GLP-1 Ileal-HC, P=0.013, PYY Ileal-HC, P=0.070

4.9.3 VBM of brain volume measures

4.9.3.1 Whole-brain volumetry between CD patients and HCs

Table 42 provides the whole brain volumetry for CD patients and the HC group. No significant difference was found in the TIV, GMV, WMV and CSF volume.

	CD [n=34]	**HC [n=34]**	**Significance [2-tailed]**
TIV cm^3	1513 ± 137	1550 ± 150	NS
GMV cm^3	688 ± 76	701 ± 75	NS
WMV cm^3	508 ± 57	529 ± 63	NS
CSF cm^3	317 ± 42	320 ± 47	NS

Table 42 Whole-brain volumetry of CD patients and the HC group. Values presented as mean ±SEM

Table 43 provides the whole brain volumetry of CD patients based on disease location i.e. ileal CD or colonic CD. No significant difference was found in the TIV, GMV and CSF volume between ileal and colonic CD patients

	Ileal CD [n=17]	**Colonic CD [n=17]**	**Significance [2-tailed]**
TIV cm^3	1525 ± 30	1496 ± 36	NS
GMV cm^3	704 ± 13	673 ± 21	NS
WMV cm^3	517 ± 14	496 ± 12.9	NS
CSF cm^3	305 ± 8.9	327 ± 11.1	NS

Table 43 Whole-brain volumetry ileal CD and colonic CD. Values presented as mean ± SEM.

4.9.3.2 Assessing GMV changes in CD

4.9.3.3 Comparison of GMV between CD patients and HCs

Figure 42 shows example slices illustrating the GMV of the CD and HC group.

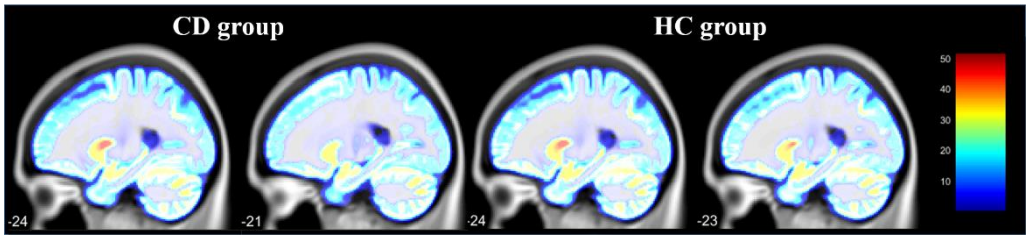


Figure 42 Mean global GMV in CD and HC

Figure 43 shows the result of the VBM analysis to assess GMV differences between the CD patients and HCs, with those areas with significantly reduced GMV in CD patients compared to HCs shown. Data are shown for each GLM models using differing covariates-of-no-interest: A) TIV alone; B) TIV and age; C) TIV, age, and gender; D) TIV, age, gender and BMI. It can be seen that CD patients showed lower GMV in the precentral gyrus, postcentral gyrus and left anterior orbital gyrus compared with the HC group Table 44. This effect was more evident when using both TIV and age as covariates-of-no-interest. There was little change on including gender and BMI as additional covariates-of-no-interest. No brain regions showed significantly greater GMV in CD patients compared with HCs.

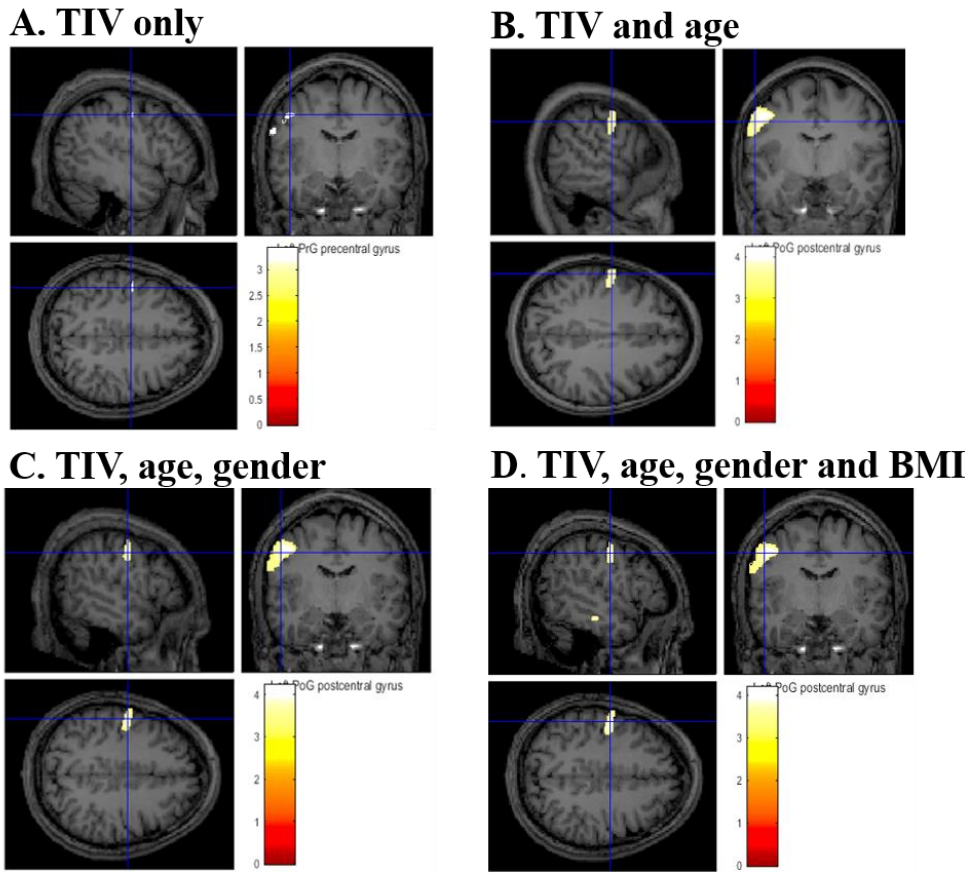


Figure 43 CD patients have significantly lower GMV in the left precentral gyrus, left postcentral gyrus and left anterior orbital gyrus compared to HCs. The SPM is displayed on a T_1-weighted normalised anatomical image (P<0.001, uncorrected, T =3.22). The colour bar represents the range of the T value. Data of **CD <HC** is shown for the inclusion of different covariates-of-no-interest: **A**. CD<HC, using TIV only as a covariate of no interest. **B**. CD < HC, using age and TIV only as covariates of no interest. **C**. CD<HC, using age, TIV and gender as covariates of no interest. **D**. CD<HC, using age, TIV, gender and, BMI as covariates of no interest. Table 44 provides those areas which showed GMV loss in CD patients compared with HCs when using age and TIV as covariates of no interest.

Anatomical regions	**uncorrected p (cluster level)**	**T value (voxel level)**	**MNI coordinates**			**Cluster size (k)**
			x	**y**	**z**	
Left precentral gyrus	0.043	4.23	-47	-11	44	893
Left postcentral gyrus		3.63	-59	-9	32	Sub-cluster
Left postcentral gyrus		3.58	-66	-12	27	Sub-cluster
left anterior orbital gyrus	0.329	3.55	-29	59	-11	187

Table 44: GMV, CD <HC using age and TIV as covariates of no interest, see Figure 43.

4.9.3.4 The association of GMV with age in CD patients and HC

Figure 44 shows those brain areas which had a negative association with age in the CD and HC group (i.e. reduced GMV with age - see Figure 32). A stronger negative correlation with age was observed in the CD group compared with HC.

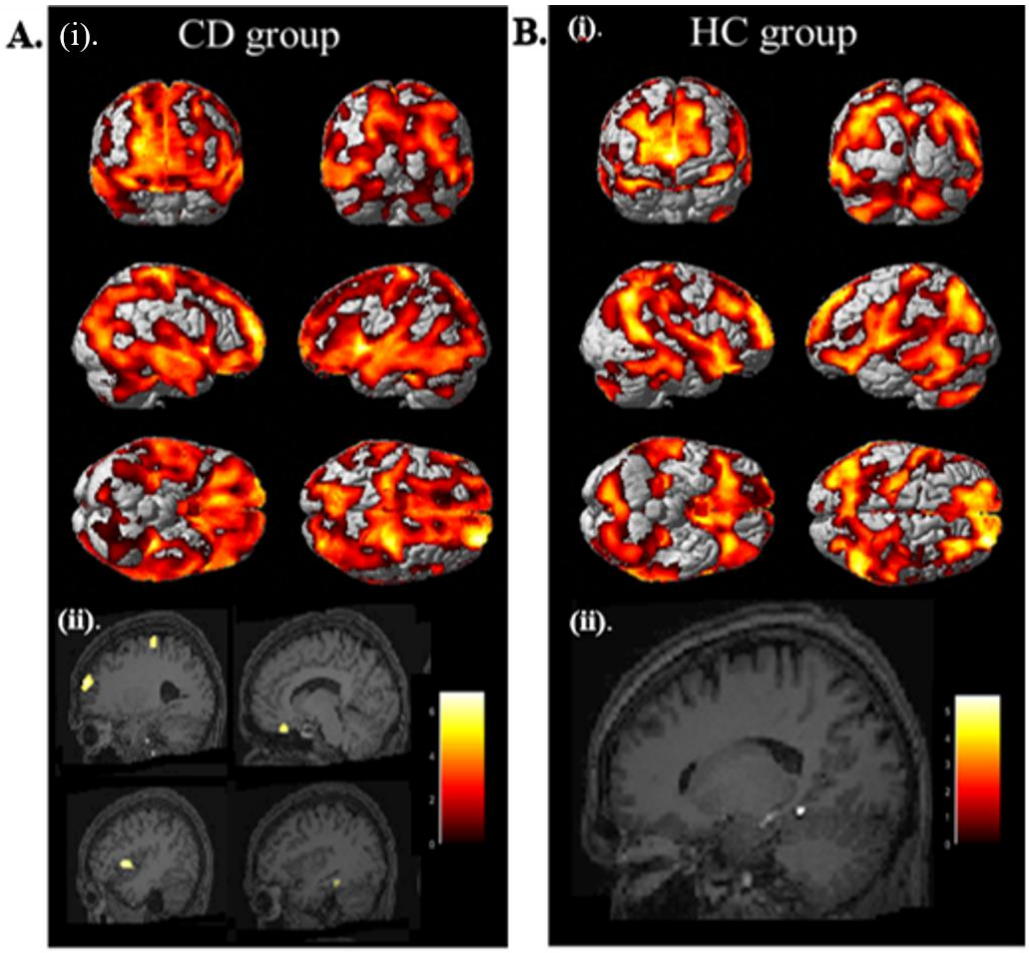


Figure 44 Brain regions demonstrating a negative correlation of GMV with age. **A**.(i) CD group, FDR corrected, P<0.05, k=5, T=2.08 using 3D rendering for display purposes. (ii) CD group FWE corrected P<0.05, k=5, T=5.4. **B**.(i) HC group, FDR corrected P<0.05 k=5, T= 2.14, using 3 D rendering for display purposes, **(ii)**. HC group FWE corrected P<0.05, k=5, T=5.35.

Anatomical regions	P FWE corrected (cluster level)	T value (voxel level)	MNI coordinates			Cluster size (k)
			x	y	z	
Right precentral gyrus	0.001	6.45	29	-23	63	246
RSFG	0.000	6.88	30	62	20	339
Left frontal operculum	0.000	6.62	-42	12	0	327
Left fusiform gyrus	0.003	6.52	-33	-33	-24	156
Right medial orbital gyrus	0.008	6.34	11	32	-30	80
Right lingual gyrus	0.028	5.56	20	-41	-12	17

Table 45 Brain regions demonstrating a negative correlation of GMV with age, FWE P<0.05, corrected

To determine if the (CD vs age) and (HC vs age) correlation coefficients were statistically significantly different, a Fisher's r to z transformation was used, which tells if the two slopes are statistically different, but not the gap between them[374]. The plots below show the regions where the correlation coefficients were significantly different between the two groups C (i) right precentral gyrus R1 vs R2; P=0.004 (ii) left fusiform gyrus R1 vs R2; P=0.008 (iii) Left frontal operculum R1 vs R2; P=0.01(iv) right medial orbital gyrus R1 vs R2; P=0.009

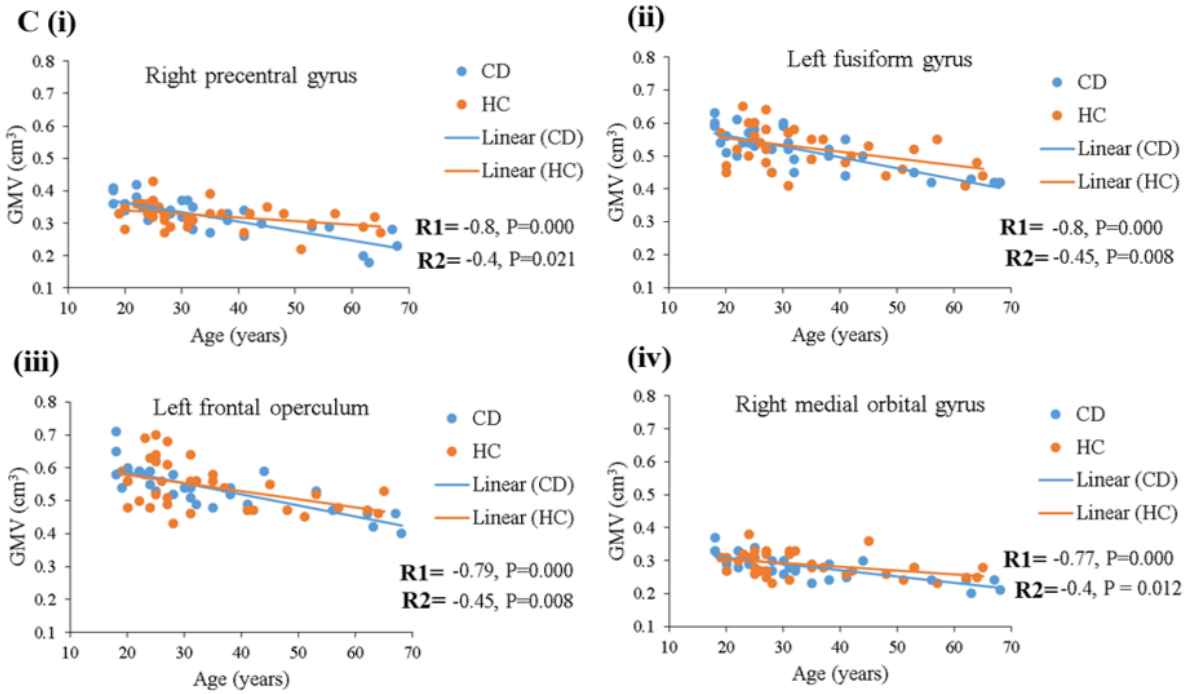


Figure 45 Plots of the negative correlation between GMV and age in CD patients and HC. CD patients exhibited a stronger negative correlation with age compared with HCs.

No brain regions in the CD or HC group showed a greater GMV with increasing age.

4.9.3.5 Comparison of GMV between CD patients with and without abdominal pain

The 20 CD patients with pain and 14 CD patients without pain were compared. Figure 46 shows those brain regions with greater GMV in CD patients with abdominal pain compared with CD patients without abdominal pain.

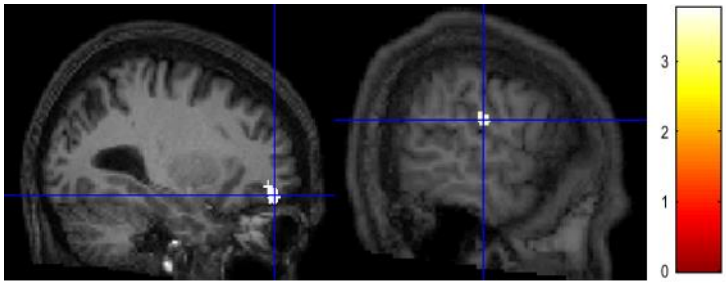


Figure 46 CD patients with abdominal pain had greater GMV than CD patients without pain in the right postcentral gyrus and left anterior orbital gyrus P = 0.001 uncorrected, k=10, T= 3.4.

Anatomical regions	**uncorrected p (cluster level)**	**uncorrected p (peak level)**	**T value (voxel level)**	**MNI coordinates**			**Cluster size (k)**
				x	**y**	**z**	
Right postcentral gyrus	0.56	0.000	3.67	60	-18	20	59
Left anterior orbital gyrus	0.38	0.000	3.76	-30	50	-20	126

Table 46. Brain regions with greater GMV in CD patients with abdominal pain compared to CD patients without abdominal pain

No significant differences were found for the CD with pain vs CD without pain condition.

4.9.3.6 Comparison of GMV between CD patients with and without EIM

11 CD patients with EIM and 23 CD patients without EIM were compared. Figure 47 shows those brain regions with greater GMV in patients without EIM compared with patients with EIM. There was significantly greater GMV in the left postcentral gyrus and right precuneus.

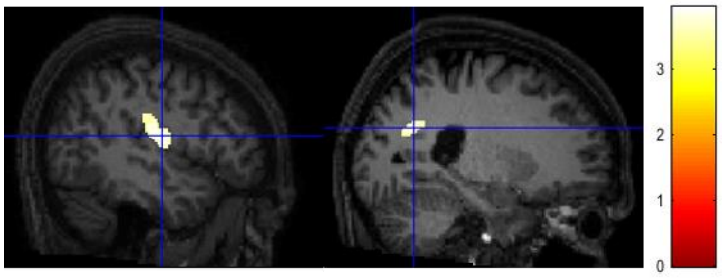


Figure 47 CD patients with no EIM had greater GMV in the left postcentral gyrus and right precuneus compared to patients with EIM. P = 0.001 uncorrected, k=10, T= 3.4

Anatomical regions	**uncorrected p**	**uncorrected p**	**T value**	**MNI coordinates**			**Cluster size (k)**
	(cluster level)	**(peak level)**	**(voxel level)**	**x**	**y**	**z**	
Left postcentral gyrus	0.075	0.000	3.96	-50	-18	23	569
Right Precuneus	0.184	0.000	3.93	27	-63	21	301

Table 47. Brain regions with greater GMV in CD patients with no EIM compared to CD patients with EIM

4.9.3.7 Correlation of GMV with IBD fatigue scores

CD patients with both ileal and colonic CD were combined in an analysis to assess GMV changes correlated with IBD fatigue scores (n= 26). Figure 48 shows that there was a significant negative correlation between GMV and IBD fatigue score bilaterally in the precentral gyrus.

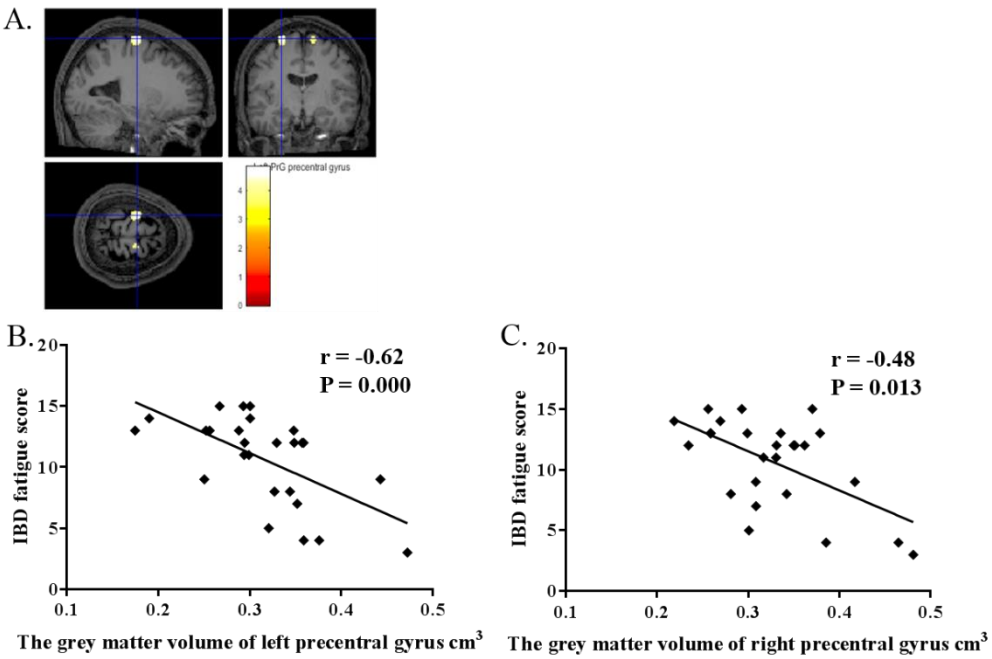


Figure 48 **A**. Brain regions with a negative correlation between GMV and IBD fatigue score. The SPM is displayed on the T_1-weighted image. P = 0.001 uncorrected, k=10, T= 3.5. The colour bar represents the range of the T value. **B**. Relationship between IBD fatigue score and the GMV of the left precentral gyrus. The higher the IBD fatigue score is associated with a GMV reduction of the left precentral gyrus (Spearman rank correlation: P=0.001, R=-0.62). **C**. Relationship between IBD fatigue score and the GMV of the right precentral gyrus. The higher the IBD fatigue score is associated with GMV reduction of the right precentral gyrus (Spearman rank correlation: P=0.013, R=-0.48).

Anatomical regions	**uncorrected p (cluster level)**	**uncorrected p (peak level)**	**T value (voxel level)**	**MNI coordinates**			**Cluster size (k)**
				x	**y**	**z**	
Left precentral gyrus	0.171	0.000	4.82	-26	-14	72	289
Right precentral gyrus	0.416	0.001	3.78	12	-15	71	101

Table 48 Brain regions showing a negative correlation between GMV and IBD fatigue score

Figure 49 shows a significant positive correlation between GMV and IBD fatigue score in the left supramarginal gyrus.

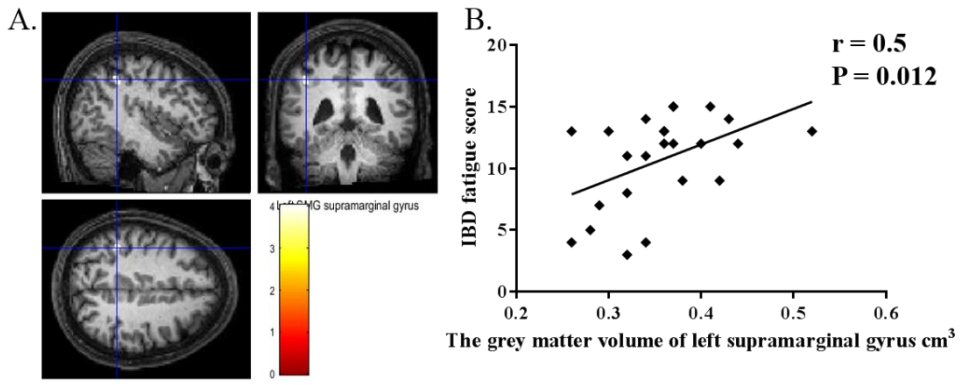


Figure 49 Relationship between IBD fatigue score and the GMV of the left supramarginal gyrus P = 0.001 uncorrected, k=10, T= 3.5. The higher the IBD fatigue score is associated with increased GMV of the left supramarginal gyrus (Spearman rank correlation: P=0.012, R=0.5)

Anatomical regions	uncorrected p (cluster level)	uncorrected p (peak level)	T value (voxel level)	MNI coordinates			Cluster size (Ke)
				x	y	z	
Left supramarginal gyrus	0.550	0.000	3.93	-42	-44	41	57

Table 49 Brain region with positive correlation with IBD fatigue score

There was no significant correlation of GMV with other clinical scores of HBI, FCP, and CRP.

4.9.3.8 Comparison of GMV between ileal and colonic CD patients and their relationship with fasting gut peptides

As an exploratory analysis of whether disease location differentially affects brain structure and if this is linked with fasting gut peptides, 17 patients with ileal CD were compared with 17 patients with colonic CD. Figure 50 shows greater GMV in ileal CD patients compared with colonic CD in the right postcentral and superior temporal gyrus.

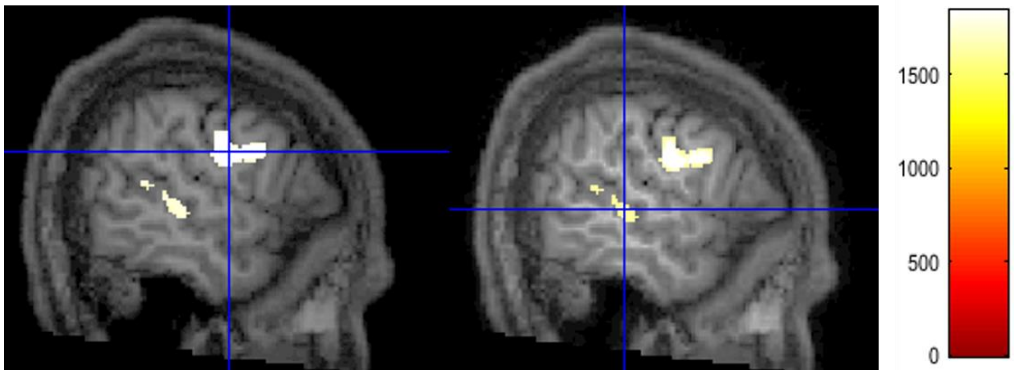


Figure 50 Patients with ileal CD had greater GMV than the colonic CD in the postcentral gyrus using age, BMI, TIV and gender as covariates of no interest. P<0.05, FWE corrected. The colour bar shows the TFCE values

Anatomical regions	$P_{FWE\text{-}corrected}$ (peak-cluster level)	TFCE value (voxel level)	MNI coordinates			Cluster size (Ke)
			x	y	z	
Right postcentral gyrus	0.024	1840.26	57	-9	23	1507
Right superior temporal gyrus	0.046	1561.34	57	-30	0	277

Table 50 Brain regions with greater GMV in ileal CD than colonic CD

Figure 51 shows the fasting GLP-1 and PYY levels in patients with ileal and colonic CD. A positive correlation was seen between fasting GLP-1 and GMV of the right postcentral gyrus, no correlation was found between GLP-1 and the right superior temporal gyrus. No correlation was found between PYY and the GMV of both regions.

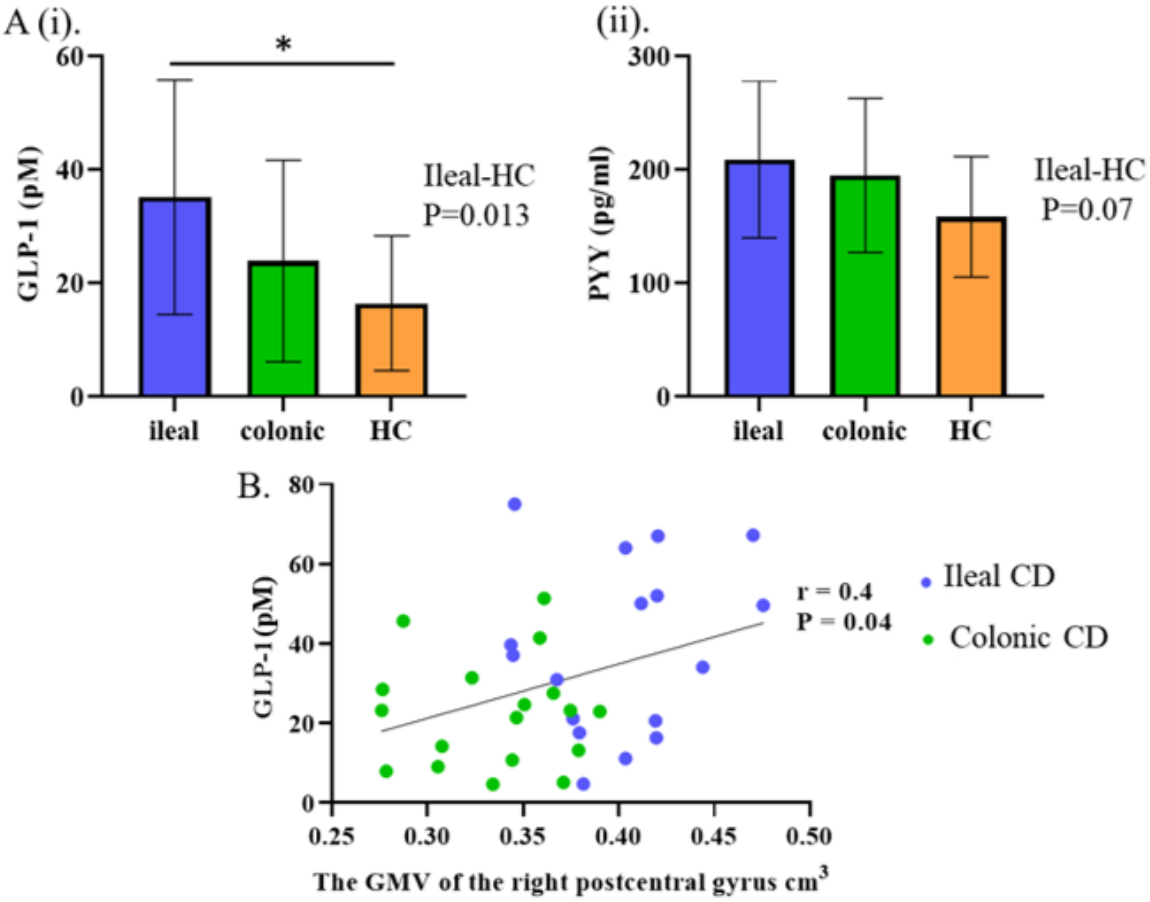


Figure 51 A. Fasting gut peptides (i) GLP-1 (pM) and (ii) PYY (pg/ml). B. Relationship between fasting GLP-1 levels and the GMV of the right postcentral gyrus (Pearson correlation: P=0.04, R=0.4)

4.9.4 Assessing WMV changes in CD

4.9.4.1 Comparison of WMV between CD and HC groups

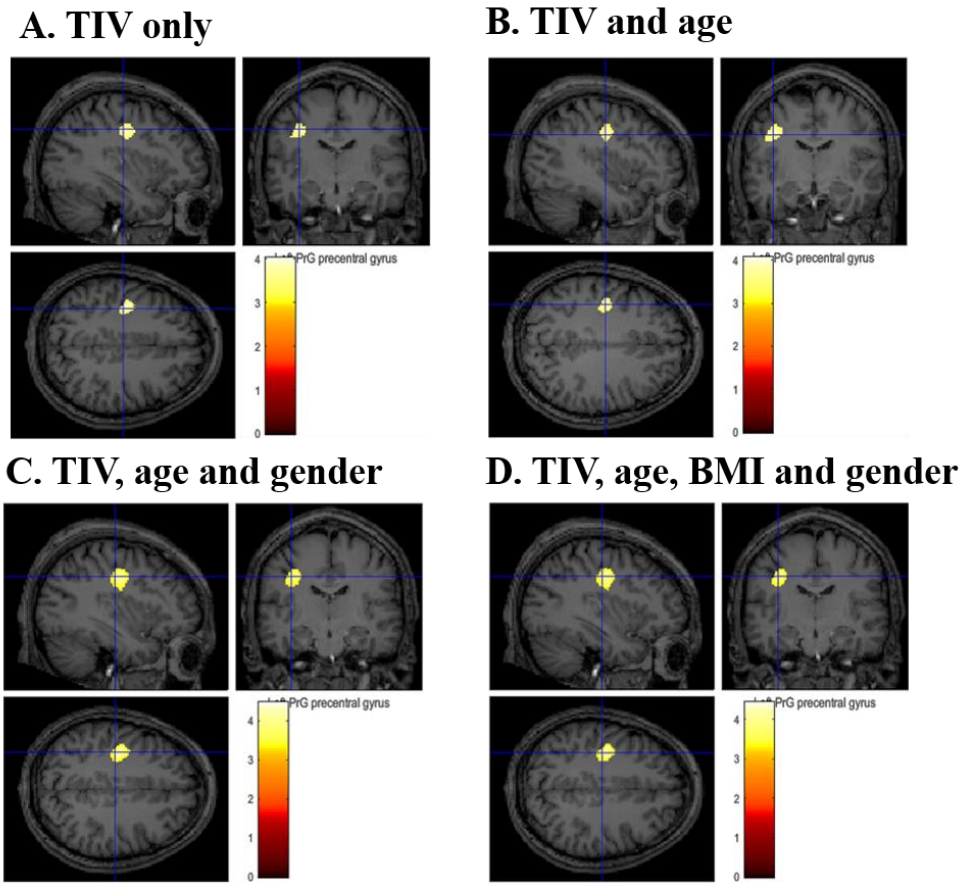


Figure 52 shows the result of VBM analysis to assess WMV differences between CD patients and HCs. CD patients have significantly lower WMV in the left precentral gyrus, compared to HCs. The SPM is displayed on a T_1-weighted normalised anatomical image (P<0.001, uncorrected, T =3.22). The colour bar represents the range of the T value. Data of **CD <HC** is shown for the inclusion of different covariates-of-no-interest: **A**. CD<HC, using TIV only as a covariate of no interest. **B**. CD < HC, using age and TIV only as covariates of no interest. **C**. CD<HC, using age, TIV, and gender as covariates of no interest. **D**. CD<HC, using age, TIV, gender and, BMI as covariates of no interest. Table 51 provides the region which showed WMV loss in CD patients compared with HCs when using age and TIV as covariates of no interest.

Anatomical regions	**uncorrected p**	**uncorrected p**	**T value**	**MNI coordinates**			**Cluster size (k)**
	(cluster level)	**(peak level)**	**(voxel level)**	**x**	**y**	**z**	
Left precentral gyrus	0.128	0.000	3.82	-41	-12	36	510

Table 51. Brain region showing CD<HC, WMV

4.9.4.2 Comparison of WMV between CD patients with and without EIM

CD patients with EIM had greater WMV than CD patients without EIM in the left PCG and the supramarginal gyrus as shown in Figure 53.

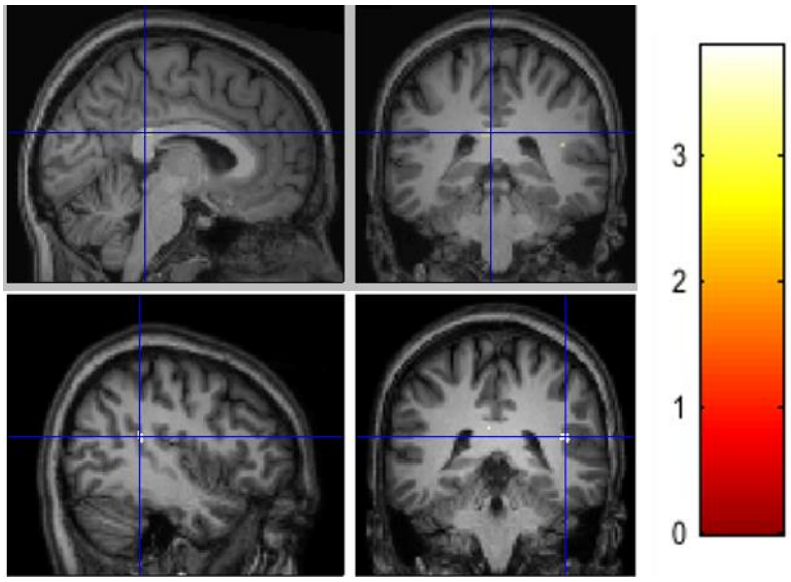


Figure 53 CD patients with EIM had significantly greater WMV than CD patients without EIM in the left PCG and the right supramarginal gyrus. SPM is displayed on a T1- weighted normalised anatomical image (P<0.001, uncorrected, k=10, T=3.37). The colour bar represents the range of T value.

Anatomical regions	**uncorrected p (cluster level)**	**uncorrected p (peak level)**	**T value (voxel level)**	**MNI coordinates**			**Cluster size (k)**
				x	**y**	**z**	
Right supramarginal gyrus	0.634	0.000	3.85	45	-41	17	47
Left PCC	0.471	0.001	3.61	-3	-38	24	100

Table 52 Brain regions showing greater WMV in CD patients with EIM compared with CD patients without EIM.

4.9.4.3 Correlation between WMV and fatigue in CD patients

A negative correlation was found between fatigue score and the WMV in the right lingual gyrus.

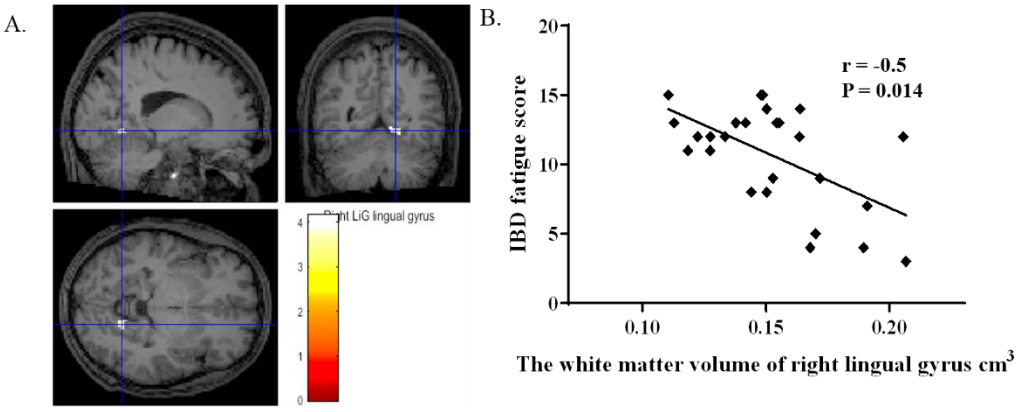


Figure 54A. A negative correlation between WMV and IBD fatigue score in the right lingual gyrus (P<0.001, uncorrected, T=3.5). B. Spearman rank correlation r=-0.5, P=0.014

Anatomical regions	**uncorrected p (cluster level)**	**uncorrected p (peak level)**	**T value (voxel level)**	**MNI coordinates**			**Cluster size (k)**
				x	**y**	**z**	
Right lingual gyrus	0.521	0.000	4.15	12	-59	-8	73

Table 53 Brain region with a negative correlation between WMV and IBD Fatigue score.

4.9.4.4 Comparison of WMV between patients with ileal and colonic CD and their relationship with fasting gut peptides

As an exploratory analysis of whether disease location differentially affects brain structure and if this is linked with fasting gut peptides, 17 CD patients with ileal CD and 17 CD patients with colonic CD were compared. Figure 55 shows those brain regions with greater WMV in patients with ileal CD compared with colonic CD. No regions survived (ileal CD < colonic CD).

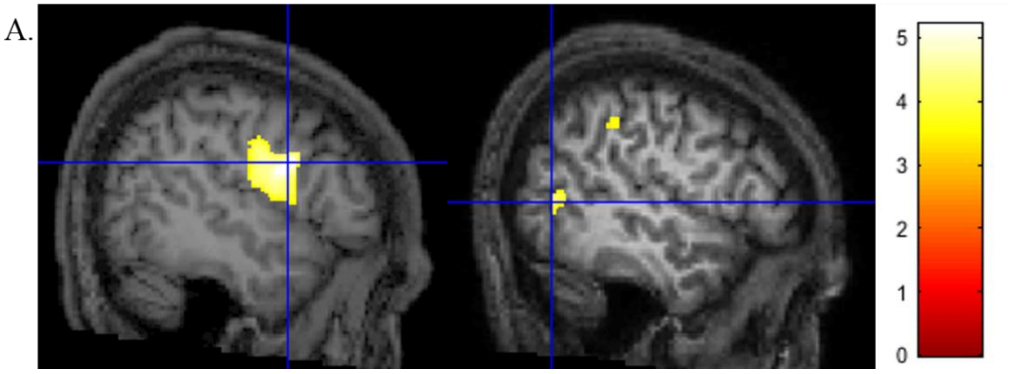


Figure 55 Brain regions with greater WMV in ileal CD patients than colonic CD patients, T=3.4, k=10 P<0.001, uncorrected

Anatomical regions	**uncorrected p (cluster level)**	**corrected p FWE (cluster level)**	**T value (voxel level)**	**MNI coordinates**			**Cluster size (k)**
				x	**y**	**z**	
Right precentral gyrus	0.004	0.010	5.21	51	6	23	2001
Left mid temporal gyrus	0.255	-	4.34	-51	-66	3	240
Left Supramarginal gyrus	0.542	-	3.80	-56	-39	39	72

Table 54 Brain regions with greater WMV in ileal CD than colonic CD

Figure 56 shows the fasting GLP-1 and PYY levels in patients with ileal and colonic CD. These fasting gut peptides were correlated with the regions above, i.e. right precentral gyrus left mid temporal gyrus and left supramarginal gyrus. A

positive correlation was found between the fasting GLP-1 and the WMV of the right precentral gyrus, no correlation was found between GLP-1 and the WMV of the left mid temporal gyrus and left supramarginal gyrus. A positive correlation was found between the fasting PYY and the WMV of the left supramarginal gyrus, no correlation was found between PYY and the WMV of the right precentral gyrus and the left mid temporal gyrus.

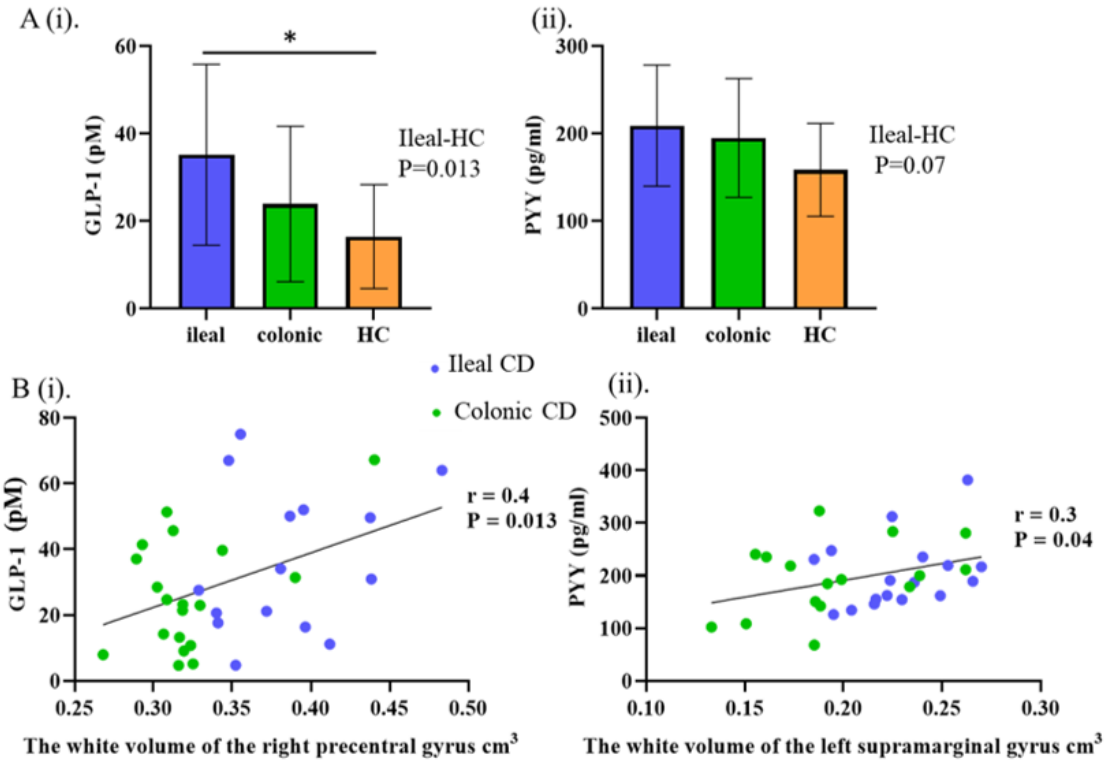


Figure 56 A. Fasting gut peptides (i) GLP-1 (pM) and (ii) PYY (pg/ml). B (i) Relationship between fasting GLP-1 levels and the WMV of the right precentral gyrus. The higher the GLP-1 levels are associated with a WMV increase of the right precentral gyrus (Pearson correlation: P=0.013, R=0.4). (ii) Relationship between fasting PYY levels and the WMV of the left supramarginal gyrus. (Pearson correlation: P=0.04, R=-0.3).

4.9.5 CT: CAT12

Both FreeSurfer and CAT12 were used to assess CT. In this thesis chapter, the results of the analysis using CAT12 are presented as the primary results, with a discussion of the comparison of results between CAT12 and FreeSurfer provided in section 4.9.5.5.

Figure 57 shows the mean CT in CD patients and HCs. No significant difference in the global mean CT was found.

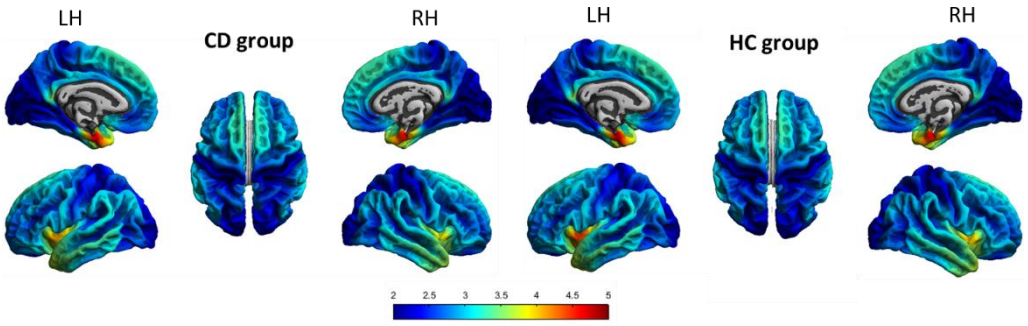


Figure 57 Mean CT (mm) in CD patients and the HC group

4.9.5.1 Comparison of CT between CD patients and HCs

4.9.5.2 Whole-brain analysis

Reduced CT was found in the CD patients compared with the HC group (CD<HC). Those brain regions with cortical thinning in CD patients compared with HCs are shown for a whole-brain analysis (Figure 58 A and Table 55) and ROI analysis (Figure 58 B and Table 56). Conversely, no cortical thickening was found in either the whole brain and ROI analysis.

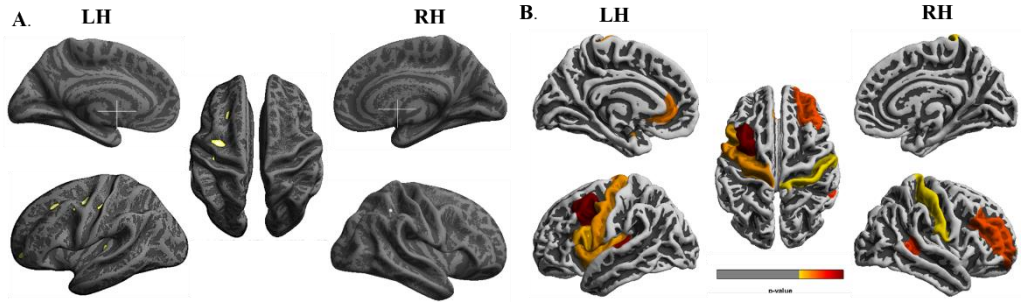


Figure 58 A. Differences in CT for CD < HC (P<0.001, uncorrected) for A. Whole-brain analysis, B. ROI analysis as defined by the aparc Desikan-Killiany atlas.

Anatomical location	MNI space (X, Y, Z in mm)	Cluster size K_E (voxels)	Peak – t values	Peak- P uncorrected values
Left precentral gyrus	-32, -7, 45	351	4.21	0.000
Left frontal pole	-32, 55, -2	115	3.90	0.000
Left superior frontal gyrus	-23, 20, 39	121	3.78	0.000
Left insula	-38, -25, 6	121	3.51	0.000
Left precentral gyrus	-34, -22, 44	120	3.43	0.001
Left middle frontal gyrus	-40, 5, 44	14	3.30	0.001
Right superior parietal	34, -44, 46	50	3.41	0.001

Table 55 CT: whole-brain analysis CD<HC

CT mm	hemisphere	Region	P-value
CD < HC	Left	caudalmiddlefrontal	0.005
		transversetemporal	0.006
		rostralanteriorcingulate	0.032
		precentral	0.035
		insula	0.037
		parsopercularis	0.039
CD < HC	Right	Bankssts	0.022
		rostralmiddlefrontal	0.026
		postcentral	0.049

Table 56 CT: ROI analysis CD<HC

4.9.5.3 Correlation between (CT) and IBD fatigue score in CD patients

In CD patients, a negative correlation between IBD fatigue score and CT was found in the mid-frontal gyrus, as shown in Figure 59.

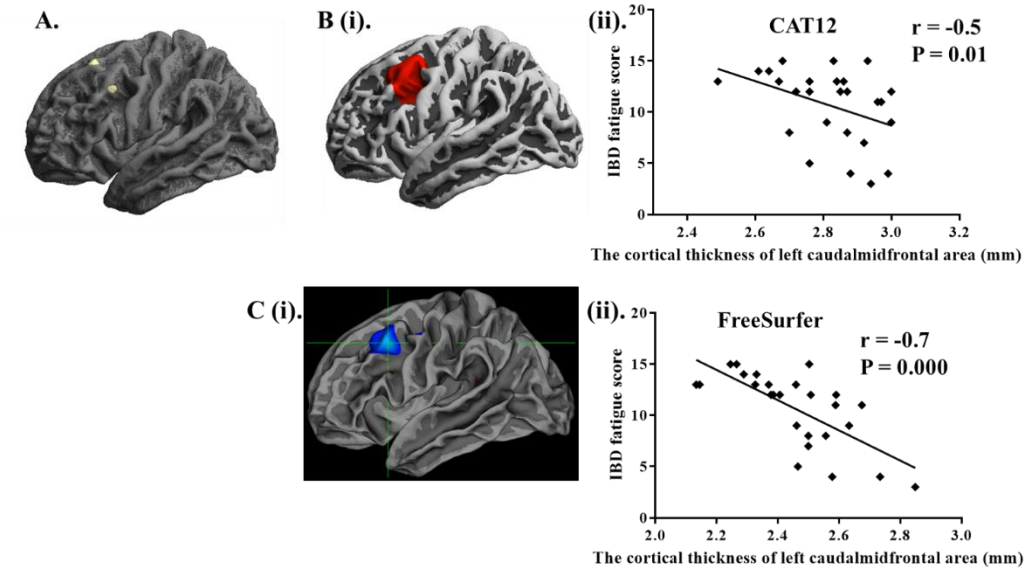


Figure 59. Brain regions showing negative correlations between IBD fatigue score and CT. A. Whole-brain analysis, P<0.001, uncorrected. B (i) ROI analysis in CAT12 as defined by aparc Desikan Killiany atlas: negative correlation of caudal midfrontal region CT and fatigue, P<0.019, uncorrected (ii) Negative correlation using CT from CAT12, Spearman correlation r = 0.5, P=0.000 C (i) FreeSurfer analysis: negative correlation in caudal midfrontal region CT and fatigue (ii) Negative correlation using CT from FreeSurfer, Pearson correlation r =0.7, P=0.000.

Anatomical location	**MNI space (X, Y, Z in mm)**	**Cluster size (k)**	**Peak – t values**	**Peak-, uncorrected values**
Middle frontal gyrus	-42, 13, 40	77	4.15	0.000
Superior frontal gyrus	-22, 23, 58	89	3.88	0.000

Table 57: Brain regions showing a negative correlation between fatigue and CT in the: whole-brain analysis P<0.001, uncorrected

4.9.5.4 Comparison of CT between patients with ileal CD and colonic CD and their relationship with fasting gut peptides

Greater CT was found in ileal CD patients compared with colonic CD, as shown in Figure 60A and Table 58 using a whole-brain analysis and Figure 60B and Table 59 using an ROI analysis. Conversely, no greater CT was observed for colonic CD as compared to ileal CD. No significant correlation was found between fasting PYY and GLP-1 and CT.

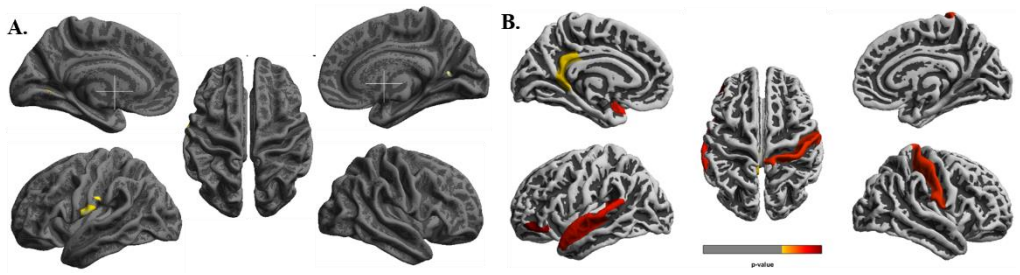


Figure 60 A. Ileal CD had greater CT than colonic CD, P<0.001 uncorrected, T=3.4 B. ROI analysis as defined by aparc Desikan-Killiany atlas, P<0.05, uncorrected.

Anatomical location	**MNI space X, Y, Z**	**Cluster size (k)**	**Peak t-value**	**Peak uncorrected p values**	**Peak FWE corrected**	**Cluster FWE corrected**
Left secondary somatosensory cortex	-62, -8, 10	470	5.17	0.000	0.018	0.017
Left postcentral gyrus	-60, -21, 26	73	3.91	0.000	0.338	0.510
Left lingual gyrus	-11, -64, 3	65	3.57	0.001	0.585	0.537

Table 58 Whole-brain analysis: Brain regions with greater CT in ileal CD patients compared with colonic CD patients

CT mm	hemisphere	Region	P-value P<0.05
Ileal>colonic CD	Left	parsorbitalis	0.010
		Superior temporal	0.019
		isthmuscingulate	0.046
Ileal>colonic CD	Right	postcentral	0.022

Table 59 ROI analysis: Brain regions with greater CT in ileal CD compared with colonic CD, P<0.05, uncorrected.

4.9.5.5 Comparison of FreeSurfer and CAT12 CT results

As expected, strong similarities were found between FreeSurfer and CAT12 results, however, there was an exception that cortical thinning was not detected in the most superior regions of the brain for FreeSurfer as compared with CAT12. Figure 61 illustrates an example of the negative correlation of CT with age. It can be seen there is a lower significance in the superior regions in FreeSurfer, and this was found to be attributed to an error in the segmentation in the superior slices, as shown in Figure 62, which would require extensive manual redrawing to correct.

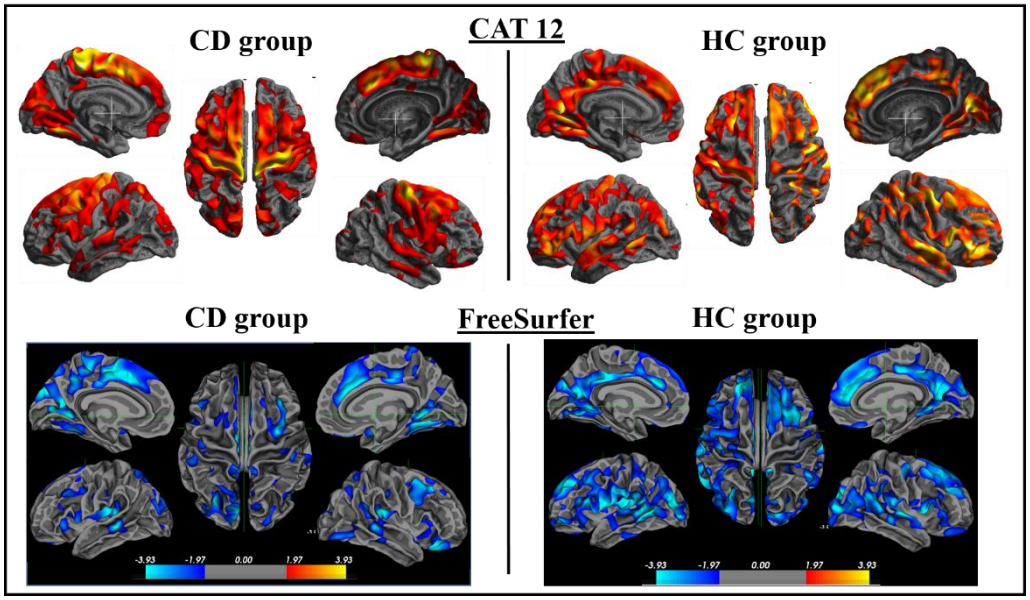


Figure 61 Comparison of the negative correlation of CT and age in CD and HC using CAT12 and FreeSurfer FDR corrected P<0.05, k=5. A. Negative correlation with age in CD group (CAT12). B. Negative correlation with age in the HC group (CAT12). C. Negative correlation with age in the CD group (FreeSurfer). D. Negative correlation with age in the HC group (FreeSurfer)

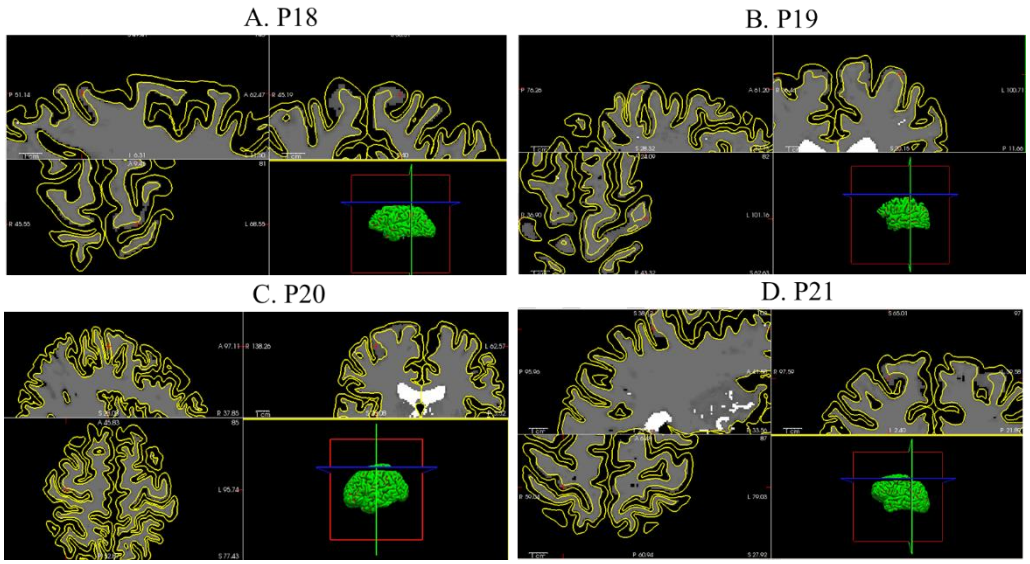


Figure 62 Examples of subjects with segmentation errors. 47% of CD patients and 40% of HCs had segmentation error at the top of the brain respectively

4.10 Discussion

This chapter studies the structural differences that exist in the brains of the patients with CD. The key findings are:

- GM, WM atrophy and cortical thinning in active CD patients compared with HCs.
- CD patients showed a stronger negative correlation of GMV with age compared with HCs.
- CD patients with pain showed greater GMV in the right postcentral gyrus and left anterior orbital gyrus compared with CD patients without pain, potentially representing use-dependent plasticity effects.
- CD patients with EIM had reduced GMV in the left postcentral gyrus and right precuneus compared with patients without EIM, suggesting systemic inflammation related GM atrophy. CD patients with EIM also had greater WMV than CD patients without EIM.
- Increased IBD fatigue was associated with GM, WM atrophy and cortical thinning.
- Ileal CD had greater GMV, WMV, and CT compared with colonic CD. GMV changes were linked with fasting GLP-1 but not PYY. WMV changes were associated with both fasting GLP-1 and PYY. No association between CT and fasting gut peptides were found.

These key findings are each discussed in the sections below.

4.10.1 Comparison of GMV and CT, and WMV between CD and HC

CD patients had lower GMV in the left precentral, left postcentral and left anterior orbital gyrus. The precentral gyrus is the site of the primary motor cortex, implicated in motor function and motor speech production[375]. The postcentral gyrus is the location of the primary somatosensory cortex, which responds to a sense of touch and movement[376] and flavour perception[104]. The anterior orbital gyrus has been shown to be involved in executive control and task switching[377].

The loss of GMV in the left precentral and postcentral gyrus has previously been reported by Bao et al[352] in CD patients in remission (using TIV, gender, age, and weight as covariates-of-no-interest). In this present study loss of GMV was also found in the left anterior orbital gyrus in active CD patients compared with HCs, which has not been previously reported in the literature.

Changes in GM CT alone were also explored. CD patients exhibited reduced CT compared with HCs in the left caudal middle frontal, left transverse temporal, left rostral anterior cingulate, left precentral and left insula, left parsopercularis, right banks of the superior temporal sulcus, rostral midfrontal and right postcentral gyrus. Table 60 lists these regions and their respective functions.

Region	Function
Left caudal middle frontal	Working memory and attentional control[378]
Right rostral middle frontal	
Left parsopercularis	
Left rostral anterior cingulate	Detection of salient stimuli[378]
Left insula	Detection of salient stimuli[378], pain processing[341], appetite regulation[118]
Left transverse temporal	Auditory and language processing[379]
Left precentral	Motor function
Right postcentral	Sense of touch, smell, flavour perception
Right banks of the superior temporal sulcus	Language perception and social functioning[380]

Table 60 Brain regions showing reduced CT in CD patients compared with HCs and their functions

Reduced CT in the left caudal middle frontal region and rostral ACC, left insula and superior temporal region, precentral, postcentral gyrus in CD patients compared with HC is in agreement with Bao et al[358]. Cortical thinning in the superior temporal region is in line with both Bao et al[358] and Nair et al[339].

Several VBM studies have been conducted in CD, however, only GMV and not WMV has been assessed. In this chapter, WMV differences between CD patients and HC were also assessed using VBM. Reduced WMV, along with GMV, was found in the left precentral gyrus (the primary motor cortex) in CD patients compared with HCs. Three studies have investigated WM alterations in CD using Diffusion Tensor Imaging (DTI) (Zikou et al[359], Van

Erp et al[350] and Hou et al (unpublished)). DTI is a non-invasive tool that measures the integrity of microstructural WM by measuring molecular diffusion of water molecules and provides high sensitivity in detecting axonal injury[381]. This method allows the analysis of fractional anisotropy and mean diffusivity (MD). FA indicates the overall directionality of the water diffusion, which is higher in organised WM tracts and lower in CSF and disorganised fibres[382]. MD measures the average diffusion properties of a voxel, which describes the rotationally invariant magnitude of the diffusion of water within a brain tissue[382]. Zikou et al[359] reported reduced axial diffusivity in the right corticospinal tract and the right superior longitudinal fasciculus in patients with IBD (11 CD, 8 UC) compared with matched HCs. They also reported a higher number of WM hyperintensities in IBD patients than controls. Van erp et al[350] found no difference across the WM MD and FA values between 20 CD patients and 17 HCs. In contrast, Hou et al[383] reported decreased FA values in the bilateral cingulate gyrus, increased MD values in the left cingulate gyrus, left inferior fronto-occipital fasciculus and bilateral superior longitudinal fasciculus in 20 CD patients and 20 matched HCs. It has been proposed that decreased/increased axial diffusivity could is linked to impaired WM fibre tract integrity, possibly due to cerebral small vessel vasculitis and the neurotoxic effects of proinflammatory cytokines[384].

The alterations observed in this present study in GMV and CT, and WMV in patients with active CD compared to HCs could be due to multiple factors such as systemic inflammatory response, fatigue, abdominal pain, psychological comorbidities, and medication use. Intestinal inflammation and pain may activate central sensitization pathways that convey visceral

nociceptive afferent signals from the gut to the brain[342,346], leading to brain structural changes. Additionally proinflammatory cytokines such TNFα, IL-1β, IL-6 are soluble regulatory proteins produced by immune cells and have the ability to interact with the CNS via the vagus nerve or directly with the BBB via cytokine receptors and can also cross the BBB via transporters or compromised leaks in BBB, propagating inflammatory signals within the brain via the activation of the endothelial cells, glial cells and macrophages[347], resulting in neuronal cell death. This could be manifested in the form of grey and WMV loss and cortical atrophy. To further understand if these structural brain changes are specific to CD, further investigation is required using a non-gastrointestinal chronic inflammatory disease patient group (such as rheumatoid arthritis/psoriasis) as a comparator group. This comparison will help to dissect the relationship between intestinal, systemic inflammation and brain structure. Furthermore, due to the cross-sectional nature of this study, it is hard to say if the structural brain changes precede CD diagnosis or is a result of the disease symptoms, chronic inflammation and treatments. Longitudinal studies investigating the impact of psychological disorders on the development of CD have shown conflicting results. For example, one study found that depressive symptoms increased the risk of CD in women[385], whereas another study found that anxiety and depression were more common after CD diagnosis but preceded UC diagnosis[386]. Further studies are needed to elucidate if any premorbid gut-brain stimulation increases the risk of CD.

4.10.2 The association of GMV with age in CD patients and HCs

CD patients exhibited a stronger negative correlation of GMV with age compared with HCs in the right precentral gyrus, left frontal operculum, left fusiform gyrus and the right medial orbital gyrus. These regions are implicated in functions shown in Table 61.

Brain regions	**Function**
Right precentral gyrus	(primary motor cortex), motor function and motor speech production
Left frontal operculum	Language and speech processing[387]
Left fusiform gyrus	Object and face recognition and facial expression recognition[388]
Right medial orbital gyrus	Reward processing[389]

Table 61 Brain regions showing a stronger negative correlation of GMV with age in CD patients compared with HC

The stronger negative correlation of GMV with age could be reflective of CD manifestations, medication use, and related to other inflammatory condition predating the diagnosis of CD such as psoriatic arthropathy and rheumatoid arthritis. It could be argued that age is a proxy for disease duration, as it accounts for brain structural changes pre and post CD diagnosis. It is important to note that disease duration only considers brain structural changes post CD diagnosis and is not a good surrogate for disease burden and this measure does not account for the number and severity of relapses, surgical history, type/duration of treatment. Longitudinal studies are required to assess the time course of brain structural changes in CD and to assess the effect of ageing on brain structure.

Furthermore, comparisons must be made with a non-gastrointestinal disease group to better understand if the brain regions implicated are specific to CD.

4.10.3 Comparison of GMV and CT, and WMV in CD patients with and without pain

CD patients with pain showed greater GMV in the right postcentral gyrus and left anterior orbital gyrus compared with CD patients without pain. The increase in GMV in the right postcentral gyrus seen is in line with studies in fibromyalgia[390] and chronic pain patients[391] and could be linked with ongoing nociceptive inputs, where patients are increasingly attentive to nociceptive and unpleasant sensory stimuli leading to use-dependent plasticity effects[341,390]. Although pain-related GMV modifications have been widely reported in the literature, there is still some controversy regarding the direction of change (i.e. increase or decrease of GM)[392,393]. Also, the GMV alterations implicated in pain processing are not solely limited to the pain matrix (cingulate cortex, insula, thalamus, amygdala), as non-pain processing regions have also found to be affected[392,393]. The finding from the present study contradicts previous findings[349], where CD patients in remission with abdominal pain, CD patients without abdominal pain and HCs were compared using total GM volume, age, gender weight, and anxiety and depression scores as covariates (the addition of the HAD score was unnecessary in this study as all groups were in the normal range). CD patients in remission with abdominal pain had reduced GMV in the insula and anterior cingulate compared with CD without abdominal pain and HCs. CD patients without abdominal pain showed higher GMV in the hippocampal and PHG compared with HC and CD with pain. The inconsistency between Bao et al and the present study could be due to variations in the CD

population studied, statistical models used in the analysis, variation in disease burden, disease activity (i.e. active vs remission) and medication used. No difference was found in the CT or WMV between CD patients with pain and without pain.

4.10.4 Comparison of GMV and CT, and WMV in CD patients with and without EIM

CD patients with no EIM had greater GMV in the left postcentral gyrus and right precuneus compared with CD patients with EIM. The postcentral gyrus is involved in somatosensory processing and the precuneus is involved in episodic memory/mental imagery[394] and also is the functional core of the DMN[395]. No difference in GM CT was found between CD patients with and without EIM.

CD patients with EIM had greater WMV than CD patients without EIM in the left PCG and the supramarginal gyrus. The cingulate activity has been linked with anxiety symptoms in CD patients[396] and the supramarginal gyrus is involved in language perception and processing[397]. This is the first study to report GMV and WMV changes in CD patients with and without EIM. Only one previous study by Thomann et al[351] investigated structural brain measures (except GMV and WMV) in CD patients with EIM. They found no difference in CT between CD patients with and without EIM, in line with the findings of this present study. EIM in CD predominantly affects the joints, eyes, and liver indicating systemic inflammation, which is also thought to be genetically determined[398]. The reduction in GMV in the left postcentral and right precuneus in CD with EIM could be attributed to chronic systemic inflammation resulting in GM atrophy.

4.10.5 Correlation of GMV and CT, and WMV with IBD fatigue scores

IBD fatigue scores were found to correlate negatively with GMV in the left and right precentral gyrus, the primary motor cortex. Also, a positive correlation was found between IBD fatigue scores and the GMV of the left supramarginal gyrus, an area involved in language perception and processing[397]. The underlying mechanism for fatigue-related brain structural changes is still poorly understood. In CD patients, disease severity, chronic inflammation, depression, anxiety, sleep disturbances and IBS-like symptoms may all lead to severe fatigue[399]. It can be hypothesised that GM atrophy of the primary motor cortex is linked with feelings of weakness, tiredness resulting in reduced physical activity. These findings contrast those of Van Erp et al[350], who showed reduced GMV in the left superior frontal gyrus in CD patients in remission with fatigue compared to HC without fatigue. However, Van Erp et al[350] did not have a negative control group of CD patients without fatigue, therefore, it is not possible to conclude whether the differences in GMV were related to CD per se or reflective of patients with both CD and fatigue. To address this question, our research group is undertaking a study investigating brain structural changes in CD patients with fatigue, CD patients without fatigue and HCs (McGing et al unpublished). In chronic fatigue syndrome, reduction in GMV in the bilateral PFC[400], occipital, parahippocampal regions[401] and increase in GMV in the amygdala and insula[402] have been reported.

IBD fatigue scores negatively correlated with the WMV of the right lingual gyrus, a region involved in visual information processing[403]. Studies investigating WMV using VBM in chronic fatigue syndrome (CFS) have

reported inconsistent results. For example, reduced WMV has been reported in the left occipital lobe in CFS patients compared with HCs[401].

IBD fatigue score also correlated negatively with the CT of the caudal middle frontal cortex, an area involved in working memory and attention control[378]. Presently, no studies have investigated brain CT in CD patients with fatigue. In CFS, cortical thickening has been reported in the middle temporal, precentral gyrus and occipital lobe[404].

The neuroplasticity observed in the present study in the lingual gyrus, caudal midfrontal region and the left supramarginal gyrus could be linked with cognitive fatigue.

4.10.6 Comparison of GMV and CT, and WMV ileal and colonic CD and their relationship with fasting gut peptides

In the present study, a significant difference was found between fasting GLP-l in ileal CD compared with HC, however, there was no difference between ileal and colonic CD in plasma GLP-1 levels as hypothesised. In contrast, a study by Moran et al[95] found no difference in fasting plasma GLP-1 levels between ileal, colonic and HC. However, an increase in the expression of GLP-1 positive cells and an increase in GLP-1 gene expression have been found the terminal ileum tissue of CD patients compared with HCs[95]. These findings may explain the increase in fasting GLP-1 plasma levels in ileal CD patients compared with controls found in the present study.

Ileal CD had greater GMV in the right postcentral gyrus and right superior temporal gyrus compared with colonic CD. In the combined CD group analysis, i.e. (ileal + colonic CD) vs HCs, a reduction in GMV of the left postcentral gyrus

was found. It could be postulated that the variance across CD patients in the right postcentral gyrus due to this difference between the ileal and colonic subgroups, may explain the lack of survival of the postcentral gyrus in the right hemisphere in the combined CD group analysis.

The GMV of the right postcentral gyrus correlated positively with the fasting GLP-1 levels. Presently, there are no studies that have investigated the association between fasting GLP-1 and GMV and WMV and CT in healthy or diseased states. The somatosensory cortex in the precentral gyrus has been implicated in flavour perception[405] and sensory processing. fMRI studies have found precentral gyrus to be implicated in appetite regulation[406,407]. It could be hypothesised that in GLP-1 mediates the neuroplasticity of the right postcentral gyrus with possible hedonic or homeostatic effects on appetite. The positive correlation was found between GLP-1 and the WMV of the right precentral gyrus. The precentral gyrus or the motor cortex has been implicated in appetite-related fMRI studies[126157], however, its significance is not understood. Similarly, the relationship between PYY and the left supramarginal gyrus is unclear. Only one VBM study by Weise et al[408] has investigated the effects of fasting and postprandial PYY on GMV and WMV in HCs, however, the left supramarginal gyrus was not reported in their findings. Further studies, investigating the effects of gut peptides on the brain structure are warranted.

4.11 Conclusion

Structural brain changes in active CD patients likely reflect the neuroplasticity to a chronic systemic inflammatory response and chronic symptom stimuli like abdominal pain and fatigue. The relative atrophy of the motor cortex could be a

possible central cause of IBD fatigue, and the neuroplasticity observed in the caudal midfrontal, lingual gyrus and supramarginal gyrus could be linked with cognitive fatigue. In the future, it would be interesting to compare CD patients with and without fatigue to further elucidate the central cause of IBD fatigue. It is important to note that, the cross-sectional nature of this study only provided a small window to assess the association between mild abdominal pain or fatigue and structural brain measures. Furthermore, it is hard to describe the chronology of events in the pathogenesis of CD and whether brain involvement precedes CD diagnosis or is a manifestation of the disease. The stronger negative correlation of GMV with age in CD patients compared with HC could be reflective of CD manifestations, medication use, surgery or effect of any other inflammatory condition predating the diagnosis of CD. Longitudinal studies are required to assess time course of brain structural changes in CD and to assess the effect of ageing on brain structure and function in CD patients. Future studies assessing brain structures in CD should use a non-gastrointestinal chronic inflammatory disease patient group as a comparator to dissect the relationship between gastrointestinal, systemic inflammation and brain structure. Future studies should also compare the same CD patients during the active phase of the disease and in remission, to see if the brain structural changes are reversible and associated with improved disease outcomes. Structural brain changes based on disease location in CD and the effects of fasting and postprandial gut peptides on brain structure require further investigation.

5 Resting-state fMRI functional connectivity and its alteration in CD

Alterations in RSFC have been previously documented in adult CD patients in remission, however, the data are inconsistent and not available in the active disease state. Studies on RSFC in CD also appear biased towards investigating major networks such as the DMN and the frontal-parietal network (FPN), hence neglecting the effect the disease may have on other resting-state networks RSNs. This chapter aims to investigate the differences in RSFC between patients with active CD and HCs across all known (RSNs). Finally, RSFC in CD patients is correlated with abdominal pain scores, IBD fatigue scores, disease duration and fasting GLP-1 and PYY.

This work was presented at the following meeting:

A resting-state fMRI study in patients with active CD. 14th Congress of European Crohn's and Colitis organisation ECCO- Inflammatory bowel Diseases, Copenhagen, March 2019. Poster presentation.

5.1 Background

Resting-state fMRI (RS-fMRI) measures the intrinsic functional connectivity (FC) of the brain. This relies on spontaneous low-frequency fluctuations (<0.1 Hz) in the BOLD signal generated from spatially distant but functionally connected and continuously communicating areas within a network[409]. FC provides a measure of the connections between two spatial regions that are linearly temporally correlated[409]. In contrast to FC, structural connectivity measures physical connections or interactions between two anatomical regions of the brain (via WM tracts) that can be measured using structural imaging techniques such as DTI which generate tractography maps[410]. It has been suggested that FC depends on structural connectivity, however, structural connectivity cannot predict FC patterns[411], because a single brain structure supports a variety of functions, and functional networks have characteristics that are context or time dependent[412]

The brain is always active and despite representing only 2% of the body's weight, it consumes 20% of the body's energy[413]. Studies have shown that brain energy metabolism from glucose oxidation correlates with BOLD signal processes[414]. These processes involve synaptic transmission, glutamate or gamma-Aminobutyric acid (GABA) recycling, calcium activities and haemodynamics through neurovascular coupling[414,415]. The non-signalling processes are involved in housekeeping functions such as maintenance of resting potential, biosynthesis and proton leaks[416]. However, the cost of signalling and non-signalling processes in the human brain are still unclear, making the quantitative interpretation of brain fMRI signals difficult[417]. Resting-state brain activity represents 60-80% of the brain's energy, possibly in the form of glutamate cycling reflecting neural

signalling processes[418]. In contrast, energy consumption during task performance is less than 5%[418]. The difference between task-based fMRI and resting fMRI[409] is outlined in Table 62.

Task-based fMRI	**Resting-state fMRI**
Measures spontaneous BOLD signal in the presence of a task or stimulus (e.g. finger-tapping, eye blinking, meal administration)	Measures spontaneous BOLD signal in the absence of an explicit task or any input
Highlights single brain network associated with any given task	Allows the observation of many networks at once
Takes ~ 20-30 mins to acquire data	Takes ~ 8-10 mins to acquire data
The signal during task-related activity is very small compared to the noise (80% of BOLD modulation discarded as noise)	The signals discarded as noise in task fMRI is taken as a signal in RS-fMRI. This is a low-frequency spontaneous fluctuation in the BOLD signal.
The removal of the signal as noise results in low SNR	Improved SNR due to the measurement of overall spontaneous low-frequency fluctuations of the BOLD signal
Participant cooperation is essential	Easier to perform resting-state fMRI in young children or patients unable to complete long experiments or perform cognitive tasks.

Table 62 Difference between tasked-based fMRI and resting-state fMRI[409]

5.2 Different RSNs and their behavioural interpretation

The importance of resting-state brain activity was first appreciated by Biswal et al[419] who correlated the time course of a seed ROI in the motor area with the time course of all other brain voxels. They demonstrated that the fMRI BOLD time series at rest in the left and right hemispheric regions of the primary motor cortex were highly correlated, indicating information processing and FC between these regions[419]. These observations reflect FC as defined by 'spatial patterns that are neuroanatomically distinct and functionally linked generating RSNs. Several other studies replicated Biswal et al's original findings[420], and other studies identified networks such as the visual network[420], auditory network[420], language network[421], dorsal and ventral attention networks[422] and DMN[423]. The most commonly reported RSNs in the literature are shown in Figure 63[424] with the brain regions involved and behavioural interpretations of the different RSNs shown in Table 63.

RSN	Regions	Function
Lateral visual	Middle temporal visual association area at the temporal-occipital junction	Most important in complex (emotional) stimuli (e.g. viewing faces/films)
Medial visual		Simple visual stimuli (e.g. flickering checkerboard)
Occipital visual		High order visual stimuli (orthography)[425]
Sensorimotor network	Involves SMA/MCC, bilateral primary motor cortex, and bilateral middle frontal gyri	The sensorimotor network resembles the activations seen in motor and sensory tasks[419]
Dorsal attention network (DAN)	Involves the intraparietal sulcus, the junction of the precentral and superior	Orienting focus to a particular task[426], also involved in cognitive top-down processing, which

	frontal sulcus (frontal eyelids)	involves factors such as knowledge, expectation and current goals[426]
Salience network	Involves fronto-insular and ACC with connections to the subcortical and limbic region	Implicated in orientation toward salient emotional stimuli, conflict monitoring, response choice, information integration, pain-related processes during acute stimulus-induced pain[427]
Temporal RSN	Involves inferior frontal gyrus, medial temporal gyrus, superior temporal gyrus	Involved in reading and language processing [428]
DMN	Involves precuneus, PCC, mesiofrontal/ACC and temporoparietal junction regions	Less active during task performance, compared with resting state, linked to self-related and internal process such as thoughts independent of any stimulus[429]
FPN	Involves frontal and parietal lobules and cingulate gyrus	FPN has been associated with different functions, i.e., executive function working memory, language, attention and visual processes[428].
Cerebellar network	Cerebellum	Associated with action and somesthesis (sense of touch, pressure, temperature, etc.), involved in processing humorous stimuli[425]
Executive control network (ECN)	Involves the medial frontal gyrus, superior frontal gyrus, and ACC	Involved in tasks relying on executive functions, such as control processes and working memory. [430].

Table 63 Different RSNs and their behavioural interpretation

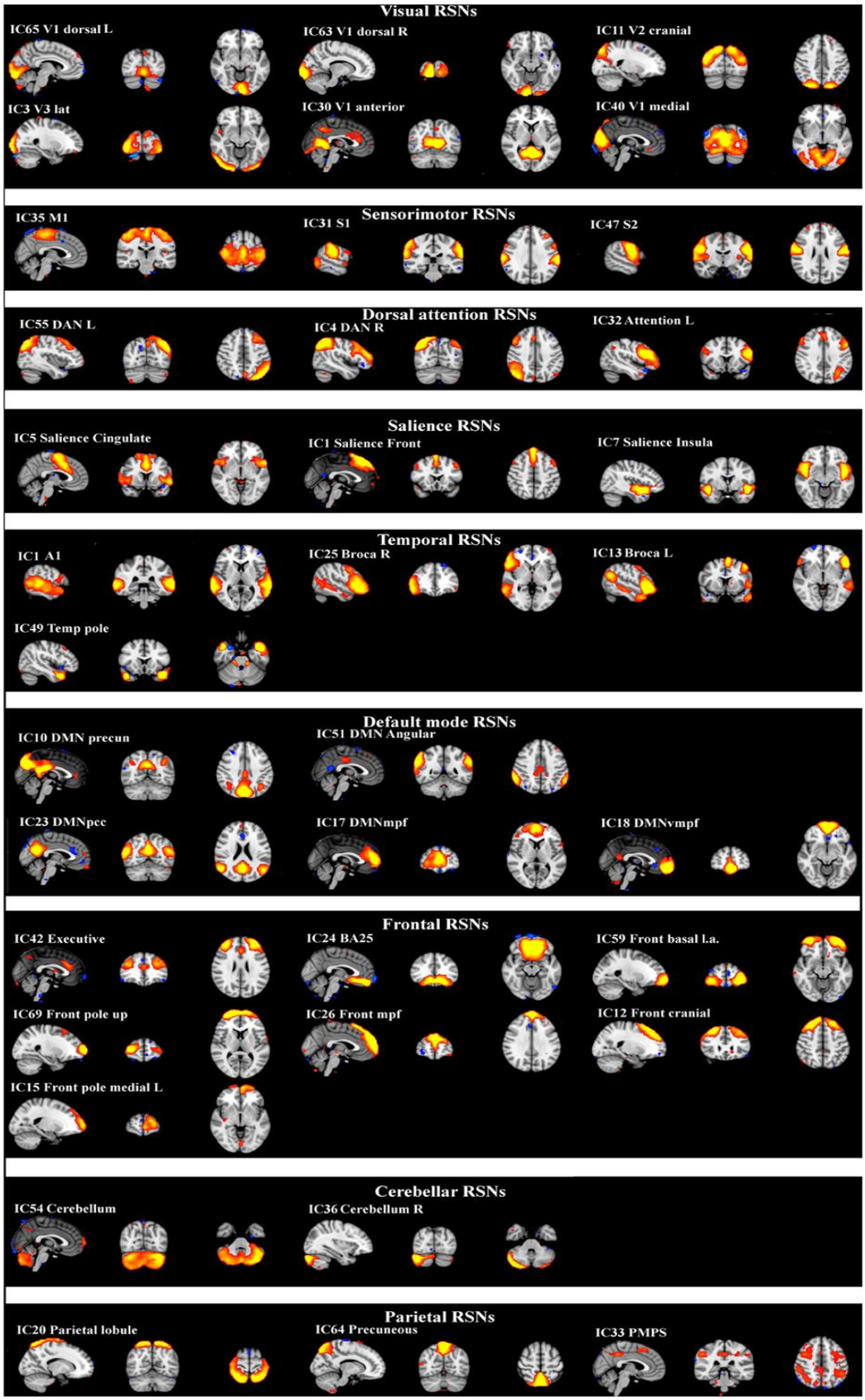


Figure 63 Different RSNs reported in the literature[424]

5.3 RSFC analysis techniques

Different analysis methods have been employed to investigate RSFC in CD. These include seed-based connectivity, the amplitude of low-frequency fluctuation (ALFF), regional homogeneity (ReHo) method, graph theory method, and independent component analysis (ICA).

5.3.1 Seed based method

Seed based analysis was the original method used by Biswal *et al.* to identify resting-state networks[419]. This is a model-based method, where a seed or ROI is selected and the resting state time-series of the specified seed region is linearly correlated with the time-series of all other voxels in the entire brain, producing a seed-based FC map[409]. The straightforwardness of the results and the simplicity of this analysis method is an advantage however, this method does not allow the examination of functional connections patterns on a whole-brain scale and is limited to the functional connections of the selected seed region[409].

The seed-based analysis method is used to quantify the ALFF, Kendall coefficient of concordance, and ReHo measures[409,431]. The ALFF reflects the average power of the low-frequency fluctuations in the range 0.01-0.08 Hz, where the pre-processed time series is transformed into the frequency domain using a Fourier transform to obtain the power spectrum[409]. In other words, the power spectrum for a resting state signal captures the amount of power per unit time the signal has a frequency between 0.01-0.08 Hz[409]. The Kendall coefficient of concordance measures the similarity of a number of time series, whereas ReHo examines the similarity of the time series of a particular voxel with that of nearby neighbours[432].

5.3.2 Graph theory method

In the graph-based method, RSN's are viewed as a collection of nodes connected by edges, where ROIs are represented as nodes and the correlation between ROIs as the connectivity of the edges[433,434]. This method measures the average path length, a measure of global connectedness (i.e. the average length of the shortest connection between all pairs of nodes[433]). In addition, a clustering coefficient is used which reflects the connectedness of neighbouring nodes and reflects the presence of smaller subgraphs[433].

5.3.3 ICA

ICA was first applied to fMRI data in 1998 by McKeown et al[435]. ICA employs mathematical algorithms that are purely data-driven and model-free in order to decompose the signal from whole-brain voxels into a set of independent components (ICs), with each IC consisting of a spatial map (that is statistically independent of other IC maps) and a corresponding time course[436]. ICA aims to identify the spatiotemporal processes that coexist to give rise to the BOLD response. These spatial-temporal processes correspond to the spontaneous fluctuations in resting-state networks[436]. Resting-state analysis typically uses spatial ICA (rather than temporal ICA). Spatial ICA decomposition is applied to the 4-dimensional resting-state BOLD data set by first rearranging it into a 2-dimensional matrix, arranging all voxels for each time point into a single row[436]. This data set is then decomposed into two other matrices (i) time course of the signal in each column (ii) spatial components map in each row[436], as showed in Figure 64.

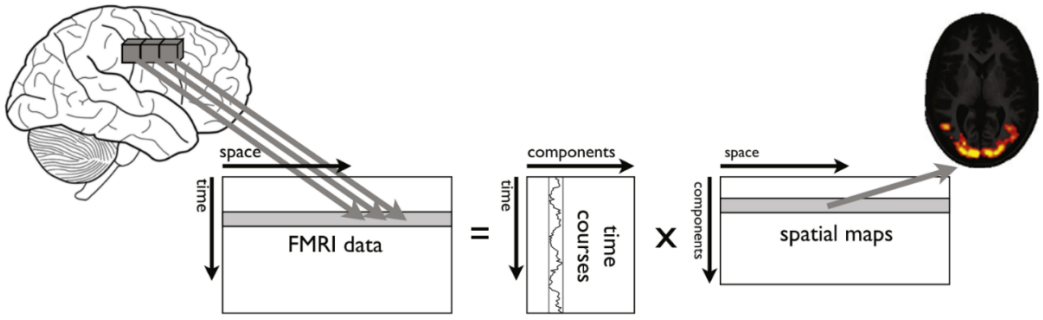


Figure 64 Spatial decomposition performed by spatial ICA on fMRI data [436]

A multi-subject analysis is carried out by concatenating all subjects' fMRI data to produce a group IC map[437], common networks in the entire dataset[438]. Alternatively, a set of template networks can be derived from the group ICA of an independent set of subjects (e.g. HCs)[424] or from an atlas[438]. However, these templates will not reflect specific artefacts or noise sources in the data being studied as compared to the group ICA of the study population[438].

In the ICA method, subject-specific network maps corresponding to each group ICA map need to be identified[438]. In comparison to the seed-based method, the ICA method does not require the user to specify subject-specific seed time courses from ROIs[438]. Group ICA identifies the spatiotemporal signals linked with RSNs, artefacts, and noise that is inherently present in the fMRI data[438]. Group differences in RSNs can be examined using a dual regression, which is a mathematical tool that uses group IC maps as network templates to identify the corresponding FC maps in each subject[438].

The strengths and limitations of each RSFC analysis method are shown in Table 64.

Method	Purpose	Strengths	Limitations
Seed-based analysis	Estimating correlations between predefined voxel or region and the rest of the brain voxels	Straight forward, easy to calculate and understand	Priori selection of ROI may lead to potential biases
ReHo	Using Kendall's coefficient concordance to measure the similarity of a given voxel with its nearest neighbours based on the BOLD time series	Easy to calculate	Bias linked with prior seed selection
ALFF	Estimating the intensity of regional spontaneous brain activity by calculating voxel-wise magnitude within a low-frequency range	Can be used as a potential confounding variable when examining FC and network	Sensitive to physiological noise-making fractional ALFF a better option
ICA	Separating RSN that is spatially (or temporally) independent of each other	Model-free, data-driven, with few priori assumptions	Maybe less sensitive to inter-individual variation and maybe more likely to produce errors at the

	and identifying noise within the BOLD signal		group level if a network is fragmented across multiple components in some subjects. Manual denoising of individual subjects requires prior knowledge and experience[439]
Graph theory	Calculating connectional characteristics of the graph comprising of nodes (voxels) and edges (connections between voxels)	Directly compares different brain networks utilizing topological parameters	Difficult to interpret

Table 64 Comparison of resting-state fMRI analysis methods[440]

5.4 RSFC in healthy subjects

5.4.1 The association of age and RSFC

Age-related decreases in RSFC in the DMN, DAN, salience network, and sensorimotor network have been associated with age-related cognitive decline[441–443]. Such a decrease in connectivity implies a reduction in information transfer between different brain regions[443]. For instance, it has been found that the anterior to posterior components within the DMN become disconnected with increased age, hence this disruption over time may explain age-related cognitive decline[444]. It has also been reported that older adults exhibit weaker deactivation of the DMN during task performance compared with younger adults[444]. Decreased motor capacity is a part of healthy ageing, it has been reported that older adults have reduced RSFC in the mid-posterior insula in the sensory-motor network associated with ageing[445]. Decreased connectivity linked with ageing persists even after controlling for age-related brain atrophy, indicating that the age-related decrease in connectivity in several RSNs is not just due to reduced GMV[446].

5.4.2 Gender-specific differences in RSFC

The effect of gender on RSFC is less clear. Scheinost et al[447] reported that both males and females exhibit an age-related reduction in RSFC in networks such as the DMN, but at different rates[447], whereas other studies have reported women having higher RSFC than men in the DMN[442,448]. Gender-specific differences in attention[449], salience[448], sensorimotor[449,450], and visual network[449] have also been reported in the literature. For, instance, Filippi et al[449] found that men exhibited increased RSFC in parietal and occipital regions, whereas women showed a

higher RSFC in frontal and temporal regions, and in the cerebellum in various cognitive and sensory networks[449]. In contrast, Weissman-Fogel[451] found no gender-specific differences in the ECN, DMN, and salience network[451]

5.4.3 RSFC in fasting and fed states

The human brain uses blood glucose as its main energy substrate for metabolism and the adenosine triphosphate produced by glucose catabolism supports intrinsic brain activity. A study in healthy volunteers which investigated RSFC in an overnight fasted state compared to a state of high glucose following glucagon infusion found a significant difference in the DMN, with a small cluster of superior parietal lobule showing greater connectivity with the rest of the DMN in the high glucose state compared with the fasting state. Additionally, increased connectivity was found in the insula, pallidum and inferior parietal lobule, and other regions in the FPN following a cognitive task in the fasted state. Therefore, it was concluded that fasting only has a small impact on the DMN, however, fasting had a negative impact on attention in the FPN following cognitive effort[452]. Another study using a seed-based method investigated the physiological role of endogenous GLP-1 on the resting-state brain with the use of exendin9-39 (GLP-1 receptor antagonist) following glucose IG infusion to understand the RSFC in the fed state. Inhibiting glucose-induced GLP-1 production (glucose infusion + GLP-1 antagonist) resulted in increased connectivity compared with glucose infusion alone between (i) the hypothalamus and the left lateral OFC as well as the left amygdala; (ii) the right nucleus accumbens and the right lateral OFC; and (iii) result in decreased connectivity between the midbrain and the right caudate. These findings indicate endogenous GLP- 1 modulates RSFC in homeostatic and reward-related brain

regions in a GLP-1 receptor-dependent manner[453]. The effect of fasting and satiation (following a standard breakfast) on the RSFC of the left and right anterior, middle, and posterior insula, and left and right hypothalamus[131] was also investigated. It was observed that RSFC between the left posterior insula and cerebellum/superior frontal gyrus, and between left hypothalamus and inferior frontal gyrus was stronger during fasting[131]. Additionally, FC between the right middle insula and default mode structures (left and right posterior parietal cortex, cingulate cortex), and between right hypothalamus and superior parietal cortex was stronger during satiation[131]. It was concluded that the insula and hypothalamic RSFC patterns were altered by changes in the homeostatic energy balance and that the RSFC observed with the frontal cortex possibly forms a part of a circuit motivating feeding, terminating feeding upon satiation and prevent overeating.

Nutrient specific effects on RSFC have also been reported, with differential responses to lipids, sugars, protein/amino acids. Table 65 summaries the key resting-state fMRI studies investigating the effect of nutrients (sugars, lipids, and amino acids) on RSFC.

Author	Nutrients received	Method	Main findings
Page et al 2013[454]	Glucose 75g Fructose 75g	Seed based	-Glucose ingestion (compared with baseline) increased FC between the hypothalamus and the thalamus and striatum. -Fructose increased connectivity between the hypothalamus and thalamus but not the striatum
Carbonell et al 2014[455]	-nutritionally balanced amino acid mixture drink -tyrosine and phenylalanine deficient drink (lowered dopamine state) - acute phenylalanine/tyrosine depletion technique, which decreases dopamine synthesis and reduces both baseline dopamine levels and stimulated dopamine release	Graph theory	-The amino acid-deficient drink reduced the regional efficiency in the OFC and amygdala, indicating that connections between these regions, receiving dopaminergic innervation, and the rest of the brain were made less efficient by dopamine depletion. - Greater connectivity was also found between the typically anti-correlated task-positive and DMN.
Wölnerhanssen et al 2015[155]	Glucose 75 g Fructose 25g Placebo - water	ICA	Fructose differentially increased the activity of the left amygdala, left hippocampus, right PHG, OFC, and precentral gyrus more than glucose, indicating stronger reward-driven responses compared with glucose.
Zanchi et al 2016[456]	Nasogastric infusion of: -300 ml tap water with 1.56 g L-tryptophan, -1.56 g L-leucine, -75 g glucose, -300 ml of pure tap water (placebo)	ICA	-In comparison to glucose and water, L-tryptophan consistently modified the connectivity of the cingulate cortex in the DMN, of the insula in the saliency network and of the sensory cortex in the somatosensory network. -L-leucine had lesser effects on these functional networks.
Jastreboff et al 2016[150]	Glucose 75g Fructose 75g	Seed based	- Reduced connectivity between executive, homeostatic, and hedonic brain regions (using hypothalamus and nucleus accumbens as seed regions) was observed in obese adolescents

			compared with lead adolescents in response to glucose and fructose ingestion
Deza-Araujo et al 2018[141]	one of the following drinks: -acute tryptophan depletion, -a balanced mixture of amino acids or -acute tryptophan loading * tryptophan is the dietary precursor of serotonin.	template-based approach	-Tryptophan loading drink increased tryptophan plasma levels and decreased DMN connectivity with visual cortices and brain regions involved in emotion and affect regulation (i.e., putamen, subcallosal cortex, thalamus, and frontal cortex), indicating changes in the serotonin modulatory system. -Acute Tryptophan Depletion – no effect on RSFC
Al-Zubaidi et al 2018[457]	oral administration of 75 g of glucose in a fasted state or fed state	ReHo	-After glucose administration previously, fasted subjects showed greater connectivity in the left thalamus compared with prior fed subjects
Van Opstal et al 2019[140]	received shakes sweetened with glucose, fructose, allulose or sucralose.	Eigenvector Centrality Mapping	-Glucose and fructose led to significantly decreased BOLD signal in the cingulate cortex, insula and the basal ganglia. -Sucralose and allulose had no effect on BOLD signal or network connectivity -indicating that non-nutritive sweeteners do not exert the same satiating effects as nutritive sugars
Podlech et al 2019[158]	High-fat yoghurt (8% fat) Low-fat yoghurt (<0.01% fat)	Seed based	-FC between NTS and reward and gustatory areas was lower after ingestion regardless of fat content. - Oral fat sensitivity was positively correlated with FC between homeostatic regions and limbic areas in the high-fat condition, but negatively correlated with FC between the dorsal striatum and somatosensory regions in the low-fat condition

Table 65 Summary of key resting-state fMRI studies investigating the effect of nutrients (sugars, lipids, and amino acids) on RSFC

5.5 RFFC alterations in CD

RSFC alterations have been reported in CD in remission but have not been investigated in the active phase of the disease. The findings reported by previous studies have been inconsistent, possibly due to the heterogeneity in the patient population, sample size, disease activity, concomitant medication, disease symptoms (e.g. abdominal pain and fatigue) and fMRI resting-state data TA. Additionally, all studies have been cross-sectional in nature, therefore changes in brain activity over time due to disease activity or psychological symptoms or medication usage are unknown. Studies on RSFC in CD also appear biased towards investigating major networks such as DMN, FPN, and ECN, hence neglecting the effect the disease may have on other RSNs.

A study by Hou et al[458] investigated RSFC within the ECN and the DMN in 18 CD patients in remission and 18 HCs. They found that CD patients had increased connectivity compared with HCs between the right middle frontal gyrus and right inferior parietal lobe in the ECN. Similarly, increased connectivity was reported between the right precuneus and right PCC in the DMN in CD patients compared with HCs. No significant correlations were found between the ECN, DMN and behavioural scores in each group[458]. However, this study was limited by small sample size, short TA (5mins resting-state time series, a longer time series can significantly enhance the strength of connectivity), and the investigation of two specific networks only based on prior assumptions, with the potential effects of CD on other brain networks not investigated. Increased connectivity in the middle and ACC in the DMN has been reported by Thomann et al[396]. A study by Bao et al [459] in 60 CD patients in remission and 40 HCs found alterations in ALFF values and FC using a seed-based method between CD

patients and HC, see Table 66. Abnormalities in the DMN were found, as indicated by lower ALFF values in the anterior DMN medial PFC and higher ALFF values in the posterior DMN (precuneus), suggesting a lower coupling between anterior and posterior DMN in CD patients than HC. Liu et al[460] found that CD patients had decreased nodal graph metrics compared with HCs in the DMN. Another study by Bao et al[461] found that CD patients following electro-acupuncture treatment showed a significant increase in RSFC values between the bilateral hippocampus and MCC and insula, and the increase in RSFC negatively correlated with CDAI (disease activity score). The major limitation of the study by Bao et al[461] is the lack of a control group, and the general drawbacks of the seed-based method (see Table 66). A study by Thomann et al[396] investigated RSFC using ICA within the DMN and FPN in 15 CD patients and 14 HCs. They found increased connectivity in the anterior cingulate and left superior medial frontal gyrus (anterior DMN) and the MCC (posterior DMN). The mid-cingulate activity showed a significant positive correlation with anxiety scores in CD patients but not in HCs. The FPN showed no significant difference between CD patients and HCs. This study was however limited by its small sample size and the lack of interrogation of other RSNs that may have been affected by CD. Another study by Bao et al[462] found that ReHo levels (a voxel-based measure of brain activity which evaluates the similarity or synchronization between the time series of a given voxel and its nearest neighbours[432] in different parts of the brain) were significantly increased or decreased compared with HCs as shown in Table 66. The alterations in the PCC, mPFC, precuneus (key regions of the DMN), in CD patients, compared with HCs suggested abnormalities in the DMN. A further study by Bao et al[463] compared 25 CD patients with abdominal

pain and 25 patients without abdominal pain to 32 HCs. Abdominal pain was assessed using a 0-10 cm VAS, with 0 representing no pain and 10 indicating excruciating pain. An average score was taken from the daily pain score log a week before the MRI scan. The CD patients in the pain group had mild abdominal pain as indicated by the average score of 3.0 ± 1.5. CD patients with pain showed an increase or decrease in various brain regions compared with CD without pain and HCs, as showed in Table 66. CD patients with abdominal pain showed decreased ReHo values in the insula, MCC and SMA and increased ReHo values in the temporal pole. The decrease in ReHo values in the insula and MCC (which form part of the pain modulatory system) negatively correlated with the daily pain score suggesting reduced synchronization and coordination of neural activities in these brain regions. This study was limited by the subjective nature pain measurement using VAS and the known drawbacks of the seed-based method. In contrast to all the studies mentioned above, a study by Agostini et al[208] which investigated RSFC in 17 CD patients and 17 HCs using the seed-based method found no significant difference between CD patients and HCs using the MCC as a seed region. This study was limited by the seed-based method and selection of one specific seed only based on prior knowledge.

Author, Country	Study population	Methods	Main Findings	Correlation Findings
Hou et al 2019[458], USA	-18 CD in remission -18 HC	- 3T GE -Seed based method -TA: 5mins -Data Processing Assistant for Resting-state fMRI Basic Edition toolbox (DPARSF v4.3)	**CD>HC**: increased RSFC between the right middle frontal gyrus and right inferior parietal lobule in the (ECN) **CD>HC**: increased RSFC between the right precuneus and right PCC in the (DMN)	No significant correlations were found between ECN/DMN and behavioural scores (e.g. VF, behavioural approach, and behaviour inhibition) in each group
Bao et al 2018[459], CHINA	-60 CD in remission -40 HC	-3T Siemens - ALFF - Seed-based FC - ALFF: REST v1.8 software - Data Processing Assistant for resting-state fMRI (DPARSF v3.1)	**CD>HC**: Higher ALFF values in hippocampus and PHG (HIPP/PHG), ACC, insula, superior frontal cortex and precuneus **CD<HC**: lower ALFF values in secondary somatosensory cortex (S2), precentral gyrus, and medial PFC (mPFC) **CD<HC**: Lower FC between left HIPP and left inferior temporal cortex, and right MCC, HIPP, and fusiform area **CD<HC:** lower FC between right HIPP and right inferior OFC and left HIP	No significant correlation was found between the ALFF values and disease duration in patients with CD
Liu et al, 2018[460], CHINA	-43 CD patients in remission -37 HC -21 CD patients with >7 i.e. abnormal HAD scores -22 with normal HAD score	-3T Siemens - ICA -Graph theory method -automated pipeline on the CONN FC toolbox	**CD<HC**: decreased nodal graph metrics in the subcortical, sensorimotor, cognitive control and DMN. **CD with anxiety (A) and depression (D) > CD with no A and D:** increased connectivity strength in the medial PFC (mPFC) and ACC.	The connectivity strength of putamen negatively correlated with CD duration in patients

		-GIFT toolbox	**CD with A and D > CD with no A and D:** increased clustering coefficient in mPFC, ACC and PCC. **CD with A and D > CD with no A and D:** increased local efficiency in mPFC, ACC and PCC. **CD with A and D > CD with no A and D:** increased connectivity between putamen and PCC, and caudate and mPFC.	
Bao et al 2017[461], CHINA	-18 CD remission at baseline and after 12 weeks of electro-acupuncture -20 CD patients in remission at baseline and after 12 weeks of moxibustion treatment - No control group	-3T, Siemens -Seed based analysis -SPM8 -Conn Toolbox	- No difference in RSFC baseline characteristics between CD patients receiving acupuncture or moxibustion treatment. -CD patients after electro-acupuncture treatment showed a significant increase in RSFC values between the bilateral hippocampus and anterior MCC and insula. -CD patients after moxibustion treatment showed a significant increase in RSFC values between bilateral hippocampus and precuneus and inferior parietal lobe	-After electro-acupuncture treatment, the increase of RSFC between the left hippocampus seed and the left anterior MCC and the right insula was negatively correlated with CDAI score. -After moxibustion treatment, the increase of RSFC between the left hippocampus seed and the right precuneus and left inferior parietal lobe was negatively correlated with the CDAI score.
Thomann et al 2017[396], GERMANY	-15 CD in remission -14 HCs	-3T, Siemens -ICA -SPM8	CD>HC: Increased connectivity was found in the anterior cingulate and left superior medial frontal gyrus (aDMN) and the MCC (pDMN).	MCC activity showed a significant positive correlation with anxiety scores in CD patients

		-Functional Network Connectivity Toolbox, FNCTB Vers. 2.3		
Bao et al 2016[462], CHINA	-52 CD in remission -36 HCs - 36 CD patients were randomly assigned to receive either electro-acupuncture or acupuncture for 12 weeks	-3T Siemens -TA: 6 mins -ReHo - REST software	**-CD>HC:** CD patients had significantly higher ReHo values in the bilateral ACC, superior frontal medial cortex, middle frontal cortex, superior temporal pole, precuneus RSFG, inferior temporal cortex, angular gyrus, left middle temporal cortex, superior parietal cortex and middle occipital cortex ($P < 0.05$, corrected) **-CD<HC:** CD patients had significantly lower ReHo values in the bilateral thalamus, insula, MCC, PCC, lingual gyrus, cerebellum, PAG, brainstem, left HIPP, SMA, postcentral gyrus, inferior frontal operculum cortex, right amygdala and superior temporal cortex ($P < 0.05$, corrected)	
Bao et al 2016[463], CHINA	-25 CD in remission with pain - 25 CD in remission without pain - 32 HCs	-3T, Siemens -ReHo -SPM8 -DPARSF software -REST software	**CD patients with pain < CD patients without pain and HC**: ReHo values of the insula, SMA, and MCC in the patients from the Pain CD group were significantly lower than the Non-pain CD group and the HC group. **CD patients with pain > CD patients without pain and HC:** ReHo values of the temporal pole in patients from the	ReHo values of the insula and MCC were significantly negatively correlated with daily pain scores for patients with abdominal pain

			Pain CD group were significantly higher than the non-pain CD group and the HC group ($P < 0.05$, corrected) **CD patients with no pain < CD patients with pain and HC:** the ReHo values for HIPP/PHG in patients from the Non-pain CD group were significantly lower than the Pain CD group and the HC group **CD patients with no pain > CD patients with pain and HC:** the ReHo values of the dorsomedial PFC in patients from the non-pain CD group were significantly higher than the Pain CD group and the HC group (all $P < 0.05$, corrected)	
Agostini et al[208] 2017	-17 CD in remission -17 HC	-3T Philips - seed-based method - TA: 8mins	No significant difference between CD patients and controls in the FC maps using the MCC as the seed region	

Table 66 Literature on RSFC in CD

5.6 Methods

5.6.1 Imaging protocol

Data were collected in the pre-cannulation section of the protocol Figure 65. Resting-state BOLD data were collected on a 3T Achieva scanner (Philips Medical Systems, Best, Netherlands) with a 32 channel head receive coil using a double-echo gradient-echo EPI acquisition scheme with TE)20/49ms, 64 x 64 matrix, 3x3x3 mm^3, 34 axial slices, TR = 2.5 s. Subjects were instructed to lay still inside the scanner with their eyes open. Physiological heart rate and respiratory data were collected throughout. Each acquisition lasted for 10 mins, yielding 240 volumes per subject as shown in Figure 65. Ten minutes was chosen as being optimal for increased detection of RSNs based on recent literature[464]. A high resolution T_1-weighted image was also acquired using an MPRAGE sequence (1mm isotropic resolution; TE/TR = 8.3/3.8 ms, flip angle = 8 º, SENSE factor =2, 160 slices, 256 x256 matrix).

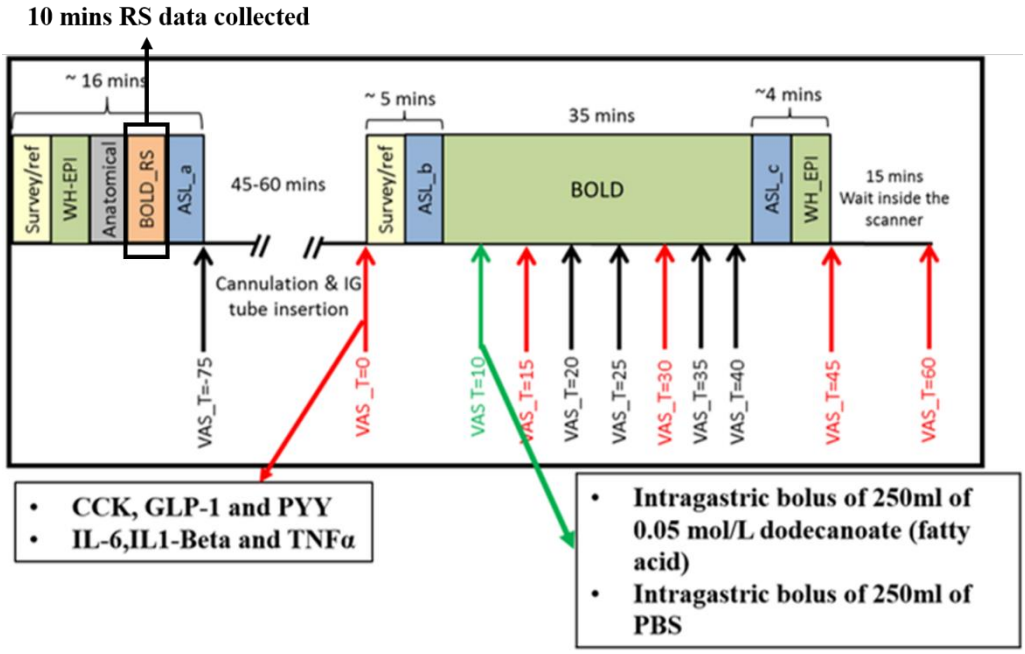


Figure 65 showing scanning protocol, 10-minute resting state was acquired in a fasted state, pre nasogastric infusion and cannulation

5.6.2 Pre-processing

Physiological noise associated with cardiac pulsation and respiration were removed using RETROICOR[465]. The subsequent pre-processing and analysis were then performed in the FMRIB Software Library (FSL; FMRIB Software Library) package (http://fsl.fmrib.ox.ac.uk/fsl/fslwiki/). Head motion in the fMRI data were corrected using multi-resolution rigid body co-registration of volumes, as used in the MCFLIRT software[466]. Brain extraction was performed on the motion-corrected BOLD volumes with optimization of the deforming smooth surface model using the Brain Extraction Tool software[467]. The fMRI volumes were registered to the 3D MPRAGE (brain extracted) volumes of the corresponding subjects and subsequently the 3D MPRAGE volume to MNI152 standard space. A high-pass temporal filter cut-off of 100s was applied to the resting state data, and the images were smoothed with a 6-mm spatial filter.

5.6.3 ICA analysis

The Multivariate Exploratory Linear Decomposition into Independent Components (MELODIC) tool was used to perform single session ICA on all subjects to produce 30 ICs maps. The noisy components were removed following visual inspection, as described by[439], and shown in Figure 66. After the noisy components were identified, the *fslregfilt* function was used to regress out the time series from the components labelled as noise from the dataset.

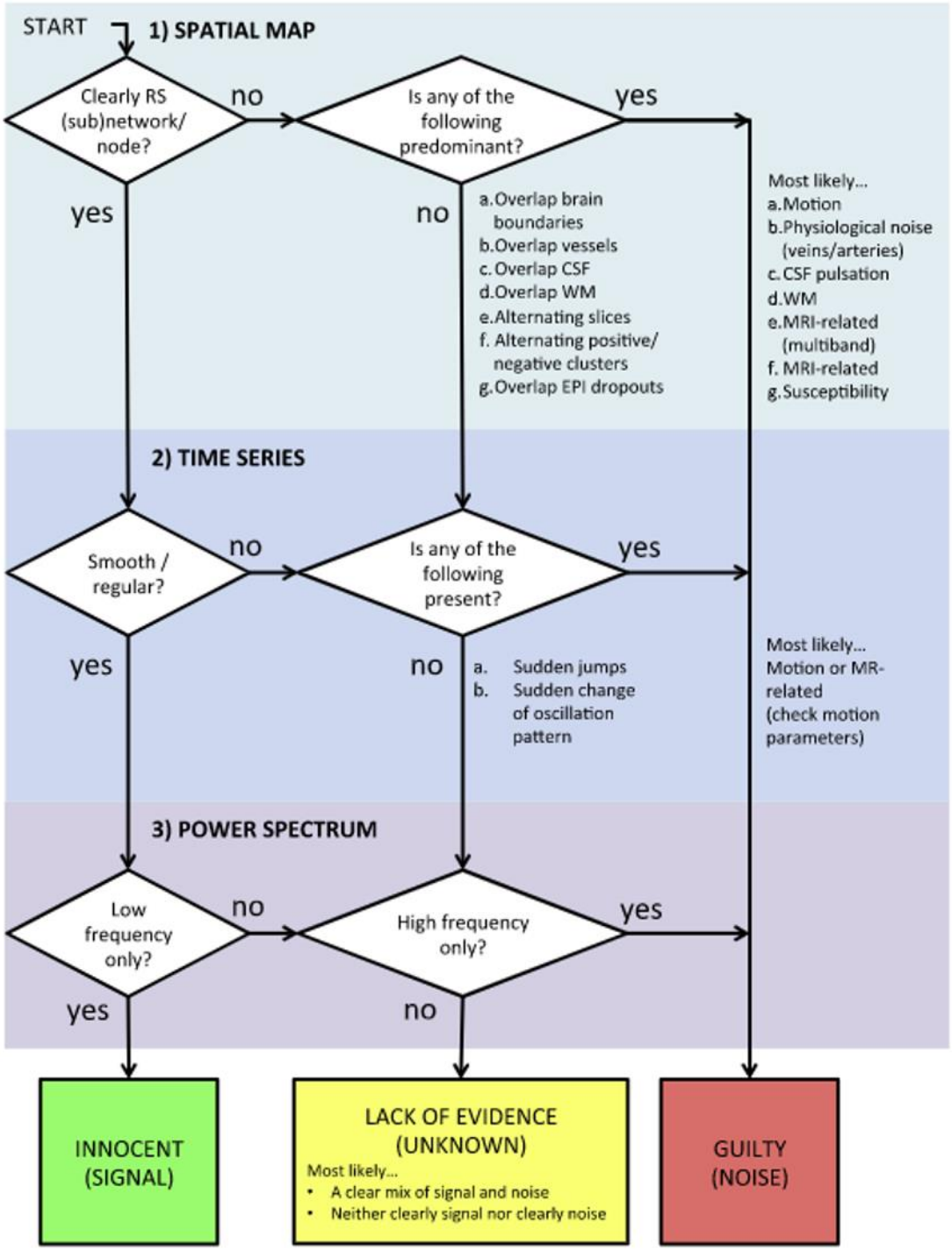


Figure 66 A flowchart of the procedure for visual inspection and manual classification of ICs[439]

Group ICA was performed on the noise-free datasets from the single session ICA step using multisession temporal concatenation to produce 30 maps (IC maps) representing average RSNs of the entire study population (i.e. the fMRI data

from every subject was included in the analysis). A separate group ICA was performed for both the CD patients and the HCs using the noise-free datasets.

5.6.4 Group ICA with dual regression

Dual regression was performed using two approaches: i) the cleaned group IC maps from the entire study population (i.e. CD and HC groups) as a network template as is standard practice in ICA analysis; (ii) the cleaned group IC maps from the HC group only as the network template. The use of the HC group only network template was included based on recent literature[424] suggesting that the HC ICA result is more robust in the absence of disease-related alterations and more sensitive in detecting group differences in the dual regression as compared with ICA maps from both patients and controls.

Variance normalisation was used, reflecting the differences in both activity and spatial spread of RSNs. Dual regression was carried out in three stages. In stage 1, the subject-specific time course for each template network was extracted using a multivariate spatial regression of the template maps against each subject's fMRI data. In Stage 2, the subject-specific time courses from stage 1 were used in a second multivariate temporal regression against the subjects' fMRI data to identify the subject-specific spatial maps corresponding to each template network of interest. In Stage 3, statistical analysis was performed i.e. a two-sample unpaired t-test between the CD and HC group, where different component maps were collected across subjects into single 4 D files (i.e. per original ICA map) and tested voxel-wise by non-parametric permutation using the FSL randomise tool[468] with 5000 permutations and TFCE to control for multiple comparisons. The hypothesized differences between groups were

calculated using a $p < 0.05$ threshold with voxel-wise changes in the FSL randomize tool. It is important to highlight that a two-group t-test using the spatial maps output by dual-regression can result in areas of significant difference both "within" and not "within" the (group-average) ICA map for that RSN. Areas which are not "within" the (group-average) ICA map for that RSN means that the connectivity of this area with the main regions of this RSN is different between the two groups, despite on average (across both groups) not being strongly connected. For example, an area might have a weak positive correlation with the main areas of this RSN in the control group and a weak negative correlation in the patient group.

Correlation analyses within the CD patients group were calculated between the RSFC in different RSNs and abdominal pain scores, IBD fatigue scores, disease duration and (fasting GLP-1 and PYY – methods details in section 2.8.6 of this thesis) using the (CD+HC) RSNs as a network template in the dual regression stage. The Juelich histological atlas incorporated in FSL and the Harvard-Oxford cortical and subcortical atlases (Harvard Centre for Morphometric Analysis) provided within the FSL4 software were used to identify anatomical characteristics of the resulting maps.

5.7 Results

5.7.1 Recruitment

Figure 67 provides a consort diagram outlining the number of participants included in this chapter. Please refer to Figure 70 in Chapter 6 which shows the summary consort diagram of the number of participants that appeared in each chapter. **Twenty-three CD patients and 8 HCs in this chapter appeared in Chapter 1. Fifteen CD patients and 8 HCs in this chapter appeared in Chapter 3. All subjects in this chapter appeared in Chapter 4**

In total, 25 CD patients and 25 age, BMI and gender-matched HCs with **10-minute resting-state datasets** are included in this study. This was used as a longer (10-minute) time series has been shown to significantly enhance the strength of connectivity over a 5-minute time series.

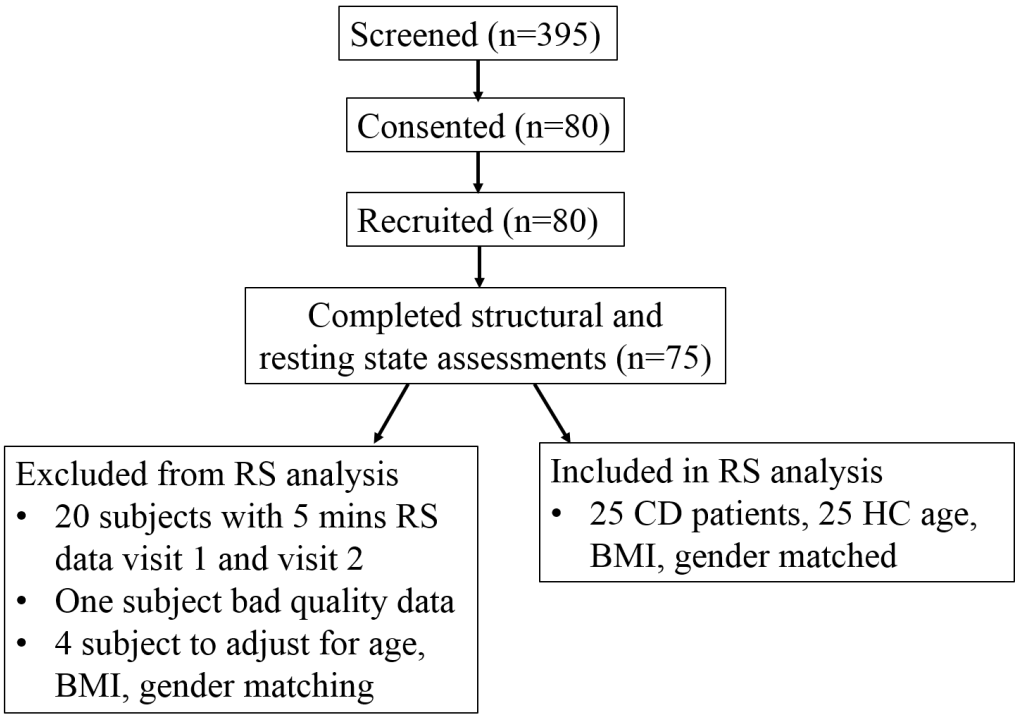


Figure 67 Consort diagram outlining the number of participants included in this chapter.

5.7.2 Participant demographics

Table 67 provides the demographic, behavioural, and clinical characteristics of the CD patients and HCs included in the resting state analysis.

	CD [n=25]	HC [n=25]	P- values
Age [years]	33.9 ± 15.8	36.1 ± 13.6	NS
BMI [kg/m^2]	24.3 ± 4.79	24.8 ± 3.36	NS
Gender [M/F]	16 M, 9 F	16 M, 9 F	NS
[Ileal/colonic]	14 ileal, 11 colonic		
Abdominal pain score	23.4 ± 20.0	0 ± 0	P<0.05*
Disease duration [years]	7.4 ± 5.87	-	-
HBI	4.0 ± 2.9	-	-
IBD- Fatigue	10.9 ± 3.6	-	-
CRP [mg/dl]	21.3 ± 51.2	-	-
FCP [µg/g]	703 ± 618	-	-
EIM	8 with EIM, 17 without EIM		

Table 67 Demographic, behavioural, clinical characteristics of CD patients and HC. Values are presented as mean ± SEM. HBI scores (<5 remission, 5-7= mild disease, 8-16 = moderate disease, >16 = severe disease. IBD fatigue score= (ranges from 0 to 20, where 0 = no fatigue, 1 to 10 = moderate fatigue, 11 to 20 = severe fatigue.

5.7.3 Comparison of RSFC between CD patients and HCs using a CD and HC network template in dual regression

This section presents the comparison of RSFC between CD patients and HCs using the cleaned group IC maps from the entire study population (i.e. CD and HC) as a network template, as is typically used in ICA analysis. Figure 68 shows the combined CD and HC RSNs that were investigated.

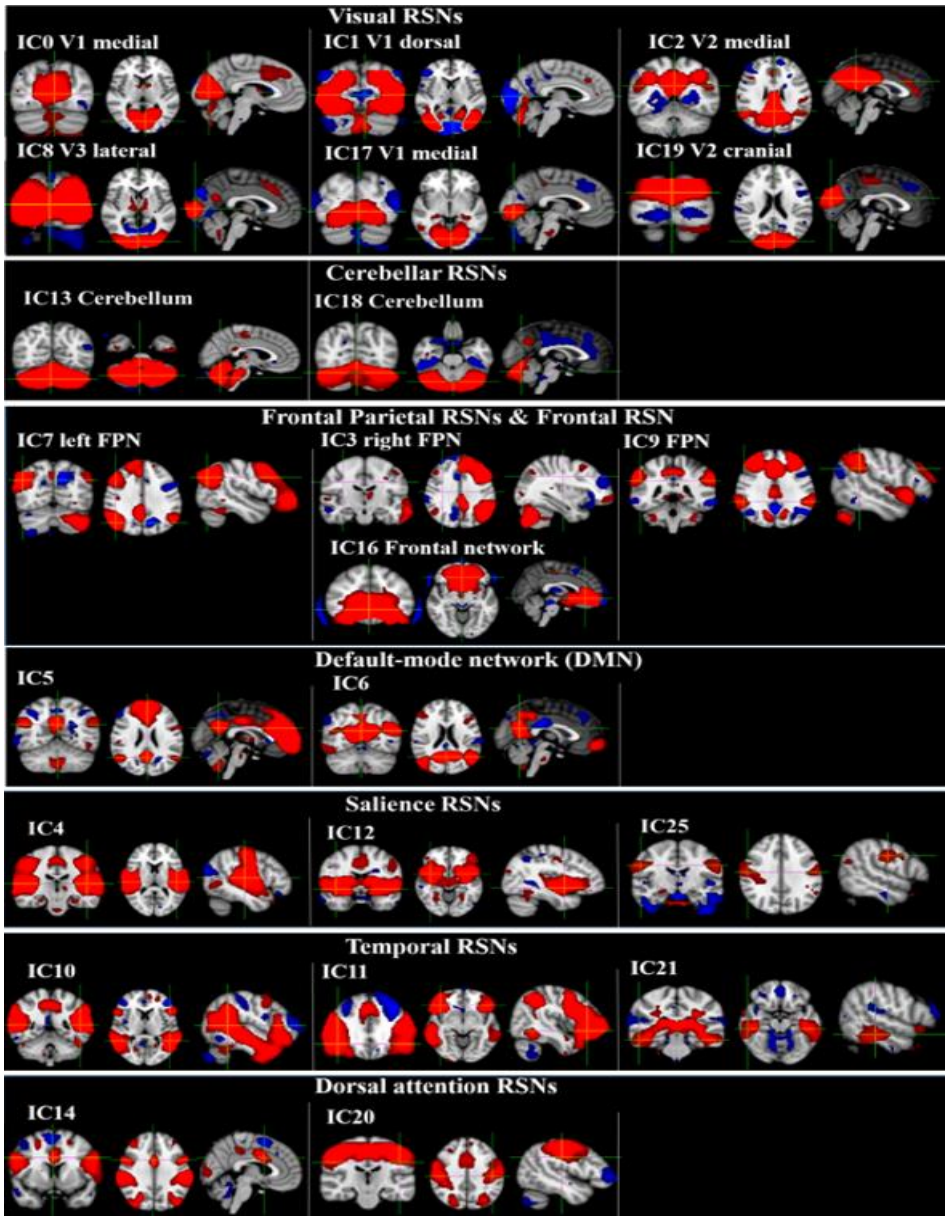


Figure 68 RSNs from using *CD and HCs* in the dual regression analysis. Red = positive networks (2 <z-score<5), and blue = negative networks (-2<z-score<-5).

Table 68 shows those RSNs with significant differences in RSFC between the HC group and CD patients using the *(CD+HC) network* template in the dual regression analysis. There were a number of areas which showed greater connectivity in the CD patients compared to the HC group.

RSN	**L/R**	**Voxels**	**P-value corrected**	**MNI (x, y, z)**
IC1 dorsal visual RSN				
CD >HC				
Inferior temporal gyrus	L	5171	<0.005	-45, -48, -18
Occipital fusiform gyrus	L	5637	<0.005	-25, -74, -7
Lingual gyrus	R	4991	<0.005	11, -64, -7.2
Lateral occipital gyrus	R	6798	<0.005	40, -86, -7.2
IC9 FPN				
CD>HC				
Left occipital fusiform cortex	L	4953	<0.05	-19, -70, -14
IC11 Temporal RSN				
CD<HC				
Brain Stem	L	4871	<0.05	-7.6, -36, -43
Pallidum	L	7124	<0.05	23, -9.8, -1.6
IC13 Cerebellar RSN				
CD>HC				
Inferior temporal gyrus	R	3377	<0.05	59, -46, -25
Middle temporal gyrus	R	5701	<0.05	59, 35, 14
Brain stem	R	6002	<0.05	0.8, -35, -43
IC18 Cerebellar RSN				
CD>HC				
Frontal medial cortex	R	6489	P<0.005	9, 45, -19.6
Frontal pole	R	5731	P<0.005	40, 42, 6
Precentral gyrus	R	6344	P<0.005	32, 10, 28.5
Paracingulate gyrus	L	7883	P<0.005	-13, 39, 24
Occipital fusiform gyrus	L	4644	P<0.005	-37, -73, -22
Cerebellum		6023	P<0.005	4.5, -68, -39
IC19 cranial visual RSN				
CD>HC				
Lateral occipital cortex/visual cortex	R	7590	P<0.05	18, -80, -18
Occipital pole/ visual cortex	R	6074	P<0.05	25, -95, 13

Table 68 shows the RSNs and regional alterations in RSFC between CD and HC using *(CD+HC) network* template in the dual regression analysis.

5.7.4 Correlation of pain scores, fatigue scores, disease duration and fasting GLP-1 and PYY in CD patients

Table 69 shows those RSNs in which brain regions correlated with IBD fatigue scores in the CD patients. An increase in fatigue scores was associated with an increase in RSFC in the paracingulate gyrus in the visual RSN and increased RSFC in the lateral occipital cortex in the salience network.

RSN	**L/R**	**Voxels**	**P-value corrected**	**MNI (x, y, z)**
IC17 medial visual network **(positive correlation)** Paracingulate gyrus	L	5830	P<0.05	(-3, 46, 23)
IC25 salience network **(positive correlation)** Lateral occipital cortex	L	6547	P<0.05	(-39, -64, 25)

Table 69 Relationship between RSFC in different brain regions and IBD fatigue scores in the visual and salience network.

Table 70 shows that in RSNs of the DMN and FPN brain regions correlated with abdominal pain scores in the CD patients.

RSN	L/R	Voxels	P-value corrected	MNI (x, y, z)
IC5 DMN **(negative correlation)**				
Inferior temporal gyrus	R	4367	P<0.05	(45, -14, -40)
IC6 DMN **(positive correlation)**				
Middle temporal gyrus	L	5350	P<0.05	(-64, -52, -10)
IC7 left lateral FPN **(negative correlation)**				
Frontal pole	R	7096	P<0.05	(27, 37, -8.6)
Frontal pole	R	6608	P<0.05	(45, 46, -8.6)
IC10 temporal RSN **(positive correlation)**				
Superior parietal lobule	L	6080	P<0.05	(-35, -40, 41)
IC13 cerebellar RSN **(positive correlation)**				
Inferior temporal gyrus	R	6285	P<0.05	(49, -22, -28)

Table 70 Relationship between RSFC in different brain regions and abdominal pain scores in the DMN, left lateral FPN and temporal RSN

Table 71 shows that in RSNs of the visual and salience networks brain regions correlated with disease duration in CD patients.

RSN	L/R	Voxels	P-value corrected	MNI (x, y, z)
IC2 medial visual RSN **(positive correlation)**				
Inferior temporal gyrus	R	5953	P<0.05	(62, -31, -20)
Planum temporale	R	6134	P<0.05	(53, -28, 13)
IC20 Salience network **(positive correlation)**				
Precentral gyrus	R	7372	<0.05	(52, -2.8, 32)
Precentral gyrus	L	4098	<0.05	(62, -2.7,30)
Inferior frontal gyrus	R	5135	<0.05	(57, 12, 1.8)
Frontal medial cortex	L	5415	<0.05	(2.1, 38, -16)

Table 71 Relationship between RSFC in different brain regions and disease duration in the visual and salience RSN

Table 72 shows that in the visual RS, the precentral gyrus correlated with fasting GLP-1 plasma levels in CD patients

RSN	L/R	Voxels	P-value corrected	MNI (x, y, z)
IC0 medial visual RSN **(positive correlation)**				
Precentral gyrus	R	4549	<0.05	(63, 1.5, 5.0)

Table 72 Positive correlation between RSFC in the precentral gyrus and fasting GLP-1plasma in the visual RSN.

Table 73 shows that in temporal and frontal RSNs brain regions correlated with fasting PYY plasma levels in the CD patients.

RSN	L/R	Voxels	P-value corrected	MNI (x, y, z)
IC11 temporal RSN **(positive correlation)**				
Central opercular cortex	L	7342	<0.05	(-44, -16,21)
Thalamus	L	5681	<0.05	(-10.6, 37, 6)
IC16 frontal network **(negative correlation)**				
Precentral gyrus	L	7032	<0.05	(-49, -5.8, 31)
Central opercular cortex	L	6811	<0.05	(-42, -5.8, 18)
Supracalcarine cortex	R	5343	<0.05	(22, -65, 19)

Table 73 Relationship between RSFC in different brain regions and fasting PYY plasma levels in the temporal and salience RSN

5.7.5 Comparison of RSFC between CD patients and HCs using HC RSNs as a network template in dual regression

As a further analysis, the dual regression analysis to assess RSFC between the CD patients and HC was also performed using the cleaned group IC maps from the *HC group only* as a network template in the dual regression[424]. Figure 69 shows the RSNs generated for the HC group only.

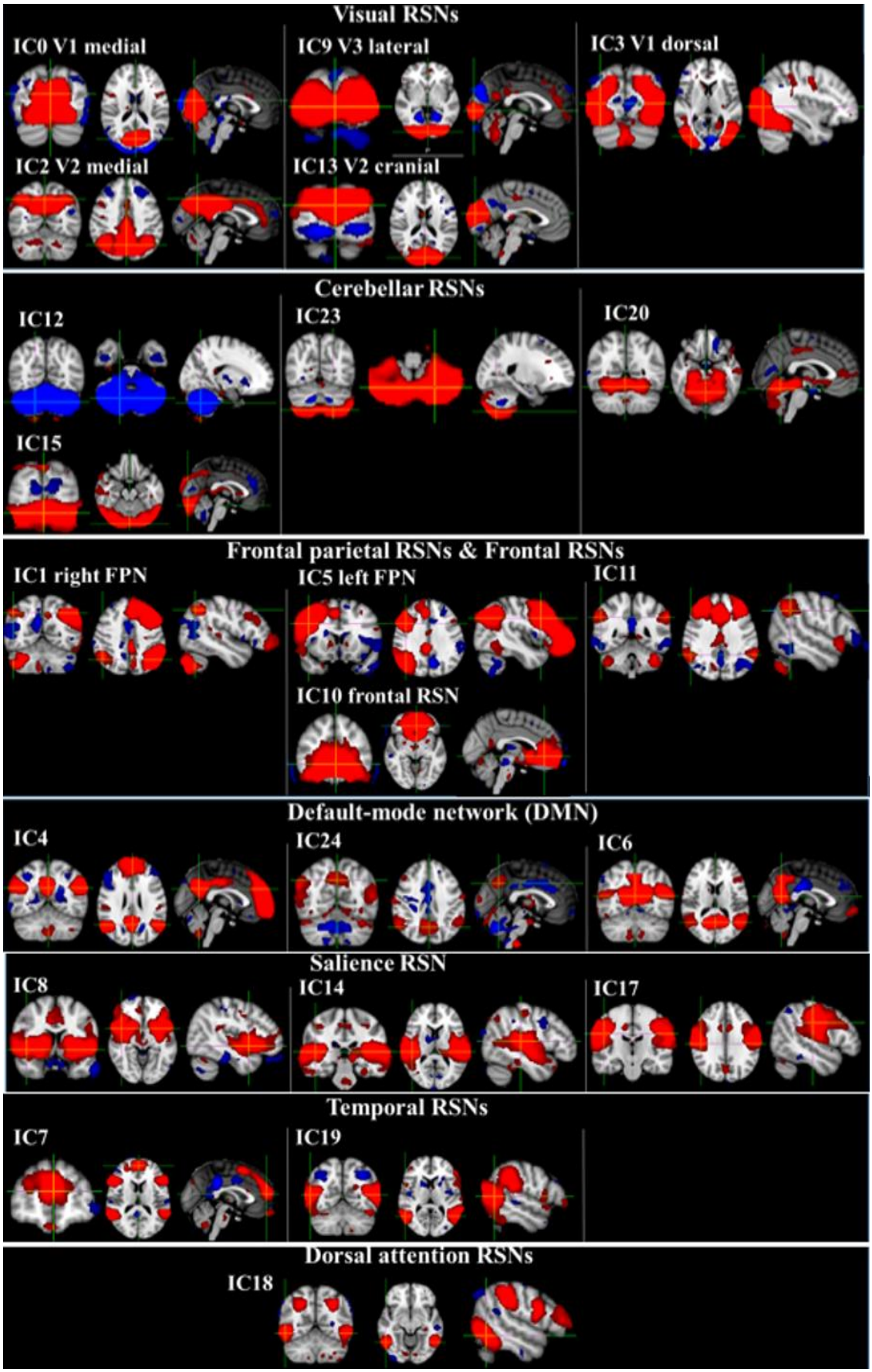


Figure 69 RSNs for *HC only* used in the dual regression analysis. Red = positive networks (2 <z-score<5) and blue = negative networks (-2<z-score<-5).

Table 74 shows the RSNs and regional alterations in RSFC between HC and CD using the *HC only* network template in the dual regression analysis.

RSN	**L/R**	**Voxels**	**P-value corrected**	**MNI (x, y, z)**
IC2 medial visual RSN				
CD>HC				
Frontal orbital cortex	R	5629	<0.05	22, 25, -17
IC3 dorsal visual RSN				
CD>HC				
Inferior temporal gyrus	L	5585	<0.01	-47, -48, -22
Lateral occipital cortex	L	5795	<0.01	-38, -68, 19
IC5 left FPN				
CD>HC				
Inferior temporal gyrus	R	5122	<0.05	46, -40, -28
IC8 salience network				
CD<HC				
Cerebellum	L	6660	<0.05	-35, -58, -36
Lingual gyrus	R	3094	<0.05	6, -58, -1.6
Postcentral gyrus	R	5960	<0.05	60, -13, 27
IC11 FPN				
CD>HC				
Occipital fusiform gyrus	L	5536	<0.01	-25, -72, -14
Thalamus	R	6299	<0.01	8.6, -6.7, 2.2
Caudate	R	5544	<0.01	8.6, 16, 0.8
PCG	R	6619	<0.01	21, -44, 0.1
Postcentral gyrus	R	6219	<0.01	67, -17, 20
Lingual gyrus	R	5417	<0.01	25, -50, -8
IC12 Cerebellar network				
CD<HC				
Occipital fusiform gyrus	L	4315	<0.05	-32, -73, -19
Cerebellum	L	5990	<0.05	-16, -71, -21
IC13 cranial visual RSN				
CD>HC				
Lateral occipital cortex	L	7453	<0.05	-33, -77, 16
IC24 DMN				
CD<HC				
PHG	L	4259	<0.05	-23, -32, -24
Cerebellum	L	6852	<0.05	-18, -50, -30

Table 74 shows the RSNs and regional alterations in RSFC between CD and HC using the *HC group only* network template in the dual regression analysis.

5.7.6 Comparison of results between the two dual regression approaches

Table 75 compares the outcomes of the two dual regression approaches, which used either a (CD and HC) or HC only network template, showing similar results in the visual RSNs and FPNs

CD and HC RSNs as a network template in dual regression	**HC only RSNs as a network template in dual regression**
IC1 dorsal visual RSN **CD >HC** Inferior temporal gyrus Occipital fusiform gyrus Lingual gyrus Lateral occipital gyrus	*IC3 dorsal visual RSN* **CD>HC** Inferior temporal gyrus Lateral occipital cortex
IC9 FPN **CD>HC** Occipital fusiform gyrus	*IC11 FPN* **CD>HC** Occipital fusiform gyrus Thalamus Caudate PCG Postcentral gyrus Lingual gyrus
IC19 cranial visual RSN **CD>HC** Lateral occipital cortex/visual cortex Occipital pole/ visual cortex	*IC13 cranial visual RSN* **CD>HC** Lateral occipital cortex

Table 75 Networks showing similar results for the two dual regression approaches.

The use of HC only network as the template in the dual regression analysis resulted in a greater number of regions with significant differences between the CD patients and the HC group.

5.8 Discussion

This chapter studies the resting-state FC differences that exist in the brains of patients with CD as compared to an age-matched HCs group. The key findings are:

- Using (CD+HC) RSNs as a network template, altered RSFC was found between CD patients and HC in the dorsal/cranial visual RSN, FPN, temporal RSN, and cerebellar RSN.
- Using HC RSNs only as a network template, altered RSFC was found between CD patients and HCs in a larger number of RSNs including the medial visual RSN, left lateralised FPN, salience RSN and the DMN. Both dual regression approaches yielded similar results in the dorsal visual RSN, FPN and cranial visual RSN.
- IBD fatigue scores positively correlated with the RSFC in regions in visual and salience RSNs.
- Abdominal pain scores negatively correlated with RSFC in regions in the DMN and left lateral FPN. Positive correlations were found between abdominal pain scores and the RSFC in regions associated with the temporal and cerebellar RSNs as well as DMN.
- Disease duration correlated positively with the RSFC in regions in the visual RSN and salience network.
- Fasting GLP-1 levels positively correlated with the RSFC in the precentral gyrus in the visual RSN.
- Fasting PYY levels were associated with RSFC in regions in the temporal and frontal RSNs.

5.8.1 Comparison of RSFC between active CD patients and HC

This is the first study to study differences in RSFC in active CD patients compared with HCs. Here we observe differences in the cerebellar, visual, FPN, and temporal RSNs for the *(CD+HC) network* template. Using the *HC only* network in the dual regression resulted in more RSNs showing a significant difference between CD patients and HCs i.e. additional differences in the salience network and DMN.

CD patients showed increased RSFC compared to HCs in the cerebellar RSN (IC13, Figure 68) in the inferior temporal gyrus (visual perception[469]), middle temporal gyrus (language and semantic memory processing[469]) and the brain stem. The cerebellar network is associated with action and somesthesis (bodily perception and somatosensory processing) and is also found to be involved in processing humorous stimuli[425]. CD patients showed increased RSFC compared with HCs in cerebellar RSN (IC18, Figure 68) in the right frontal medial cortex (memory and decision making)[470], right frontal pole (task switching)[377], right precentral gyrus (motor cortex), left para-cingulate gyrus (language processing/word generation)[471], left occipital fusiform gyrus (object and facial recognition[388]) and the cerebellum (involved in motor function and cognition[472,473]). CD patients showed reduced connectivity in the cerebellar network (IC12, Figure 69) in the left occipital fusiform gyrus and cerebellum using the HC only network template. Altered RSFC in the cerebellar RSN in CD patients may be linked with abnormal cognitive functioning and emotional processing, and possibly heightened pain sensitivity. The cerebellar network has been implicated in age-related brain amyloidosis and inflammation[474].

CD patients showed reduced connectivity in the temporal RSN (involved in reading and language processing[425]) compared with HCs in the brain stem (involved in emotion, attention, executive function, and self regulation[475]) and left pallidum (emotional processing[476]). It could be postulated that reduced communication and information processing in these regions may result in impaired cognitive and emotion processing and attention deficits in CD patients.

CD patients showed increased RSFC in the medial visual RSN (associated with simple visual stimuli such as flashing checkerboards[425]) in the frontal orbital cortex (decision making and emotional processing[477,478]), and in the cranial visual RSN in the visual cortex.

CD patients showed increased connectivity compared with HCs in the left lateralised FPN (involved in working memory, language processing, word generation, and reading tasks[425]) in the inferior temporal gyrus (visual perception[469]). CD patients showed reduced RSFC in the salience network compared with HC (IC8, Figure 69) in the left cerebellum (motor function and cognition)[472,473], right lingual gyrus (visual information processing[403]) and right postcentral gyrus (somatosensory processing). The salience network has been implicated in orientation toward salient emotional stimuli, conflict monitoring, response choice, information integration, and pain-related processes during acute stimulus-induced pain[427]. As reported in the structural chapter of this thesis, the right postcentral gyrus showed reduced CT in CD compared with HC, it could be that this structural change may have contributed to the decreased RSFC seen in the right postcentral gyrus in the salience network. Decreased RSFC in regions of cortical thinning has been reported before in systemic inflammatory conditions such as systemic lupus erythematosus[479].

CD patients showed reduced connectivity in the DMN (IC24 Figure 69) (involved in self-referential processing[425]) in the PHG (visuospatial processing and episodic memory)[480] and cerebellum (motor function and cognition[472,473]). This finding contrasts with a study by Thomann et al[396] where increased connectivity was found in the anterior cingulate, left superior medial frontal gyrus and MCC in CD patients with remission compared with HC using ICA approach. These inconsistencies could be due to variations in the patient population, disease activity/severity, sample size, concomitant medication, and disease-related symptoms.

The two dual regression approaches used in this chapter yielded similar results in the dorsal visual RSN and cranial visual RSN and the FPN. The dual regression approach using HC RSNs only in the network template showed significant differences in more regions in the FPN such as the right thalamus, caudate, PCG, postcentral gyrus and lingual gyrus. This larger number of network differences in dual regression using the HC only network is in line with recent literature that the HC only ICA result is more robust in the absence of disease-related alterations[424].

CD patients showed increased connectivity in FPN in the left occipital fusiform gyrus (object and facial expression recognition[388]), right thalamus (relaying and integrating information, working memory, reward processing)[481], right caudate (executive function, information processing speed, memory)[482], right PCG (implicated in depression, emotion/pain processing, processing rewards, and self-reflection)[483], right postcentral gyrus (somatosensory processing) and right lingual gyrus (visual information processing[469]) compared with HC. The FPN has been associated with various functions such as executive function, working

memory, language, and visual information processing[425]. As reported in the structural chapter of this thesis, CD patients showed greater cortical thinning in the right postcentral gyrus compared with HC, which may have contributed to the increased connectivity observed in this region in the FPN (i.e. a compensatory effect to gain normal function of the atrophied region). Increased connectivity in regions of brain atrophy has been reported previously[484]. The left and right FPN have been investigated in CD patients in remission and HC before using ICA, however, no difference was detected between the groups[396].

CD patients showed increased connectivity compared with HC, in the left inferior temporal gyrus (visual perception[469]), left occipital fusiform gyrus (object and facial expression recognition[388]), right lingual gyrus (visual information processing[403]) and right lateral occipital regions (human object recognition[485]) in the dorsal visual RSN. The dorsal visual RSN is involved in the visually guided analysis of the spatial location, shape, and orientation of objects[486].

The underlying mechanisms of cognitive dysfunction in CD are poorly understood. A study investigating dysfunctions of cognitive flexibility (task switching) in IBD patients found that in IBD patients there were task-switching deficits (increased switch costs) compared with HCs[487]. It was concluded that IBD affects the cognitive neurophysiological pathways linked with the fronto-striatal networks and that these circuits are overstrained in IBD during task switching[487]. It could be postulated that the increase in RSFC observed in various RSNs in this chapter, is a compensatory mechanism that CD patients' brains undergo, i.e. overstraining of neural circuits to achieve normal brain function. It could be hypothesised that failure in compensatory mechanisms to restore

normal brain function, may lead to impairments in cognitive and emotional processing. For example, it has been found that CD patients in remission and HCs performing a phonemic VF test show no difference in the VF task performance. However, it was found that in response to the cognitive task, HCs exhibited activation patterns predominantly in the left lateralised regions. In contrast, CD patients exhibited a bihemispheric activation and decreased deactivation of the DMN, whereby the right-hemispheric language areas were recruited in response to the cognitive task. These findings indicate that CD patients may have recruited additional language areas as a compensatory mechanism to achieve equivalence in the behaviour performance, much like the phenomenon observed in older adults also scanned in this study. In addition, impairment in the information processing speed[488], task switching abilities[487] and verbal function[488,489] have been reported in adult CD patients where cognitive performance was linked to CD activity and nutritional status[488]. Similarly, CD patients have been shown to have slower response times in a cognitive impairment test compared with controls, where the slow response time observed in CD patients was associated with systemic inflammation, abdominal pain, and concurrent fatigue[490].

5.8.2 Correlation of pain scores, fatigue scores, disease duration and fasting GLP-1 and PYY in CD patients

IBD fatigue scores correlated positively with (i) the paracingulate gyrus in the medial visual RSN and (ii) the lateral occipital cortex (object recognition[485]) in the salience network. The effect of mental exhaustion has been shown to alter RSFC in the medial visual RSN in healthy volunteers[491]. Increased activity of the paracingulate gyrus has been associated with poorer visual memory task

performance in healthy volunteers[492]. Also, the salience network is one of the major RSNs implicated in CFS[493,494]. These findings may reflect overstraining of the neural circuits in the visual RSN and salience network, possibly forming part of the underlying processes involved in central fatigue in CD. In the present study, the measurement of fatigue is limited by the subjective nature of self-reported questionnaires and the questionnaire administered only identified fatigue, its severity, frequency, and duration (i.e. trait and state level fatigue). In future studies, multidimensional fatigue scales should be used to cover the general, physical and mental aspects of fatigue[495,496]

Abdominal pain scores correlated negatively with (i) the right inferior temporal gyrus (visual perception[469]) in the DMN (ii) the right frontal pole (task switching[377]) in the left lateralised FPN. Abdominal pain scores correlated positively with (i) left middle temporal gyrus (language and semantic memory processing[469]) in the DMN (ii) the left superior parietal lobule (manipulation of information in working memory[497]) in the temporal RSN (iii) the right inferior temporal gyrus (visual perception[469]) in the cerebellar RSN. A previous study showed more deactivation in the DMN in response to thermal pain stimulus in the IBD patients compared with IBS patients and controls indicating that IBD patients may show more cognitive control of painful stimuli. The FPN has been implicated in the cognitive modulation of pain in response to thermal pain stimulus in healthy volunteers[498]. The cerebellar RSN has also been implicated in chronic pain disorders.[499] A previous resting-state fMRI study in CD patients in remission found that abdominal pain scores correlated negatively with the ReHo values of the insula and the MCC, which contrasts with the findings of this study[463]. This inconsistency could be due to variations in the data analysis

methods, patient population, disease activity/severity, sample size, concomitant medication, and disease-related symptoms.

Disease duration correlated positively with (i) the right inferior temporal gyrus (visual perception[469]) and the right planum temporale (auditory perception and attention[500]) in the medial visual RSN (ii) the right and left precentral gyrus (motor cortex), the right inferior frontal gyrus (inhibition and attention control)[501] and the left frontal medial cortex (memory and decision making[470]) in the salience network. A previously resting-state study in CD patients in remission found that disease duration correlated negatively with the connectivity strength of the putamen. This finding is in contrast with the present study. It could be postulated that disease duration is one of the variables that affect disease burden which may be related to the changes seen in RSNs due to the increased chronic exposure of the CNS to symptom and chronic inflammatory stimuli

Fasting GLP-1 levels correlated positively with the right precentral gyrus (motor cortex) in CD patients. Fasting PYY levels correlated (i) positively with the left central opercular cortex (implicated in taste[502]) and left thalamus (relaying and integrating information, reward processing)[481] in the temporal RSN (ii) negatively with the left precentral gyrus, the left central opercular cortex (implicated in taste[502]) and the supracalcarine cortex (visual function[503]) in the frontal network. It has been found that PYY modulates reward-related feeding behaviour[89], which may be linked with the increased connectivity observed in the left thalamus in the temporal RSN. The significance of the association of PYY in supracalcrine, central operculum and precentral gyrus in the frontal network is unclear.

5.9 Conclusion

Taken together, alteration in RSFC between CD and HC in the RSNs implicated in cognition, attention, emotion, and pain may reflect neuroplasticity in response to chronic systemic inflammation, abdominal pain, and fatigue. It is important to note that, the cross-sectional nature of this study only provided a small window to assess the association between mild abdominal pain or fatigue and RSFC. Also investigating the RSFC in CD patients with and without fatigue and HCs would shed more light on the central causes of fatigue. Future studies assessing brain RSFC in CD, should use a non-gastrointestinal chronic inflammatory disease patient group as a comparator to dissect the relationship between gastrointestinal, systemic inflammation and RSFC. Future studies should also compare CD patients during the active phase of the disease and in remission, to see if the brain RSFC changes are reversible and associated with improved disease outcomes. Finally, comparing RSFC between fasting and postprandial states and associations with fasting/postprandial gut peptides in CD patients would be of interest to explain the gut peptide and meal driven functional effects on the brain.

6 Conclusion

Specific hypotheses to be tested in this thesis were that ileal CD patients when compared with colonic CD patients and HCs will show A) an alteration in brain-gut stimulation, B) an increase in the postprandial plasma EEC peptides response (CCK, GLP-1 and PYY) with associated appetite scores, C) a change in eating behaviour, and D) an altered brain structure and RSFC.

Figure 70 provides a summary consort diagram of the participants that were included in each chapter.

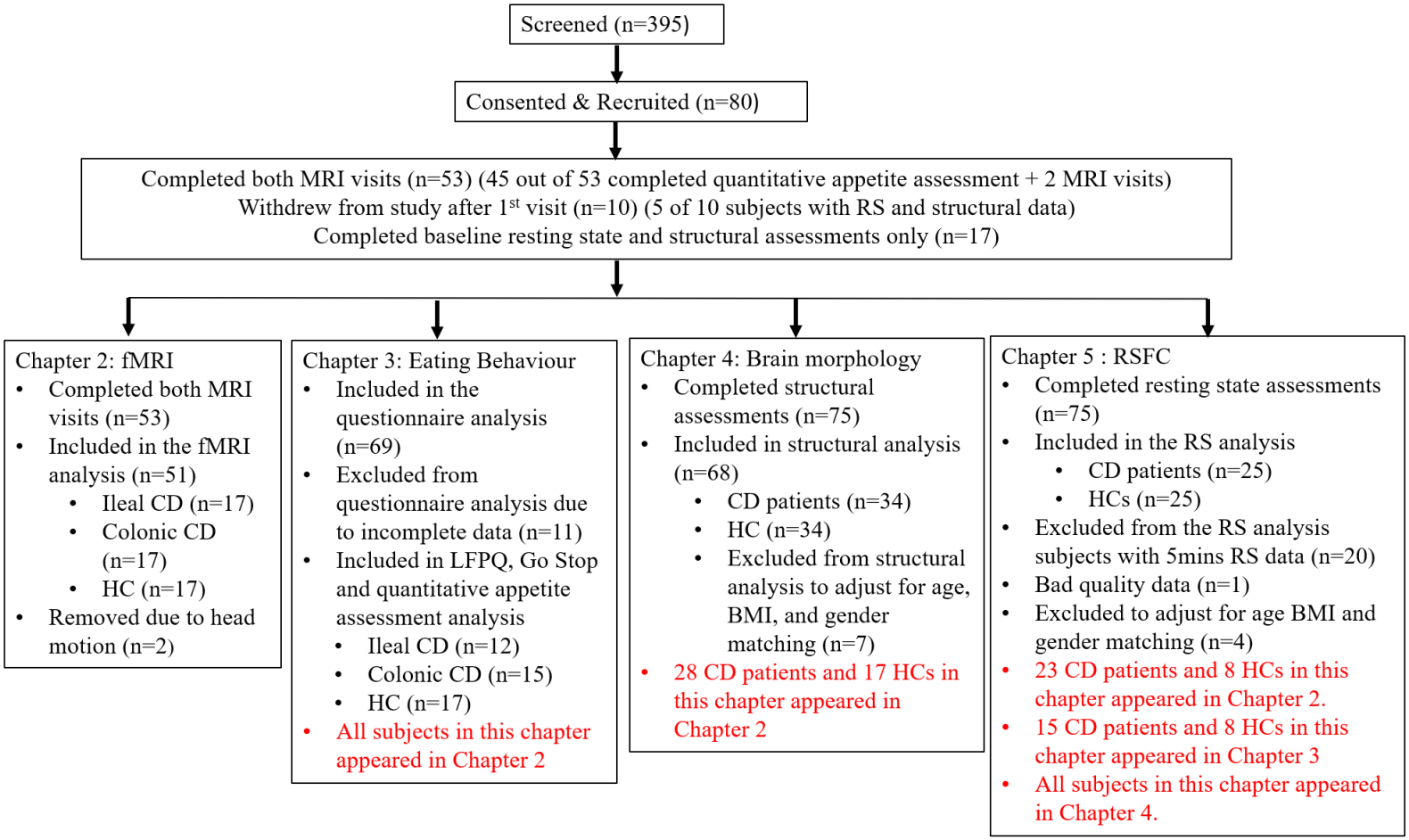


Figure 70 A summary consort diagram showing the number of participants included in each chapter

The overall purpose of the study was to investigate the role of the gut-brain axis and the EEC pathways in the control of food intake using MRI. The primary objective of this thesis was to compare the relevant changes in measures of brain activity following the C12 fatty acid test meal between ileal and colonic CD and age-, BMI- and gender-matched HCs. The secondary objectives were to compare the following measures amongst the ileal and colonic CD groups and HCs (i) the postprandial EEC hormones (CCK, GLP-1 and PYY) response (ii) changes in appetite and eating behaviour (iii) fasting plasma levels of IL-1β, IL-6 and TNFα (iii) brain structural and RSFC measures.

At the time of submission of this thesis, the CCK plasma data had just become available. Ongoing analyses of brain activity (BOLD and CBF) following the test meal is underway to generate second level, random-effects statistical maps of those regions which correlate with CCK levels and fullness ratings by using these measures as parametric modulators.

6.1 Postprandial EEC peptides and BOLD responses in response to the C12 fatty acid test meal

The investigation of the postprandial EEC peptides and BOLD responses in patients with active ileal CD, colonic CD and HCs showed that fasting baseline concentrations of GLP-1 in the ileal CD patients were significantly higher when compared with HC; with no difference found between ileal and colonic CD patients. No significant difference was found in the fasting baseline PYY concentrations and postprandial iAUC between the 3 groups. A significant postprandial increase in CCK concentrations was found in the ileal, colonic CD patients and HCs in response to fat. No significant difference was found in the fasting baseline CCK concentrations and postprandial iAUC between the three

groups in response to fat and saline. The probable explanation for this is that the absence of co-localisation of intestinal inflammation and the location of the CCK-secreting I cells in the proximal gut rather than in the distal ileum and colon. CD patients had significantly higher ratings compared with HC for fullness, distension, bloating, abdominal pain and discomfort. These symptoms could have been driven through the central anorectic effects of GLP-1 or through a state of intestinal hypomotility in the CD patients as our group has very recently shown[203].

Both saline and fat-induced a decrease in the postprandial BOLD response in the DMN. In addition, there was a greater decrease in the BOLD response in the RSFG for the saline meal compared with the fat meal. It was found that this response in the RSFG was driven by the ileal CD patients. The frontal lobe has been implicated in impulsive behaviours[204], and in particular, the RSFG[205] has been implicated in the control of impulse responses. Previous studies have shown feeding induced reduction in DMN activity[139141]. The mechanisms underlying this phenomenon is not understood, and is thought to be linked with the activity of the cholinergic and glutamatergic neurotransmitter systems[139]

Greater postprandial BOLD responses were found in areas including cerebellum, hippocampus, PCG, middle temporal gyrus, thalamus and medulla in response to fat. This is in line with previous findings by Lassman et al[157]. In the PCG, the BOLD response was greater following the fat meal compared with the saline meal. The activity of this region was driven by CD patients, with colonic CD patients showing stronger activation in this region compared with the ileal CD patients. The PCG activation was specific to CD patients in response to fat. Both colonic and ileal CD patients showed a significant postprandial increase in

abdominal pain in response to the fat meal. It could be postulated that abdominal pain may be one of the factors inducing the greater PCG activity in CD patients. Although, lower BOLD activation in the anterior[90] and posterior[210] cingulate gyrus has been reported in obese patients after RYGB surgery in response to viewing high-calorie foods[90], with reduced desire to eat, and reduced liking of high-calorie foods possibly linked with increased postoperative GLP-1 and PYY concentrations[90]. As shown in the eating behaviour chapter of this thesis, ileal CD patients exhibited explicit liking and wanting bias for high-fat foods, which may be related to emotional and comfort eating behaviours to alleviate symptoms such as low mood, abdominal pain and chronic fatigue. In HCs, sad emotion-induced activity of the PCG is found to be attenuated by C12 fatty acid infusions[165]. It could be postulated that the lower activity in PCG in the ileal CD patients, could be a lower hedonic brain response linked with the upregulation GLP-1 hormone and not driven by inflammation, as no significant difference was found in the proinflammatory cytokines (TNFα, IL-6, IL-1β) between the ileal and colonic CD groups and HCs. It is not possible to postulate whether the reduced PCG activity is a fat-induced attenuation in the homeostatic-hedonic response compared to colonic CD, or a response linked with pain. To confirm, if the PCG activity is linked with CCK, GLP-1 or PYY concentration, further analysis is required including these measures as parametric modulators in the fMRI GLM model.

6.2 Eating behaviour in active CD

Ileal CD patients exhibited greater impulsivity than colonic CD patients. Ileal CD patients had a lower positive mood than HCs and showed stronger explicit liking and wanting fat appeal bias in relation to food preference relative to HCs.

However, there was no difference in dietary intake across the three groups. The preload meal did not show a difference in appetite measures between the ileal and colonic CD groups. Lastly, no difference in the SQ was found across the three groups, however, the ileal CD ate significantly less of the *ad libitum* test meal compared with HC. It may be concluded that eating behaviour in ileal CD is likely to be impulse and reward-driven to alleviate symptoms such as low mood, abdominal pain and chronic fatigue. Stronger hedonic control of food intake was observed in the ileal CD patients based on their explicit wanting/liking appeal bias for high-fat foods, however, this was not translated into actual increased calorie intake, perhaps because of fear of triggering or worsening symptoms. Therefore, a complex interplay of gut peptides, psychological factors, disease-related symptoms, inflammatory burden may ultimately guide eating behaviour in ileal CD patients.

6.3 Altered brain structure in CD

GM, WM atrophy and cortical thinning were found in active CD patients compared with HCs in regions such as the precentral gyrus (motor cortex) and the postcentral gyrus. IBD fatigue scores negatively correlated with the GMV of the motor cortex. The relative atrophy of the motor cortex could be a possible central cause of IBD fatigue. The stronger negative correlation of GMV with age seen in CD patients relative to HCs could be reflective of CD manifestations, medication use, and related to other inflammatory conditions predating the diagnosis of CD such as psoriatic arthropathy and rheumatoid arthritis. However, longitudinal studies are required to understand the relationship between brain structure and age in CD. In addition, using a non-gastrointestinal chronic disease

group as a comparator would allow to determine if the brain regions implicated are specific to CD.

CD patients with pain showed greater GMV in the right postcentral gyrus and left anterior orbital gyrus compared with CD patients without pain, potentially representing use-dependent plasticity effects. CD patients with EIM had reduced GMV in the left postcentral gyrus and right precuneus compared with patients without EIM, suggesting systemic inflammation related GM atrophy. It is important to note that, CD patients with EIM tend to have more disease burden and hence a stronger inflammatory response. CD patients with EIM also had greater WMV than CD patients without EIM. Structural brain changes in active CD patients likely reflect the neuroplasticity to a chronic systemic inflammatory response and chronic symptom stimuli like abdominal pain and fatigue.

6.4 Altered RSFC in active CD

RSFC was assessed between CD and HCs using two dual regression analysis approaches including i) the cleaned group IC maps from the entire study population (i.e. CD and HC groups) as a network template as is standard practice in ICA analysis; (ii) the cleaned group IC maps from the HC group only as the network template. The use of the HC group only network template was included based on recent literature[424] suggesting that the HC ICA result is more robust in the absence of disease-related alterations and more sensitive in detecting group differences in the dual regression as compared with ICA maps from both patients and controls. Both dual regression approaches yielded similar results in the dorsal visual RSN, FPN and cranial visual RSN. For example, CD patients showed increased connectivity in FPN in the left occipital fusiform gyrus, right thalamus, right caudate, right PCG, right postcentral gyrus and right lingual

gyrus compared with HC. The FPN has been associated with various functions such as executive function, working memory, language, and visual information processing[425]. As reported in the structural chapter of this thesis, CD patients showed greater cortical thinning in the right postcentral gyrus compared with HC, which may have contributed to the increased connectivity observed in this region in the FPN (i.e. a compensatory effect to gain normal function of the atrophied region). It could be postulated that the increase in RSFC observed in various RSNs, is a compensatory mechanism that CD patients' brains undergo, i.e. overstraining of neural circuits to achieve normal brain function. It could be hypothesised that failure in compensatory mechanisms to restore normal brain function, may lead to impairments in cognitive and emotional processing. Taken together, alteration in RSFC between CD and HC in the RSNs implicated in cognition, attention, emotion, and pain may reflect neuroplasticity in response to chronic systemic inflammation, abdominal pain, and fatigue.

6.5 Limitations of the study

In the present study, the experiments were blinded to the participants but not the student. Patient standardisation was another limitation, due to variations in disease duration, the severity of inflammation and medication use. It should be noted that the fat meal used in the fMRI environment specifically stimulated CCK, so a different test meal with mixed nutrients (protein, CHO and fat) may have shown stronger postprandial responses in GLP-1 and PYY. The habitual diets of the participants were not assessed using more robust measures like FFQ or weighed food records, to see if the fat stimulus used was comparable between groups. However, based on the 24-hour recall there was no difference in fat intake between the 3 groups. In relation to the structural and functional brain

changes observed in CD patients, the cross-sectional nature of this study only provided a small window to assess the association between mild abdominal pain or fatigue and structural brain measures. Furthermore, it is hard to describe the chronology of events in the pathogenesis of CD and whether brain involvement precedes CD diagnosis or is a manifestation of the disease.

6.6 Future Directions

In relation to eating behaviour in CD, given the explicit liking/wanting appeal bias for fatty foods in the ileal CD group relative to HC, it might be more revealing to use a buffet-style test meal in future studies comprising of high-fat sweet/savoury, low-fat sweet/savoury. By using this, the effect of preload manipulation on food preference could be assessed. In the present study, the Go Stop impulsivity paradigm did not include any food stimulus, so future research could use food-based impulsivity tasks to better understand the lower inhibitory control observed in ileal CD patients.

With regards to the structural and functional brain changes, it would be interesting to compare CD patients with and without fatigue to further elucidate the central cause of IBD fatigue. Longitudinal studies are required to assess the time course of structural brain changes in CD, and to assess the effect of ageing on brain structure and function in CD patients. Future studies assessing brain structure and RSFC in CD should use a non-gastrointestinal chronic inflammatory disease patient group as a comparator to dissect the relationship between gastrointestinal, systemic inflammation and brain measures. It would be of interest to compare the brain structure and RSFC in the same CD patients during the active phase of the disease and in remission, to see if the brain changes

are reversible and associated with improved disease outcomes. It is possible in the future to use the BOLD time series currently used to perform an RSFC analysis between fasting and postprandial states. This will allow assessment of the association of RSFC measures with fasting/postprandial gut peptides in CD patients to further explain the gut peptide and meal driven functional associations with the brain

Finally, a better understanding of the role EEC peptides in altered eating behaviour, malnutrition and in the modulation of the gut-brain axis is relevant in elucidating new therapeutic pathways in CD treatment, thus improving nutritional status, disease outcomes, and QoL. Dietetic advice for healthy eating is recommended to improve disordered eating traits. Psychological, cognitive and behavioural therapeutic interventions may be beneficial to manage disease related symptoms such as low mood, chronic fatigue, abdominal pain, increased self monitoring and impulse behaviours.

Figure 71 shows the integration of the major findings from this thesis and their clinical relevance.

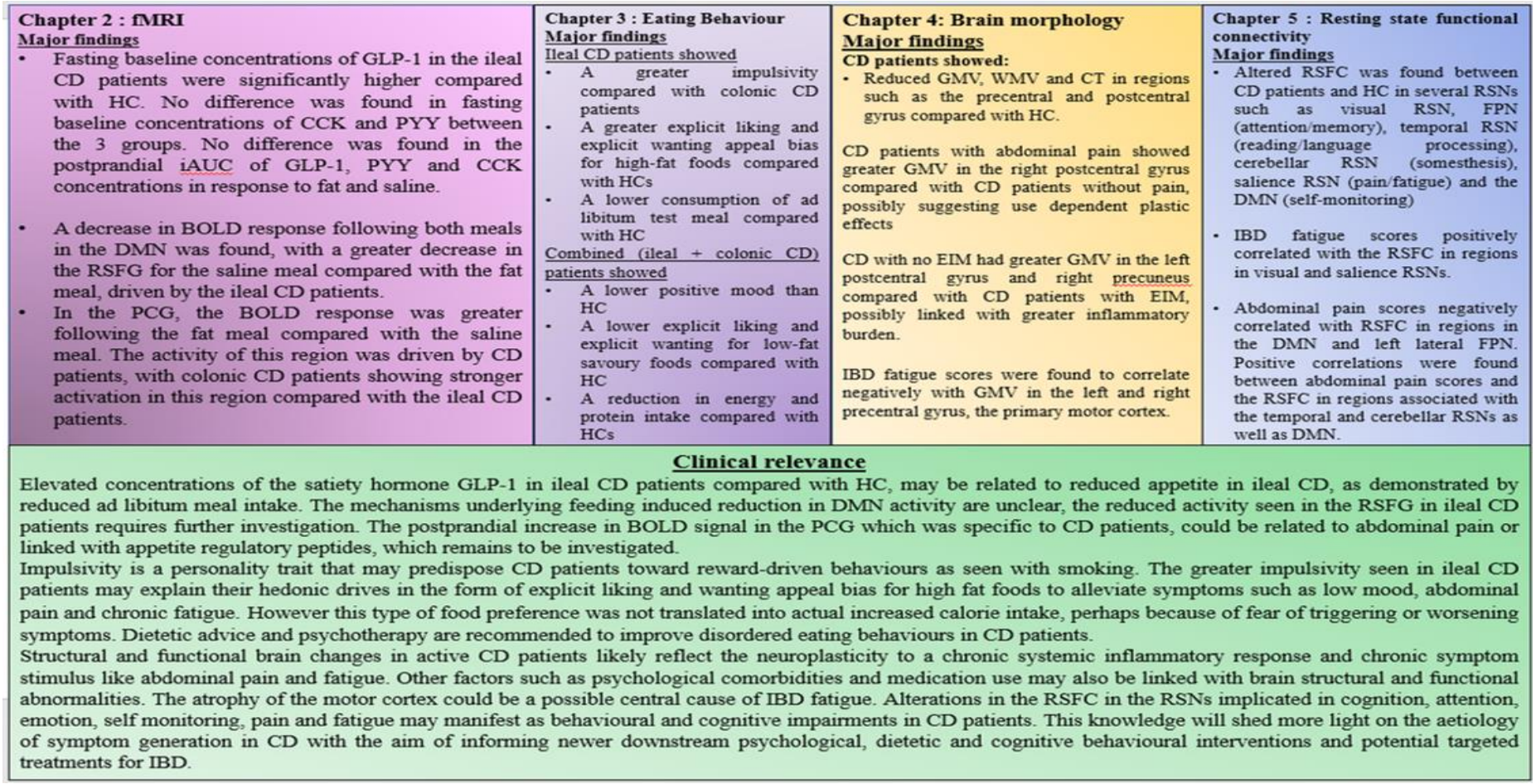


Figure 71 Integrating major findings from this thesis with their clinical relevance

7 References

1. Hancock L, Windsor AC, Mortensen NJ. Inflammatory bowel disease: The view of the surgeon. Color Dis 2006;8:10–14.

2. Mowat, Cole, Windsor, et al. Guidelines for the management of inflammatory bowel disease in adults. Gut 2011;60:571–607. Available at: http://gut.bmj.com/content/60/5/571.full.pdf%5Cnhttp://ovidsp.ovid.com/ovidweb.cgi?T=JS&PAGE=reference&D=emed10&NEWS=N&AN=2011191478.

3. Assche G Van, Dignass A, Reinisch W, et al. The second European evidence-based Consensus on the diagnosis and management of Crohn's disease: Special situations. J Crohn's Colitis 2010;4:63–101.

4. Peyrin-Biroulet L, Loftus E V, Colombel J-F, et al. The natural history of adult Crohn's disease in population-based cohorts. Am J Gastroenterol 2010;105:289–297. Available at: http://dx.doi.org/10.1038/ajg.2009.579.

5. Jeuring SFG, Heuvel TRA van den, Zeegers MP, et al. Epidemiology and Long-term Outcome of Inflammatory Bowel Disease Diagnosed at Elderly Age—An Increasing Distinct Entity? Inflamm Bowel Dis 2016;0:1. Available at: http://content.wkhealth.com/linkback/openurl?sid=WKPTLP:landingpage&an=00054725-900000000-98887.

6. Molodecky NA, Soon IS, Rabi DM, et al. Increasing incidence and prevalence of the inflammatory bowel diseases with time, based on systematic review. Gastroenterology 2012;142:46-54.e42. Available at: http://dx.doi.org/10.1053/j.gastro.2011.10.001.

7. Ghosh N, Premchand P. A UK cost of care model for inflammatory bowel disease. Frontline Gastroenterol 2015;6:169–174. Available at: http://fg.bmj.com/cgi/doi/10.1136/flgastro-2014-100514.

8. Ponder A, Long MD. A clinical review of recent findings in the epidemiology of inflammatory bowel disease. Clin Epidemiol 2013;5:237–247.

9. Molodecky NA, Kaplan GG. Environmental risk factors for inflammatory bowel disease. Gastroenterol Hepatol (N Y) 2010;6:339–346. Available at: http://www.ncbi.nlm.nih.gov/pubmed/20567592%5Cnhttp://www.pubmedcentral.nih.gov/articlerender.fcgi?artid=PMC2886488%5Cnhttp://www.ncbi.nlm.nih.gov/pubmed/20567592%5Cnhttp://www.pubmedcentral.nih.gov/articlerender.fcgi?artid=PMC2886488.

10. Arebi N, Misra R, Faiz O, et al. Epidemiology of inflammatory bowel disease in racial and ethnic migrant groups. World J Gastroenterol 2018;24:424–437.

11. Luther J, Dave M, Higgins PDR, et al. Association between Helicobacter pylori infection and inflammatory bowel disease: A meta-analysis and systematic review of the literature. Inflamm Bowel Dis 2010;16:1077–1084.

12. Calkins BM. A meta-analysis of the role of smoking in inflammatory bowel disease. Dig Dis Sci 1989;34:1841–1854.

13. Cornish JA, Tan E, Simillis C, et al. The risk of oral contraceptives in the etiology of inflammatory bowel disease: A meta-analysis. Am J Gastroenterol 2008;103:2394–2400.

14. Ungaro R, Bernstein CN, Gearry R, et al. Antibiotics associated with increased risk of New-Onset Crohn's disease but not ulcerative colitis: A meta-analysis. Am J Gastroenterol 2014;109:1728–1738.

15. Loddo I, Romano C. Inflammatory bowel disease: Genetics, epigenetics, and pathogenesis. Front Immunol 2015;6:6–11.

16. Brant SR. Update on the heritability of inflammatory bowel disease: The importance of twin studies. Inflamm Bowel Dis 2011;17:1–5.

17. Yang SK, Hong M, Zhao W, et al. Genome-wide association study of Crohn's disease in Koreans revealed three new susceptibility loci and common attributes of genetic susceptibility across ethnic populations. Gut 2014;63:80–87.

18. Hugot JP, Chamaillard M, Zouali H, et al. Association of NOD2 leucine-rich repeat variants with

susceptibility to Crohn's disease. Nature 2001;411:599–603.

19. Ogura Y, Bonen DK, Inohara N, et al. A frameshift mutation in NOD2 associated with susceptibility to Crohn's disease. Nature 2001;411:603–606.

20. Cooney R, Baker J, Brain O, et al. NOD2 stimulation induces autophagy in dendritic cells influencing bacterial handling and antigen presentation. Nat Med 2010;16:90–97. Available at: http://dx.doi.org/10.1038/nm.2069.

21. Murthy A, Li Y, Peng I, et al. A Crohn ' s disease variant in Atg16l1 enhances its degradation by caspase 3. Nature 2014;506:456–462. Available at: http://dx.doi.org/10.1038/nature13044.

22. Schwerd T, Pandey S, Yang H-T, et al. Impaired antibacterial autophagy links granulomatous intestinal inflammation in Niemann–Pick disease type C1 and XIAP deficiency with NOD2 variants in Crohn's disease. Gut 2016:gutjnl-2015-310382. Available at: http://gut.bmj.com/lookup/doi/10.1136/gutjnl-2015-310382.

23. Lauro ML, Burch JM, Grimes CL. The effect of NOD2 on the microbiota in Crohn's disease. Curr Opin Biotechnol 2016;40:97–102. Available at: http://linkinghub.elsevier.com/retrieve/pii/S0958166916300507.

24. Sanders DSA. Mucosal integrity and barrier function in the pathogenesis of early lesions in Crohn's disease. 2005:568–573.

25. Silverberg MS, Satsangi J, Ahmad T, et al. Toward an integrated clinical, molecular and serological classification of inflammatory bowel disease: report of a Working Party of the 2005 Montreal World Congress of Gastroenterology. Can J Gastroenterol 2005;19 Suppl A:5A-36A. Available at: http://www.researchgate.net/publication/7610226_Silverberg_MS_Satsangi_J_Ahmad_T_Arnott_ID_Bernstein_CN_Brant_SR_Caprili_R_Colombel_JF_Gasche_C_Geboes_K_Jewell_DP_Karban_A_Loftus_EV_Jr_Pene_AS_Riddel_RH_Schar_DB_Schreiber_S_Steinhart_AH_Targan_SR_Vermeire.

26. Baumgart DC, Sandborn WJ. Crohn's disease. Lancet 2012;380:1590–1605. Available at: http://dx.doi.org/10.1016/S0140-6736(12)60026-9.

27. D'Incà R, Dal Pont E, Leo V Di, et al. Can calprotectin predict relapse risk in inflammatory bowel disease? Am J Gastroenterol 2008;103:2007–2014.

28. Voderholzer W a, Beinhoelzl J, Rogalla P, et al. Small bowel involvement in Crohn's disease: a prospective comparison of wireless capsule endoscopy and computed tomography enteroclysis. Gut 2005;54:369–73. Available at: http://www.pubmedcentral.nih.gov/articlerender.fcgi?artid=1774420&tool=pmcentrez&rendertype=abstract.

29. Canavan C, Abrams KR, Mayberry J. Meta-analysis: Colorectal and small bowel cancer risk in patients with Crohn's disease. Aliment Pharmacol Ther 2006;23:1097–1104.

30. Louis E, Michel V, Hugot JP, et al. Early development of stricturing or penetrating pattern in Crohn's disease is influenced by disease location, number of flares, and smoking but not by NOD2/CARD15 genotype. Gut 2003;52:552–557.

31. Sandborn W, J A, Feagan BG, et al. Vedolizumab as induction and maintenance therapy for Crohn's disease. N Engl J Med 2013;369:711–21. Available at: http://www.ncbi.nlm.nih.gov/pubmed/23964933.

32. Peyrin-Biroulet L, Loftus E V, Colombel J-F, et al. The natural history of adult Crohn's disease in population-based cohorts. Am J Gastroenterol 2010;105:289–297.

33. Frolkis AD, Dykeman J, Negron ME, et al. Risk of surgery for inflammatory bowel diseases has decreased over time: A systematic review and meta-analysis of population-based studies. Gastroenterology 2013;145:996–1006. Available at: http://dx.doi.org/10.1053/j.gastro.2013.07.041.

34. Graaf C De, Blom WAM, Smeets PAM, et al. Biomarkers of satiation and satiety. Am J Clin Nutr 2004;79:946–961.

35. Bruen CM, O'Halloran F, Cashman KD, et al. The effects of food components on hormonal signalling in gastrointestinal enteroendocrine cells. Food Funct 2012;3:1131–1143. Available at: http://www.ncbi.nlm.nih.gov/pubmed/22914860.

36. Gerasimidis K, Mcgrogan P, Edwards CA. The aetiology and impact of malnutrition in paediatric inflammatory bowel disease. J Hum Nutr Diet 2011;24:313–326.

37. Catia Sternini, Laura Anselmia and ERP. Enteroendocrine cells : a site of "taste" in gastrointestinal chemosensing. Curr Opin Endocrinol Diabetes Obes 2008;15:73–78.

38. Posovszky C, Wabitsch M. Regulation of appetite, satiation, and body weight by enteroendocrine cells. Part 1: Characteristics of enteroendocrine cells and their capability of weight regulation. Horm Res Paediatr 2015;83:1–10.

39. Furness JB, Kunze WAA, Clerc N, et al. The intestine as a sensory organ: neural, endocrine and immune responses. Am J Physiol 1999;277:G922–G928.

40. Schwartz GJ. The role of gastrointestinal vagal afferents in the control of food intake: Current prospects. Nutrition 2000;16:866–873.

41. Date Y, Murakami N, Toshinai K, et al. The role of the gastric afferent vagal nerve in Ghrelin-induced feeding and growth hormone secretion in rats. Gastroenterology 2002;123:1120–1128.

42. Sukkar SG, Vaccaro A, Ravera GB, et al. Appetite control and gastrointestinal hormonal behavior (CCK, GLP-1, PYY 1-36) following low doses of a whey protein-rich nutraceutic. Med J Nutrition Metab 2013;6:259–266.

43. Perry B, Wang Y. Appetite regulation and weight control: the role of gut hormones. Nutr Diabetes 2012;2:e26. Available at: http://dx.doi.org/10.1038/nutd.2011.21.

44. Cummings DE, Overduin J. Review series Gastrointestinal regulation of food intake. Health Care (Don Mills) 2007;117:13–23.

45. McLaughlin JT, Lomax RB, Hall L, et al. Fatty acids stimulate cholecystokinin secretion via an acyl chain length-specific, Ca2+-dependent mechanism in the enteroendocrine cell line STC-1. J Physiol 1998;513:11–8. Available at: http://www.pubmedcentral.nih.gov/articlerender.fcgi?artid=2231256&tool=pmcentrez&rendertype=abstract.

46. Liou AP, Lu X, Sei Y, et al. The G-protein-coupled receptor GPR40 directly mediates Long-chain fatty acid-induced secretion of cholecystokinin. Gastroenterology 2011;140:903–912.

47. Valassi E, Scacchi M, Cavagnini F. Neuroendocrine control of food intake. Nutr Metab Cardiovasc Dis 2008;18:158–168.

48. Huda MSB, Wilding JPH, Pinkney JH. Gut peptides and the regulation of appetite. Obes Rev 2006;7:163–182.

49. Moran T, Sheng B. Hyperphagia and Obesity of OLETF Rats Lacking CCK1 Receptors: Developmental Aspects. Dev Psychobiol 2007:832–840. Available at: http://onlinelibrary.wiley.com/doi/10.1002/dev.20200/abstract%5Cnhttp://www.ncbi.nlm.nih.gov/pubmed/17299788.

50. F.C. Leslie, D.G. Thompson, J.T. McLaughlin, A. Varro, G.J. Dockray BKM. Plasma cholecystokinin concentrations are elevated in acute upper gastrointestinal infections. QJM - Mon J Assoc Physicians 2003;96:870–871.

51. Cummings DE, Overduin J. Review series Gastrointestinal regulation of food intake. Health Care (Don Mills) 2007;117:13–23. Available at: http://www.pubmedcentral.nih.gov/articlerender.fcgi?artid=1716217&tool=pmcentrez&rendertype=abstract.

52. Crawley JN, Corwin RL. Biological actions of cholecystokinin. Peptides 1994;15:731–755.

53. Matson C a, Reid DF, Cannon T a, et al. Cholecystokinin and leptin act synergistically to reduce body weight. Am J Physiol Regul Integr Comp Physiol 2000;278:R882–R890.

54. Holmes GM, Browning KN, Tong M, et al. Vagally mediated effects of glucagon-like peptide 1: *in vitro* and *in vivo* gastric actions. J Physiol 2009;587:4749–4759. Available at: http://doi.wiley.com/10.1113/jphysiol.2009.175067.

55. Lim GE, Brubaker PL. Glucagon-like peptide 1 secretion by the L-cell: The view from within. Diabetes 2006;55:S70–S77.

56. Chaudhri OB, Wynne K, Bloom SR. Can gut hormones control appetite and prevent obesity? Diabetes Care 2008;31 Suppl 2:S284–S289.

57. Sisley S, Gutierrez-Aguilar R, Scott M, et al. Neuronal GLP1R mediates liraglutide's anorectic but not glucose-lowering effect. J Clin Invest 2014;124:2456–2463.

58. Baggio LL, Drucker DJ. Glucagon-like peptide-1 receptors in the brain : controlling food intake and body weight. J Clin Invest 2014;124:4223–4226.

59. Secher A, Jelsing J, Baquero AF, et al. The arcuate nucleus mediates GLP-1 receptor agonist liraglutide-dependent weight loss. J Clin Invest 2014;124:4473–4488.

60. Farr OM, Sofopoulos M, Tsoukas MA, et al. GLP-1 receptors exist in the parietal cortex, hypothalamus and medulla of human brains and the GLP-1 analogue liraglutide alters brain activity related to highly desirable food cues in individuals with diabetes: a crossover, randomised, placebo-controlled. Diabetologia 2016. Available at: http://link.springer.com/10.1007/s00125-016-3874-y.

61. Veltman DJ, Bloemendaal L Van, Groot PFC, et al. Endogenous GLP-1 and GLP-1 analogue alter CNS responses to palatable food consumption. J Endocrinol 2016:1–32.

62. Filippatos TD, Panagiotopoulou T V, Elisaf MS. Adverse Effects of GLP-1 Receptor Agonists. Rev Diabet Stud 2015:202–230.

63. Batterham R, Cowley M, Small C, et al. Does gut hormone PYY3-36 decrease food intake in rodents? Reply. Nature 2004;168:8–9. Available at: http://discovery.ucl.ac.uk/762737/.

64. Anini Y, Fu-Cheng X, Cuber JC, et al. Comparison of the postprandial release of peptide YY and proglucagon- derived peptides in the rat. Pflugers Arch Eur J Physiol 1999;438:299–306.

65. Lin HC, Chey WY, Zhao X. Release of distal gut peptide YY (PYY) by fat in proximal gut depends on CCK. Peptides 2000;21:1561–3. Available at: http://www.ncbi.nlm.nih.gov/pubmed/14687704.

66. Kim BJ, Carlson OD, Jang HJ, et al. Peptide YY is secreted after oral glucose administration in a gender-specific manner. J Clin Endocrinol Metab 2005;90:6665–6671.

67. Lumb KJ, DeCarr LB, Milardo LF, et al. Novel selective neuropeptide Y2 receptor PEGylated peptide agonists reduce food intake and body weight in mice. J Med Chem 2007;50:2264–2268.

68. Abbott CR, Small CJ, Kennedy AR, et al. Blockade of the neuropeptide Y Y2 receptor with the specific antagonist BIIE0246 attenuates the effect of endogenous and exogenous peptide YY (3-36) on food intake. Brain Res 2005;1043:139–144.

69. Vincent RP, Roux CW le. The satiety hormone peptide YY as a regulator of appetite. J Clin Pathol 2008;61:548–52. Available at: http://www.ncbi.nlm.nih.gov/pubmed/18441153.

70. Koda S, Date Y, Murakami N, et al. The role of the vagal nerve in peripheral PYY 3-36-induced feeding reduction in rats. Endocrinology 2005;146:2369–2375.

71. Savage AP, Adrian TE, Carolan G, et al. Effects of peptide YY (PYY) on mouth to caecum intestinal transit time and on the rate of gastric emptying in healthy volunteers. Gut 1987;28:166–170. Available at: http://gut.bmj.com/content/28/2/166.abstract.

72. Roux CW le, Borg CM, Murphy KG, et al. Supraphysiological doses of intravenous PYY3-36 cause nausea, but no additional reduction in food intake. Ann Clin Biochem 2008;45:93–5. Available at: http://www.scopus.com/inward/record.url?eid=2-s2.0-41649099750&partnerID=tZOtx3y1.

73. Ueno H, Nakazato M. Mechanistic relationship between the vagal afferent pathway, central nervous system and peripheral organs in appetite regulation. J Diabetes Investig 2016:1–7.

74. Lartigue G De, Lur G, Dimaline R, et al. EGR1 is a target for cooperative interactions between cholecystokinin and leptin, and inhibition by ghrelin, in vagal afferent neurons. Endocrinology 2010;151:3589–3599.

75. Smeets PAM, Erkner A, Graaf C De. Cephalic phase responses and appetite. Nutr Rev 2010;68:643–655.

76. Teff K. Nutritional implications of the cephalic-phase reflexes: endocrine responses. Appetite 2000;34:206–213.

77. Berthoud HR, Neuhuber WL. Functional and chemical anatomy of the afferent vagal system. Auton Neurosci Basic Clin 2000;85:1–17.

78. Berthoud HR. Vagal and hormonal gut-brain communication: From satiation to satisfaction. Neurogastroenterol Motil 2008;20:64–72.

79. Perry B, Wang Y. Appetite regulation and weight control: the role of gut hormones. Nutr Diabetes 2012;2:e26.

80. Schwartz MW, Jr DP. Diabetes , Obesity , and the Brain. Science (80-) 2005;307:375–379.

81. Farr OM, Li C-SR, Mantzoros CS. Central nervous system regulation of eating: Insights from human brain imaging. Metabolism 2016;65:699–713. Available at: http://www.sciencedirect.com/science/article/pii/S0026049516000330.

82. Ziauddeen H, Alonso-alonso M, Hill JO, et al. Obesity and the Neurocognitive Basis of Food Reward and the Control of Intake. Adv Nutr 2015:474–86.

83. DiLeone RJ, Taylor JR, Picciotto MR. The drive to eat: comparisons and distinctions between mechanisms of food reward and drug addiction. Nat Neurosci 2012;15:1330–1335. Available at: http://dx.doi.org/10.1038/nn.3202.

84. Kelley AE, Baldo BA, Pratt WE, et al. Corticostriatal-hypothalamic circuitry and food motivation: Integration of energy, action and reward. Physiol Behav 2005;86:773–795.

85. Morton GJ, Meek TH, Schwartz MW. Neurobiology of food intake in health and disease. Nat Rev Neurosci 2014;15:367–78. Available at: http://www.ncbi.nlm.nih.gov/pubmed/24840801.

86. Pannacciulli N, Le DSNT, Salbe AD, et al. Postprandial glucagon-like peptide-1 (GLP-1) response is positively associated with changes in neuronal activity of brain areas implicated in satiety and food intake regulation in humans. Neuroimage 2007;35:511–517. Available at: http://dx.doi.org/10.1016/j.neuroimage.2006.12.035.

87. Nederkoorn C, Smulders FTY, Havermans RC, et al. Impulsivity in obese women. Appetite 2006;47:253–256.

88. Nederkoorn C, Jansen E, Mulkens S, et al. Impulsivity predicts treatment outcome in obese children. Behav Res Ther 2007;45:1071–1075.

89. Batterham RL, Dominic H, Rosenthal JM, et al. PYY modulation of cortical and hypothalamic brain areas predicts feeding behaviour in humans. Nature 2007;450:2–7.

90. Scholtz S, Miras AD, Chhina N, et al. Obese patients after gastric bypass surgery have lower brain-hedonic responses to food than after gastric banding. Gut 2014;63:891–902.

91. Goldstone AP, Miras AD, Scholtz S, et al. Link between increased satiety gut hormones and reduced food reward following gastric bypass surgery for obesity. J Clin Endocrinol Metab 2015:jc.2015-2665. Available at: http://press.endocrine.org/doi/10.1210/jc.2015-2665.

92. Cornier MA, Kaenel SS Von, Bessesen DH, et al. Effects of overfeeding on the neuronal response to visual food cues. Am J Clin Nutr 2007;86:965–971.

93. Goldstone AP, Prechtl De Hernandez CG, Beaver JD, et al. Fasting biases brain reward systems towards high-calorie foods. Eur J Neurosci 2009;30:1625–1635.

94. Moran GW, Pennock J, Mclaughlin JT. Enteroendocrine cells in terminal ileal Crohn ' s disease ☆. J Crohn's Colitis 2012;6:871–880. Available at: http://dx.doi.org/10.1016/j.crohns.2012.01.013.

95. Moran GW, Leslie FC, McLaughlin JT. Crohn's disease affecting the small bowel is associated with reduced appetite and elevated levels of circulating gut peptides. Clin Nutr 2013;32:404–411. Available at: http://dx.doi.org/10.1016/j.clnu.2012.08.024.

96. Moran GW, Leslie FC, Levison SE, et al. Enteroendocrine cells: neglected players in gastrointestinal disorders? Therap Adv Gastroenterol 2008;1:51–60.

97. Pauling L, Coryell CD. The Magnetic Properties and Structure of the Hemochromogens and Related Substances. Proc Natl Acad Sci 1936;22:159–163.

98. Thulborn KR, Waterton JC, Matthews PM, et al. Oxygenation dependence of the transverse relaxation time of water protons in whole blood at high field. BBA - Gen Subj 1982;714:265–270.

99. Lin AL, Qin Q, Zhao X, et al. Blood longitudinal (T 1) and transverse (T 2) relaxation time constants at 11.7 Tesla. Magn Reson Mater Physics, Biol Med 2012;25:245–249.

100. Ogawa, S, Lee T.M, Kay A.R and DWT. Brain magnetic resonance imaging with contrast dependent on blood oxygenation. Proc Natl Acad Sci U S A 1990;87:9868–9872.

101. Kwong KK, Belliveau JW, Chesler DA, et al. During Primary. Proc Natl Acad Sci U S A 1992;89:1–5. Available at: papers3://publication/uuid/B967F349-9A1A-47B9-B27D-80E674C7E945.

102. Bandettini PA, Wong EC, Hinks RS, et al. Time course EPI during task activation. Magn Res Med 1992;25:390–397.

103. Chow MS, Wu SL, Webb SE, et al. Functional magnetic resonance imaging and the brain: A brief review. World J Radiol 2017;9:5.

104. Francis ST, Eldeghaidy S. Imaging methodologies and applications for nutrition research: what can functional MRI offer? Proc Nutr Soc 2015;74:89–98.

105. Lee SP, Duong TQ, Yang G, et al. Relative changes of cerebral arterial and venous blood volumes during increased cerebral blood flow: Implications for bold fMRI. Magn Reson Med 2001;45:791–800.

106. Báez-Yánez MG, Ehses P, Mirkes C, et al. The impact of vessel size, orientation and intravascular contribution on the neurovascular fingerprint of BOLD bSSFP fMRI. Neuroimage 2017;163:13–23.

107. Kim SG, Ogawa S. Biophysical and physiological origins of blood oxygenation level-dependent fMRI signals. J Cereb Blood Flow Metab 2012;32:1188–1206.

108. Menon RS, Ogawa S, Hu X, et al. BOLD Based Functional MRI at 4 Tesla Includes a Capillary Bed Contribution: Echo-Planar Imaging Correlates with Previous Optical Imaging Using Intrinsic Signals. Magn Reson Med 1995;33:453–459.

109. Yacoub E, Shmuel A, Pfeuffer J, et al. Investigation of the initial dip in fMRI at 7 Tesla. NMR Biomed 2001;14:408–412.

110. Buxton RB. The physics of functional magnetic resonance imaging (fMRI). Reports Prog Phys 2013;76.

111. Krüger G, Kleinschmidt A, Frahm J. Dynamic MRI sensitized to cerebral blood oxygenation and flow during sustained activation of human visual cortex. Magn Reson Med 1996;35:797–800.

112. Mandeville JB, Marota JJA, Kosofky BZ, et al. Dynamic functional imaging of relative CBV during rat fore paw stimulation. Magn Res Med 1998;39:619–624.

113. Buxton RB, Uludağ K, Dubowitz DJ, et al. Modeling the hemodynamic response to brain activation. Neuroimage 2004;23:220–233.

114. Hoge RD, Atkinson J, Gill B, et al. Investigation of BOLD signal dependence on CBF and CMRO2: The deoxyhemoglobin dilution model. Neuroimage 1999;9:849–863.

115. Marciani Luca, Eldeghaidy Sally, Spiller Robin, Gowland Penny FS. *Brain imaging : Food technology*. Taylor, A. J., Linforth, S. T., Eds.; Wiley: Oxford, U.K; 2010.

116. Purdon PL, Weisskoff RM. Effect of temporal autocorrelation due to physiological noise and stimulus paradigm on voxel-level false-positive rates in fMRI. Hum Brain Mapp 1998;6:239–249.

117. Arco JE, González-García C, Díaz-Gutiérrez P, et al. Influence of activation pattern estimates and statistical significance tests in fMRI decoding analysis. J Neurosci Methods 2018;308:248–260.

118. Zanchi D, Depoorter A, Egloff L, et al. The impact of gut hormones on the neural circuit of appetite and satiety: A systematic review. Neurosci Biobehav Rev 2017;80:457–475.

119. McLaughlin JT, McKie S. Human brain responses to gastrointestinal nutrients and gut hormones. Curr Opin Pharmacol 2016;31:8–12. Available at: http://dx.doi.org/10.1016/j.coph.2016.08.006.

120. Anderson IM, McKie S, Elliott R, et al. Assessing human 5-HT function in vivo with pharmacoMRI. Neuropharmacology 2008;55:1029–1037. Available at: http://dx.doi.org/10.1016/j.neuropharm.2008.06.029.

121. Lancaster JL, Tordesillas-Gutiérrez D, Martinez M, et al. Bias between MNI and talairach

coordinates analyzed using the ICBM-152 brain template. Hum Brain Mapp 2007;28:1194–1205.

122. Friston KJ, Holmes J, Poline P, Grasby P.J, Williams, SC, Frackowlak TR. Analysis of fMRI Time-Series Revisited. 1995:45–53.

123. Friston K.J, Holmes A.P, Worsley J.P, Poline, Frith F. Statistical Parametric Maps in Functional Imaging: A General Linear Approach. Hum Brain Mapp 1995;2:189–210.

124. Poldrack RA, Fletcher PC, Henson RN, et al. Guidelines for reporting an fMRI study. Neuroimage 2008;40:409–414. Available at: http://dx.doi.org/10.1016/j.neuroimage.2007.11.048.

125. Chumbley JR, Friston KJ. False discovery rate revisited: FDR and topological inference using Gaussian random fields. Neuroimage 2009;44:62–70. Available at: http://dx.doi.org/10.1016/j.neuroimage.2008.05.021.

126. Jones RB, Mckie S, Astbury N, et al. Functional neuroimaging demonstrates that ghrelin inhibits the central nervous system response to ingested lipid. Gut 2012;61:1543–1551.

127. Lassman DJ, McKie S, Gregory LJ, et al. Defining the Role of Cholecystokinin in the Lipid-Induced Human Brain Activation Matrix. Gastroenterology 2010;138:1514–1524. Available at: http://dx.doi.org/10.1053/j.gastro.2009.12.060.

128. Spetter MS, Graaf C de, Mars M, et al. The sum of its parts--effects of gastric distention, nutrient content and sensory stimulation on brain activation. PLoS One 2014;9:e90872. Available at: http://www.pubmedcentral.nih.gov/articlerender.fcgi?artid=3948722&tool=pmcentrez&rendertype=abstract.

129. Silva A De, Salem V, Long CJ, et al. The Gut Hormones PYY3-36 and GLP-17-36 amide Reduce Food Intake and Modulate Brain Activity in Appetite Centers in Humans Akila. Cell Metab 2011;14:700–706. Available at: http://dx.doi.org/10.1016/j.cmet.2011.09.010.

130. Eldeghaidy S, Marciani L, Hort J, et al. Prior Consumption of a Fat Meal in Healthy Adults Modulates the Brain's Response to Fat. J Nutr 2016;146:2187–2198.

131. Wright H, Li X, Fallon NB, et al. Differential effects of hunger and satiety on insular cortex and hypothalamic functional connectivity. Eur J Neurosci 2016:1–9.

132. Timper K, Brüning JC. Hypothalamic circuits regulating appetite and energy homeostasis: Pathways to obesity. DMM Dis Model Mech 2017;10:679–689.

133. Myers MG, Olson DP. Central nervous system control of metabolism. Nature 2012;491:357–363.

134. Führer D, Zysset S, Stumvoll M. Brain activity in hunger and satiety: An exploratory visually stimulated fMRI study. Obesity 2008;16:945–950.

135. LaBar KS, Gitelman DR, Parrish TB, et al. Hunger selectively modulates corticolimbic activation to food stimuli in humans. Behav Neurosci 2001;115:493–500.

136. Mohanty A, Gitelman DR, Small DM, et al. The spatial attention network interacts with limbic and monoaminergic systems to modulate motivation-induced attention shifts. Cereb Cortex 2008;18:2604–2613.

137. Laan LN van der, Ridder DTD de, Viergever MA, et al. The first taste is always with the eyes: A meta-analysis on the neural correlates of processing visual food cues. Neuroimage 2011;55:296–303. Available at: http://dx.doi.org/10.1016/j.neuroimage.2010.11.055.

138. Killgore WDS, Young AD, Femia LA, et al. Cortical and limbic activation during viewing of high- versus low-calorie foods. Neuroimage 2003;19:1381–1394.

139. Ishibashi K, Sakurai K, Shimoji K, et al. Altered functional connectivity of the default mode network by glucose loading in young, healthy participants. BMC Neurosci 2018;19:1–8. Available at: https://doi.org/10.1186/s12868-018-0433-0.

140. Opstal AM Van, Hafkemeijer A, Berg-Huysmans AA van den, et al. Brain activity and connectivity changes in response to nutritive natural sugars, non-nutritive natural sugar replacements and artificial sweeteners. Nutr Neurosci 2019;0:1–11. Available at: https://doi.org/10.1080/1028415X.2019.1639306.

141. Deza-Araujo YI, Neukam PT, Marxen M, et al. Acute tryptophan loading decreases functional

connectivity between the default mode network and emotion-related brain regions. Hum Brain Mapp 2019;40:1844–1855.

142. Becker CA, Flaisch T, Renner B, et al. From thirst to satiety: The anterior mid-cingulate cortex and right posterior insula indicate dynamic changes in incentive value. Front Hum Neurosci 2017;11:1–9.

143. Denton D, Shade R, Zamarippa F, et al. Neuroimaging of genesis and satiation of thirst and an interoceptor-driven theory of origins of primary consciousness. Proc Natl Acad Sci U S A 1999;96:5304–5309.

144. Farrell MJ, Bowala TK, Gavrilescu M, et al. Cortical activation and lamina terminalis functional connectivity during thirst and drinking in humans. Am J Physiol - Regul Integr Comp Physiol 2011;301.

145. Liu Yijun, Gao Jia-Hong, Liu Ho-Ling FP. The temporal response of the brain after eating revealed by functional MRI. Nature 2000;405:1058–1062.

146. Smeets PAM, Graaf C De, Stafleu A, et al. Functional MRI of human hypothalamic responses following glucose ingestion. Neuroimage 2005;24:363–368.

147. Smeets Paul, Graaf Cees de, Stafleu Annette, Van Osch Matthias van der GJ. Functional magnetic resonance imaging of human hypothalamic responses to sweet taste and calories. Am J Clin Nutr 2005;82:1011–6.

148. Smeets PAM, Vidarsdottir S, Graaf C De, et al. Oral glucose intake inhibits hypothalamic neuronal activity more effectively than glucose infusion. Am J Physiol - Endocrinol Metab 2007;293:754–758.

149. Little TJ, McKie S, Jones RB, et al. Mapping glucose-mediated gut-to-brain signalling pathways in humans. Neuroimage 2014;96:1–11. Available at: http://dx.doi.org/10.1016/j.neuroimage.2014.03.059.

150. Jastreboff AM, Sinha R, Arora J, et al. Altered brain response to drinking glucose and fructose in obese adolescents. Diabetes 2016;65:1929–1939.

151. Opstal AM Van, Berg-Huysmans AA Van Den, Hoeksma M, et al. The effect of consumption temperature on the homeostatic and hedonic responses to glucose ingestion in the hypothalamus and the reward system. Am J Clin Nutr 2018;107:20–25.

152. Opstal AM van, Kaal I, Berg-Huysmans AA van den, et al. Dietary sugars and non-caloric sweeteners elicit different homeostatic and hedonic responses in the brain. Nutrition 2019;60:80–86. Available at: https://doi.org/10.1016/j.nut.2018.09.004.

153. Purnell JQ, Klopfenstein BA, Stevens AA, et al. Brain functional magnetic resonance imaging response to glucose and fructose infusions in humans. Diabetes, Obes Metab 2011;13:229–234.

154. Stopyra MA, Friederich HC, Sailer S, et al. The effect of intestinal glucose load on neural regulation of food craving. Nutr Neurosci 2019;0:1–10. Available at: https://doi.org/10.1080/1028415X.2019.1600275.

155. Wölnerhanssen BK, Meyer-Gerspach AC, Schmidt A, et al. Dissociable behavioral, physiological and neural effects of acute glucose and fructose ingestion: A pilot study. PLoS One 2015;10:1–15.

156. Luo S, Monterosso JR, Sarpelleh K, et al. Differential effects of fructose versus glucose on brain and appetitive responses to food cues and decisions for food rewards. Proc Natl Acad Sci 2015;112:6509–6514.

157. Lassman DJ, Mckie S, Gregory LJ, et al. Defining the Role of Cholecystokinin in the Lipid-Induced Human Brain Activation Matrix. Gastroenterology 2010;138:1514–1524. Available at: http://dx.doi.org/10.1053/j.gastro.2009.12.060.

158. Frank-Podlech S, Heinze JM, Machann J, et al. Functional Connectivity Within the Gustatory Network Is Altered by Fat Content and Oral Fat Sensitivity – A Pilot Study. Front Neurosci 2019;13:1–10.

159. Leidy HJ, Ortinau LC, Douglas SM, et al. Beneficial effects of a higher-protein breakfast on the appetitive, hormonal, and neural signals controlling energy intake regulation in overweight/obese, “breakfast-skipping,” late-adolescent girls. Am J Clin Nutr 2013;97:677–688.

160. Li J, An R, Zhang Y, et al. Correlations of macronutrient-induced functional magnetic resonance imaging signal changes in human brain and gut hormone responses. Am J Clin Nutr 2012;96:275–282.

161. Kroemer NB, Krebs L, Kobiella A, et al. (Still) longing for food: Insulin reactivity modulates response to food pictures. Hum Brain Mapp 2013;34:2367–2380.

162. B.S. L, D.C. A, L.M. H, et al. Effects of dietary glycemic index on brain areas associated with addiction: A randomized controlled feeding study. Endocr Rev 2013;34:641–647. Available at: http://www.embase.com/search/results?subaction=viewrecord&from=export&id=L71785240%0Ahttp://press.endocrine.org/doi/abs/10.1210/endo-meetings.2013.OABA.10.SAT-698.

163. Heni M, Kullmann S, Ketterer C, et al. Differential effect of glucose ingestion on the neural processing of food stimuli in lean and overweight adults. Hum Brain Mapp 2014;35:918–928.

164. Dorton HM, Luo S, Monterosso JR, et al. Influences of dietary added sugar consumption on striatal food-cue reactivity and postprandial GLP-1 response. Front Psychiatry 2018;8:1–9.

165. Oudenhove L Van, Mckie S, Lassman D, et al. Fatty acid – induced gut-brain signaling attenuates neural and behavioral effects of sad emotion in humans. J Clin Invest 2011;121:3094–3099.

166. Byrne CS, Chambers ES, Alhabeeb H, et al. Increased colonic propionate reduces anticipatory reward responses in the human striatum to high-energy foods. Am J Clin Nutr 2016;104:5–14.

167. Poulia KA, Klek S, Doundoulakis I, et al. The two most popular malnutrition screening tools in the light of the new ESPEN consensus definition of the diagnostic criteria for malnutrition. Clin Nutr 2017;36:1130–1135. Available at: http://dx.doi.org/10.1016/j.clnu.2016.07.014.

168. Wędrychowicz A. Advances in nutritional therapy in inflammatory bowel diseases: Review. World J Gastroenterol 2016;22:1045. Available at: http://www.wjgnet.com/1007-9327/full/v22/i3/1045.htm.

169. Lochs H, Dejong C, Hammarqvist F, et al. ESPEN Guidelines on Enteral Nutrition: Gastroenterology. Clin Nutr 2006;25:260–274. Available at: http://linkinghub.elsevier.com/retrieve/pii/S0261561406000252.

170. Donnellan CF, Yann LH, Lal S. Nutritional management of Crohn's disease. Therap Adv Gastroenterol 2013;6:231–242.

171. Sonnenberg a, Collins JF. Vicious circles in inflammatory bowel disease. Inflamm Bowel Dis 2006;12:944–949. Available at: http://ep.fjernadgang.kb.dk/login?url=http://ovidsp.ovid.com/ovidweb.cgi?T=JS&CSC=Y&NEWS=N&PAGE=fulltext&D=emed7&AN=2006486180.

172. Prince A, Whelan K, Moosa A, et al. Nutritional problems in inflammatory bowel disease : The patient perspective. J Crohn's Colitis 2011;5:443–450. Available at: http://dx.doi.org/10.1016/j.crohns.2011.04.016.

173. Limdi JK, Aggarwal D, McLaughlin JT. Dietary Practices and Beliefs in Patients with Inflammatory Bowel Disease. Inflamm Bowel Dis 2016;22:164–170.

174. Casanova MJ, Chaparro M, Molina B, et al. Prevalence of malnutrition and nutritional characteristics of patients with inflammatory bowel disease. J Crohn's Colitis 2017;11:1430–1439.

175. Vries JHM De, Dijkhuizen M, Tap P, et al. Patient's Dietary Beliefs and Behaviours in Inflammatory Bowel Disease. Dig Dis 2019;37:131–139.

176. Wędrychowicz A, Zając A, Tomasik P. Advances in nutritional therapy in inflammatory bowel diseases: Review. World J Gastroenterol 2016;22:1045–1066.

177. Hart AL, Lomer M, Verjee A, et al. What Are the Top 10 Research Questions in the Treatment of Inflammatory Bowel Disease? A Priority Setting Partnership with the James Lind Alliance. J Crohns Colitis 2017;11:204–211.

178. Wardle RA, Thapaliya G, Nowak A, et al. An examination of appetite and disordered eating in active crohn's disease. J Crohn's Colitis 2018;12:819–825.

179. Mahida YR, Wu K, Jewell DP. Enhanced production of interleukin 1-beta by mononuclear cells isolated from mucosa with active ulcerative colitis of Crohn's disease. Gut 1989;30:835–8.

Available at: http://www.pubmedcentral.nih.gov/articlerender.fcgi?artid=1434123&tool=pmcentrez&rendertype=abstract.

180. Mahida YR, Kurlac L, Gallagher A, et al. High circulating concentrations of interleukin-6 in active Crohn ' s disease but not ulcerative colitis. 1991:1531–1534.

181. Macdonald TT, Hutchings P, Choy M, et al. Tumour necrosis factor-alpha and interferon-gamma production measured at the single cell level in normal and inflamed human intestine. 1990:301–305.

182. Chrousos G. The Hypothalmic-pituitary-adrenal axis and immune- mediated inflammation. N Engl J Med 1995;332:1351–1362.

183. Plata-Salaman CR, Oomura Y, Kai Y. Tumor necrosis factor and interleukin-1 beta: suppression of food intake by direct action in the central nervous system. Brain Res 1988;448:106–114.

184. Mcdermott JR, Leslie FC, Thompson DG, et al. Immune contorl of food intake: enteroendocrine cells are regulated by CD4+ T lymphocytes during small intestinal inflammtion. Neurogastroenterology 2006;55:492–497.

185. Besterman HS, Cook GC, Sarson DL, et al. Gut hormones in tropical malabsorption. Br Med J 1979;2:1252–1255.

186. Solteszb XW, Andersson JAR. Cholecystokinin increases small intestinal motility and reduces enteric bacterial overgrowth and translocation in rats with surgically induced acute liver failure. Digestion 1996;57:67–72.

187. S. Freier, M. Eran JF. Effect of cholecystokinin and of its antagonist, of atropine, and of food on the release of immunoglobulin A and immunoglobulin G specific antibodies in the rat intestine. Gastroenterology 1987;93:1242–1246. Available at: http://www.ravishingbeasts.com/adventures-with-taxidermy/2011/6/22/third-place-merle-patchett.html.

188. Keller J, Beglinger C, Holst JJ, et al. Mechanisms of gastric emptying disturbances in chronic and acute inflammation of the distal gastrointestinal tract. Am J Physiol Gastrointest Liver Physiol 2009;297:G861-8. Available at: http://www.ncbi.nlm.nih.gov/pubmed/20501434.

189. Keller J, Binnewies U, Rosch M, et al. Gastric emptying and disease activity in inflammatory bowel disease. Eur J Clin Invest 2015;45:1234–1242.

190. Jacobsen SH, Olesen SC, Dirksen C, et al. Changes in gastrointestinal hormone responses, insulin sensitivity, and beta-cell function within 2 weeks after gastric bypass in non-diabetic subjects. Obes Surg 2012;22:1084–1096.

191. Dirksen C, Jørgensen NB, Bojsen-Møller KN, et al. Gut hormones, early dumping and resting energy expenditure in patients with good and poor weight loss response after Roux-en-Y gastric bypass. Int J Obes 2013;37:1452–1459.

192. Scholtz S, Miras AD, Chhina N, et al. Obese patients after gastric bypass surgery have lower brain-hedonic responses to food than after gastric banding. Gut 2014;63:891–902. Available at: http://www.pubmedcentral.nih.gov/articlerender.fcgi?artid=4033279&tool=pmcentrez&rendertype=abstract%5Cnhttp://gut.bmj.com/content/early/2013/08/20/gutjnl-2013-305008.short.

193. Kulve JS Ten, Veltman DJ, Gerdes VEA, et al. Elevated postoperative endogenous GLP-1 levels mediate effects of roux-en-Y gastric bypass on neural responsivity to food cues. Diabetes Care 2017;40:1522–1529.

194. Zoon HFA, Bruijn SEM de, Smeets PAM, et al. Altered neural responsivity to food cues in relation to food preferences, but not appetite-related hormone concentrations after RYGB-surgery. Behav Brain Res 2018;353:194–202. Available at: https://doi.org/10.1016/j.bbr.2018.07.016.

195. McLaughlin J, Grazia Lucà M, Jones MN, et al. Fatty acid chain length determines cholecystokinin secretion and effect on human gastric motility. Gastroenterology 1999;116:46–53.

196. Lal S, McLaughlin J, Barlow J, et al. Cholecystokinin pathways modulate sensations induced by gastric distension in humans. Am J Physiol - Gastrointest Liver Physiol 2004;287:72–79.

197. Corp ES, McQuade J, Moran TH, et al. Characterization of type A and type B CCK receptor

binding sites in rat vagus nerve. Brain Res 1993;623:161–166.

198. Moriarty P, Dimaline R, Thompson DG, et al. Characterization of cholecystokinin(A) and cholecystokinin(B) receptors expressed by vagal afferent neurons. Neuroscience 1997;79:905–913.

199. Holzer HH, Turkelson CM, Solomon TE, et al. Intestinal lipid inhibits gastric emptying via CCK and a vagal capsaicin- sensitive afferent pathway in rats. Am J Physiol - Gastrointest Liver Physiol 1994;267.

200. Rehfeld JF. Accurate measurement of cholecystokinin in plasma. Clin Chem 1998;44:991–1001.

201. Alhussain MH, Macdonald IA, Taylor MA. Irregular meal-pattern effects on energy expenditure, metabolism, and appetite regulation: A randomized controlled trial in healthy normal-weight women. Am J Clin Nutr 2016;104:21–32.

202. Houghton LA, Lea R, Agrawal A, et al. Relationship of Abdominal Bloating to Distention in Irritable Bowel Syndrome and Effect of Bowel Habit. Gastroenterology 2006;131:1003–1010.

203. Khalaf A, Hoad CL, Menys A, et al. Gastrointestinal peptides and small-bowel hypomotility are possible causes for fasting and postprandial symptoms in active Crohn ' s disease. Am J Clin Nutr 2019;00:1–10.

204. Inuggi A, Sanz-Arigita E, González-Salinas C, et al. Brain functional connectivity changes in children that differ in impulsivity temperamental trait. Front Behav Neurosci 2014;8:1–14.

205. Hu S, Ide JS, Zhang S, et al. The right superior frontal gyrus and individual variation in proactive control of impulsive response. J Neurosci 2016;36:12688–12696.

206. Vogt BA. Inflammatory bowel disease : perspectives from cingulate cortex in the first brain. Neurogastroenterol Motil 2013:93–98.

207. Rubio A, Pellissier S, Oudenhove L Van, et al. Brain responses to uncertainty about upcoming rectal discomfort in quiescent Crohn's disease - a fMRI study. Neurogastroenterol Motil 2016. Available at: http://doi.wiley.com/10.1111/nmo.12844.

208. Agostini A, Ballotta D, Righi S, et al. Stress and brain functional changes in patients with Crohn's disease: A functional magnetic resonance imaging study. Neurogastroenterol Motil 2017:00:e13108.

209. Gray MA, Chao CY, Staudacher HM et al. Anti- TNFα therapy in IBD alters brain activity reflecting visceral sensory function and cognitive-affective biases. PLoS One 2013;13:1–17.

210. Ochner CN, Stice E, Hutchins E, et al. Relation between changes in neural responsivity and reductions in desire to eat high-calorie foods following gastric bypass surgery. Neuroscience 2012;209:128–135. Available at: http://dx.doi.org/10.1016/j.neuroscience.2012.02.030.

211. Satherley RM, Howard R, Higgs S. The prevalence and predictors of disordered eating in women with coeliac disease. Appetite 2016;107:260–267. Available at: http://dx.doi.org/10.1016/j.appet.2016.07.038.

212. Satherley R, Howard R, Higgs S. Disordered eating practices in gastrointestinal disorders. Appetite 2014;84:240–250. Available at: http://dx.doi.org/10.1016/j.appet.2014.10.006.

213. Prince A, Whelan K, Moosa A, et al. Nutritional problems in inflammatory bowel disease: The patient perspective. J Crohn's Colitis 2011;5:443–450. Available at: http://dx.doi.org/10.1016/j.crohns.2011.04.016.

214. Addolorato G, Capristo E, Stefanini GF, et al. Inflammatory Bowel Disease : A Study of the Association between Anxiety and Depression , Physical Morbidity , and Nutritional Status. Scand J Gastroenterol 1997:1013–21.

215. Navabi S, Gorrepati VS, Yadav S, et al. Influences and Impact of Anxiety and Depression in the Setting of Inflammatory Bowel Disease. Inflamm Bowel Dis 2018;24:2303–2308.

216. Fuller-Thomson E, Sulman J. Depression and inflammatory bowel disease: Findings from two nationally representative Canadian surveys. Inflamm Bowel Dis 2006;12:697–707.

217. Growdon JH, Wurtman RJ. Dietary Influences on the Synthesis of Neurotransmitters in the Brain. Nutr Rev 1979;37:129–136.

218. Mikocka-Walus A, Knowles SR, Keefer L, et al. Controversies Revisited: A Systematic Review

of the Comorbidity of Depression and Anxiety with Inflammatory Bowel Diseases. Inflamm Bowel Dis 2015;22:752–762.

219. Vidal de Lima FD, Rocha Ribeiro TC da, Andrade Chebli L, et al. Mood swings in patients with Crohn's disease: incidence and associated factors. Rev da Assoc Médica Bras (English Ed 2012;58:481–488. Available at: http://linkinghub.elsevier.com/retrieve/pii/S2255482312702333.

220. Anon. *National institute fro health and care excellence (NICE) briefing paper*. 2014. Available at: https://www.nice.org.uk/guidance/qs81/resources/inflammatory-bowel-disease-briefing-paper2.

221. Goodhand JR, Greig FIS, Koodun Y, et al. Do antidepressants influence the disease course in inflammatory bowel disease? A retrospective case-matched observational study. Inflamm Bowel Dis 2012;18:1232–1239.

222. Szigethy E, Bujoreanu SI, Youk AO, et al. Randomized efficacy trial of two psychotherapies for depression in youth with inflammatory bowel disease. J Am Acad Child Adolesc Psychiatry 2014;53:726–735.

223. Mikocka-Walus A, Bampton P, Hetzel D, et al. Cognitive-behavioural therapy has no effect on disease activity but improves quality of life in subgroups of patients with inflammatory bowel disease: A pilot randomised controlled trial. BMC Gastroenterol 2015;15:1–12.

224. Schoultz M, Atherton I, Watson A. Mindfulness-based cognitive therapy for inflammatory bowel disease patients: Findings from an exploratory pilot randomised controlled trial. Trials 2015;16:1–13.

225. Berrill JW, Sadlier M, Hood K, et al. Mindfulness-based therapy for inflammatory bowel disease patients with functional abdominal symptoms or high perceived stress levels. J Crohn's Colitis 2014;8:945–955. Available at: http://dx.doi.org/10.1016/j.crohns.2014.01.018.

226. Berthoud HR. Metabolic and hedonic drives in the neural control of appetite: Who is the boss? Curr Opin Neurobiol 2011;21:888–896. Available at: http://dx.doi.org/10.1016/j.conb.2011.09.004.

227. Karlsson J, Persson LO, Sjöström L, et al. Psychometric properties and factor structure of the Three-Factor Eating Questionnaire (TFEQ) in obese men and women. Results from the Swedish Obese Subjects (SOS) study. Int J Obes Relat Metab Disord 2000;24:1715–1725.

228. Gormally JIM, Black S, Daston S, et al. The Assessment of Binge Eating Severity Among Obese Persons. Addict Behav 1982;7:47–55.

229. Cappelleri JC, Bushmakin a G, Gerber R a, et al. Evaluating the Power of Food Scale in obese subjects and a general sample of individuals: development and measurement properties. Int J Obes (Lond) 2009;33:913–922. Available at: http://www.ncbi.nlm.nih.gov/pubmed/19506564.

230. Hill AJ, Weaver CF, Blundell JE. Food craving, dietary restraint and mood. Appetite 1991;17:187–197.

231. Dougherty DM, Mathias CW, Marsh DM, et al. Laboratory behavioral measures of impulsivity. Behav Res Methods 2005;37:82–90.

232. Finlayson G, King N, Blundell J. The role of implicit wanting in relation to explicit liking and wanting for food: implications for appetite control. Appetite 2008;50:120–7. Available at: http://www.ncbi.nlm.nih.gov/pubmed/17655972.

233. Stunkard a. J and MS. The Three-factor Eating Questionnaire to measure dietary restraint, disinhibition and hunger. J Psychomatic Res 1985;29:71–83.

234. Bryant EJ, King NA, Blundell JE. Disinhibition: Its effects on appetite and weight regulation. Obes Rev 2008;9:409–419.

235. Freitas SR, Lopes CS, Appolinario JC, et al. The assessment of binge eating disorder in obese women: A comparison of the binge eating scale with the structured clinical interview for the DSM-IV. Eat Behav 2006;7:282–289.

236. Dalton M, Finlayson G, Hill A, et al. Preliminary validation and principal components analysis of the Control of Eating Questionnaire (CoEQ) for the experience of food craving. Eur J Clin Nutr 2015;69:1313–1317. Available at: http://dx.doi.org/10.1038/ejcn.2015.57.

237. Finlayson G, Bryant E, Blundell JE, et al. Acute compensatory eating following exercise is

associated with implicit hedonic wanting for food. Physiol Behav 2009;97:62–67. Available at: http://dx.doi.org/10.1016/j.physbeh.2009.02.002.

238. Griffioen-Roose S, Finlayson G, Mars M, et al. Measuring food reward and the transfer effect of sensory specific satiety. Appetite 2010;55:648–655. Available at: http://dx.doi.org/10.1016/j.appet.2010.09.018.

239. Greenwald AG, Nosek BA, Banaji MR. Understanding and Using the Implicit Association Test: I. An Improved Scoring Algorithm. J Pers Soc Psychol 2003;85:197–216.

240. Rhodes DG, Clemens JC, Rumpler W V, et al. The US Department of Agriculture Automated Multiple-Pass Method reduces bias in the collection of energy intakes. Am J Clin Nutr 2018:324–332.

241. Drapeau V, Blundell J, Therrien F, et al. Appetite sensations as a marker of overall intake. Br J Nutr 2005;93:273–280.

242. Green SM, Delargy HJ, Joanes D, et al. A satiety quotient: a formulation to assess the satiating effect of food. Appetite 1997;29:291–304.

243. Srinath AI, Goyal A, Zimmerman LA, et al. Predictors of abdominal pain in depressed pediatric inflammatory bowel disease patients. Inflamm Bowel Dis 2014;20:1329–1340.

244. Taylor-Gjevre R, Gjevre JA, Skomro R, et al. Assessment of sleep health in patients with rheumatic disease. Int J Clin Rheumtol 2011;6:207–218.

245. Tyring S, Gottlieb A, Papp K, et al. Etanercept and clinical outcomes, fatigue, and depression in psoriasis: Double-blind placebo-controlled randomised phase III trial. Lancet 2006;367:29–35.

246. Koloski NA, Jones M, Talley NJ. Evidence that independent gut-to-brain and brain-to-gut pathways operate in the irritable bowel syndrome and functional dyspepsia: a 1-year population-based prospective study. Aliment Pharmacol Ther 2016;44:592–600.

247. Abautret-Daly Á, Dempsey E, Parra-Blanco A, et al. Gut-brain actions underlying comorbid anxiety and depression associated with inflammatory bowel disease. Acta Neuropsychiatr 2018;30:275–296.

248. Miller AH, Haroon E, Raison CL, et al. Cytokine targets in the brain: Impact on neurotransmitters and neurocircuits. Depress Anxiety 2013;30:297–306.

249. Wardle Richard, WardleAJ, C Charadava, Ghosh S MG. Literature review: impacts of socioeconomic status on the risk of inflammatory bowel disease and its outcomes. Eur J Gastroenterol Hepatol 2017;29:879–884.

250. Dalley JW, Everitt BJ, Robbins TW. Impulsivity, Compulsivity, and Top-Down Cognitive Control. Neuron 2011;69:680–694. Available at: http://dx.doi.org/10.1016/j.neuron.2011.01.020.

251. Evenden JL. Varieties of impulsivity. Psychopharmacology (Berl) 1999;146:348–361.

252. Kagan J. The generality and dynamics of conceptual tempo. J Abnorm Psychol 1966;71:17–24.

253. Barbera D La, Bonanno B, Rumeo M V., et al. Alexithymia and personality traits of patients with inflammatory bowel disease. Sci Rep 2017;7:1–11. Available at: http://dx.doi.org/10.1038/srep41786.

254. Sybil B, G. Eysenck HJE. Impulsiveness and venturesomeness: Their position in a dimensional system of personality. Psychol Rep 1978;43:1247–1255.

255. Hyphantis T, Antoniou K, Tomenson B, et al. Is the personality characteristic “impulsive sensation seeking” correlated to differences in current smoking between ulcerative colitis and Crohn’s disease patients? Gen Hosp Psychiatry 2010;32:57–65. Available at: http://dx.doi.org/10.1016/j.genhosppsych.2009.09.002.

256. Reuter M, Netter P. The influence of personality on nicotine craving: A hierarchical multivariate statistical prediction model. Neuropsychobiology 2001;44:47–53.

257. Berridge Kent, Robinson Terry AJW. Dissecting components of reward: “liking”, “wanting”, and learning. Curr Opin Pharmacol 2010;3:65–73.

258. Houben K. Overcoming the urge to splurge: Influencing eating behavior by manipulating inhibitory control. J Behav Ther Exp Psychiatry 2011;42:384–388. Available at: http://dx.doi.org/10.1016/j.jbtep.2011.02.008.

259. Murray S, Tulloch A, Gold MS, et al. Hormonal and neural mechanisms of food reward, eating behaviour and obesity. Nat Rev Endocrinol 2014;10:540–552. Available at: http://dx.doi.org/10.1038/nrendo.2014.91.

260. Berridge KC, Robinson TE, Aldridge JW. Dissecting components of reward: "liking", "wanting", and learning. Curr Opin Pharmacol 2009;9:65–73.

261. Finlayson G, King N, Blundell JE. Liking vs. wanting food: Importance for human appetite control and weight regulation. Neurosci Biobehav Rev 2007;31:987–1002.

262. Berridge KC. Measuring hedonic impact in animals and infants: Microstructure of affective taste reactivity patterns. Neurosci Biobehav Rev 2000;24:173–198.

263. Finlayson G, King N, Blundell JE. Is it possible to dissociate "liking" and "wanting" for foods in humans? A novel experimental procedure. Physiol Behav 2007;90:36–42.

264. Finlayson G, Arlotti A, Dalton M, et al. Implicit wanting and explicit liking are markers for trait binge eating. A susceptible phenotype for overeating. Appetite 2011;57:722–728. Available at: http://dx.doi.org/10.1016/j.appet.2011.08.012.

265. Dalton M, Hollingworth S, Blundell J, et al. Weak satiety responsiveness is a reliable trait associated with hedonic risk factors for overeating among women. Nutrients 2015;7:7421–7436.

266. Kober H, Barrett LF, Joseph J, et al. Functional grouping and cortical-subcortical interactions in emotion: A meta-analysis of neuroimaging studies. Neuroimage 2008;42:998–1031.

267. Moran Gordon WA. Paediatric Crohn's disease patients in remission have a reduced skeletal muscle protein balance after feeding. Gut 2018;67:3–4.

268. Filippi J, Al-Jaouni R, Wiroth J, et al. Nutritional deficiencies in patients with Crohn's disease in remission. Inflamm Bowel Dis 2006;12:185–91. Available at: http://www.ncbi.nlm.nih.gov/pubmed/16534419.

269. Aghdassi E, Wendland BE, Stapleton M, et al. Adequacy of Nutritional Intake in a Canadian Population of Patients with Crohn's Disease. J Am Diet Assoc 2007;107:1575–1580.

270. Blundell J, Graaf C De, Hulshof T, et al. Appetite control: Methodological aspects of the evaluation of foods. Obes Rev 2010;11:251–270.

271. Azevedo FAC, Carvalho LRB, Grinberg LT, et al. Equal numbers of neuronal and nonneuronal cells make the human brain an isometrically scaled-up primate brain. J Comp Neurol 2009;513:532–541.

272. Fischl B and DA. Measuring the thickness of the human cerebral cortex from magnetic resonance images. PNAS 2011;36:1–18. Available at: http://linkinghub.elsevier.com/retrieve/pii/S0165027008002458%5Cnhttp://dx.doi.org/10.1016/j.neuroimage.2012.03.026%5Cnhttp://www.pubmedcentral.nih.gov/articlerender.fcgi?artid=3793581&tool=pmcentrez&rendertype=abstract%5Cnhttp://linkinghub.elsevier.com/r.

273. Geschwind DH, Rakic P. Cortical evolution: Judge the brain by its cover. Neuron 2013;80:633–647. Available at: http://dx.doi.org/10.1016/j.neuron.2013.10.045.

274. Winkler AM, Kochunov P, Blangero J, et al. NeuroImage Cortical thickness or grey matter volume ? The importance of selecting the phenotype for imaging genetics studies. Neuroimage 2010;53:1135–1146. Available at: http://dx.doi.org/10.1016/j.neuroimage.2009.12.028.

275. Gouttard S, Wilber K, Gerig G, et al. A Structural MRI Study of Human Brain Development from Birth to 2 Years. J Neurosci 2008;28:12176–12182.

276. Groeschel S, Vollmer B, King MD, et al. Developmental changes in cerebral grey and white matter volume from infancy to adulthood. Int J Dev Neurosci 2010;28:481–489. Available at: http://dx.doi.org/10.1016/j.ijdevneu.2010.06.004.

277. Beheshti I, Maikusa N, Matsuda H. Effects of aging on brain volumes in healthy individuals across adulthood. Neurol Sci 2019;6:1191–1198. Available at: http://link.springer.com/10.1007/s10072-019-03817-3.

278. Matsuzawa J, Matsui M, Konishi T. Age-related Volumetric Changes of Brain Gray and White Matter in Healthy Infants and Children. Cereb Cortex 2001;11:335–342.

279. Herting MM, Dahl RE, Crone EA, et al. Structural brain development between childhood and adulthood: Convergence across four longitudinal samples. Neuroimage 2016;141:273–281.

280. Castro-Fornieles J, Bargalló N, Lázaro L, et al. A cross-sectional and follow-up voxel-based morphometric MRI study in adolescent anorexia nervosa. J Psychiatr Res 2009;43:331–340.

281. Prado EL, Dewey KG. Nutrition and brain development in early life. Nutr Rev 2014;72:267–284.

282. Lu S, Xu R, Cao J, et al. The left dorsolateral prefrontal cortex volume is reduced in adults reporting childhood trauma independent of depression diagnosis. J Psychiatr Res 2019;112:12–17. Available at: https://linkinghub.elsevier.com/retrieve/pii/S002239561831450X.

283. Nosarti C, Allin MPG, Cuddy M, et al. Preterm birth and structural brain alterations in early adulthood. NeuroImage Clin 2014;6:180–191. Available at: http://dx.doi.org/10.1016/j.nicl.2014.08.005.

284. Tolsa CB, Zimine S, Warfield SK, et al. Early alteration of structural and functional brain development in premature infants born with intrauterine growth restriction. Pediatr Res 2004;56:132–138.

285. Good CD, Johnsrude IS, Ashburner J, et al. A voxel-based morphometric study of ageing in 465 normal adult human brains. Neuroimage 2001;14:21–36.

286. Hakonarson H, Ruparel K, Satterthwaite TD, et al. Age-Related Effects and Sex Differences in Gray Matter Density, Volume, Mass, and Cortical Thickness from Childhood to Young Adulthood. J Neurosci 2017;37:5065–5073.

287. Schaufelberger MS, Busatto GF, Curiati PK, et al. Age-related gray matter volume changes in the brain during non-elderly adulthood. Neurobiol Aging 2009;32:354–368.

288. Raz N, Erickson KI, Voss MW, et al. Age-related differences in regional brain volumes: A comparison of optimized voxel-based morphometry to manual volumetry. Neurobiol Aging 2008;30:1657–1676.

289. Matsuda H. Voxel-based Morphometry of Brain MRI in Normal aging and Alzheimer's Disease. 2013;4:29–37.

290. Li G, Wang L, Shi F, et al. Dynamic Development of Regional Cortical Thickness and Surface Area in Early Childhood. Cereb Cortex 2014;25:2204–2212.

291. Nie J, Wang L, Lin W, et al. Longitudinal development of cortical thickness, folding, and fiber density networks in the first 2 years of life. Hum Brain Mapp 2013;35:3726–3737.

292. Remer J, Croteau-Chonka E, Dean DC, et al. Quantifying cortical development in typically developing toddlers and young children, 1–6 years of age. Neuroimage 2017;153:246–261. Available at: http://dx.doi.org/10.1016/j.neuroimage.2017.04.010.

293. Zhou D, Lebel C, Evans A, et al. Cortical thickness asymmetry from childhood to older adulthood. Neuroimage 2013;83:66–74. Available at: http://dx.doi.org/10.1016/j.neuroimage.2013.06.073.

294. Giedd JN, Raznahan A, Mills KL, et al. Review: Magnetic resonance imaging of male/female differences in human adolescent brain anatomy. Biol Sex Differ 2012;3:1–9.

295. Giorgio A, Watkins KE, Chadwick M, et al. Longitudinal changes in grey and white matter during adolescence. Neuroimage 2010;49:94–103. Available at: http://dx.doi.org/10.1016/j.neuroimage.2009.08.003.

296. Liu H, Wang L, Geng Z, et al. A voxel-based morphometric study of age- and sex-related changes in white matter volume in the normal aging brain. Neuropsychiatr Dis Treat 2016;12:453–465.

297. Giorgio A, Santelli L, Tomassini V, et al. Age-related changes in grey and white matter structure throughout adulthood. Neuroimage 2010;51:943–951. Available at: http://dx.doi.org/10.1016/j.neuroimage.2010.03.004.

298. Smith CD, Chebrolu H, Wekstein DR, et al. Age and gender effects on human brain anatomy: A voxel-based morphometric study in healthy elderly. Neurobiol Aging 2007;28:1075–1087.

299. Lueders E, Neumann N, Lotze M, et al. Novel findings from 2,838 Adult Brains on Sex Differences in Gray Matter Brain Volume. Sci Rep 2019;9:1–7. Available at: http://dx.doi.org/10.1038/s41598-018-38239-2.

300. Ruigrok ANV, Salimi-Khorshidi G, Lai MC, et al. A meta-analysis of sex differences in human

brain structure. Neurosci Biobehav Rev 2014;39:34–50. Available at: http://dx.doi.org/10.1016/j.neubiorev.2013.12.004.

301. Bellis MD De. Sex Differences in Brain Maturation during Childhood and Adolescence. Cereb Cortex 2001;11:552–557. Available at: https://academic.oup.com/cercor/article-lookup/doi/10.1093/cercor/11.6.552.

302. Shiino A, Chen YW, Tanigaki K, et al. Sex-related difference in human white matter volumes studied: Inspection of the corpus callosum and other white matter by VBM. Sci Rep 2017;7:3–9.

303. Ritchie SJ, Cox SR, Shen X, et al. Sex differences in the adult human brain: Evidence from 5216 UK biobank participants. Cereb Cortex 2018;28:2959–2975.

304. Mechelli A, Price C, Friston K, et al. Voxel-Based Morphometry of the Human Brain: Methods and Applications. Curr Med Imaging Rev 2005;1:105–113.

305. Ashburner J, Friston KJ. Voxel-based morphometry - The methods. Neuroimage 2000;11:805–821.

306. Greve DN. An Absolute Beginner's Guide to Surface and Voxel - Based Morphometric Analysis. Proc Intl Soc Mag Reson Med 19 2011.

307. Mazziotta John, Toga Arthur, Evans Alan LJ. A Probabilistic Atlas of the Human Brain: Theory and Rationale for Its Development. Neuroimage 1995;2:89–101.

308. Maintz Antoine VM. A survey of medical image registration. Meical Image Anal 1998;2:1–36.

309. Chau W, McIntosh AR. The Talairach coordinate of a point in the MNI space: How to interpret it. Neuroimage 2005;25:408–416.

310. Mechelli A, Price CJ, Friston KJ, et al. Voxel-based morphometry of the human brain: methods and applications. Curr Med Imaging Rev 2005;1:105–113.

311. Whitwell JL. Voxel-Based Morphometry: An Automated Technique for Assessing Structural Changes in the Brain. J Neurosci 2009;29:9661–9664.

312. Ridgway GR, Henley SMD, Rohrer JD, et al. Ten simple rules for reporting voxel-based morphometry studies. Neuroimage 2008;40:1429–1435.

313. Friisoni G B, Testa C, Zorzan A, Sabattoli F, Beltramello, Soininen H LMP. Detection of grey matter loss in mild Alzheimer's disease with voxel based morphometry. J Neurol Neurosurg Psychiatry 2002;73:657–664.

314. Minkova L, Gregory S, Scahill RI, et al. Cross-sectional and longitudinal voxel-based grey matter asymmetries in Huntington's disease. NeuroImage Clin 2018;17:312–324.

315. Wenger E, Brozzoli C, Lindenberger U, et al. Expansion and Renormalization of Human Brain Structure During Skill Acquisition. Trends Cogn Sci 2017;21:930–939. Available at: http://dx.doi.org/10.1016/j.tics.2017.09.008.

316. Draganski B, Christian G, Volker B, et al. Changes in grey matter induced by training. Nature 2004;427:312–312. Available at: https://www.nature.com/nature/journal/v427/n6972/pdf/427311a.pdf.

317. Lövdén M, Schaefer S, Noack H, et al. Spatial navigation training protects the hippocampus against age-related changes during early and late adulthood. Neurobiol Aging 2012;33:620.e9-620.e22. Available at: http://dx.doi.org/10.1016/j.neurobiolaging.2011.02.013.

318. Mårtensson J, Eriksson J, Bodammer NC, et al. Growth of language-related brain areas after foreign language learning. Neuroimage 2012;63:240–244. Available at: http://dx.doi.org/10.1016/j.neuroimage.2012.06.043.

319. Teixeira-Machado L, Arida RM, Jesus Mari J de. Dance for neuroplasticity: A descriptive systematic review. Neurosci Biobehav Rev 2019;96:232–240.

320. Foster NE V, Zatorre RJ. Cortical structure predicts success in performing musical transformation judgments. Neuroimage 2010;53:26–36. Available at: http://dx.doi.org/10.1016/j.neuroimage.2010.06.042.

321. Horstmann A, Draganski B, Ragert P, et al. Dynamic Properties of Human Brain Structure: Learning-Related Changes in Cortical Areas and Associated Fiber Connections. J Neurosci 2010;30:11670–11677.

322. Takeuchi H, Taki Y, Sassa Y, et al. Working memory training using mental calculation impacts regional gray matter of the frontal and parietal regions. PLoS One 2011;6:1–10.

323. Fischl B, Salat DH, Busa E, et al. Whole brain segmentation: Automated labeling of neuroanatomical structures in the human brain. Neuron 2002;33:341–355.

324. Fischl B, Salat DH, Kouwe AJW Van Der, et al. Sequence-independent segmentation of magnetic resonance images. Neuroimage 2004;23:69–84.

325. Sled JG, Zijdenbos AP, Evans AC. A nonparametric method for automatic correction of intensity nonuniformity in MRI data. IEEE Trans Med Imaging 2002;17:87–97.

326. Espinosa A, Serrano J. A, Montori A. Automated Manifold Surgery: Constructing Geometrically Accurate and Topologically Correct Models of the Human Cerebral Cortex. IEEE Trans Med Imaging 2001;20:70–80. Available at: https://surfer.nmr.mgh.harvard.edu/docs/ftp/pub/articles/fischl01-topology-fixing.pdf.

327. Dale AM, Fischl B, Sereno MI. Cortical surface-based analysis: I. Segmentation and surface reconstruction. Neuroimage 1999;9:179–194.

328. Dahnke R, Yotter RA, Gaser C. Cortical thickness and central surface estimation. Neuroimage 2013;65:336–348. Available at: http://dx.doi.org/10.1016/j.neuroimage.2012.09.050.

329. Yotter RA, Nenadic I, Ziegler G, et al. Local cortical surface complexity maps from spherical harmonic reconstructions. Neuroimage 2011;56:961–973. Available at: http://dx.doi.org/10.1016/j.neuroimage.2011.02.007.

330. Yotter RA, Thompson PM, Gaser C. Algorithms to Improve the Reparameterization of Spherical Mappings of Brain Surface Meshes. J Neuroimaging 2011;21:1–14.

331. Ashburner J. A fast diffeomorphic image registration algorithm. Neuroimage 2007;38:95–113.

332. Rosas HD, Liu AK, Hersch S, et al. Regional and progressive thinning of the cortical ribbon in Huntington's disease. Neurology 2002;05886:695–702.

333. Kuperberg, G.R., Broome, M.R., McGuire, P.K., David, A.S., Eddy, M., Ozawa, F., Goff, D., West, W.C., Williams, S.C., van der Kouwe, A.J., Salat, D.H., Dale, A.M., Fischl B. Regionally localized thinning of the cerebral cortex in schizophrenia. Arch Gen Psychiatry 2003;60:878–888.

334. Han X, Jovicich J, Salat D, et al. Reliability of MRI-derived measurements of human cerebral cortical thickness: The effects of field strength, scanner upgrade and manufacturer. Neuroimage 2006;32:180–194.

335. Reuter M, Schmansky NJ, Rosas HD, et al. Within-Subject Template Estimation for Unbiased Robust and Sensitive Longitudinal Image Analysis. Neuroimage 2012;61:1402–1418.

336. Seiger R, Ganger S, Kranz GS, et al. Cortical Thickness Estimations of FreeSurfer and the CAT12 Toolbox in Patients with Alzheimer's Disease and Healthy Controls. J Neuroimaging 2018;28:515–523.

337. Righart R, Schmidt P, Dahnke R, et al. Volume versus surface-based cortical thickness measurements: A comparative study with healthy controls and multiple sclerosis patients. PLoS One 2017;12:1–10.

338. Sowell ER, Peterson BS, Thompson PM, et al. Mapping cortical change across the human life span. Nat Neurosci 2003;6:309–315.

339. Nair VA, Beniwal-Patel P, Mbah I, et al. Structural imaging changes and behavioral correlates in patients with Crohn's disease in remission. Front Hum Neurosci 2016;10:1–11. Available at: http://www.embase.com/search/results?subaction=viewrecord&from=export&id=L612269284%5Cnhttp://dx.doi.org/10.3389/fnhum.2016.00460.

340. Ito U, Kuroiwa T, Nagasao J, et al. Temporal Profiles of Axon Terminals, Synapses and Spines in the Ischemic Penumbra of the Cerebral Cortex. Stroke 2006;37:2134–2139.

341. May A. Chronic pain may change the structure of the brain. Pain 2008;137:7–15.

342. Hubbard CS, Becerra L, Heinz N, et al. Abdominal pain, the adolescent and altered brain structure and function. PLoS One 2016;11:1–30.

343. Erpelding N, Moayedi M, Davis KD. Cortical thickness correlates of pain and temperature

sensitivity. Pain 2012;153:1602–1609. Available at: http://dx.doi.org/10.1016/j.pain.2012.03.012.

344. Piché M, Chen JI, Roy M, et al. Thicker posterior insula is associated with disease duration in women with irritable bowel syndrome (IBS) whereas thicker orbitofrontal cortex predicts reduced pain inhibition in both IBS patients and controls. J Pain 2013;14:1217–1226.

345. Zatorre RJ, Fields RD, Johansen-Berg H. Plasticity in gray and white: Neuroimaging changes in brain structure during learning. Nat Neurosci 2012;15:528–536. Available at: http://dx.doi.org/10.1038/nn.3045.

346. Jones MP, Dilley JB, Drossman D, et al. Brain-gut connections in functional GI disorders: Anatomic and physiologic relationships. Neurogastroenterol Motil 2006;18:91–103.

347. Dantzer R, O'Connor JC, Freund GG, et al. From inflammation to sickness and depression: When the immune system subjugates the brain. Nat Rev Neurosci 2008;9:46–56.

348. Foster JA, Rinaman L, Cryan JF. Stress & the gut-brain axis: Regulation by the microbiome. Neurobiol Stress 2017;7:124–136. Available at: https://doi.org/10.1016/j.ynstr.2017.03.001.

349. Bao C, Liu P, Shi Y, et al. Differences in brain gray matter volume in patients with Crohn's disease with and without abdominal pain. Oncotarget 2017;8:93624–93632. Available at: http://www.oncotarget.com/fulltext/21161.

350. Erp S van, Ercan E, Breedveld P, et al. Cerebral magnetic resonance imaging in quiescent Crohn's disease patients with fatigue. World J Gastroenterol 2017;23:1018–1029. Available at: http://www.wjgnet.com/1007-9327/full/v23/i6/1018.htm.

351. Thomann AK, Thomann PA, Wolf RC, et al. Altered markers of brain development in Crohn's disease with extraintestinal manifestations - A pilot study. PLoS One 2016;11:1–14.

352. Bao CH, Liu P, Liu HR, et al. Alterations in brain gray matter structures in patients with Crohn's disease and their correlation with psychological distress. J Crohns Colitis 2015;9:532–540. Available at: http://www.ncbi.nlm.nih.gov/pubmed/25895879.

353. Agostini A, Campieri M, Bertani A, et al. Absence of change in the gray matter volume of patients with ulcerative colitis in remission: a voxel based morphometry study. Biopsychosoc Med 2015;9:1–4. Available at: http://www.pubmedcentral.nih.gov/articlerender.fcgi?artid=4302580&tool=pmcentrez&rendertype=abstract.

354. Zikou AK, Kosmidou M, Astrakas LG, et al. Brain involvement in patients with inflammatory bowel disease: a voxel-based morphometry and diffusion tensor imaging study. Eur Radiol 2014:2499–2506.

355. Agostini A, Benuzzi F, Filippini N, et al. New insights into the brain involvement in patients with Crohn's disease: a voxel-based morphometry study. Neurogastroenterol Motil 2013;25:147–153. Available at: http://doi.wiley.com/10.1111/nmo.12017.

356. Schaer M, Bach Cuadra M, Tamarit L, et al. A Surface-based approach to quantify local cortical gyrification. IEEE Trans Med Imaging 2008;27:161–170.

357. Mrakotsky C, Anand R, Watson C, Vu C, Matos A, Friel S, Rivkin M SS. New Evidence for Structural Brain Differences in Pediatric Crohn's Disease: Impact of Underlying Disease Factors. Inflamm Bowel Dis 2016:S6-7.

358. Bao CH, Liu P, Liu HR, et al. Alterations in brain grey matter structures in patients with Crohn's disease and their correlation with psychological distress. J Crohn's Colitis 2015;9:532–540.

359. Zikou AK, Kosmidou M, Astrakas LG, et al. Brain involvement in patients with inflammatory bowel disease: a voxel-based morphometry and diffusion tensor imaging study. Eur Radiol 2014:2499–2506.

360. Agostini A, Filippini N, Benuzzi F, et al. Functional magnetic resonance imaging study reveals differences in the habituation to psychological stress in patients with Crohn's disease versus healthy controls. J Behav Med 2013;36:477–487.

361. Bao CH, Liu P, Liu HR, et al. Alterations in brain grey matter structures in patients with Crohn's disease and their correlation with psychological distress. J Crohn's Colitis 2015;9:532–540.

362. Zigmond AS, Snaith RP. The Hospital Anxiety and Depression Scale. Traduction française : J.F.

Lépine. Acta Psychiatr Scand 1983;67:361–370.

363. Nair V, Prabhakaran V, Beniwal-Patel P, et al. Sa1886 Altered Brain Functional Activation and Connectivity Patterns in Patients With Crohn's Disease in Remission. Gastroenterology 2016;150:S392. Available at: http://dx.doi.org/10.1016/S0016-5085(16)31375-0.

364. Best WR. Predicting the Crohn's disease activity index from the Harvey-Bradshaw Index. Inflamm Bowel Dis 2006;12:304–310.

365. Cameron JD, Cyr M-J, Doucet E. Increased meal frequency does not promote greater weight loss in subjects who were prescribed an 8-week equi-energetic energy-restricted diet. Br J Nutr 2010;103:1098–101. Available at: http://journals.cambridge.org/abstract_S0007114509992984.

366. Bang L, Rø Ø, Endestad T. Normal gray matter volumes in women recovered from anorexia nervosa: A voxel-based morphometry study. BMC Psychiatry 2016;16:1–7. Available at: http://dx.doi.org/10.1186/s12888-016-0856-z.

367. Salimi-Khorshidi G, Smith SM, Nichols TE. Adjusting the effect of nonstationarity in cluster-based and TFCE inference. Neuroimage 2011;54:2006–2019. Available at: http://dx.doi.org/10.1016/j.neuroimage.2010.09.088.

368. Eklund A, Nichols TE, Knutsson H. Cluster failure: Why fMRI inferences for spatial extent have inflated false-positive rates. Proc Natl Acad Sci U S A 2016;113:7900–5. Available at: http://www.ncbi.nlm.nih.gov/pubmed/27357684%0Ahttp://www.pubmedcentral.nih.gov/articlerender.fcgi?artid=PMC4948312.

369. Smith SM, Nichols TE. Threshold-free cluster enhancement: addressing problems of smoothing, threshold dependence and localisation in cluster inference. Neuroimage 2009;44:83–98. Available at: http://www.ncbi.nlm.nih.gov/pubmed/18501637.

370. Ségonne F, Dale AM, Busa E, et al. A hybrid approach to the skull stripping problem in MRI. Neuroimage 2004;22:1060–1075.

371. Desikan RS, Ségonne F, Fischl B, et al. An automated labeling system for subdividing the human cerebral cortex on MRI scans into gyral based regions of interest. Neuroimage 2006;31:968–980.

372. Destrieux C, Fischl B, Dale A, et al. Automatic parcellation of human cortical gyri and sulci using standard anatomical nomenclature. Neuroimage 2010;53:1–15. Available at: http://dx.doi.org/10.1016/j.neuroimage.2010.06.010.

373. Fischl B, Kouwe A Van Der, Destrieux C, et al. Automatically Parcellating the Human Cerebral Cortex. Cereb Cortex 2004;14:11–22.

374. Cox NJ. Speaking Stata: Correlation with confidence, or Fisher's z revisited. Stata J 2008;8:413–439.

375. Itabashi R, Nishio Y, Kataoka Y, et al. Damage to the left precentral gyrus is associated with apraxia of speech in acute stroke. Stroke 2016;47:31–36.

376. Lamp G, Goodin P, Palmer S, et al. Activation of bilateral secondary somatosensory cortex with right hand touch stimulation: A meta-analysis of functional neuroimaging studies. Front Neurol 2019;10:1–14.

377. Mansouri FA, Buckley MJ, Mahboubi M, et al. Behavioral consequences of selective damage to frontal pole and posterior cingulate cortices. Proc Natl Acad Sci 2015;112:E3940–E3949.

378. Metzler-Baddeley C, Caeyenberghs K, Foley S, et al. Task complexity and location specific changes of cortical thickness in executive and salience networks after working memory training. Neuroimage 2016;130:48–62. Available at: http://dx.doi.org/10.1016/j.neuroimage.2016.01.007.

379. Warrier C, Wong P, Penhune V, et al. Relating structure to function: Heschl's gyrus and acoustic processing. J Neurosci 2009;29:61–69.

380. Beauchamp MS. The social mysteries of the superior temporal sulcus. Trends Cogn Sci 2015;19:489–490. Available at: http://dx.doi.org/10.1016/j.tics.2015.07.002.

381. Schaefer PW, Grant PE, Gonzalez RG. Diffusion MRbrain State of the Art. Radiology 2000:331–345.

382. Clark KA, Nuechterlein KH, Asarnow RF, et al. Mean diffusivity and fractional anisotropy as indicators of disease and genetic liability to schizophrenia. J Psychiatr Res 2011;45:980–988.

Available at: http://dx.doi.org/10.1016/j.jpsychires.2011.01.006.

383. Hou J, Dodd K, Nair VA, et al. Alterations in brain white matter microstructural properties in patients with Crohn ' s disease in remission.

384. Dolapcioglu C, Dolapcioglu H. Structural brain lesions in inflammatory bowel disease. World J Gastrointest Pathophysiol 2015;6:124–130.

385. Ananthakrishnan AN, Khalili H, Pan A, et al. Association Between Depressive Symptoms and Incidence of Crohn's Disease and Ulcerative Colitis: Results From the Nurses' Health Study. Clin Gastroenterol Hepatol 2013;11:57–62. Available at: http://dx.doi.org/10.1016/j.cgh.2012.08.032.

386. Kurina LM, Goldacre MJ, Yeates D, et al. Depression and anxiety in people with inflammatory bowel disease. J Epidemiol Community Health 2001;55:716–720.

387. Rolston JD, Englot DJ, Benet A, et al. Frontal operculum gliomas: language outcome following resection. J Neurosurg 2015;122:725–734.

388. Perlman SB, Hudac CM, Pegors T, et al. Experimental manipulation of face-evoked activity in the fusiform gyrus of individuals with autism. Soc Neurosci 2011;6:22–30.

389. Cheng W, Rolls ET, Qiu J, et al. Medial reward and lateral non-reward orbitofrontal cortex circuits change in opposite directions in depression. Brain 2016;139:3296–3309.

390. Pomares FB, Funck T, Feier NA, et al. Histological Underpinnings of Grey Matter Changes in Fibromyalgia Investigated Using Multimodal Brain Imaging. J Neurosci 2017;37:1090–1101.

391. Riederer F, Landmann G, Gantenbein AR, et al. Nondermatomal somatosensory deficits in chronic pain are associated with cerebral grey matter changes. World J Biol Psychiatry 2017;18:227–238.

392. Torta DME, Vercelli U, Cauda F, et al. Gray matter alterations in chronic pain: A network-oriented meta-analytic approach. NeuroImage Clin 2014;4:676–686. Available at: http://dx.doi.org/10.1016/j.nicl.2014.04.007.

393. Smallwood RF, Laird AR, Ramage AE, et al. Structural brain anomalies and chronic pain: A quantitative meta-analysis of gray matter volume. J Pain 2013;14:663–675. Available at: http://dx.doi.org/10.1016/j.jpain.2013.03.001.

394. Mashal N, Vishne T, Laor N. The role of the precuneus in metaphor comprehension: evidence from an fMRI study in people with schizophrenia and healthy participants. Front Hum Neurosci 2014;8:1–11.

395. Utevsky A V., Smith D V., Huettel SA. Precuneus Is a Functional Core of the Default-Mode Network. J Neurosci 2014;34:932–940.

396. Thomann AK, Griebe M, Thomann PA, et al. Intrinsic neural network dysfunction in quiescent Crohn's Disease. Sci Rep 2017;7:1–10. Available at: http://dx.doi.org/10.1038/s41598-017-11792-y.

397. Hartwigsen G, Baumgaertner A, Price CJ, et al. Phonological decisions require both the left and right supramarginal gyri. Proc Natl Acad Sci U S A 2010;107:16494–16499.

398. Vavricka SR, Schoepfer A, Scharl M, et al. Extraintestinal manifestations of inflammatory bowel disease. Inflamm Bowel Dis 2015;21:1982–1992.

399. Graff LA, Clara I, Walker JR, et al. Changes in Fatigue Over 2 Years Are Associated With Activity of Inflammatory Bowel Disease and Psychological Factors. Clin Gastroenterol Hepatol 2013;11:1140–1146. Available at: http://dx.doi.org/10.1016/j.cgh.2013.03.031.

400. Okada T, Tanaka M, Kuratsune H, et al. Mechanisms underlying fatigue: A voxel-based morphometric study of chronic fatigue syndrome. BMC Neurol 2004;4:1–6.

401. Puri BK, Jakeman PM, Agour M, et al. Regional grey and white matter volumetric changes in myalgic encephalomyelitis (chronic fatigue syndrome): A voxel-based morphometry 3 T MRI study. Br J Radiol 2012;85.

402. Finkelmeyer A, He J, Maclachlan L, et al. Grey and white matter differences in Chronic Fatigue Syndrome – A voxel-based morphometry study. NeuroImage Clin 2018;17:24–30. Available at: https://doi.org/10.1016/j.nicl.2017.09.024.

403. Yang YL, Deng HX, Xing GY, et al. Brain functional network connectivity based on a visual task: Visual information processing-related brain regions are significantly activated in the task state. Neural Regen Res 2015;10:298–307.

404. Zeineh MM, Kang J, Atlas SW, et al. Right arcuate fasciculus abnormality in chronic fatigue syndrome. Radiology 2015;274:517–526.

405. Grabenhorst F, Rolls ET. The representation of oral fat texture in the human somatosensory cortex. Hum Brain Mapp 2014;35:2521–2530.

406. Rosenbaum M, Sy M, Pavlovich K, et al. Leptin reverses weight loss-induced changes in regional neural activity responses to visual food stimuli. J Clin Invest 2008;118:2583–2591.

407. Kiortsis DN, Spyridonos P, Margariti PN, et al. Brain activation during repeated imagining of chocolate consumption: a functional magnetic resonance imaging study. Hormones 2018;17:367–371.

408. Weise CM, Thiyyagura P, Reiman EM, et al. Postprandial plasma PYY concentrations are associated with increased regional gray matter volume and rCBF declines in caudate nuclei - A combined MRI and H 215O PET study. Neuroimage 2012;60:592–600. Available at: http://dx.doi.org/10.1016/j.neuroimage.2011.12.023.

409. Smitha KA, Akhil Raja K, Arun KM, et al. Resting state fMRI: A review on methods in resting state connectivity analysis and resting state networks. Neuroradiol J 2017;30:305–317.

410. Gong G, He Y, Concha L, et al. Mapping anatomical connectivity patterns of human cerebral cortex using in vivo diffusion tensor imaging tractography. Cereb Cortex 2009;19:524–536.

411. Friston KJ. Functional and Effective Connectivity: A Review. Brain Connect 2011;1:13–36.

412. Park HJ, Friston K. Structural and functional brain networks: From connections to cognition. Science (80-) 2013;342:1238411-1–6.

413. SOKOLOFF L, MANGOLD R, WECHSLER RL, et al. The effect of mental arithmetic on cerebral circulation and metabolism. J Clin Invest 1955;34:1101–1108.

414. Shulman RG, Hyder F, Rothman DL. Insights from neuroenergetics into the interpretation of functional neuroimaging: An alternative empirical model for studying the brain's support of behavior. J Cereb Blood Flow Metab 2014;34:1721–1735.

415. Sanganahalli BG, Herman P, Blumenfeld H, et al. Oxidative Neuroenergetics in Event-Related Paradigms. J Neurosci 2009;29:1707–1718.

416. Engl E, Attwell D. Non-signalling energy use in the brain. J Physiol 2015;593:3417–3429.

417. Yu Y, Herman P, Rothman DL, et al. Evaluating the gray and white matter energy budgets of human brain function. J Cereb Blood Flow Metab 2018;38:1339–1353.

418. Raichle ME. Two views of brain function. Trends Cogn Sci 2010;14:180–190. Available at: http://dx.doi.org/10.1016/j.tics.2010.01.008.

419. Biswal B, Yetkin FZ HV. Functional Connectivity in the Motor Cortex of Resting Human Brain Using Echo-Planar MRI. Magn Reson Med 1995;34:537–41.

420. Biswal BB, Kylen J Van, Hyde JS. Simultaneous assessment of flow and BOLD signals in resting-state functional connectivity maps. NMR Biomed 1997;10:165–170.

421. Tomasi D, Volkow ND. Resting functional connectivity of language networks: Characterization and reproducibility. Mol Psychiatry 2012;17:841–854. Available at: http://dx.doi.org/10.1038/mp.2011.177.

422. Michael D. Fox, Corbetta M, Snyder AZ, et al. Spontaneous neuronal activity distinguishes human. Proc Natl Acad Sci 2006;103:9381–9386.

423. Greicius MD, Krasnow B, Reiss AL, et al. Functional connectivity in the resting brain: a network analysis of the default mode hypothesis. Proc Natl Acad Sci U S A 2003;100:253–8.

424. Rytty R, Nikkinen J, Paavola L, et al. GroupICA dual regression analysis of resting state networks in a behavioral variant of frontotemporal dementia. Front Hum Neurosci 2013;7:1–10.

425. Laird, P. Mickle Fox, Simon B. Eickhoff, Jessica A. Turner, Kimberly L. Ray, D. Reese McKay, David C. Glahn, Christian F. Beckmann, Stephen M. Smith and PTF. Behavioral Interpretations

of Intrinsic Connectivity Networks. J Cogntive Neurosci 2011;12:4022–4037. Available at: file:///Users/cpt3270/Documents/Library.papers3/Articles/2013/Unknown/2013-5.pdf%5Cnpapers3://publication/uuid/34445F0C-8ECF-437F-BA5A-2C8CDBE7481E.

426. Corbetta M, Patel G, Shulman GL. The Reorienting System of the Human Brain: From Environment to Theory of Mind. Neuron 2008;58:306–324.

427. Heine L, Soddu A, Gómez F, et al. Resting state networks and consciousness Alterations of multiple resting state network connectivity in physiological, pharmacological, and pathological consciousness states. Front Psychol 2012;3:1–12.

428. Rosazza C, Minati L. Resting-state brain networks: Literature review and clinical applications. Neurol Sci 2011;32:773–785.

429. McKiernan KA, D'Angelo BR, Kaufman JN, et al. Interrupting the "stream of consciousness": An fMRI investigation. Neuroimage 2006;29:1185–1191.

430. Seeley WW, Menon V, Schatzberg AF, et al. Dissociable Intrinsic Connectivity Networks for Salience Processing and Executive Control. J Neurosci 2007;27:2349–2356. Available at: http://www.jneurosci.org/cgi/doi/10.1523/JNEUROSCI.5587-06.2007.

431. Yan. DPARSF: a MATLAB toolbox for "pipeline" data analysis of resting-state fMRI. Front Syst Neurosci 2010;4:1–7. Available at: http://journal.frontiersin.org/article/10.3389/fnsys.2010.00013/abstract.

432. Zang Y, Jiang T, Lu Y, et al. Regional homogeneity approach to fMRI data analysis. Neuroimage 2004;22:394–400.

433. Heuvel MP van den, Stam CJ, Boersma M, et al. Small-world and scale-free organization of voxel-based resting-state functional connectivity in the human brain. Neuroimage 2008;43:528–539. Available at: http://dx.doi.org/10.1016/j.neuroimage.2008.08.010.

434. Heuvel MP van den, Hulshoff Pol HE. Exploring the brain network: A review on resting-state fMRI functional connectivity. Eur Neuropsychopharmacol 2010;20:519–534. Available at: http://dx.doi.org/10.1016/j.euroneuro.2010.03.008.

435. Mckeown MJ, Makeig S, Brown GG, et al. Analysis of fMRI Data by Blind Separation Into Independent Spatial Components. Hum Brain Mapp 1998;6:160–188.

436. Beckmann CF. Modelling with independent components. Neuroimage 2012;62:891–901. Available at: http://dx.doi.org/10.1016/j.neuroimage.2012.02.020.

437. Matthews PM, Jezzard P. Functional Magnetic Resonance Imaging Analyses. Neurosci Neurol 2004;75:6–12.

438. Nickerson LD, Smith SM, Öngür D, et al. Using dual regression to investigate network shape and amplitude in functional connectivity analyses. Front Neurosci 2017;11:1–18.

439. Griffanti L, Douaud G, Bijsterbosch J, et al. Hand classification of fMRI ICA noise components. Neuroimage 2017;154:188–205.

440. Zhan X, Yu R. A Window into the Brain: Advances in Psychiatric fMRI. Biomed Res Int 2015;2015:1–12.

441. Geerligs L, Renken RJ, Saliasi E, et al. A Brain-Wide Study of Age-Related Changes in Functional Connectivity. Cereb Cortex 2015;25:1987–1999.

442. Tomasi D, Volkow ND. Gender differences in brain functional connectivity density. Hum Brain Mapp 2012;33:849–860.

443. Sala-Llonch R, BartrÃ©s-Faz D, JunquÃ© C. Reorganization of brain networks in aging: a review of functional connectivity studies. Front Psychol 2015;6:1–11.

444. Andrews-Hanna JR, Snyder AZ, Vincent JL, et al. Disruption of Large-Scale Brain Systems in Advanced Aging. Neuron 2007;56:924–935.

445. He H, Luo C, Chang X, et al. The functional integration in the sensory-motor system predicts aging in healthy older adults. Front Aging Neurosci 2017;8:1–12.

446. Ferreira LK, Busatto GF. Resting-state functional connectivity in normal brain aging. Neurosci Biobehav Rev 2013;37:384–400. Available at: http://dx.doi.org/10.1016/j.neubiorev.2013.01.017.

447. Scheinost D, Finn ES, Tokoglu F, et al. Sex differences in normal age trajectories of functional brain networks. Hum Brain Mapp 2015;36:1524–1535.

448. Jamadar SD, Sforazzini F, Raniga P, et al. Sexual Dimorphism of Resting-State Network Connectivity in Healthy Ageing. Journals Gerontol Ser B 2018;00:1–11.

449. Filippi M, Valsasina P, Misci P, et al. The organization of intrinsic brain activity differs between genders: A resting-state fMRI study in a large cohort of young healthy subjects. Hum Brain Mapp 2013;34:1330–1343.

450. Allen EA, Erhardt EB, Damaraju E, et al. A Baseline for the Multivariate Comparison of Resting-State Networks. Front Syst Neurosci 2011;5:1–23.

451. Weissman-Fogel I, Moayedi M, Taylor KS, et al. Cognitive and default-mode resting state networks: Do male and female brains "rest" differently? Hum Brain Mapp 2010;31:1713–1726.

452. Orfanos S, Toygar T, Berthold-Losleben M, et al. Investigating the impact of overnight fasting on intrinsic functional connectivity: a double-blind fMRI study. Brain Imaging Behav 2018;12:1150–1159. Available at: http://dx.doi.org/10.1007/s11682-017-9777-9.

453. Meyer-Gerspach AC, Ly HG, Borgwardt S, et al. Endogenous GLP-1 alters postprandial functional connectivity between homeostatic and reward-related brain regions involved in regulation of appetite in healthy lean males: A pilotstudy. Diabetes, Obes Metab 2018;20:2330–2338.

454. Page KA, Chan O, Cline GW, et al. Incomplete Conflict of Interest Disclosures in: Effects of Fructose vs Glucose on Regional Cerebral Blood Flow in Brain Regions Involved With Appetite and Reward Pathways. Jama 2013;309:1773.

455. Carbonell F, Nagano-Saito A, Leyton M, et al. Dopamine precursor depletion impairs structure and efficiency of resting state brain functional networks. Neuropharmacology 2014;84:90–100. Available at: http://dx.doi.org/10.1016/j.neuropharm.2013.12.021.

456. Zanchi D, Meyer-Gerspach AC, Suenderhauf C, et al. Differential effects of L-Tryptophan and L-leucine administration on brain resting state functional networks and plasma hormone levels. Sci Rep 2016;6:1–9. Available at: http://dx.doi.org/10.1038/srep35727.

457. Al-Zubaidi A, Heldmann M, Mertins A, et al. Influences of Hunger, Satiety and Oral Glucose on Functional Brain Connectivity: A Multimethod Resting-State fMRI Study. Neuroscience 2018;382:80–92.

458. Hou J, Mohanty R, Nair VA, et al. Alterations in resting-state functional connectivity in patients with Crohn's disease in remission. Sci Rep 2019;9:1–9.

459. Bao C, Liu P, Liu H, et al. Difference in regional neural fluctuations and functional connectivity in Crohn's disease: a resting-state functional MRI study. Brain Imaging Behav 2018;0:1–9. Available at: http://dx.doi.org/10.1007/s11682-018-9850-z.

460. Liu P, Li R, Bao C, et al. Altered topological patterns of brain functional networks in Crohn's disease. Brain Imaging Behav 2018;12:1466–1478. Available at: http://dx.doi.org/10.1007/s11682-017-9814-8.

461. Bao C, Wang D, Liu P, et al. Effect of Electro-Acupuncture and Moxibustion on Brain Connectivity in Patients with Crohn's Disease: A Resting-State fMRI Study. Front Hum Neurosci 2017;11:1–10. Available at: http://journal.frontiersin.org/article/10.3389/fnhum.2017.00559/full.

462. Bao C, Liu P, Liu H, et al. Different brain responses to electro-acupuncture and moxibustion treatment in patients with Crohn's disease. Sci Rep 2016;6:1–12. Available at: http://dx.doi.org/10.1038/srep36636.

463. Bao C-H, Liu P, Liu H-R, et al. Differences in Regional Homogeneity Between Crohn's Disease Patients With and Without Abdominal Pain Revealed by Resting-State fMRI. Pain 2016;157:1037–1044. Available at: http://www.ncbi.nlm.nih.gov/pubmed/26761381.

464. Birn RM, Molloy EK, Patriat R, et al. The effect of scan length on the reliability of resting-state fMRI connectivity estimates. Neuroimage 2013;83:550–558. Available at: http://dx.doi.org/10.1016/j.neuroimage.2013.05.099.

465. Glover GH, Li TQ, Ress D. Image-based method for retrospective correction of physiological motion effects in fMRI: RETROICOR. Magn Reson Med 2000;44:162–167.

466. Jenkinson M, Bannister P, Brady M, et al. Improved optimization for the robust and accurate linear registration and motion correction of brain images. Neuroimage 2002;17:825–41. Available at: http://www.ncbi.nlm.nih.gov/pubmed/12377157.

467. Smith SM. Fast robust automated brain extraction. Hum Brain Mapp 2002;17:143–55. Available at: http://www.ncbi.nlm.nih.gov/pubmed/12391568.

468. Winkler AM, Ridgway GR, Webster MA, et al. Permutation inference for the general linear model. Neuroimage 2014;92:381–397. Available at: http://dx.doi.org/10.1016/j.neuroimage.2014.01.060.

469. Onitsuka T, Shenton ME, Salisbury DF, et al. Middle and inferior temporal gyrus gray matter volume abnormalities in chronic schizophrenia: An MRI study. Am J Psychiatry 2004;161:1603–1611.

470. Euston DR, Gruber AJ, McNaughton BL. The Role of Medial Prefrontal Cortex in Memory and Decision Making. Neuron 2012;76:1057–1070. Available at: http://dx.doi.org/10.1016/j.neuron.2012.12.002.

471. Fornito A, Yücel M, Wood S, et al. Individual Differences in Anterior Cingulate/Paracingulate Morphology Are Related to Executive Functions in Healthy Males. Cereb Cortex 2004;14:424–431.

472. Fuentes CT, Bastian AJ. "Motor cognition" - What is it and is the cerebellum involved? Cerebellum 2007;6:232–236.

473. Rabellino D, Densmore M, Théberge J, et al. The cerebellum after trauma: Resting-state functional connectivity of the cerebellum in posttraumatic stress disorder and its dissociative subtype. Hum Brain Mapp 2018;39:3354–3374.

474. Steininger SC, Liu X, Gietl A, et al. Cortical amyloid beta in cognitively normal elderly adults is associated with decreased network efficiency within the cerebro-cerebellar system. Front Aging Neurosci 2014;6:1–11.

475. Luo L, Wu K, Lu Y, et al. Increased Functional Connectivity Between Medulla and Inferior Parietal Cortex in Medication-Free Major Depressive Disorder. Front Neurosci 2018;12:1–7.

476. Lee YJG, Kim S, Kim N, et al. Changes in subcortical resting-state functional connectivity in patients with psychophysiological insomnia after cognitive–behavioral therapy: Changes in resting-state FC after CBT for insomnia patients. NeuroImage Clin 2018;17:115–123. Available at: https://doi.org/10.1016/j.nicl.2017.10.013.

477. Neubert FX, Mars RB, Sallet J, et al. Connectivity reveals relationship of brain areas for reward-guided learning and decision making in human and monkey frontal cortex. Proc Natl Acad Sci U S A 2015;112:E2695–E2704.

478. Rolls ET. The orbitofrontal cortex and emotion in health and disease, including depression. Neuropsychologia 2019;128:14–43. Available at: https://doi.org/10.1016/j.neuropsychologia.2017.09.021.

479. Niu C, Tan X, Liu X, et al. Cortical thickness reductions associate with abnormal resting-state functional connectivity in non-neuropsychiatric systemic lupus erythematosus. Brain Imaging Behav 2018;12:674–684.

480. Aminoff EM, Kveraga K, Bar M. The role of the parahippocampal cortex in cognition. Trends Cogn Sci 2013;17:379–390. Available at: http://dx.doi.org/10.1016/j.tics.2013.06.009.

481. Zhang S, Li CSR. Functional Connectivity Parcellation of the Human Thalamus by Independent Component Analysis. Brain Connect 2017;7:602–616.

482. Simoni S De, Jenkins PO, Bourke NJ, et al. Altered caudate connectivity is associated with executive dysfunction after traumatic brain injury. Brain 2018;141:148–164.

483. Cheng W, Rolls ET, Qiu J, et al. Increased functional connectivity of the posterior cingulate cortex with the lateral orbitofrontal cortex in depression. Transl Psychiatry 2018;8:1–10.

484. Anon. GroupICA dual regression analysis of resting state networks in a behavioral variant of frontotemporal dementia.

485. Grill-Spector Kalanit, Kourtzi Zoe KN. The lateral occipital complex and its role in object recognition. Vision Res 2001;41:1409–1422.

486. Hebart MN, Hesselmann G. What visual information is processed in the human dorsal stream? J Neurosci 2012;32:8107–8109.

487. Petruo VA, Zeißig S, Schmelz R, et al. Specific neurophysiological mechanisms underlie cognitive inflexibility in inflammatory bowel disease. Sci Rep 2017;7:1–9.

488. Golan D, Gross B, Miller A, et al. Cognitive Function of Patients with Crohn's Disease is Associated with Intestinal Disease Activity. Inflamm Bowel Dis 2016;22:364–371.

489. Nair VA, Dodd K, Rajan S, et al. A Verbal Fluency Task-Based Brain Activation fMRI Study in Patients with Crohn's Disease in Remission. J Neuroimaging 2019:1–10.

490. Langenberg DR van, Yelland GW, Robinson SR, et al. Cognitive impairment in Crohn's disease is associated with systemic inflammation, symptom burden and sleep disturbance. United Eur Gastroenterol J 2017;5:579–587.

491. Esposito F, Otto T, Zijlstra FRH, et al. Spatially distributed effects of mental exhaustion on resting-state FMRI networks. PLoS One 2014;9:1–13.

492. Gennari SP, Millman RE, Hymers M, et al. Anterior paracingulate and cingulate cortex mediates the effects of cognitive load on speech sound discrimination. Neuroimage 2018;178:735–743. Available at: https://doi.org/10.1016/j.neuroimage.2018.06.035.

493. Wortinger LA, Endestad T, Melinder AMD, et al. Aberrant resting-state functional connectivity in the salience network of adolescent chronic fatigue syndrome. PLoS One 2016;11:1–16.

494. Gay CW, Robinson ME, Lai S, O'Shea A, Craggs JG, Price DD SR. Abnormal Resting-state Functional connectivity in patients with chronic fatigue syndrome: results of seed and data-driven analyses. Brain Connect 2016:48–56.

495. Tinsley A, MacKlin EA, Korzenik JR, et al. Validation of the Functional Assessment of Chronic Illness Therapy-Fatigue (FACIT-F) in patients with inflammatory bowel disease. Aliment Pharmacol Ther 2011;34:1328–1336.

496. Terry H, Forbes A, Ream E, et al. P242 Development and psychometric testing of an inflammatory bowel disease fatigue (IBD-F) patient self-assessment scale. J Crohn's Colitis 2014;8:S163.

497. Koenigs M, Barbey AK, Postle BR, et al. Superior parietal cortex is critical for the manipulation of information in working memory. J Neurosci 2009;29:14980–14986.

498. Kong J, Jensen K, Loiotile R, et al. Functional connectivity of the frontoparietal network predicts cognitive modulation of pain. Pain 2013;154:459–467. Available at: http://dx.doi.org/10.1016/j.pain.2012.12.004.

499. Zhao Z, Huang T, Tang C, et al. Altered resting-state intra- and inter- network functional connectivity in patients with persistent somatoform pain disorder. PLoS One 2017;12:1–16.

500. Hirnstein M, Westerhausen R, Hugdahl K. The Right Planum Temporale Is Involved in Stimulus-Driven, Auditory Attention - Evidence from Transcranial Magnetic Stimulation. PLoS One 2013;8:1–7.

501. Hampshire A, Chamberlain SR, Monti MM, et al. The role of the right inferior frontal gyrus: inhibition and attentional control. Neuroimage 2010;50:1313–1319. Available at: http://dx.doi.org/10.1016/j.neuroimage.2009.12.109.

502. Kringelbach ML. The pleasure of food: underlying brain mechanisms of eating and other pleasures. Flavour 2015;4:1–12.

503. Zhang Y, Fan L, Zhang Y, et al. Connectivity-based parcellation of the human posteromedial cortex. Cereb Cortex 2014;24:719–727.

8 Appendix

May 2018
Alice Lieth

Radioimmunoassay (RIA) measurements of Cholecystokinin (CCK) in plasma

Reagents

Barbital buffer I:	20 mmol/l barbital pH 8.4 0.6 mmol/l thiomersal 0.11 % bovine albumin (Sigma)
Barbital buffer II:	20 mmol/l barbital buffer pH 8.4 Natriumazid 0.13 g/l
Human albumin:	Human albumin 5 % CSL Behring. Extract 400 µl Human albumin 5 % CSL Behring with 800 µl of 96 % vol/vol ethanol. After vigorous vortexing for 10 s, centrifuge the mixture 15 min 4000 rpm. The supernatant is decanted and evaporated in a vacuum concentrator. The dried albumin-extracts are stored at -20 °C.
Standard concentrations:	0, 1, 2.5, 5, 10, 20, 30 and 50 pmol/l of synthetic sulphated CCK-8 dissolved in barbital buffer II (BACHEM).
Controls:	4, 7.5 and 15 pmol/l synthetic sulphated CCK-8, dissolved in barbital buffer I.
Antibody:	Ab. 92128/6 is diluted to a concentration that binds approximately 35 % of the tracer. The final dilution of Ab. 92128-6 in our set-up is 1:300.000.
Tracer:	^{125}I-CCK8-sulfated labelled with Bolton. Hunter reagent, 1000 CPM/tube (Perkin Elmer).
Separation:	6 g activated Charcoal (Merck) 20 ml human plasma (outdated blood bank plasma) 80 ml barbital buffer II

Samples

Blood samples are collected in ice-chilled plastic tubes containing 5 µl EDTA per ml blood and left in an ice-bath until centrifugation (within 30 min) at 4 °C. The samples are centrifuged for 10 min at 30000 rpm and plasma stored at -20 °C.

Sample preparation

Extraction of samples on ice-bath:

400 µl of plasma is extracted with 800 µl of 96 % vol/vol ethanol. After vigorous vortexing for 2 x 10 s, the mixture is centrifuged for 15 min 4000 rpm. The supernatant is decanted and evaporated in a vacuum concentrator. The dried plasma-extract can be stored at -20 °C. Before assay, the samples are reconstituted in 400 µl barbital buffer I, which stays at 4 °C for 15 min before mixing.

Blank, standards and controls:

Before RIA, 400 µl of blank, standard and control are dissolved in extracted and evaporated human albumin (400 µl). Mix.

Assay procedure

1. **Blank in double**
   150 µl 0 sample +
   1000 µl barbital buffer I + tracer

   Standard, controls and sample are prepared for double determinations

   150 µl sample/standard/control +
   1000 µl barbital buffer I + antibody + tracer

2. Time of incubation 3-7 days at 4 °C

3. Separation with 20 % human plasma

   The suspension kept on ice is rigorously shaken on a magnetic stirrer for 30 minutes before use. Half a ml suspension is added to each tube. The samples are mixed, left for 15 min at room temp. (max 30 min) and then centrifuged for 10 min at 4000 rpm, 4 °C. The separation is performed on a SepRia separator. The supernatant is counted for 5 min in an automatic gamma counter.

4. Results are calculated with MultiCalc program from Perkin Elmer.

5. The concentrations are calculated in pmol/l and given with 1 decimal.

6. Concentrations measured to be >30 pmol/l are diluted with 0 sample.

Reference

Rehfeld JF. Accurate measurement of cholecystokinin in plasma. Clin. Chem. 1998;44:5:991-1001.

PPID:

Time:

Date:

UNIVERSITY OF LEEDS

Instructions*.* Below are groups of numbered statements. Read all of the statements in each group and mark on this sheet the one that best describes the way you feel about the problems you have controlling your eating behaviour.

#1.

1. I don't feel self-conscious about my weight or body size when I'm with others.
2. I feel concerned about how I look to others, but it normally does not make me feel disappointed with myself.
3. I do get self-conscious about my appearance and weight which makes me feel disappointed in myself.
4. I feel very self-conscious about my weight and frequently, I feel intense shame and disgust for myself. I try to avoid social contacts because of my self-consciousness.

#2.

1. I don't have any difficulty eating slowly in the proper manner.
2. Although I seem to "gobble down" foods, I don't end up feeling stuffed because of eating too much.
3. At times, I tend to eat quickly and then, I feel uncomfortably full afterwards.
4. I have the habit of bolting down my food, without really chewing it. When this happens I usually feel uncomfortably stuffed because I've eaten too much.

#3.

1. I feel capable to control my eating urges when I want to.
2. I feel like I have failed to control my eating more than the average person.
3. I feel utterly helpless when it comes to feeling in control of my eating urges.
4. Because I feel so helpless about controlling my eating I have become very desperate about trying to get in control.

#4

1. I don't have the habit of eating when I'm bored.
2. I sometimes eat when I'm bored, but often I'm able to "get busy" and get my mind off food.
3. I have a regular habit of eating when I'm bored, but occasionally, I can use some other activity to get my mind off eating.
4. I have a strong habit of eating when I'm bored. Nothing seems to help me break the habit.

#5

1. I'm usually physically hungry when I eat something.
2. Occasionally, I eat something on impulse even though I really am not hungry.
3. I have the regular habit of eating foods that I might not really enjoy, to satisfy a hungry feeling even though physically, I don't need the food.
4. Even though I'm not physically hungry, I get a hungry feeling in my mouth that only seems to be satisfied when I eat a food, like a sandwich, that fills my mouth. Sometimes, when I eat the food to satisfy my mouth hunger, I then spit the food out so I won't gain weight.

PPID:

Time:

Date:

#6

1. I don't feel any guilt or self-hate after I overeat.
2. After I overeat, occasionally I feel guilt or self-hate.
3. Almost all the time I experience strong guilt or self-hate after I overeat.

#7

1. I don't lose total control of my eating when dieting even after periods when I overeat.
2. Sometimes when I eat a "forbidden food" on a diet, I feel like I "blew it" and eat even more.
3. Frequently, I have the habit of saying to myself, "I've blown it now, why not go all the way" when I overeat on a diet. When that happens I eat even more.
4. I have a regular habit of starting strict diets for myself, but I break the diets by going on an eating binge. My life seems to be either a "feast" or "famine."

#8

1. I rarely eat so much food that I feel uncomfortably stuffed afterwards.
2. Usually about once a month, I eat such a quantity of food, I end up feeling very stuffed.
3. I have regular periods during the month when I eat large amounts of food, either at mealtime or at snacks.
4. I eat so much food that I regularly feel quite uncomfortable after eating and sometimes a bit nauseous.

#9

1. My level of calorie intake does not go up very high or go down very low on a regular basis.
2. Sometimes after I overeat, I will try to reduce my caloric intake to almost nothing to compensate for the excess calories I've eaten.
3. I have a regular habit of overeating during the night. It seems that my routine is not to be hungry in the morning but overeat in the evening.
4. In my adult years, I have had week-long periods where I practically starve myself. This follows periods when I overeat. It seems I live a life of either "feast or famine."

#10

1. I usually am able to stop eating when I want to. I know when "enough is enough."
2. Every so often, I experience a compulsion to eat which I can't seem to control.
3. Frequently, I experience strong urges to eat which I seem unable to control, but at other times I can control my eating urges.
4. I feel incapable of controlling urges to eat. I have a fear of not being able to stop eating voluntarily.

#11

1. I don't have any problem stopping eating when I feel full.
2. I usually can stop eating when I feel full but occasionally overeat leaving me feeling uncomfortably stuffed.
3. I have a problem stopping eating once I start and usually I feel uncomfortably stuffed after I eat a meal.
4. Because I have a problem not being able to stop eating when I want, I sometimes have to induce vomiting to relieve my stuffed feeling.

PPID:
Time:
Date:

#12
1. I seem to eat just as much when I'm with others (family, social gatherings) as when I'm by myself.
2. Sometimes, when I'm with other persons, I don't eat as much as I want to eat because I'm self-conscious about my eating.
3. Frequently, I eat only a small amount of food when others are present, because I'm very embarrassed about my eating.
4. I feel so ashamed about overeating that I pick times to overeat when I know no one will see me. I feel like a "closet eater."

#13
1. I eat three meals a day with only an occasional between meal snack.
2. I eat 3 meals a day, but I also normally snack between meals.
3. When I am snacking heavily, I get in the habit of skipping regular meals.
4. There are regular periods when I seem to be continually eating, with no planned meals.

#14
1. I don't think much about trying to control unwanted eating urges.
2. At least some of the time, I feel my thoughts are pre-occupied with trying to control my eating urges.
3. I feel that frequently I spend much time thinking about how much I ate or about trying not to eat anymore.
4. It seems to me that most of my waking hours are pre-occupied by thoughts about eating or not eating. I feel like I'm constantly struggling not to eat.

#15
1. I don't think about food a great deal.
2. I have strong cravings for food but they last only for brief periods of time.
3. I have days when I can't seem to think about anything else but food.
4. Most of my days seem to be pre-occupied with thoughts about food. I feel like I live to eat.

#16
1. I usually know whether or not I'm physically hungry. I take the right portion of food to satisfy me.
2. Occasionally, I feel uncertain about knowing whether or not I'm physically hungry. At these times it's hard to know how much food I should take to satisfy me.
3. Even though I might know how many calories I should eat, I don't have any idea what is a "normal" amount of food for me.

PPID:

Time:

Date:

UNIVERSITY OF LEEDS

Please read each question carefully and put a mark through the line at the point that best represents your experience. Answer all questions according to your experience over the **last 7 days**.

1. How hungry have you felt?

Not at all hungry _____ Extremely hungry

2. How full have you felt?

Not at all full _____ Extremely full

3. How strong was your desire to eat sweet foods?

Not at all strong _____ Extremely strong

4. How strong was your desire to eat savoury foods?

Not at all strong _____ Extremely strong

5. How happy have you felt?

Not at all happy _____ Extremely happy

6. How anxious have you felt?

Not at all anxious _____ Extremely anxious

7. How alert have you felt?

Not at all alert _____ Extremely alert

8. How contented have you felt?

Not at all contented _____ Extremely contented

A food craving is a strong urge to eat a particular food or drink

9. During the last 7 days how often have you had food cravings?

Not at all _____ Very often

PPID:

Week:

Date:

UNIVERSITY OF LEEDS

10. How strong have any food cravings been?

Not at all strong _____ Extremely strong

11. How difficult has it been to resist any food cravings?

Not at all difficult _____ Extremely difficult

12. How often have you eaten in response to food cravings?

Not at all _____ After every one

How often have you had food cravings for the following types of food/drink?

13. Chocolate or chocolate flavoured foods

Not at all _____ Extremely often

14. Other sweet foods (cakes, pastries, biscuits, etc)

Not at all _____ Extremely often

15. Fruit or fruit juice

Not at all _____ Extremely often

16. Dairy foods (cheese, yoghurts, milk, etc)

Not at all _____ Extremely often

17. Starchy foods (bread, rice, pasta, etc)

Not at all _____ Extremely often

18. Savoury foods (french fries, crisps, burgers, pizza, etc)

Not at all _____ Extremely often

19. Generally, how difficult has it been to control your eating?

Not at all difficult _____ Extremely difficult

20. Which one food makes it most difficult for you to control eating?

.....

21. How difficult has it been to resist eating this food during the last 7 days?

Not at all difficult _____ Extremely difficult

PPID:

Time:

Date:

UNIVERSITY OF LEEDS

Please indicate the extent to which you agree that the following items describe you. Use the following 1-5 scale for you responses.

1 don't agree at all
2 agree a little
3 agree somewhat
4 agree
5 strongly agree

---

1. I find myself thinking about food even when I'm not physically hungry.	1	2	3	4	5
2. I get more pleasure from eating than I do from almost anything else.	1	2	3	4	5
3. If I see or smell a food I like, I get a powerful urge to have some.	1	2	3	4	5
4. When I'm around a fattening food I love, it's hard to stop myself from at least tasting it.	1	2	3	4	5
5. It's scary to think of the power that food has over me.	1	2	3	4	5
6. When I know a delicious food is available, I can't help myself from thinking about having some.	1	2	3	4	5
7. I love the taste of certain foods so much that I can't avoid eating them even if they're bad for me.	1	2	3	4	5
8. Just before I taste a favorite food, I feel intense anticipation.	1	2	3	4	5
9. When I eat delicious food I focus a lot on how good it tastes.	1	2	3	4	5
10. Sometimes, when I'm doing everyday activities, I get an urge to eat "out of the blue" (for no apparent reason).	1	2	3	4	5
11. I think I enjoy eating a lot more than most other people.	1	2	3	4	5
12. Hearing someone describe a great meal makes me really want to have something to eat.	1	2	3	4	5
13. It seems like I have food on my mind a lot.	1	2	3	4	5
14. It's very important to me that the foods I eat are as delicious as possible.	1	2	3	4	5
15. Before I eat a favorite food my mouth tends to flood with saliva.	1	2	3	4	5

PPID:
Time:
Date:

UNIVERSITY OF LEEDS

This booklet contains a number of statements. Each statement should be answered either TRUE or FALSE. Read each statement and decide how you feel about it in PART 1.

If you agree with the statement , or if you feel that it is true about you then circle T next to the statement.

If you disagree with a statement, or if you feel that it is false as applied to you, circle the F next to the statement.

1) When I smell a sizzling steak or see a juicy piece of meat I find it very difficult to keep from eating, even if I have just finished a meal	**T**	**F**
2) I usually eat too much at social occasions, like parties and picnics.	**T**	**F**
3) I am usually so hungry that I eat more than 3 times a day.	**T**	**F**
4) When I have eaten my quota of calories I am usually very good about not eating any more.	**T**	**F**
5) Dieting is so hard for me because I just get too hungry.	**T**	**F**
6) I deliberately take small helpings as a means of controlling my weight.	**T**	**F**
7) Sometimes things just taste so good that I keep on eating, even when I am no longer hungry.	**T**	**F**
8) Since I am often hungry, I sometimes wish that while I am eating an expert would tell me that I have had enough or that I can have something more to eat.	**T**	**F**
9) When I feel anxious I find myself eating.	**T**	**F**
10) Life is too short to worry about dieting.	**T**	**F**
11) Since my weight goes up and down, I have gone on reducing diets more than once.	**T**	**F**
12) I often feel so hungry I just have to eat something.	**T**	**F**
13) When I am with someone who is overeating I usually overeat too.	**T**	**F**
14) I have a pretty good idea of the number of calories in common foods	**T**	**F**
15) Sometimes when I start eating, I just can't seem to stop.	**T**	**F**
16) It is not difficult for me to leave something on my plate.	**T**	**F**

PPID:
Time:
Date:

17) At certain times of the day I get hungry because I have gotten used to eating then. **T** **F**

18) While on a diet, if I eat food that is not allowed, I consciously eat less for a period of time to make up for it. **T** **F**

19) Being with someone who is overeating often makes me hungry enough to eat also. **T** **F**

20) When I feel blue I often overeat. **T** **F**

21) I enjoy eating too much to spoil it by counting calories or watching my weight. **T** **F**

22) When I see a real delicacy I often get so hungry that I have to eat it right away. **T** **F**

23) I often stop eating when I am not really full as a conscious means of limiting the amount I eat. **T** **F**

24) I get so hungry my stomach feels like a bottomless pit. **T** **F**

25) My weight has hardly changed at all in the last ten years. **T** **F**

26) I am always hungry so it is hard for me to stop eating before I finish the food on my plate. **T** **F**

27) When I feel lonely, I console myself by eating. **T** **F**

28) I consciously hold back at meals in order not to gain weight. **T** **F**

29) I sometimes get very hungry late in the evening or at night. **T** **F**

30) I eat anything I want, anytime. **T** **F**

31) Without even thinking about it I take a long time to eat. **T** **F**

32) I count calories as a conscious means of controlling my weight. **T** **F**

33) I do not eat some foods because they make me fat. **T** **F**

34) I am always hungry enough to eat at anytime. **T** **F**

35) I pay a great deal of attention to changes in my figure. **T** **F**

36) While on a diet, if I eat food that is not allowed, I often then splurge and eat other high calorie foods. **T** **F**

PPID:
Time:
Date:

Please answer the following questions by circling the number above the response that is appropriate to you.

37) How often are you dieting in a conscious effort to control your weight?

1	2	3	4
rarely	sometimes	usually	always

38) Would a weight fluctuation of 5lbs affect the way you live your life?

1	2	3	4
not at all	slightly	moderately	very much

39) How often do you feel hungry?

1	2	3	4
only at meal times	sometimes between meals	often between meals	almost always

40) Do your feelings of guilt about overeating help you to control your food intake?

1	2	3	4
never	rarely	often	always

41) How difficult would it be for you to stop eating halfway through dinner and not eat for the next four hours?

1	2	3	4
easy	slightly difficult	moderately difficult	very difficult

42) How conscious are you of what you are eating?

1	2	3	4
not at all	slightly	moderately	extremely

43) How frequently do you avoid 'stocking up' on tempting foods.

1	2	3	4
almost never	seldom	usually	almost always

44) How likely are you to shop for 'low calorie' foods?

1	2	3	4
unlikely	slightly likely	moderately likely	very likely

45) Do you eat sensibly in front of others and splurge alone?

1	2	3	4
never	rarely	often	always

PPID:
Time:
Date:

46) How likely are you to consciously eat slowly in order to cut down on how much you eat?

1	2	3	4
unlikely	slightly likely	moderately likely	very likely

47) How frequently do you skip dessert because you are no longer hungry?

1	2	3	4
never	seldom	at least once a week	almost every day

48) How likely are you to consciously eat less than you want?

1	2	3	4
unlikely	slightly likely	moderately likely	very likely

49) Do you go on eating binges even though you are not hungry?

1	2	3	4
never	rarely	sometimes	at least once a week

50) On a scale of 0-5 where 0 means no restraint in eating (eat whatever you want, whenever you want it), and 5 means total restraint (constantly limiting food intake and never 'giving in'). What number would you give yourself?

0
Eat whatever you want, whenever you want it.
1
Usually eat whatever you want, whenever you want it.
2
Often eat whatever you want, whenever you want it.
3
Often limit food intake, but often 'give in'.
4
Usually limit food, rarely ‘give in’
5
Constantly limiting food intake, never 'giving in'.

51) To what extent does this statement describe your eating behaviour?

'I start dieting in the morning, but because of any number of things that happen during the day, by evening I have given up and eat what I want, promising myself to start dieting again tomorrow.'

1	2	3	4
not like me	little like me	pretty good description of me	describes me perfectly

Short Quality of Life Questionnaire for Inflammatory Bowel Disease

Name _____ Date_____

This questionnaire is designed to find out how you have been feeling during the last 2 weeks. You will be asked about symptoms you have been having as a result of your inflammatory bowel disease, the way you have been feeling in general, and how your mood has been. Please circle the number of your choice below each question.

1. How often has the feeling of fatigue or being tired and worn out been a problem for you during the past 2 weeks?
    1. All of the time
    2. Most of the time
    3. A good bit of the time
    4. Some of the time
    5. A little of the time
    6. Hardly any of the time
    7. None of the time

2. How often during the last 2 weeks have you delayed or canceled a social engagement because of your bowel problem?
    1. All of the time
    2. Most of the time
    3. A good bit of the time
    4. Some of the time
    5. A little of the time
    6. Hardly any of the time
    7. None of the time

3. As a result of your bowel problems, how much difficulty did you experience doing leisure or sports activities you would liked to have done during the past 2 weeks?
    1. A great deal of difficulty; activities made impossible
    2. A lot of difficulty
    3. A fair bit of difficulty
    4. Some difficulty
    5. A little difficulty
    6. Hardly any difficulty
    7. No difficulty; the bowel problem did not limit sports or leisure activities

4. How often during the past 2 weeks have you been troubled by pain in the abdomen?
    1. All of the time
    2. Most of the time
    3. A good bit of the time
    4. Some of the time
    5. A little of the time
    6. Hardly any of the time
    7. None of the time

Irvine, E. J., et. al. The short inflammatory bowel disease questionnaire: A quality of life instrument for community physicians managing inflammatory bowel disease. Am J Gastroenterology. 1996; 91(8):1571-8 Aug.

5. How often during the past 2 weeks have you felt depressed or discouraged?
    1. All of the time
    2. Most of the time
    3. A good bit of the time
    4. Some of the time
    5. A little of the time
    6. Hardly any of the time
    7. None of the time

6. Overall, in the past 2 weeks, how much of a problem have you had with passing large amounts of gas?
    1. A major problem
    2. A big problem
    3. A significant problem
    4. Some problem
    5. A little trouble
    6. Hardly any trouble
    7. No trouble

7. Overall, in the past 2 weeks, how much of a problem have you had maintaining or getting to the weight you would like to be?
    1. A major problem
    2. A big problem
    3. A significant problem
    4. Some problem
    5. A little trouble
    6. Hardly any trouble
    7. No trouble

8. How often during the past 2 weeks have you felt relaxed and free of tension?
    1. All of the time
    2. Most of the time
    3. A good bit of the time
    4. Some of the time
    5. A little of the time
    6. Hardly any of the time
    7. None of the time

9. How much of the time during the past 2 weeks have you been troubled by a feeling of having to go to the bathroom even though your bowels were empty?
    1. All of the time
    2. Most of the time
    3. A good bit of the time
    4. Some of the time
    5. A little of the time
    6. Hardly any of the time
    7. None of the time

10. How often during the past 2 weeks have you felt angry as a result of your bowel problem?
    1. All of the time
    2. Most of the time
    3. A good bit of the time
    4. Some of the time
    5. A little of the time
    6. Hardly any of the time
    7. None of the time

Irvine, E. J., et. al. The short inflammatory bowel disease questionnaire: A quality of life instrument for community physicians managing inflammatory bowel disease. Am J Gastroenterology. 1996; 91(8):1571-8 Aug.

For formulary coverage:

Harvey-Bradshaw Index (HBI) — A simple index of Crohn's disease activity[1]

Patient name: _____

Date of HBI calculation: _____

Please check one box per number (except for #5)

1. General well-being *(yesterday)*	☐ Very well = 0 ☐ Slightly below par = 1 ☐ Poor = 2 ☐ Very poor = 3 ☐ Terrible = 4
2. Abdominal pain *(yesterday)*	☐ None = 0 ☐ Mild = 1 ☐ Moderate = 2 ☐ Severe = 3
3. Number of liquid or soft stools per day *(yesterday)* = _____	
4. Abdominal mass	☐ None = 0 ☐ Dubious = 1 ☐ Definite = 2 ☐ Definite and tender = 3
5. Complications *(check any that apply; score one per item except for first box)*	☐ None ☐ Arthralgia ☐ Uveitis ☐ Erythema nodosum ☐ Aphthous ulcers ☐ *Pyoderma gangrenosum* ☐ Anal fissure ☐ New fistula ☐ Abscess

Harvey-**B**radshaw **I**ndex score[2]=

(please add scores of questions 1 through 5)

Remission	<5
Mild disease	5-7
Moderate disease	8-16
Severe disease	>16

References: 1. Harvey RF, Bradshaw JM. A simple index of Crohn's-disease activity. *Lancet*. 1980;315(8167):514. **2.** British Columbia Ministry of Health Services. Worksheet based on the Harvey-Bradshaw Index. British Columbia Ministry of Health Services website. https://www.health.gov.bc.ca/exforms/pharmacare/5374fil.pdf. Accessed September 23, 2010.

Janssen Inc.
19 Green Belt Drive
Toronto, Ontario
M3C 1L9

© 2011 JANSSEN Inc.
www.janssen.ca
RGFM110565E

Member R&D PAAB

*All trademark rights used under license

janssen PHARMACEUTICAL COMPANIES OF Johnson & Johnson

The University of Nottingham

NDDC Nottingham Digestive Diseases Centre

Reduced Appetite in Crohn disease: Investigating the role of the gut-brain pathways.

Volunteer's Health Questionnaire

SUBJECT…….....SIC……

INITIALS ……DATE …….

During the past 4 weeks, how much have you been bothered by any of the following problems?	Not Bothered at all	Bothered a little	Bothered a lot
Stomach pain			
Back pain			
Pain in your arms, legs, or joints (knees, hips, etc)			
Menstrual cramps or other problems with your periods (Women only)			
Headaches			
Chest pain			
Dizziness			
Fainting spells			
Feeling your heart pound or race			
Shortness of breath			
Pain or problems during sexual intercourse			
Constipation, loose bowels, or diarrhoea			
Nausea, gas, or indigestion			
Feeling tired or having low energy			
Trouble sleeping			

Abdominal pain score

Do you currently suffer from abdominal (tummy) pain? **YES** **NO**

Circle appropriate box

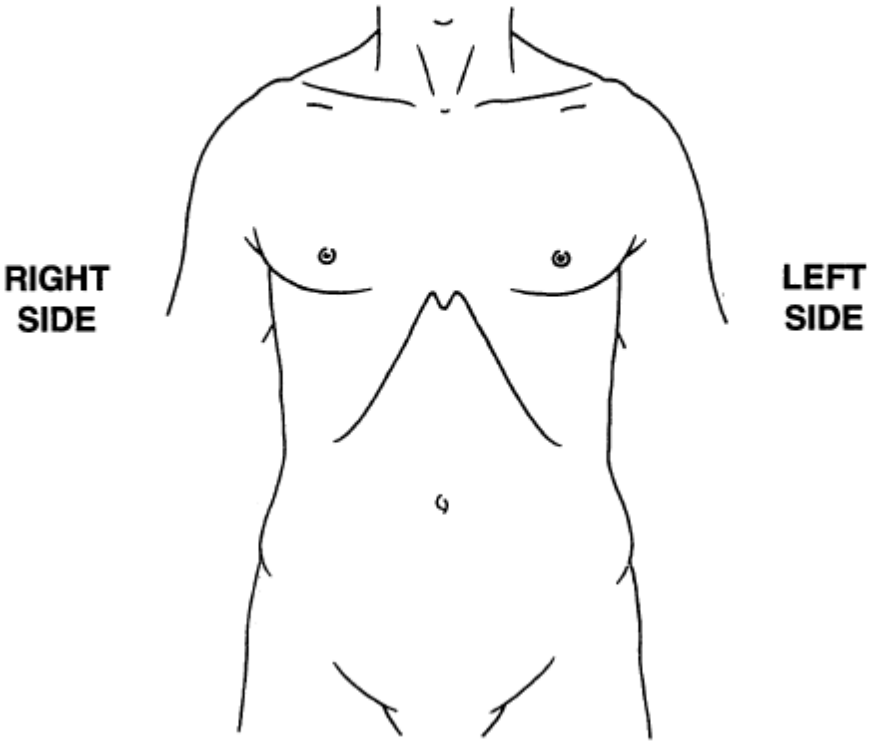
If yes, how severe is your abdominal (tummy) pain?

0% —— **100%**

no pain | not very severe | quite severe | severe | very severe

SITE OF PAIN

Please mark with a cross (x) on the diagram below where you get your pain
(use more than one x if necessary)



Reduced Appetite in Crohns Disease: Investigating the role of the gut-brain pathways
Inflammatory Bowel Disease-Fatigue (IBD-F) Self-assessment Scale

SECTION I - Fatigue Assessment Scale Date: …….. Time: ……...

Study ID No……INITIALS ……

This section of the questionnaire will identify fatigue, its severity, frequency and duration. Sometimes people with inflammatory bowel disease feel fatigued. The term 'fatigue' is used throughout the questionnaire. Fatigue has been defined as a sense of continuing tiredness, with periods of sudden and overwhelming lack of energy or feeling of exhaustion that is not relieved following rest or sleep.

Please tick ONE number for each question	Score from 0 - 4 with 0 = no fatigue				Severe fatigue = 4
1. What is your fatigue level right NOW	0	1	2	3	4
2. What was your HIGHEST fatigue level in the past two weeks	0	1	2	3	4
3. What was your LOWEST fatigue level in the past two weeks	0	1	2	3	4
4. What was your AVERAGE fatigue level in the past two weeks	0	1	2	3	4
5. How much of your waking time have you felt fatigued in the past two weeks	0 None of the time	1 Some of the time	2 Often	3 Most of the time	4 All the time